DOCTOR OF PHILOSOPHY

Identification of MMS22 as a regulator of DNA repair

Duro, Eris

Award date:
2010

Awarding institution:
University of Dundee

DOCTOR OF PHILOSOPHY

Identification of MMS22 as a regulator of DNA repair

Eris Duro

2010

University of Dundee

Identification of *MMS22* as a regulator of DNA repair

by

Eris Duro

A thesis submitted for the degree of Doctor of Philosophy, University of Dundee

Table of contents

List of figures

List of tables

Abbreviations

Amp	ampicillin
ASF1	anti-silencing function 1
AP	apurinic/apyrimidinic
AT	ataxia telangiectasia
ATM	ataxia telangiectasia mutated
ATP	adenosine 5'-triphosphate
ATR	ATM- and Rad3-related
β-ME	β-mercaptoethanol
BER	base-excision repair
BIR	break-induced replication
bp	base pairs
BS	Bloom's syndrome
BSA	bovine serum albumin
°C	degrees Celsius
C	cytosine
C-terminal	carboxy-terminal
CDK	cyclin-dependent protein kinase
CHK1/2	checkpoint kinase 1/2
CPD	cyclobutane pyrimidine dimer
CPT	camptothecin
Ctrl	control
Da	dalton
dH_2O	distilled water
DMSO	dimethylsulphoxide
DNA	deoxyribonucleic acid
DNA-PK	DNA-dependent protein kinase
dNTP	deoxynucleoside triphosphate
DSB	double-strand break

dsDNA	double-stranded DNA
DSTT	Division of Signal Transduction Therapy
DTT	dithiotheitol
E. coli	*Escherichia coli*
ECL	enhanced chemiluminescence
EDTA	ethylenediamine tetraacetic acid
EGTA	ethyleneglycol bis (2-aminoethylether)-N'N'tetraacetic acid
FA	Fanconi anaemia
FACS	fluorescence activated cell sorting
FPLC	fast protein liquid chromatography
g	gram
G418	geneticin
GFP	green fluorescent protein
GSH-	glutathione sepharose
GST	glutathione-S-transferase
Gy	Gray
HAT	histone acetyl-transferase
HEK	human embryonic kidney
HEPES	N-[2-hydroxyethyl]piperazine-N'-[2-ethanesulphonic acid]
HPLC	high-pressure liquid chromatography
HR	homologous recombination
h	hours
HP	horseradish peroxidase
HU	hydroxyurea
ICL	interstrand crosslink
IgG	immunoglobulin G
IP	immunoprecipitation
IPTG	isopropyl β-D-thiogalactoside
IR	ionising radiation

kDa	kilodalton
l	litre
LB	Luria-Bertani medium
LDS	lithium dodecyl sulphate
m	milli
M	molar
MALDI-TOF	Matrix-assisted laser desorption/ionisation time-of-flight
μ	micro
MGMT	O^6-methyl-guanine DNA methyl transferase
min	minute
MMR	mismatch repair
MMS	methyl methanesulfonate
mol	mole
MOPS	3-(*N*-morpholino) propanesulfonic acid
MRC PPU	Medical Research Council Protein Phosphorylation Unit
MS	mass spectrometry
N	nitrogen
NBS	Nijmegen breakage syndrome
NER	nucleotide excision repair
NFκBIL2	nuclear factor of kappa light polypeptide gene enhancer in B-cells inhibitor-like 2
NHEJ	non-homologous end joining
nm	nanometer
nt	nucleotide
N-terminal	amino-terminal
O	oxygen
O^6MeG	O^6-methyl-guanine
ORC	origin recognition complex
ORF	open reading frame

OD	optical density
p	pico
PAGE	polyacrylamide gel electrophoresis
PBS	phosphate-buffered saline
PCNA	proliferating cell nuclear antigen
PCR	polymerase chain reaction
PGS	protein-G Sepharose
PI 3-kinase	phosphatidylinositol 3-kinase
PIKL	PI 3-kinase-like
POL	polymerase
PRR	post-replication repair
RFC	replication factor C
ROS	reactive oxygen species
RPA	replication protein A
rpm	revolutions per minute
RTT	Regulator of Ty1 Transposition
SCE	sister chromatid exchange
S. cerevisiae	*Saccharomyces cerevisiae*
SDS	sodium dodecyl sulfate
SDSA	synthesis dependent strand annealing
SEM	standard error of the mean
s	seconds
SSA	single-strand annealing
SSB	single-strand break
ssDNA	single-stranded DNA
T	thymine
TAE	Tris-acetate-EDTA
TBE	Tris-borate-EDTA
TBS	Tris-buffered saline
TBS-T	Tris-buffered saline-Tween
TLS	translesion synthesis
Tris	tris (hydroxymethyl) aminomethane

Triton X-100	t-octylphenoxypolyethoxyethanol
Tween	polyethylene glycol sorbitan monolaurate
U	uracil
UBA	ubiquitin-associated domain
UBL	ubiquitin-like domain
UV	ultraviolet
V	volts
v/v	volume to volume
wt	wild type
w/v	weight to volume
XP	xeroderma pigmentosum

Amino acid code

Amino acid	Three letter code	One letter
Alanine	Ala	A
Arginine	Arg	R
Asparagine	Asn	N
Aspartic acid	Asp	D
Cysteine	Cys	C
Glutamic acid	Glu	E
Glutamine	Gln	Q
Glycine	Gly	G
Histidine	His	H
Isoleucine	Ile	I
Leucine	Leu	L
Lysine	Lys	K
Methionine	Met	M
Phenylalanine	Phe	F
Proline	Pro	P
Serine	Ser	S
Threonine	Thr	T
Tryptophan	Trp	W
Tyrosine	Tyr	Y
Valine	Val	V
any amino acid	Xaa	X

List of publications

Duro, E., Vaisica, J.A., Brown, G.W. and Rouse, J. (2008) Budding yeast Mms22 and Mms1 regulate homologous recombination induced by replisome blockage. DNA Repair 7, 811-818.

Duro E., Lundin C., Ask K., Sanchez–Pulido L., MacArtney T.J., Toth R., Ponting C.P., Groth A., Helleday T. and Rouse J. (2010) Identification of the MMS22L–TONSL complex that promotes homologous recombination. Molecular Cell. 40, 632-644.

Declarations

I declare that the following thesis is based on the results of investigations conducted by myself, and that this thesis is of my own composition. Work other than my own is clearly indicated in the text by reference to the relevant researchers or to their publications. This dissertation has not in whole, or in part, been previously submitted for a higher degree.

Eris Duro

I certify that Eris Duro has spent the equivalent of at least nine terms in research work at the School of Life Sciences, University of Dundee, and that he has fulfilled the conditions of the Ordinance General No 14 of the University of Dundee and is qualified to submit the accompanying thesis in application for the degree of Doctor of Philosophy.

Dr John Rouse

Acknowledgements

I am grateful to my supervisor John Rouse for all his help and for his contagious and indefatigable enthusiasm.

I want to thank everyone in the Rouse lab for their help and for being wonderful colleagues. I hope that in my future workplaces I will find people with equally high tolerance for bad jokes.

I also want to thank all my other friends in Dundee, who made my time here so much more enjoyable. I wish to thank in particular Elton and Bea, Gerta and Ayaz, Ivan and Sandra, Michale and Jonathan, Cristina and Geoff, Severine and Aymeric, Sonia and Luis, Katie and Juanma, Dennis, Emily, and Ian.

I am much indebted to many other people without whom this thesis would have taken much longer: Thomas and Rachel for heroic cloning, and everyone else in the DSTT; the mass spec team; Kirsten and Janice for tissue culture-related help; the media kitchen for keeping the yeast nicely fed; Judith for theatre reviews and help with immigration documents; and Louise, Allison B. and Allison S. for making sure my disorganisation did not mean that I did not have reagents with which to do experiments.

Last, but not least, I thank my family – Nexhi, Luan and Era – for trusting in me and for reminding me of the things that really matter. And I thank Ruze and Nebi Jaupaj for their wonderful love.

Summary

Obstacles such as DNA damage can block the progression of DNA replication forks. This is a major source of genome instability that can lead to cell transformation or death. The budding yeast *MMS1* and *MMS22* genes were identified in a screen for mutants that were hypersensitive to DNA alkylation that blocks replisome progression. I set out to investigate the cellular roles of these genes and found that cells lacking *MMS1* or *MMS22* are hypersensitive to a wide variety of genotoxins that stall or block replication forks, and are severely defective in their ability to recover from DNA alkylation damage. Homologous recombination (HR) is an important mechanism for the rescue of stalled or blocked replication forks and for the repair of double-strand breaks (DSBs). Strikingly, *MMS1* and *MMS22* are required for HR induced by replication stress but not by DSBs, and the underlying mechanisms were explored.

I next identified the uncharacterized protein C6ORF167 (MMS22L) as a putative human Mms22 orthologue. MMS22L interacts with NFκBIL2/TONSL, the histone chaperone ASF1 and subunits of the MCM replicative helicase. MMS22L colocalizes with TONSL at perturbed replication forks and at sites of DNA damage. MMS22L and TONSL are important for the repair of collapsed replication forks as depletion of MMS22L or TONSL from human cells causes DNA damage during S–phase and hypersensitivity to agents that cause fork collapse. These defects are consistent with the observations that MMS22L and TONSL are required for the efficient loading of the RAD51 recombinase onto resected DNA ends and for efficient HR. These data indicate that MMS22L and TONSL are novel regulators of genome stability that enable efficient HR.

Chapter I

1 Introduction

DNA damage occurs frequently in cells and can pose a serious threat to the stability and integrity of the genome. DNA can be damaged by cellular metabolites and DNA metabolic processes, as well as by exogenous DNA-damaging agents. If the ensuing DNA lesions are not repaired rapidly and efficiently, mutations or cell death can result. The cellular response to DNA damage is a complex network of processes that are responsible for detecting, signalling and repairing the various types of DNA lesions. The importance of the DNA-damage response is highlighted by the several human diseases, such as Fanconi anaemia and *Xeroderma pigmentosum*, that are caused by defects in DNA repair.

1.1 Types of DNA damage

DNA is constantly exposed to agents that can damage it. The various forms of DNA lesion and the pathways that repair them are summarised in Fig.1.1.

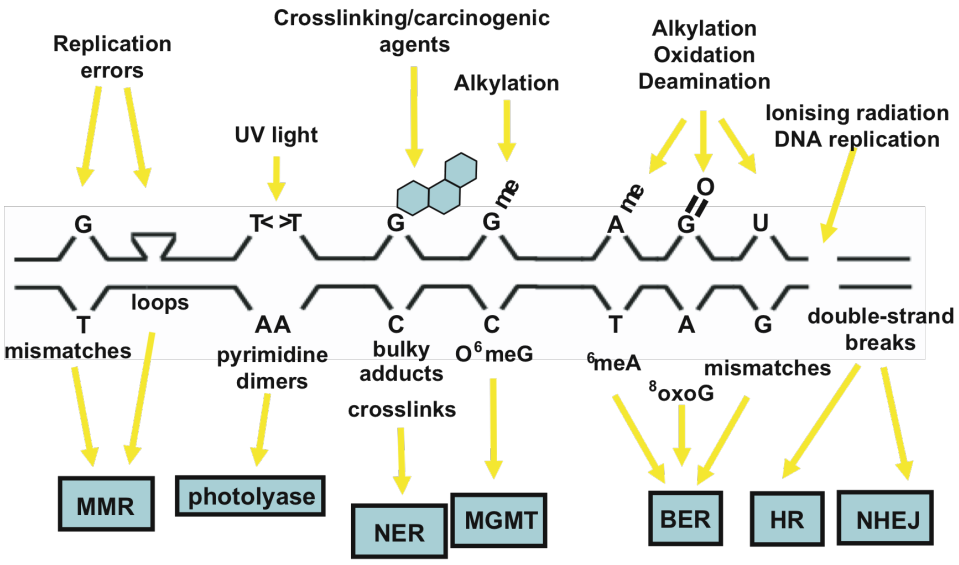

Figure 1.1 Overview of different forms of DNA damage and DNA repair.

DNA can be damaged by exogenous factors such as ultraviolet (UV) light, ionising radiation (IR) or by agents that cause DNA alkylation or cross-linking. DNA lesions can also arise due to replication errors, spontaneous DNA oxidation and deamination. Pathways or proteins responsible for repair of the different forms of DNA lesions are shown in blue boxes. (MMR: mismatch repair; NER: nucleotide excision repair; MGMT: O^6MeG DNA methyltransferase; BER: base excision repair; HR: homologous recombination; NHEJ: non-homologous end-joining).

1.2 DNA base damage

The functional groups of the DNA bases (see Fig. 1.2) make them highly reactive with the cellular environment, leading to different types of base damage (Lindahl, 1993). The majority of these lesions are caused by spontaneous, non-enzymatic chemical reactions including hydrolytic deamination, oxidation and alkylation of bases. For instance, spontaneous hydrolysis of the *N*-glycosyl bonds that link bases to the DNA sugar-phosphate backbone lead to loss of DNA bases, generating 'abasic' sites in the DNA. Bases can also spontaneously lose amine groups – a process known as deamination. Deamination thus converts cytosine to uracil and 5'-methylcytosines to thymine. At a much lower rate, adenine and guanine can also become deaminated to hypoxanthine and xanthine, respectively (Lindahl and Andersson, 1972). Further, DNA bases readily react with by-products and intermediates of cellular metabolism. Reactive oxygen species (ROS), for instance, can react with guanine to form 8-oxo-guanine, a substitution that can lead to mutation during DNA replication (Shibutani *et al.* 1991). S-adenosylmethionine is another metabolic intermediate that can readily donate alkyl groups to the nucleophilic centres in DNA bases, leading to lesions such as N^7-methylguanine and N^3–methyladenine, which impede replication fork progression (Beranek, 1990b; Sancar and Reardon, 2004). Ultraviolet (UV) light induces the formation of DNA 'photoproducts'. The most frequent photoproducts are cyclobutane pyrimidine dimers, which are formed by a UV-induced linkage between two adjacent pyrimidine bases on the same DNA strand. If left unrepaired, cyclobutane dimers can block DNA replication and transcription (Sancar et al., 2004; Sancar and Reardon, 2004; Seigneur et al., 1997).

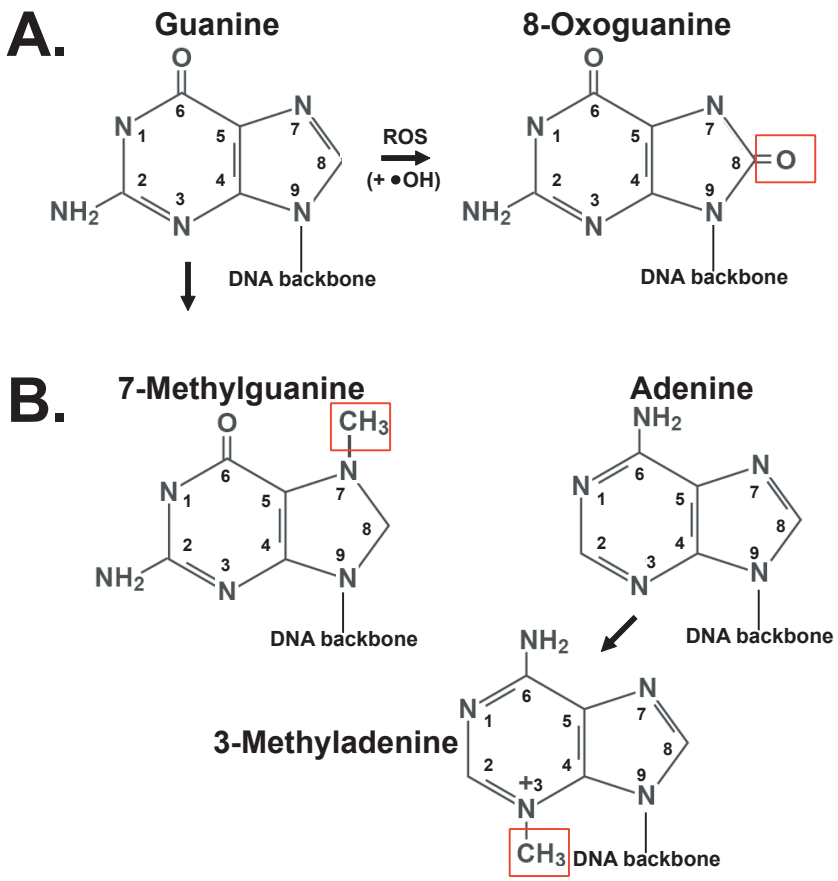
A.
Guanine
8-Oxoguanine
ROS
(+ •OH)
DNA backbone
DNA backbone
B.
7-Methylguanine
Adenine
DNA backbone
DNA backbone
3-Methyladenine
DNA backbone
C.
UV light
pyrimidine
dimer

Figure 1.2 Examples of different types of DNA base damage

(A) 8-oxo-guanine can be generated by the reaction of DNA with intracellular oxygen free-radical species.

(B) N^7-methylguanine and N^3-methyladenine are caused by alkylating agents that form covalent bonds with nucleophilic sites on DNA bases.

(C) Pyrimidine dimers form a four-membered ring structure between adjacent pyrimidines.

1.3 DNA base damage repair

1.3.1 Reversal of base damage

Certain DNA base lesions can be directly reversed. For example, in bacteria and yeast, UV-induced pyrimidine dimers can be directly reversed by photolyases (Sancar et al., 2004; Sancar et al., 1996). In humans, alkyl groups on guanines are removed by O^6MeG DNA methyltransferase (MGMT) (Scicchitano et al., 1986). For other lesions, the co-ordinated actions of groups of proteins are required for efficient repair.

1.3.2 Base excision repair

Base excision repair (BER) is the major pathway for the removal of modified DNA bases that cause little or no distortion to the DNA double helix and is thought to be the most frequent type of DNA repair event (Krokan et al., 2000). The excision of a damaged DNA base is initiated by a group of enzymes called DNA glycolyases. DNA glycolyases recognise, and bind to, specific types of base damage and then remove the damaged base by catalysing the hydrolysis of the *N*-glycosyl bond that links the modified base to the DNA sugar-phosphate backbone, resulting in an abasic site (Lindahl, 1976). Depending on the initial events in base removal, the repair patch may be a single nucleotide (short patch) or 2-10 nucleotides (long patch) (Frosina et al., 1996). When the base damage is removed by a glycolyase that cleaves the phosphodiester bond 3' to the abasic site, APE1 (apurinic/apyrimidinic endonuclease I) cleaves the phosphodiester bond 5' to the abasic site. Subsequently, POL β (DNA polymerase β) is recruited to fill in the one-nucleotide gap, which is then ligated by the LIG3 (DNA ligase 3)/XRCC1 complex (Beard and

Wilson, 2000; Matsumoto and Kim, 1995; Sancar et al., 2004). This pathway is termed short-patch BER. When the abasic site is generated by oxidative base loss or by spontaneous hydrolysis, repair usually proceeds through the long-patch pathway (Frosina et al., 1996; Klungland and Lindahl, 1997). APE1 cleaves the 5' phosphodiester bond, and DNA polymerases δ/ε carries out repair synthesis and nick translation, displacing several nucleotides (Frosina et al., 1996; Klungland and Lindahl, 1997). The flap structure is cleaved off by FEN1 endonuclease and the long-repair patch is ligated by DNA ligase 1 (Frosina et al., 1996; Klungland and Lindahl, 1997).

1.3.3 Nucleotide excision repair

Nucleotide excision repair (NER) can repair all forms of DNA base damage, including bulky DNA adducts that distort the DNA double helix, such as UV-induced lesions, and it also contributes to the removal of DNA intra- and inter-strand crosslinks (Dip et al., 2004; Reed, 2005). In humans, defects in NER cause the hereditary disease *Xeroderma pigmentosum* (XP) (Cleaver, 1968, 1969). XP patients are very sensitive to sunlight and are highly prone to skin cancer (Cleaver, 1968, 1969). The gene products mutated in XP patients are referred to as XPA to XPG and XPV, and were named after XP complementation groups that are all deficient in NER (Vermeulen et al., 1991).

In human cells there are two separate modes of NER: global genome repair (GGR) and transcription-coupled repair (TCR) (Nouspikel, 2009). TCR is selective for lesions that are present in the transcribed strand of expressed genes and is faster than GGR, which acts over the rest of the genome (Nouspikel, 2009). The main difference between the two

modes of NER is in lesion recognition. Operating in similar ways in both human cells and yeast, GGR starts with the recognition of local distortion caused by bulky lesions in the DNA double helix. This requires XPC-hHR23B in humans and Rad4-Rad23 in yeast (Costa et al., 2003; Dip et al., 2004; Reed, 2005). In humans, in the case of lesions that are poorly recognised by XPC-hHR23B, DDB1 and DDB2/XPE facilitate lesion recognition (Nouspikel, 2009). XPC-hHR23B is not required for TCR, where the signal for repair is thought to come from RNA polymerase II stalled at bulky lesions (Nouspikel, 2009). Two proteins, CSA and CSB, are required to remove the RNA polymerase to allow access of NER factors to the lesion (Nouspikel, 2009).

The recognition of lesions is followed by the formation of a pre-incision complex, an assembly of proteins that generates an unwound DNA structure around the lesion. Formation of the pre-incision complex results in the opening of DNA to create region of single-stranded DNA 24-32-nucleotides long. DNA unwinding requires the TFIIH complex, XPA (yeast Rad14) and RPA (Bankmann et al., 1992); (Friedberg, 2006). The bubble-like intermediate of unwound DNA is cleaved by structure-specific nucleases. XPG (Rad2) cleaves on the 3′ side of the damaged DNA and the ERCC1-XPF (Rad1-Rad10) enzyme cuts on the 5′ side (Friedberg, 2006). Following the incision the resulting patch is removed and the gap is filled in by DNA repair synthesis. The remaining nick is sealed by DNA ligase I (Prakash and Prakash, 2000); (Shivji et al., 1995).

1.4 Interstrand crosslinks

Certain chemotherapeutic drugs (e.g. cisplatin) and bifunctional DNA-damaging agents (e.g. mitomycin-C and nitrogen mustards) induce interstrand DNA cross-links (ICLs), i.e. the covalent linking of the two strands of the DNA helix (Noll et al., 2006). ICLs can also be induced by normal cellular metabolism, for instance by intermediates of lipid peroxidation (Marnett, 2000; Minko et al., 2008; Niedernhofer et al., 2003) and by cellular metabolites including activated estrogens (Dai and Liu, 2000). ICLs are extremely toxic lesions; it has been estimated that as few as twenty ICLs can be lethal to cells that lack the ability to remove the crosslink (Dronkert and Kanaar, 2001; Lawley and Phillips, 1996). In budding yeast several DNA repair pathways are involved in removing the crosslink – NER, homologous recombination and translesion synthesis (see below) (Henriques et al., 1997; Jachymczyk et al., 1981; McHugh et al., 2000). In mammalians, additional proteins are implicated in ICL repair, notably the proteins of the Fanconi anaemia (FA) complementation group; XPF and ERCC1 are the only NER protein involved (Moldovan and D'andrea, 2009). ICL repair can take place outside of S–phase (Akkari et al., 2000; Sarkar et al., 2006) but the major route for ICL repair probably occurs in S-phase, where ICL lesions would block the progression of the DNA replication machinery (Akkari et al., 2000; Rothfuss and Grompe, 2004; Taniguchi et al., 2002). Early during repair, the ICL must be ‘unhooked’, which requires incisions on either side of the ICL. One of these incisions is catalysed by the structure-specific nuclease MUS81-EME1 (Hanada et al., 2007; Hanada et al., 2006). The MUS81-EME1-catalysed incision generates a one-ended DSB that can be used to initiate HR. The identity of the nuclease that catalyses the second incision is yet to be elucidated. After unhooking, the resulting gap is filled in by a process termed ‘translesion synthesis’ where

specialised DNA polymerases are employed for replicating past the unhooked lesion (Knipscheer et al., 2009; Niedzwiedz et al., 2004). The unhooked ICL is then removed, but the identity of the enzyme responsible for this is yet to be firmly established (Wang, 2007). The DSBs generated by unhooking can then be resected to allow the initiation of HR to regenerate an intact replication fork. Successful HR repair also appears to depend on processing by the newly-identified FAN1 protein as well as by the SLX4 complex, which includes the scaffold protein SLX4 and the structure-specific nucleases XPF-ERCC1, MUS81-EME1 and SLX1 (Fekairi et al., 2009b; Munoz et al., 2009; Svendsen et al., 2009).

1.5 DNA single-strand breaks

DNA single-strand breaks (SSBs) are common DNA lesions. The hydroxyl groups of ROS can attack the sugars in the DNA backbone, causing both DSBs and SSBs. SSBs can also occur (often transiently) during cellular processes such as BER and DNA replication. Further, SSBs can be converted into double-strand breaks (section 1.1.6) during DNA replication. They are, thus, very deleterious lesions.

Detection and repair of SSBs involves poly(ADP-ribose) polymerase-1 (PARP-1), an enzyme with a very high affinity for SSBs. Following this binding, PARP-1 catalyses the formation of poly(ADP-ribose) polymers, causing the dissociation of PARP-1 from DNA (Dianov and Parsons, 2007). Poly(ADP-ribose) polymers facilitate chromatin remodelling, both by relaxing chromatin structure an by recruiting enzymes that catalyse nucleosome sliding (Ahel et al., 2009; Dianov and Parsons, 2007; Poirier et al., 1982). This chromatin remodelling probably facilitates the accessibility to repair factors.

PARP-1 and PARG-1 (poly(ADP-ribose) glycohydrolase) are thought to regulate the accumulation of XRCC1 at sites of oxidative DNA damage to maintain optimal levels of single-stranded DNA break repair (Fisher et al., 2007). SSBs that possess a 5'-deoxyribose phosphate are usually removed by the lyase activity of POL β after gap filling, followed by recruitment of the XRCC1-DNA ligase IIIα to seal the DNA ends (Caldecott, 2004). SSBs containing modified DNA ends of greater complexity, such as 5'-hydroxyl, 3'-phosphate, 3'-phosphoglycolate or adenylated 5'-phosphate require processing by factors such as polynucleotide kinase (PNK), APE1, flap endonuclease-1 (FEN1), tyrosyl-DNA phosphodiesterase (TDP1) and aprataxin, repectively (Caldecott, 2004). The restored termini can now be used for gap filling if necessary, in a reaction that requires POL β and other accessory factors such as PCNA (Fortini et al., 2000). Finally, DNA ligation, carried out by ligases such as DNA ligaseIIIα, completes SSB repair (Timson et al., 2000).

1.6 DNA double-strand breaks

DNA double-strand breaks (DSBs) pose a major threat to genome stability and cell viability. A single unrepaired DSB, for instance, can be sufficient to cause apoptosis (Rich et al., 2000) to lead to chromosomal translocations or to generate chromosomal abnormalities (van Gent et al., 2001). Despite their cytotoxicity, DSBs are induced in a controlled manner as part of many cellular processes. In yeast, for instance, a single DSB induced by the HO endonuclease initiates mating-type switching (Haber, 1998). In all kingdoms of life, meiotic recombination also requires the controlled induction of a DSB by the highly-conserved proteins SPO11 and MEI4 (Baudat et al., 2000; Keeney et al., 1999; Keeney et al., 1997; Kumar et al., 2010; Menees and Roeder, 1989; Romanienko

and Camerini-Otero, 1999, 2000). In mammals, DSBs are specifically induced during the rearrangements of the immunoglobulin loci in B cells and the T-cell receptor loci in T cells (Hoeijmakers, 2001; Khanna and Jackson, 2001). DSBs also arise in an uncontrolled manner in the cell, for example due to damage caused by ROS produced in the course of normal metabolism. Further, an estimated fifty DSBs occur in a single human cell during DNA replication when a replication fork encounters a nick in one strand of the DNA backbone (Saleh-Gohari et al., 2005a; Vilenchik and Knudson, 2003).

1.7 Repair of DNA double-strand breaks

Two main mechanisms operate to repair DSBs: non-homologous end joining (NHEJ) and homologous recombination (HR). NHEJ is an error-prone, ligation-based process that does not appear to be restricted to any particular cell-cycle stage (Lieber, 2010). HR relies on an intact DNA template for repair of a broken DNA strand. Thus, HR functions predominantly in the late S and G2 phases of the cell-cycle (Wyman et al., 2004).

1.7.1 Non-homologous end joining

Non-homologous end-joining (NHEJ) is a DSB repair mechanism used at all stages of the cell-cycle (Lieber, 2010). Cells defective in NHEJ show radiosensitivity (Rothkamm et al., 2003). As well as repairing unscheduled DSBs, NHEJ plays a crucial role in V(D)J recombination in developing B-cells and, as a result, defects in NHEJ cause severe combined immunodeficiency (Gu et al., 1997; Schwarz et al., 2003). NHEJ is often described as an ‘error-prone’ repair mechanism because in cases where ends cannot be

precisely joined DSB end-processing can lead to deletions at the break sites (Lieber, 2010).

NHEJ is highly conserved from bacteria to humans (Critchlow and Jackson, 1998). NHEJ is thought to proceed through the following steps: (i) detection of the DSB and tethering/protection of the DNA ends; (ii) DNA end-processing to remove damaged or non-ligatable groups; and (iii) DNA ligation. The first step of NHEJ involves binding of the heterodimer KU70/KU80 (yKu70/yKu80 in budding yeast) to the DSB ends (Turchi and Henkels, 1996). Binding of KU70/KU80 to DNA results in a conformational change in the flexible C-terminal regions of both Ku70 and Ku80, which is thought to facilitate the recruitment of other NHEJ proteins to the DSB (Lehman et al., 2008; Walker et al., 2001). In mammalian cells this includes the DNA-dependent protein kinase catalytic subunit (DNA-PKcs; absent in budding yeast), which with KU70/KU80 forms the DNA-PK holoenzyme. The binding of DNA-PK to DNA results in a large increase in the kinase activity of DNA-PK and related kinases (Gottlieb and Jackson, 1993).

DSBs are processed in order to remove lesions or non-ligatable groups and to produce the 5’ phosphate and 3’ hydroxyl groups that are necessary for ligation by all known DNA ligases. This processing step requires nucleolytic activities that resect the DNA ends. In yeast, end-processing requires the heterotrimeric nucleolytic complex Mre11-Rad50-Xrs2 (MRX), where the nuclease Mre11 provides the necessary catalytic function (Alani et al., 1989; Krogh and Symington, 2004; Paull and Gellert, 1998; Paull and Gellert, 1999; Raymond and Kleckner, 1993; Trujillo and Sung, 2001). The mammalian homologue of yeast MRX is MRE11-RAD50-NBS1 (MRN). Mre11 provides the

catalytic function – it is a manganese-dependent structure-specific nuclease with a preference for single/double-stranded DNA transitions (Krogh and Symington, 2004; Trujillo and Sung, 2001). Rad50 belongs to the structural maintenance of chromosomes (SMC) family of proteins; it may act to bridge sister chromatids in order to establish a proper architecture for NHEJ (Alani et al., 1989; Krogh and Symington, 2004; Paull and Gellert, 1998; Paull and Gellert, 1999; Raymond and Kleckner, 1993; Trujillo and Sung, 2001). The third component of the complex, yeast Xrs2 or human NBS1, interacts with MDC1, which binds to phosphorylated H2AX (Kobayashi et al., 2004; Kobayashi et al., 2002).

In yeast, MRX is required for NHEJ. In mammals, however, MRN does not seem to play an important role in NHEJ. Indeed, NBS1-null cells are normal for V(D)J recombination (Harfst et al., 2000; Yeo et al., 2000). Instead, NHEJ-related DSB processing in mammalian cells seems to require DNA-PK and one of its targets, Artemis (Moshous et al., 2001; Moshous et al., 2000). Artemis has nuclease activity that is stimulated by phosphorylation by DNA-PK (Ma et al., 2002). Consistent with this, human and mice cells deficient for Artemis are extremely sensitive to ionising radiation (Moshous et al., 2001; Moshous et al., 2000; Rooney et al., 2002). End-processing in mammalian cells has also been reported to require polynucleotide kinase, DNA polymerase μ and DNA polymerase λ (Chappell et al., 2002; Nick McElhinny et al., 2005). Once the DNA ends have been processed, they must be re-ligated to complete the repair. Ligation is carried out by DNA ligase IV (yeast Dnl4) (Frank et al., 1998; Grawunder et al., 1997; Grawunder et al., 1998; Schaer et al., 1997; Teo and Jackson, 1997; Wilson et al., 1997). DNA ligase IV exists in complex with XRCC4 (yeast Lif1) and XLF/Cernunnos (yeast

Nej1) (Ahnesorg et al., 2006; Critchlow et al., 1997; Herrmann et al., 1998; Revy et al., 2006; Valencia et al., 2001). XRCC4 has no known enzymatic activity, but rather acts as a scaffolding protein, facilitating the recruitment of other NHEJ proteins to the break (Critchlow et al., 1997; Grawunder et al., 1997). XLF serves to enhance the activity of DNA ligase IV towards non-compatible DNA ends at a subset of breaks (Gu et al., 2007).

1.7.2 Homologous recombination

Homologous recombination (HR) uses an intact homologous DNA template to accurately repair a DSB. This allows HR to restore DNA around the DSB to the sequence that it was before damage, a feature that distinguishes HR from the error-prone NHEJ. HR is crucial not only for the repair of DNA breaks, but also for the rescue of stalled or collapsed DNA replication forks, meiotic chromosome segregation and the generation of antibody diversity (Modesti and Kanaar, 2001; Moynahan and Jasin, 2010a).

Recombination can result in the physical exchange of DNA between strands of homologous sequence. The precise nature of the DNA transactions central to HR is not well understood, and several models have been proposed: the synthesis-dependent strand-annealing (SDSA) model (Haber, 1992), the Szostak (or double-strand break repair, DSBR) model (Szostak et al., 1982), and the break-induced replication (BIR) model (Kreuzer et al., 1995) (Fig. 1.3). However, certain steps remain central to each. First, a recombinogenic DNA substrate (e.g. a DSB or a gap) is generated either by specific enzymatic action (e.g. a SPO11-induced DSB in meiosis) or as a consequence of

genotoxic stress (e.g. ionizing radiation). Second, the 5' ends of the DSB need to be resected to yield single-strand 3' overhangs (Huertas, 2010). Third, a physical connection is generated between the recombinogenic substrate and an intact donor homologous duplex DNA template leading to the formation of heteroduplex (or hybrid) DNA. Fourth, contiguous DNA strands are restored by priming DNA synthesis from the invading 3′ end on the template DNA and resolving the ensuing DNA intermediates. HR is completed by DNA ligation to generate two intact duplexes.

Studies conducted two decades ago demonstrated 5' to 3' resection of DSB ends during HR (Sun et al., 1991; White and Haber, 1990). The ensuing ssDNA overhangs are crucial to the initiation of HR: they invade the donor duplex and initiate homology search (strand invasion), and their ends serve to prime DNA synthesis. 5' to 3' end resection of DSBs proceeds in two steps: an early step with limited resection, followed by a later step involving extensive resection that generates ssDNA. In the first step, resection is initiated by the MRE11 nuclease of the MRN complex (yeast MRX). MRN function requires the highly-conserved protein CtIP (budding yeast Sae2) (Huertas et al., 2008; Jazayeri et al., 2006; Myers and Cortez, 2006; Sartori et al., 2007). MRN and CtIP remove 50-100 nucleotides from the 5'end as well as any protein adducts that would render the DNA ends resistant to exonuclease action (Mimitou and Symington, 2008; Mimitou and Symington, 2009a; Mimitou and Symington, 2009b). The DNA ends created by MRN and CtIP are then resected processively and extensively by the concerted action of BLM (Sgs1) helicase, the essential helicase/nuclease DNA2 (Dna2) and EXO1 (Exo1) (Bae et al., 2008; Bolderson et al., 2010; Gravel et al., 2008; Mimitou and Symington, 2008; Nimonkar et al., 2008; Zhu et al., 2008).

The long 3' ssDNA tails that are exposed by this second phase of resection are coated by RPA, which has a high affinity for ssDNA (Iftode et al., 1999). RPA binding prevents the formation of any DNA secondary structures that may interfere with the subsequent steps of HR. In order to become competent for strand invasion, ssDNA overhangs have to be coated by one of the proteins belonging to the highly evolutionarily-conserved RecA/RAD51 family of core recombinases, which are found in prokaryotes (RecA), archae (RadA) and eukaryotes (budding yeast Rad51; mammalian RAD51) (Ogawa et al., 1993; Shinohara et al., 1993; Shinohara et al., 1992; Symington, 2002).

To bind ssDNA, RAD51 must first remove RPA from ssDNA; this requires accessory factors termed 'mediators', such as Rad52 in yeast or BRCA2 and RAD51 paralogues in mammalians (Table 1.1) (Symington, 2002). Mediators assist the formation of the RAD51-ssDNA nucleoprotein filament (Krogh and Symington, 2004; Symington, 2002). Although RAD51 can form filaments on both dsDNA and ssDNA, it is only the RAD51-ssDNA filament that is functionally relevant (Sung and Robberson, 1995). Non-productive RAD51-dsDNA filaments are disrupted by the action of the Snf2-family chromatin remodelling protein RAD54 (Rad54) (Li et al., 2007; Solinger et al., 2002). The RAD51-ssDNA nucleoprotein filament is responsible for strand invasion, homology search and strand exchange (Arnaudeau et al., 1999; Ogawa et al., 1993; Shinohara et al., 1992; Sung, 1994; Sung and Robberson, 1995). RAD51-ssDNA binds the donor dsDNA and disrupts the base-stacking in the donor duplex, thereby freeing one of the donor strands for complementary base pairing with the ssDNA substrate (Chen et al., 2008b; Davies and Pellegrini, 2007; Pellegrini et al., 2002). The local B-DNA-like conformation forces homology search to proceed strictly via Watson-Crick base pairing. The annealing

of the invading strand to the homologous sequence of the duplex DNA is termed 'displacement loop' ('D-loop'). After D-loop formation, DNA synthesis extends the annealed 3' end using the information from the intact DNA template – D-loop extension (Fig. 1.3). It is unclear which polymerase(s) mediates D-loop extension *in vivo*. However, a role for the translesion synthesis polymerase polη in the process has been suggested by work in DT40 and mammalian cells (Kawamoto et al., 2005; McIlwraith et al., 2005; McIlwraith and West, 2008). The molecular details of the steps following D-loop formation are less clear; the three models are detailed below.

In the SDSA model the newly synthesised strand is displaced from the donor sequence after repair synthesis. The displaced strand anneals to the 3' end of the original DSB, and is used as a template for repair synthesis of the other 3' end (see Fig. 1.3). The reaction is completed by ligation of the nicks and results in non-crossover products (Fig. 1.3).

The Szostak model (Szostak et al., 1983) involves a two-end strand invasion mechanism in which the displaced strand of the donor DNA (after the strand invasion of the 3' end) anneals to the free 3' end of the damaged chromosome (Fig. 1.3). The second end of the break is engaged by either second-end capture through DNA annealing, or through a second invasion event. Second-end capture has been shown to require RAD52, but not RAD51. Indeed, *in vitro* data have shown that both yeast and human RAD52 facilitate second-end capture by annealing a resected RPA-coated DNA break to the joint-molecule product of the first strand-invasion event (Grimme et al., 2010; McIlwraith and West, 2008; Miyazaki et al., 2004; Mortensen et al., 1996; Nimonkar et al., 2009; Sugiyama et al., 2006). Repair DNA synthesis can proceed from the captured second end

(McIlwraith and West, 2008). Following repair synthesis, the resulting nicks are ligated. This second-end capture mechanism leads to the formation of two four-stranded DNA (Holliday) junctions (Fig. 1.3). Holliday junctions (HJs) resolution probably involves different nucleases in different organisms: Mus81 in fission yeast (Boddy et al., 2001), Mus81 and Yen1 in budding yeast (Ip et al., 2008; Jessop et al., 2008; Oh et al., 2008), and SLX1-SLX4 and GEN1 in humans (Andersen et al., 2009; Fekairi et al., 2009a; Ip et al., 2008; Munoz et al., 2009; Rass et al., 2010; Saito et al., 2009; Svendsen et al., 2009). HJ can be resolved to yield either non-crossover or crossover products. The latter are crucial to meiotic chromosome segregation (Keeney et al., 1997; Schwacha and Kleckner, 1995, 1997); the former are more beneficial to mitotic HR. Alternatively, HJs can be dissolved to yield non-crossover products. HJ dissolution is performed by the helicase-topoisomerase complex BLM-TopoIIIα (yeast Sgs1-Top3) or the helicase FANCM (yeast Mph1) (Prakash et al., 2009).

The break-induced replication (BIR) model describes HR in those cases where only one end of the DSB can engage in recombination. This can be either because the DSB is one-ended (e.g. at broken replication forks) or because homology with only one end is available (e.g. if the DSB occurs in generally non-homologous sequences) (Haber, 1999); (Lundblad and Blackburn, 1993). The first steps of BIR are thought to be very similar to those of the Szostak model (see above), and include Rad51 filament formation, homology searching and strand invasion (Davis and Symington, 2004; Malkova et al., 2005a). The important difference lays in the absence of a second end that can either capture the first newly-synthesized strand or invade the donor sequence independently. Without second-end capture, the initial strand invasion intermediate is imagined to be

turned into a unidirectional DNA replication fork, capable of both leading and lagging strand synthesis (Bosco and Haber, 1998; Davis and Symington, 2004; Kraus et al., 2001b; Malkova et al., 1996; Malkova et al., 2005b; Morrow et al., 1997; Smith et al., 2007; Voelkel-Meiman and Roeder, 1990). This recombination-dependent DNA replication may extend to the very end of the template chromosome; alternatively, it could be terminated upon meeting a converging replication fork.

1.7.2.1 Regulation of HR

The main pathways for DSB repair are NHEJ and HR. Research in the last decade has shown that the choice of the pathway to be employed for DSB repair is influenced primarily by the cell-cycle stage. HR is restricted to the S and G2 phases of the cell-cycle by CDK-mediated phosphorylation of HR proteins. The resection step represents a major target of such regulation (Aylon et al., 2004; Huertas et al., 2008; Huertas and Jackson, 2009; Ira et al., 2004; Sartori et al., 2007; Yun and Hiom, 2009). Studies on human cells, avian DT40 cells and budding yeast show that CtIP/Sae2 are specifically phosphorylated in a CDK-dependent fashion upon entry into S-phase. Budding yeast Sae2 is phosphorylated on a single CDK site, whereas vertebrate CtIP is phosphorylated on two sites (Huertas et al., 2008; Huertas and Jackson, 2009; Sartori et al., 2007; Yun and Hiom, 2009). Phosphorylation of CtIP promotes its interaction with BRCA1, thereby promoting HR specifically at S and G2 phases (Huertas and Jackson, 2009; Yun and Hiom, 2009).

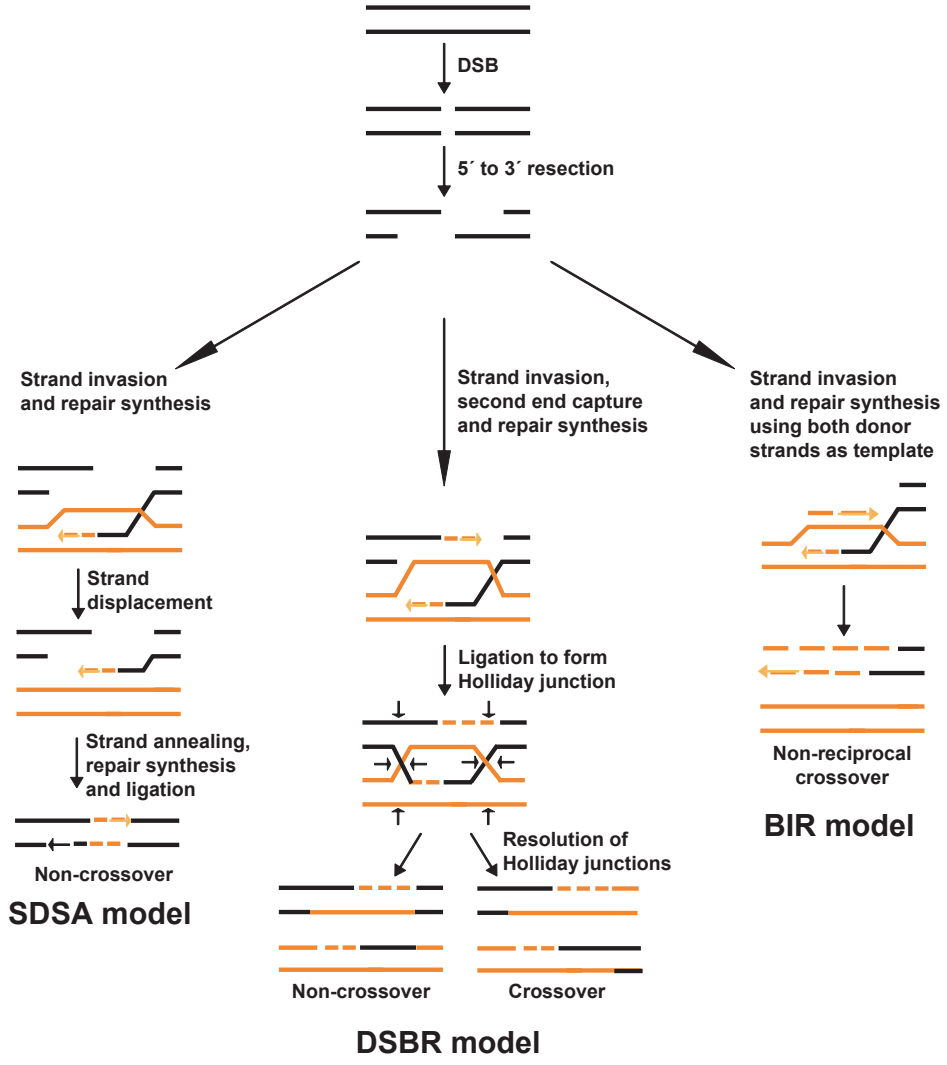

Figure 1.3 Different models for DSB repair by HR.

After DSB induction both DNA ends are resected to yield single-stranded 3' overhangs. Three models exist for the processing of these 3' ends to repair DSB: synthesis-dependent strand-annealing (SDSA) results in non-crossovers. The Szostak model involves a two-end strand invasion mechanism. This leads to the formation and resolution of Holliday junctions resulting in crossover or non-crossover products. The third model is break-induced replication (BIR), which engages a one-ended recombination event and replication for repair.

Role	Sc	Hs
Resection	Mre11-Rad50-Xrs2	MRE11-RAD50-NBS1
Resection	Sae2	CtIP
Resection	Sgs1-Dna2	BLM-DNA2
ssDNA binding	Rfa	RPA
Strand exchange	Rad51	RAD51
Annealing/second-end capture	Rad52	RAD52
Mediator	-	BRCA2
Mediator	Rad55-Rad57	RAD51B-RAD51C
		RAD51D-XRCC2
		RAD51C-XRCC3
Branch migration	Rad54	RAD54
HJ resolution	Yen1	GEN1
HJ resolution	Mus81-Eme1	MUS81-EME1
HJ resolution	Slx1-Slx4	SLX1-SLX4
HJ dissolution	Sgs1-Top3	BLM-TOPIIIα

Table 1.1 Homologous recombination factors in budding yeast (*Sc*) and humans (*Hs*).

BRCA1 is thought to ubiquitylate CtIP, thereby stimulating its resection activity (Yu et al., 2006). 53BP1, on the other hand, somehow counteracts CtIP-mediated end-resection, thereby favouring NHEJ (Bouwman et al., 2010; Bunting et al., 2010). Experiments conducted in mammalian cells have shown that cell-cycle-dependent phosphorylation also regulates other steps of HR downstream of resection. BRCA2 is a target for CDK phosphorylation on the S3291 residue of it carboxy terminus, which interacts directly with RAD51 (Esashi et al., 2005). This modification disrupts the interaction between the carboxy terminus of BRCA2 and RAD51, thereby abolishing HR. BRCA2 phosphorylation on its S3291 residue peaks in mitosis, but decreases in S and G2 phases, and this helps to restrict HR to S and G2 phases of the cell-cycle.

The mechanisms that act to restrict HR to S and G2 phases ensure that NHEJ is out-competed by HR when a sister chromatid is available, thereby promoting a repair pathway that preserves genetic information.

1.8 Single-strand annealing

An alternative recombination pathway that can occur if a DSB occurs between direct repeats is single-strand annealing (SSA) (Haber, 2006). The first step in SSA, like in NHEJ and HR, is 5'-to-3' end-resection, catalysed by the MRN complex (yeast MRX) and EXO1 (yeast Exo1). In the case of SSA, resection is particularly extensive. Resection starts adjacent to the break and extends past the repeats, thus yielding complementary single-strand overhangs. Following the coating of the single-strand overhangs by RPA, the complementary single-stranded sequences simply anneal with each other, in a reaction catalysed by RAD52 and RAD59 (Helleday, 2003) (Fig. 1.3). The non-

complementary tails that are left behind as 3´ single-strand tails are cleaved by the endonucleas ERCC1/XPF (budding yeast Rad1/Rad10) (Al-Minawi et al., 2008; Ivanov and Haber, 1995; Zhang et al., 2007), a reaction facilitated by Slx4 in budding yeast (Andersen et al., 2009; Fekairi et al., 2009a; Flott et al., 2007; Li et al., 2008a; Munoz et al., 2009; Svendsen et al., 2009; Toh et al., 2010). The remaining single-stranded gaps are then filled in by new DNA synthesis and ligated. Thus, SSA results in deletion of one copy of the repeats and all of the intervening sequence (Paques and Haber, 1999). Despite the accompanying loss of genetic information, work in both yeast and mammalian cells suggests that SSA is a frequent repair event between repetitive sequences (Liang et al., 1998). Since a large proportion of mammalian genomes consist of repetitive sequences, e.g. Alu sequences (Batzer and Deininger, 2002; Schmid, 1996), SSA may frequently be used in the repair of DSBs within these areas. It must also be borne in mind, however, that some of these repetitive sequences in the human genome display high sequence diversity (Smit, 1996), which greatly reduces the efficiency of SSA (Elliott et al., 2005; Sugawara et al., 2000).

1.9 The DNA-damage response

When DNA lesions persist or reach a certain threshold, the cell launches the DNA-damage response (DDR) in order to maintain genome stability (Rouse and Jackson, 2002a). The DDR involves recognition of persistent lesions by ‘sensors’ that relay signals to ‘transducers’, ‘mediators’ and ‘effectors’ via a protein kinase cascade (Fig. 1.4 and Table 1.2). It is important to note that there is no absolute demarcation between these various components, since some can function both as sensors and as transducers. The

DDR has a wide range of effects on transcription, protein stability and enzyme activity. Ultimately, the DDR mediates outcomes such as arrest or slowing of cell-cycle progression and an increased capacity to repair DNA lesions (Sancar et al., 2004). Over the years, many genes that are important players of the DDR have been identified; some of them are summarized in Table 1.2. Defects in the DDR can increase cellular mutation rates, and cause genome instability and cancer (Nyberg et al., 2002).

1.9.1 The DNA-damage response in budding yeast

The key proteins of the DDR in budding yeast are the kinases Mec1 and Tel1. *MEC1* (meiotic entry checkpoint 1) was isolated as a mutant sensitive to both MMS and UV light (Kato and Ogawa, 1994; Lydall et al., 1996; Weinert et al., 1994). Tel1 was initially isolated as a telomere length mutant (Lustig and Petes, 1986). Mec1 and Tel1 are members of the phosphatidylinositol 3-kinase-like (PIKK) family of kinases, so named because they contain motifs typical of the phophatidylinositol 3-kinase (PI3-kinase) family (Lovejoy and Cortez, 2009).

Deletion of *MEC1* results in loss of cell viability (Kato and Ogawa, 1994; Weinert et al., 1994). This may be due to its involvement in regulating cellular dNTP levels, since it can be rescued by artificially elevating dNTP levels (Desany et al., 1998; Zhao et al., 1998). Even though elevated dNTP pools rescue lethality of *mec1*Δ cells, these cells still have major defects in the DDR. For example, cells are extremely sensitive to a range of genotoxins, show loss of telomeric silencing, gross chromosomal instability and other defects in DNA replication and major defects in checkpoints (Kato and Ogawa, 1994; Weinert et al., 1994; Zhao et al., 1998); (Craven and Petes, 2000); (Santocanale and

Diffley, 1998a). Mec1 kinase-deficient mutants are indistinguishable from *mec1*Δ cells, indicating that the Mec1 kinase domain is required for all known Mec1 functions, including cell viability and proper DNA-damage responses (Paciotti et al., 2000a). Mec1 plays a key role in replication fork stability, as demonstrated by increased breakage at 'replication slow zones' caused by abolishing Mec1 function (Cha and Kleckner, 2002a).

A *tel1* deletion mutant is viable and does not exhibit vastly increased sensitivity to DNA damaging agents (Morrow *et al.*, 1995). Tel1 appears to function redundantly with Mec1 in repair of DNA damage, because *tel1*Δ*mec1*Δ double mutants are more sensitive to DNA damaging agents than *mec1*Δ mutants, and most other phenotypes of *tel1*Δ or *mec1*Δ single mutants are also enhanced in *mec1*Δ*tel1*Δ double mutants (Morrow *et al.*, 1995; Sanchez *et al.*, 1996).

Sensors

Sensor proteins recognize DNA damage and facilitate the activation of Mec1 and Tel1 to trigger the DDR. Tel1 is recruited to DSB ends through its interaction with the DNA-binding complex MRX, Mre11-Rad50-Xrs2 (Nakada et al., 2003). Mec1 is recruited to sites of damaged DNA via its interaction with Ddc2 (Paciotti et al., 2000a; Rouse and Jackson, 2000, 2002c; Wakayama et al., 2001). Ddc2 is thought to recognize RPA-bound ssDNA (Carr, 2002; Sogo et al., 2002). An important target of Mec1/Tel1 is the histone H2A. Phosphorylation of H2A at sites of DNA damage amplifies the DNA damage signal and recruits different chromatin remodelling complexes, resulting in the chromatin reconfiguration that is necessary for efficient DNA repair (Downs et al., 2004).

Two other protein complexes are involved in sensing DNA damage. One of them is the replication factor C -like (RFC-like) complex, which consists of the Rad24 checkpoint protein and the four small RFC subunits, Rfc2-5 (Griffiths et al., 1995); (Fairman and Stillman, 1988; Tsurimoto and Stillman, 1989) (section 1.3). The proteins of the second complex, Rad17, Ddc1 and Mec3, show sequence similarity to PCNA (Venclovas and Thelen, 2000). The precise function of the RFC-like and PCNA-like complexes is still unclear, but it is assumed that these factors promote checkpoint activation by somehow sensing DNA damage directly. It is interesting to note that the co-localisation of sensors is sufficient to activate DDR in yeast, suggesting that DNA can be viewed as a platform to increase the local concentrations of complexes involved in DDR (Bonilla et al., 2008; Majka et al., 2006).

Transducers

The transducer proteins in budding yeast DDR include Rad53 and Chk1. The Rad53 protein kinase is activated by DNA damage in a Mec1/Tel1-dependent way and plays an essential role in many aspects of the DDR (Sun et al., 1996). Several other proteins also become rapidly phosphorylated in a Mec1/Tel1-dependent manner in response to DNA damage (Rouse and Jackson, 2002).

Mediators

Mediators are an important group of proteins involved in the DDR that associate with damage sensors and signal transducers at certain phases of the cell cycle and that help to mediate phosphorylation of some downstream targets. Mediators facilitate DDR kinases: they promote their activation, regulate substrate access and control their associations with

damaged DNA. The budding yeast Rad9 protein is the prototype mediator and is involved in activation of Rad53 by Mec1. During checkpoint activation, the phospho-threonine-binding FHA domains of Rad53 interact with Mec1/Tel1-phosphorylated Rad9. This leads to catalytic activation of Rad53 and extensive Rad53 autophosphorylation (Durocher et al., 2000); (Sun et al., 1998); (Gilbert et al., 2001). It is thought that following replication stress activation of Rad53 requires the Mrc1 mediator instead of Rad9 (Alcasabas et al., 2001). Mrc1also needs to be phosphorylated by Mec1 to be able to activate Rad53 (Osborn and Elledge, 2003). Like Rad53, Chk1 also requires Rad9 for its activation (Blankley and Lydall, 2004).

Effectors

There are many different effectors in the DDR, including DNA repair proteins, chromatin components, transcriptional regulators and proteins involved in cell-cycle transitions.

1.9.2 The DNA-damage response in mammals

DDR in mammals is similar to that in yeast – it consists of damage sensors, transducers, mediators and effectors – and is mediated by evolutionarily conserved proteins (see Table 1.2). The Tel1 and Mec1 homologues in mammalians are ataxia telangiectasia mutated (ATM) and ataxia telangiectasia and Rad3 related (ATR) respectively (Morrow et al., 1995; Sanchez et al., 1996). DNA-dependent protein kinase (DNA-PK) is a third PIKK kinase that is of central importance to DDR in mammals, but absent in yeast. Like Mec1 and Tel1, ATM, ATR and DNA-PK are members of the PIKK family of kinases. The role of DNA-PK in cells is thought to be restricted to controlling NHEJ. ATR and

ATM, on the other hand, are vitally important for the general maintenance of genome stability. Both kinases are thought to function as DNA damage sensors as well as signal transducers (Abraham, 2001, 2004; Carr, 2002; Falck et al., 2005; Lovejoy and Cortez, 2009; Rouse and Jackson, 2002b).

ATM is involved primarily in the response to DSBs (Andegeko et al., 2001) and it was identified by positional cloning of the gene mutated in ataxia-telangiectasia (AT) (Savitsky et al., 1995a; Savitsky et al., 1995b). AT is characterized by clinical radiosensitivity, cancer predisposition, cerebellar degeneration, and immunodeficiency (Shiloh, 2003). At the cellular level, AT cells show high levels of genome instability, a high degree of IR sensitivity, a major DSB repair defect and increased chromosome fusions (Meyn, 1993; Pandita et al., 1995). In contrast to ATM, ATR is activated in response to a wide variety of types of DNA damage including single stranded DNA, UV damage and stalled DNA replication forks (Helt et al., 2005; Ward et al., 2004). ATR is also activated in an ATM-dependent manner in response to DSBs in the S and G2 cell cycle phases (Cuadrado et al., 2006; Jazayeri et al., 2006; Myers and Cortez, 2006). ATR was originally identified, based on sequence similarity in the protein kinase domain, as a homologue of fission yeast Rad3, whose gene product plays a critical role in sensing DNA structure defects and activating damage-response pathways (Bentley et al., 1996; Cimprich et al., 1996). ATR gene disruptions in mice causes embryonic lethality, and loss of ATR is also lethal in somatic cells (Brown and Baltimore, 2000, 2003). A splicing mutation that drastically reduces expression of ATR results in a human disorder, Seckel syndrome, with symptoms somewhat similar to AT (O'Driscoll et al., 2003).

ATR and ATM bind rapidly to sites of DNA damage (Tibbetts et al., 2000). ATM recruitment requires the NBS1 protein (Falck et al., 2005). ATR is recruited to sites of DNA damage by ATRIP, the ATR-associated protein (Falck et al., 2005) in part by the ability of ATRIP to bind RPA-coated ssDNA (Cortez et al., 2001; Zou and Elledge, 2003a; Zou et al., 2003). Translocation of ATM and ATR to sites of DNA damage results in phosphorylation of a range of proteins on Ser/Thr residues that are followed by a Gln, referred to as S/T-Q motifs (Shiloh, 2003; Traven and Heierhorst, 2005).

As for yeast Mec1 and Tel1, ATM- and ATR-mediated phosphorylation of a number of substrates requires the presence of mediator proteins; for example, activation of ATR kinase activity is dependent on the presence of the ATRIP-interacting protein TopBP1 (Mordes and Cortez, 2008). BRCT (BRCA1 C-terminal) domain-containing proteins facilitate phosphorylation-dependent interactions with other damage-responsive proteins (Stucki et al., 2005; Yu et al., 2003). BRCT domains are found in a number of DNA-damage response mediator proteins such as the Rad9 orthologues BRCA1, MDC1, PTIP, 53BP1 as well as TopBP1 (Goldberg et al., 2003; Jowsey et al., 2004; Mordes and Cortez, 2008; Schultz et al., 2000; Scully et al., 1997; Stewart et al., 2003a; Yamane et al., 2002).

The transducers in the mammalian DDR include CHK1 and CHK2. They become activated by ATM/ATR-dependent phosphorylation, and in turn phosphorylate DDR proteins (Shiloh, 2003). Unbiased screens for substrates of DDR kinases conducted in mammalian cells have shown that effectors of the mammalian DDR include proteins involved in cell-cycle regulation, DNA repair, transcription, chromosome segregation,

RNA splicing and nonsense-mediated decay (Matsuoka et al., 2007). This points to the broad role of DDR in many aspects of cellular physiology.

1.9.3 DNA damage checkpoints in yeast

DNA damage checkpoints are biochemical pathways that delay or arrest cell-cycle progression, thus giving the cell the opportunity to repair the damage (Hartwell and Weinert, 1989; Weinert and Lydall, 1993a; Weinert and Lydall, 1993b). In budding yeast, the existence of a G1-checkpoint has been challenged, but a Mec1-dependent G1 delay in response to IR has been observed (Neecke et al., 1999; Siede et al., 1996). Swi6, a subunit of the Swi4/Swi6 complex, which activates transcription specifically in late-G1, is a substrate of Rad53 in the G1-checkpoint (Sidorova and Breeden, 1997, 2003). Rad53-dependent phosphorylation of Swi6 delays the transition to S-phase by inhibiting transcription of the genes *CLN1* and *CLN2.* These genes encode for the cyclins Cln1 and Cln2 that associate with, and activate, the cyclin-dependent kinase (Cdk) promoting the G1-S transition (Sidorova and Breeden, 1997, 2003).

Activation of Mec1 by stalling of DNA replication forks or by DNA damage causes an intra-S-phase checkpoint (Fig. 1.5). Activation of the intra-S-phase checkpoint is probably the most important function of Mec1 and Rad53 in protecting cells against genotoxic insult. It is discussed in more detail in section 1.11.

Role	Sc	Hs	Type
Sensor	Ddc1	RAD9	PCNA-like
Sensor	Rad17	RAD1	PCNA-like
Sensor	Mec3	HUS1	PCNA-like
Sensor	Rad24	RAD17	RFC-like
Sensor	Rfc2-5	RFC2-5	RFC component
Sensor	Rfa1/2	RPA	ssDNA binding
Mediator	Rad9	53BP1	
Mediator		BRCA1	BRCT-domain
Mediator		MDC1	BRCT-domain
Mediator	Dpb11	TopBP1	BRCT-domain
Mediator	Mrc1	Claspin	
Mediator	Tof1	Timeless	
Sensor/transducer	Mec1	ATR	PI3K-like kinase
Sensor/transducer	Ddc2	ATRIP	ATR-binding
Sensor/transducer	Tel1	ATM	PI3K-like kinase
Transducer/effector	Chk1	CHK1	Kinase
Transducer/effector	Rad53	CHK2	Kinase
Multiple	Mre11	MRE11	Nuclease
Multiple	Rad50	RAD50	MRX/MRN complex
Multiple	Xrs2	NBS1	MRX/MRN complex
Effector		p53	Transcription factor
Effector	Cdc25	Cdc25A-C	Phosphatase

Table 1.2 Overview of DNA-damage response proteins in *Saccharomyces cerevisiae (Sc)* and humans (*Hs*).

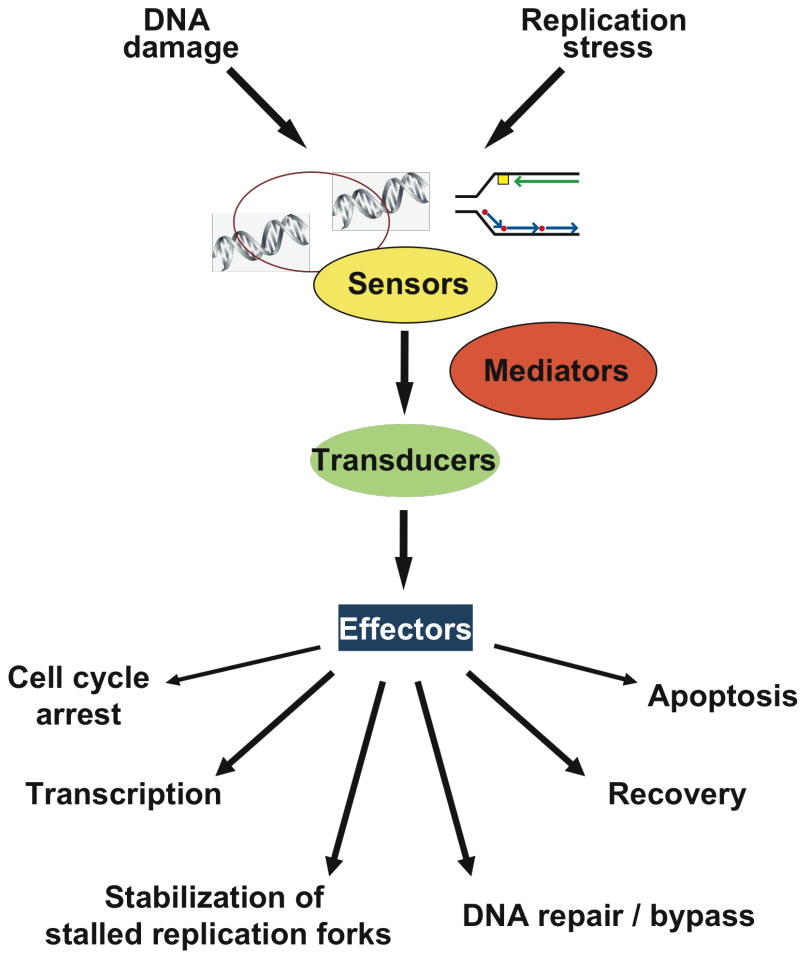

Figure 1.4 Summary of the cellular DNA-damage response.

DNA damage and replication stress are recognised by sensor proteins and result in the activation of a signal-transduction pathway consisting of transducer kinases, mediator and effector proteins. Outcomes of the DDR involve cell-cycle arrest, changes in transcription levels, stabilisation of stalled replication forks, DNA repair, DNA damage bypass, recovery and apoptosis.

In budding yeast, arrest at the G2/M-checkpoint occurs at the metaphase/anaphase transition. The anaphase-inhibitor protein Pds1, securin, is hyper-phosphorylated in a Mec1-, Rad9-, and Chk1-dependent manner in response to DNA damage (Ciosk et al., 1998); (Cohen-Fix and Koshland, 1997). In a normal cell cycle, Pds1 is degraded at the entry into mitosis, but DNA damage causes stabilization of Pds1, as its phosphorylation prevents its degradation, thus blocking entry into mitosis (Sanchez et al., 1999).

1.9.4 DNA damage-induced cell-cycle checkpoints in mammalian cells

Like in yeast, mammalian cells have three main DNA damage-induced cell-cycle checkpoints: the G1-S and intra-S-phase checkpoints, which regulate transition into and progression through S-phase following DNA damage, and the G2-M checkpoint, which regulates entry into mitosis following DNA damage (Niida and Nakanishi, 2006; Sancar et al., 2004).

The G1-S checkpoint is mediated primarily through an ATM-CHK2-p53-p21-CDK2 pathway (Kastan and Bartek, 2004). In unchallenged conditions, the phosphatase CDC25A promotes G1-S transition by dephosphorylating CDK2. Dephosphorylated CDK2 can then phosphorylate downstream targets such as Rb and CDC45 (Falck et al., 2001), events required to initiate G1-S transition (also see section 1.3). Following DNA damage, ATM is activated and phosphorylates CHK2 kinase (Shiloh, 2003). CHK2 phosphorylates CDC25A resulting in its ubiquitination and subsequent proteosomal degradation, thereby abolishing CDK2 activation (Falck et al., 2001). ATM and CHK2 have also been shown to phosphorylate the tumour suppressor p53 (Banin et al., 1998; Canman et al., 1998; Chehab et al., 2000; Chehab et al., 1999). The phosphorylation of

p53 acts to increase p53 protein levels. Further, p53 phosphorylation enhances its ability to stimulate the transcription of genes with p53-responsive elements, such as the CDK inhibitor p21 (Dornan et al., 2003; Schon et al., 2002; Tang et al., 2008); (el-Deiry et al., 1993; Kastan and Bartek, 2004). The p21 protein inhibits CDK2, preventing it from phosphorylating its downstream targets, an event that is required for G1-S transition (Dasika et al., 1999). Many cancer cells are mutated in p53 and hence lack the G1-S checkpoint; targeting the G2/M checkpoint to sensitize tumours has emerged as a promising anti-cancer strategy (Kawabe, 2004; Koniaras et al., 2001; Tse et al., 2007).

The intra S-phase checkpoint activated by DNA damage causes a transient, reversible delay in cell cycle progression, mainly by inhibiting new replicon initiation. Two parallel pathways mediate the intra-S-phase checkpoint (Falck et al., 2002). The first, the ATM - CHK2-CDC25A-CDK2 pathway, is similar to that described for the G1-S checkpoint (Lukas et al., 2004) except that the ATR-CHK1 pathway also becomes activated in response to breaks during S-phase (Cliby et al., 1998; Zou and Elledge, 2003a). The second pathway involves phosphorylation of SMC1 (structural maintenance of chromosomes-1) by ATM and this phosphorylation event is required for the downregulation of DNA replication (Bartek et al., 2004), although the underlying molecular mechanisms are unclear.

The G2-M checkpoint initially manifests as a rapid reduction in the proportion of mitotic cells, and the accumulation of cells with a 4N content of DNA (Fernandez-Capetillo et al., 2002). CHK1 and CHK2 are phosphorylated by ATM and ATM-ATR, respectively,

following exposure to IR. CHK1 is critical for the G2-M checkpoint (Liu et al., 2000; Zhao et al., 2002), whereas CHK2 is only required for cells that are already in G2 to delay mitosis (Rainey et al., 2008). ATM also phosphorylates and inactivates MDM2, a negative regulator of p53 (Maya et al., 2001). Stabilized p53 can then upregulate transcription of p21 and 14-3-3σ (Niida and Nakanishi, 2006). 14-3-3σ binds to CDK1-cyclin B1 and sequesters it in the cytoplasm (Chan et al., 1999). p21 inhibits the CDK2-cyclin A and CDK4/6 complexes, which will result in the inhibition of E2F-dependent transcription via Rb (Cann and Hicks, 2007). Important G2-M regulators targeted by E2F include CDK1, cyclin A, cyclin B1 and cyclin B2 (DeGregori, 2002). Interestingly, cells exposed to UV rather than IR also require the p38 kinase and the p38 substrate kinase MAPKAP-K2 for G2/M arrest (Bulavin et al., 2001; Manke et al., 2005).

1.10 DNA replication

The integrity of DNA is vital to faithful transmission of genetic information from mother to daughter cell. Faithful inheritance also requires the timely, complete and accurate replication of the genome once and only once per cell cycle. The general molecular mechanism of DNA replication is highly conserved between species, as are the protein complexes involved therein. DNA replication initiates from *cis*-acting sequences termed 'origins of replication', which are distributed throughout the eukaryotic genome. Origins of replications are defined by the binding of proteins that 'license' origins so they are competent to initiate DNA replication (Blow and Tada, 2000).

In yeast, origins of replication, also known as autonomously-replicating sequences (ARSs), have defined consensus sequences (Brewer and Fangman, 1987; Fangman et al.,

1983). By contrast, there is no evidence for consensus DNA sequences in metazoan origins, which remain much less well-defined than in yeast (Blow and Tada, 2000). Nevertheless, in all eukaryotes origins of replication guide the formation of a number of protein complexes leading to the assembly of two bidirectional DNA replication forks.

A pre-replicative complex (pre-RC) has to be formed at origins of replication during late M and G1 phase of the cell cycle (Sclafani and Holzen, 2007). First, origin DNA is bound by ORC (origin replication complex), which induces some unwinding of the DNA (Dueber et al., 2007; Gaudier et al., 2007). ORC subsequently recruits CDC6 and CDT1 (Bell and Stillman, 1992; Donovan et al., 1997). These proteins then load the MCM2-7 (minichromosome maintenance 2-7) replicative helicase complex onto the DNA in a reaction that is dependent on ATP hydrolysis by CDC6 and assisted by MCM9 (Aparicio et al., 1997; Bowers et al., 2004; Lutzmann and Méchali, 2008; Randell et al., 2006; Speck et al., 2005). Once the MCM2-7 helicase complex is loaded, the origin is said to be 'licensed'; ORC, CDC6 and CDT1 are not required for the subsequent association of the MCM helicase with chromatin (Hua and Newport, 1998; Labib et al., 2000).

The controlled recruitment of additional factors to the MCM2-7 complex constitutes the next phase – the assembly of the replicative complex (RC). Subsequently, the helicase activity of MCM2-7 is activated in a manner that requires the CDC7-DBF4 kinase (DDK) and the S-phase cyclin-dependent kinase (CDK), a process also known as origin 'firing' (Donovan et al., 1997; Early et al., 2004; Hisao and Ken-Ichi, 2002; Labib, 2010; Sheu and Stillman, 2006; Zou and Stillman, 2000). Importantly, CDK and DDK become active only in late G1, thus directing the co-ordination of DNA replication with the cell-

cycle. DDK and CDK phosphorylation of pre-RC complex components is thought to recruit the replication factor CDC45 and the GINS complex, both of which are essential for DNA replication and travel with the replication fork (Im et al., 2009; Sheu and Stillman, 2006; Zou and Stillman, 1998). GINS was first identified in budding yeast (Gambus et al., 2006; Moyer et al., 2006; Takayama et al., 2003) and later demonstrated to exist in human cells, too (Boskovic et al., 2007; Christina et al., 2007; Im et al., 2009). Lastly, RPA and the DNA polymerases are recruited. After the MCM complex unwinds the DNA, bidirectional replication can begin. Origins fire in a temporally-regulated manner, with some firing soon after G1 exit (early origins), and others much later in S phase (late origins) (Masai et al., 2010). In organisms from yeast to humans, the status of histone acetylation of the surrounding chromatin (Knott et al., 2009; Miotto and Struhl, 2008; Vogelauer et al., 2002) and nucleosome positioning (Lipford and Bell, 2001) are important regulators of temporal firing.

Once a replication origin fires, it is important to prevent it becoming re-licensed during the same cell-cycle, in order to avoid re-replication. Because ORC, CDC6 and CDT1 are required for the loading of MCM2–7 onto DNA, but are not required for the continued association of MCM2–7 with DNA, downregulation of their activity at the end of G1 is an effective way of preventing the re-licensing of replicated DNA (Blow and Dutta, 2005a). In budding yeast pre-RC assembly is inhibited by CDK activity. Low CDK levels at the beginning of the cell cycle (in late mitosis and early G1) permit origin licensing, whereas rising CDK levels at the end of G1 both prevent further licensing and at the same time promote the initiation of replication. CDKs target components of the licensing system, including CDC6, which is targeted for degradation following

phosphorylation by CDKs at the G1–S-phase transition (Dahmann et al., 1995; Nguyen et al., 2001), and ORC, which is directly inhibited by CDK phosphorylation (Drury et al., 2000; Vas et al., 2001). CDKs are directly recruited to origin-bound ORC and CDC6, and this helps to maintain ORC in an inactive state during S phase and G2 (Wilmes et al., 2004; Wuarin et al., 2002). In addition, the passage of a replication fork through an origin inactivates it, thereby preventing re-replication (Santocanale et al., 1999). In metazoan cells licensing during S and G2 phases is prevented mainly by downregulating CDT1 activity and levels. CDT1 is degraded at the end of G1 and early S-phase (Blow and Dutta, 2005b; Senga et al., 2006), concomitant with the activation of the CDT1-inhibiting protein geminin, the levels of which increase during S, G2 and M (Blow and Dutta, 2005b).

Following replication origin firing, DNA synthesis begins. DNA synthesis cannot occur *de novo*, so all known DNA polymerases, which can only synthesise DNA in the 5'-to-3' direction, use the 3'-OH of a nucleoside as a primer and synthesise DNA. Because of this, DNA replication begins with the synthesis of short RNA primers by POL α/primase that are then extended by POL α to about 30 bases of DNA (Burgers, 1991; Chen et al., 1992; Eliasson and Reichard, 1978; Fien and Stillman, 1992; Murakami et al., 1992; Murakami et al., 1986; Tsurimoto and Stillman, 1990). The template primed by this RNA-DNA primer provides a unique structure to which replication factor C (RFC) can bind specifically (Burgers, 1991; Chen et al., 1992; Fien and Stillman, 1992; Majka and Burgers, 2004; Tsurimoto and Stillman, 1990, 1991). RFC expels POL α/primase to load the ring-shaped proliferating cell nuclear antigen (PCNA) onto the DNA and releases the primer to the more processive and accurate DNA polymerases POL δ and POL ε. PCNA

is topologically linked to the replicated DNA and binds the polymerase, thereby enhancing the processivity of the polymerase (Krishna et al., 1994; Prelich et al., 1987).

Since DNA polymerases can only synthesise DNA in the 5'-to-3' direction and the DNA double helix is antiparallel, one of the DNA strands is synthesised continuously (the leading strand) and the other is synthesised discontinuously (the lagging strand) (Olivera and Bonhoeffer, 1972; Yudelevich et al., 1968). The leading and the lagging strands are copied by POL ε and POL δ respectively (Nick McElhinny et al., 2008; Pursell et al., 2007). On the leading strand, priming is believed to occur only once and replication can then proceed continuously in the 5'-to-3' direction. Synthesis on the lagging strand is discontinuous and results in 'Okazaki' fragments (Langston and O'Donnell, 2006; Maiorano et al., 2006). When the lagging strand polymerase encounters the 5' end of an Okazaki fragment, the 5' end is displaced to form a short 5'flap, which is degraded by enzymes that include DNA2 and FEN1, to allow the two fragments to be ligated together (Lieber, 1997; Liu et al., 2004).

As parental DNA is unwound and the replication fork advances during DNA replication, the helical intertwines of the DNA ahead of the fork are forced into a progressively shorter region, thereby causing a build-up of superhelical strain. Because eukaryotic chromosomes are large and their ends are attached to the nuclear membrane, the strain cannot simply diffuse by the swiveling of the extremities of the chromosomes. Thus, torsional stress builds up, opposing further helicase action and fork progression (Kanaar and Cozzarelli, 1992; Postow et al., 2001). In addition, DNA behind the replication fork becomes underwound and entangled (Fig.1.5). Topoisomerases are the enzymes that

solve these topological challenges. Topoisomerases TOP1 (budding yeast Top1) and TOP2A/TOP2B (budding yeast Top2) promote the smooth progression of the replication machinery by removing the positive supercoils ahead of the replication fork (Bermejo et al., 2007; Wang, 2002). TOP1 is a type I topoisomerase that acts by introducing a transient break in the DNA, which allows the passage of one of the DNA strands relative to the other, thereby reducing superhelicity. It catalyses a transesterification reaction between its active site tyrosyl and the DNA phosphate group to break the DNA backbone, thus forming a covalent enzyme-DNA intermediate (Wang, 2002). After the strands have rotated relative to each other to relax DNA, the transesterification reaction is reversed to rejoin the DNA backbone. TOP2A and TOP2B are type II topoisomerases: they cut both strands of one DNA double helix, allowing the passage of another unbroken DNA helix through it before reannealing the cut strand (Fig. 1.5).

Recent studies in budding yeast have identified an essential role for Top2 in the termination of DNA replication, too (Baxter and Diffley, 2008; Fachinetti et al., 2010). Top2 associates with DNA replication termination (*TER*) sites and resolves the topological structures that occur when two converging replication forks fuse (Fachinetti et al., 2010). The topological changes that Top2 facilitates at *TER* sites are essential for the completion of DNA replication.

1.11 DNA damage in S-phase and replication stress

DNA replication is a challenging task for the cell. The different constraints (temporal, spatial and topological) and the unusual structures that arise (Postow et al., 2001) make

DNA replication a particularly challenging process. In this light, impaired DNA replication and replication-dependent DNA damage has been reported in early stages of tumour development, and this highlights the importance of coping with this challenge (Bartkova et al., 2006; Di Micco et al., 2006).

1.11.1 Repair of DNA errors in S-phase by mismatch repair

Errors during DNA replication, such as base misincorporation, can cause base mismatches. The mismatch repair (MMR) system is specialized to repair such errors. Mismatch repair (MMR) is an important mutation avoidance system in both prokaryotes and eukaryotes as it corrects mismatched base pairs and thereby prevents inheritance of mutations (Fishel, 1998; Jiricny, 2006). Briefly, following mismatch recognition in the newly-synthesised strand, the DNA is endonucleolytically cleaved and then unwound. Exonucleases then digest the unwound DNA, allowing DNA polymerase III to fill in the gap and DNA ligase to seal the nick (Jiricny, 2006). Members of the MMR system have also been reported to play important roles in both mitotic and meiotic recombination (Hoffmann and Borts, 2004). During mitotic recombination, MMR proteins have been proposed to prevent strand exchange between non-identical sequences (Harfe and Jinks-Robertson, 2000; Jiricny, 2006).

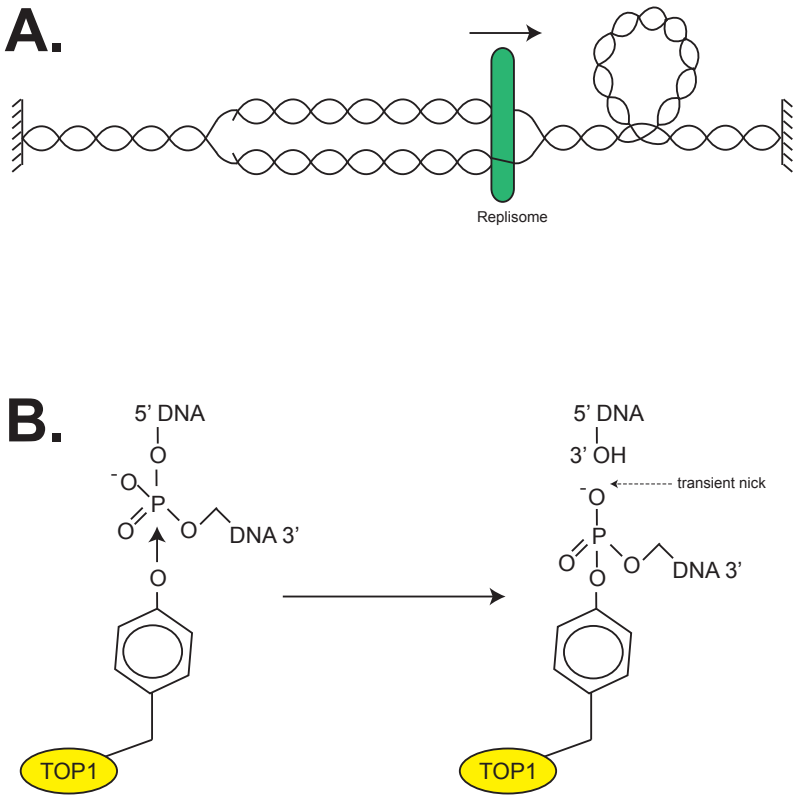

Figure 1.5 The role of topoisomerases in DNA replication.

(A) The ends of the chromosome are attached to the nuclear membrane. The DNA helix ahead of the fork is forced into a progressively shorter region, leading to positive supercoiled DNA accumulating ahead of the advancing replication fork.

(B) Transesterification between a topoisomerase tyrosyl and a DNA phosphate group leads to the breakage of the DNA backbone bond and the formation of a covalent topoisomerase-DNA intermediate. Rejoining of the DNA backbone bond occurs by the reversal of the reaction shown.

1.11.2 Obstacles to replication fork progression

Errors that occur during DNA replication are not the only threat to genome stability during S phase. Another threat comes from damage in the DNA template, which can arise endogenously in any of the ways described in section 1.1. Such damage can interfere with the function of DNA topoisomerases, for instance, which perform the essential task of relieving the topological strain created by the progression of the replication fork (see Fig. 1.5). When the transient topoisomerase-induced DNA breaks happen to be near damaged sites, topoisomerases can become trapped to the DNA termini by 3'- or 5'-phosphotyrosyl bonds. This can lead to replication fork collapse and DSBs (Fig. 1.6). Two enzymes, tyrosyl-DNA phosphodiesterase 1 and 2 (TDP1 and TDP2), cleave these bonds to restore the DNA termini for ligation (Cortes Ledesma et al., 2009; Nitiss et al., 2006; Pouliot et al., 1999a; Yang et al., 1996). These enzymes are crucial to replication fork progression and their importance to genome stability is illustrated by the progressive neurodegenerative diseases caused by mutations in TDP1 (El-Khamisy et al., 2005).

DNA lesions also present a direct obstacle to replication forks, impeding their progression and causing them to stall and/or collapse. Due to the asymmetric nature of DNA replication, a collision between the replication fork and a DNA lesion on the leading strand can have different outcomes from a collision on the lagging strand. When the blocking lesion is located in the lagging-strand template replication fork progression is not compromised, since lagging-strand synthesis can simply resume after the next cycle of Okazaki fragment priming, leaving a small daughter-strand gap in the nascent DNA that can be repaired by HR (Kumiko et al., 2003; McInerney and O'Donnell, 2004;

Pages and Fuchs, 2003). However if the block is located in the leading-strand template the replicative helicase and the DNA polymerase become uncoupled. This leads to regions of single stranded DNA that, if left unprotected, can invade homologous sequences, posing a high risk of genome destabilization (Michel et al., 1997; Saleh-Gohari et al., 2005a). Additionally, the long ssDNA regions created at stalled forks are intrinsically fragile and can break to create one-ended DSBs. Also, progression of a replication fork into a nick in the DNA template is thought to lead to a DSB. It is also thought that DSBs may be created actively at blocked replication forks by the action of structure-specific endonucleases such as MUS81-EME1 (Doe et al., 2002; Whitby et al., 2003). These DSBs may be targeted by the HR machinery to re-initiate replication.

Certain genomic regions pose a challenge to the replication machinery even in the absence of damage. Repetitive DNA sequences, such as centromeres and telomeres, are particularly challenging to replicate, most probably due to the secondary structures, such as hairpins, that can arise (Fig. 1.6) (Greenfeder and Newlon, 1992; Ivessa et al., 2002; Weitzmann et al., 1997). Secondary structures also arise at sites of tri-nucleotide repeats, resulting in replication fork stalling and expansion of repeats (Freudenreich et al., 1998). The expansion of tri-nucleotide repeats has been shown to be responsible for several human genetic diseases, including myotonic dystrophy, Huntington's disease and fragile X syndrome (Cummings and Zoghbi, 2000; Warren and Nelson, 1993). In addition, regions of DNA repeats can take alternative structures, such as left-handed Z-DNA, which can also inhibit replication (Mirkin and Mirkin, 2007).

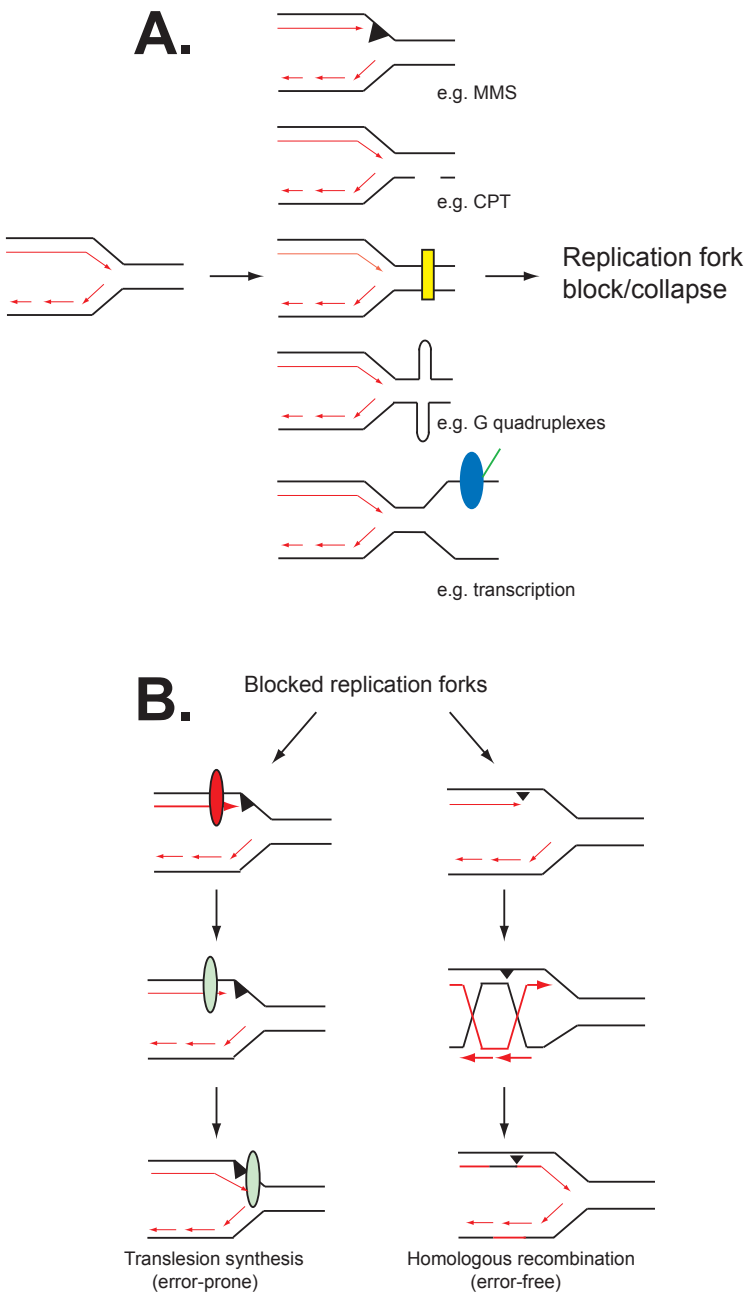

Figure 1.6 Common barriers to replication fork progression and the pathways employed to overcome them.

The densely-packed heterochromatic regions of genomes also present a challenge to the replication machinery. Proteins such as RIF1 have been proposed to have specific roles in replicating through heterochromatic regions (Buonomo, 2010). Replication can also be obstructed by non-nucleosomal stable protein-DNA complexes. In yeast the helicase Rrm3 has been shown to be required for the replication machinery to overcome this challenge (Ivessa et al., 2003; Ivessa et al., 2002).

DNA replication also has to contend with other processes that use DNA as a template, notably transcription. Indeed, collisions between the replisome and the RNA polymerase have been shown to slow down fork progression (Azvolinsky et al., 2009; Deshpande and Newlon, 1996; Takeuchi et al., 2003). This can be caused both by the physical barrier imposed by the DNA-bound transcription complex and the topological strain of the excessive superhelicity (Fig. 1.6) (Bermejo et al., 2009; Bermejo et al., 2007; Deshpande and Newlon, 1996; Olavarrieta et al., 2002). Consistent with this idea, topoisomerases have been shown to prevent replication fork collapse at sites of S phase transcription by resolving positive supercoils and insulating transcription units in chromatin loops (Bermejo et al., 2009; Bermejo et al., 2007; Tuduri et al., 2009).

In organisms from yeast to humans, the highly-transcribed ribosomal DNA arrays, which are transcribed by RNA polymerase I, contain a so-called ‘programmed pause sites’. In budding yeast, Replication Fork Barriers (RFBs) are found downstream of the 35S gene, where they block replication forks progressing opposite to the direction of transcription in a manner dependent on the protein Fob1 (Brewer and Fangman, 1988; Kobayashi and

Horiuchi, 1996; Tsang and Carr, 2008). In a similar way, transfer RNA (tRNA) genes also have polar barriers that cause replication forks to pause (de la Loza et al., 2009; Ivessa et al., 2003; McFarlane and Whitehall, 2009).

There are specific sites in the eukaryotic genome that are particularly sensitive to chromosome breakage when replication is perturbed, known as fragile sites. Fragile sites were first visualised in mammalian cells after treatment with the DNA polymerase inhibitor aphidicolin (Casper et al., 2002). Similar sites, termed 'replication slow zones', have also been described in budding yeast (Cha and Kleckner, 2002; Raveendranathan et al., 2006). Importantly, the introduction of human fragile sites in the yeast genome induces site-specific replication fork stalling (Zhang and Freudenreich, 2007). Experiments in budding yeast have shown that fragile sites are often associated with sequences that contain tRNAs and Ty transposons (Admire et al., 2006; Labib and Hodgson, 2007). This has led to a model in which fragile sites require the slowing of replication, for example at the tRNA sequences, as well as sequences such as inverted repeats which can form recombinogenic substrates when unwound.

To conclude, many obstacles prevent the smooth progression of the replication machinery even in the absence of exogenous genotoxic insult. Indeed, it is estimated that as many as 50% of replication forks may stall during a single round of DNA replication (Cox et al., 2000). However, cells are equipped with mechanisms that detect stalled replication forks and ensure resumption and eventual completion of DNA replication.

1.11.3 Dormant origins and DNA replication stress

In eukaryotes, DNA replication starts from multiple origins. There is an approximately 20-fold excess of the MCM2-7 complex over replication origins used in a normal S-phase (Ge et al., 2007; Lei et al., 1996; Olivier et al., 2003; Roland et al., 1995; Rowles et al., 1996). These factors ensure that, during replication stress, a genomic region left un-replicated by a stalled replication fork can be replicated by a converging replication fork. In addition, eukaryotic genomes contain many licensed replication origins that are not used during a normal S-phase, but remain dormant and are passively replicated – and thereby inactivated – by replication forks from neighbouring regions (Anglana et al., 2003; Dijkwel et al., 2002; Li et al., 2003). When replication fork progression is inhibited, dormant origins are less likely to be passively replicated and, consequently, more likely to fire. The firing of dormant origins has been shown to be important for the completion of DNA replication in both budding yeast and human cells (Blow and Ge, 2009; Ge et al., 2007; Santocanale et al., 1999). This is not an active mechanism – it simply depends on the stochastic nature of origin firing. Other mechanisms of dealing with replication stress, however, rely on complex regulatory pathways that are essential to cell viability.

1.11.4 The DNA replication checkpoint

The Mec1/Rad53 pathway in yeast (ATR/CHK1 in humans) is key to the replication stress response (Lopes et al., 2001; Tercero and Diffley, 2001). Activation of the DNA replication checkpoint is probably the most important function of Mec1/ATR and Rad53/CHK1 in protecting cells against genotoxic insult. Crucial to the activation of this

response is the formation of ssDNA regions, which are created for example from the uncoupling between the replicative helicase and the DNA polymerase (Byun et al., 2005; Sogo et al., 2002). These regions are then coated with the RPA, and it is thought that the RPA-ssDNA filaments recruit and activate Mec1/ATR (Zou and Elledge, 2003). RPA-ssDNA is the common intermediate arising from the many abnormal structures that may arise at stalled replication forks, thereby channeling many primary lesions into a single signal-transduction pathway. In the DNA replication checkpoint Rad53/CHK2 activation requires Mrc1/Claspin, as well as other factors such as Dpb11/TopBP1, NBS1, RAD17 and the Rad9-Rad1-Hus1 (9-1-1) complex (Kumagai et al., 2006; Lee et al., 2007).

The essential function of the DNA replication checkpoint is to ensure completion of DNA replication. To this end, the replication checkpoint orchestrates a response that operates at several levels. Firstly, the DNA replication checkpoint prevents replication fork collapse, i.e. the irreversible dissociation of replisome components from chromatin (Cobb et al., 2005; Frei and Gasser, 2000; Lopes et al., 2001; Segurado and Diffley, 2008; Sogo et al., 2002). This is thought to be the most important role of the checkpoint response in dealing with replication stress. Secondly, dNTP levels are increased, which is essential for survival during DNA replication stress (Chabes et al., 2003; Hakansson et al., 2006; Yao et al., 2003; Zhao et al., 2001; Zhao and Rothstein, 2002). Thirdly, the checkpoint inhibits further origin firing (Arnaudeau et al., 2001; Lundin et al., 2002; Merrick et al., 2004; Petermann et al., 2010; Saleh-Gohari et al., 2005b; Santocanale and Diffley, 1998a; Shirahige et al., 1998; Tercero and Diffley, 2001). This is probably achieved by inducing inhibitory phosphorylation of CDK and DDK (Costanzo et al., 2000; Costanzo et al., 2003; Lopez-Mosqueda et al., 2010; Mailand et al., 2000; Maya-

Mendoza et al., 2007; Merrick et al., 2004; Santocanale and Diffley, 1998b; Shirahige et al., 1998; Zegerman and Diffley, 2010). Furthermore, a transcriptional response is activated such that genes involved in DNA repair are upregulated (Allen et al., 1994; Huang et al., 1998; Zhou and Elledge, 1993). Lastly, replication fork re-start requires the deactivation, through de-phosphorylation, of Rad53 (Szyjka et al., 2008).

In addition to dealing with replication stress, the replication checkpoint may also have a role during an S-phase that is not exogenously challenged. Consistent with this, Mec1 and Rad53 are essential for cellular viability in budding yeast, as are ATR and CHK1 in mammals. Even in the absence of replication-blocking agents, budding yeast Ddc1, Ddc2 and Rpa2 are phosphorylated during S-phase in a Mec1-dependent manner (Brush et al., 1996; Longhese et al., 1997; Paciotti et al., 2000), suggesting that the replication checkpoint is at least partially activated during S-phase, perhaps by certain replication intermediates. Furthermore, the yeast Mrc1-Tof1 complex is required for replication fork progression in the absence of exogenous genotoxic stress in a manner independent of Rad53 (Szyjka et al 2005; Tourriere et al 2005). All of these proteins may act to facilitate the ability of replication forks to go through spontaneous DNA lesions and various chromosomal structures. This is supported by observations that certain regions on chromosomes are replicated slowly in *mec1* or ATR mutants and are prone to breakages (Cha and Kleckner, 2002).

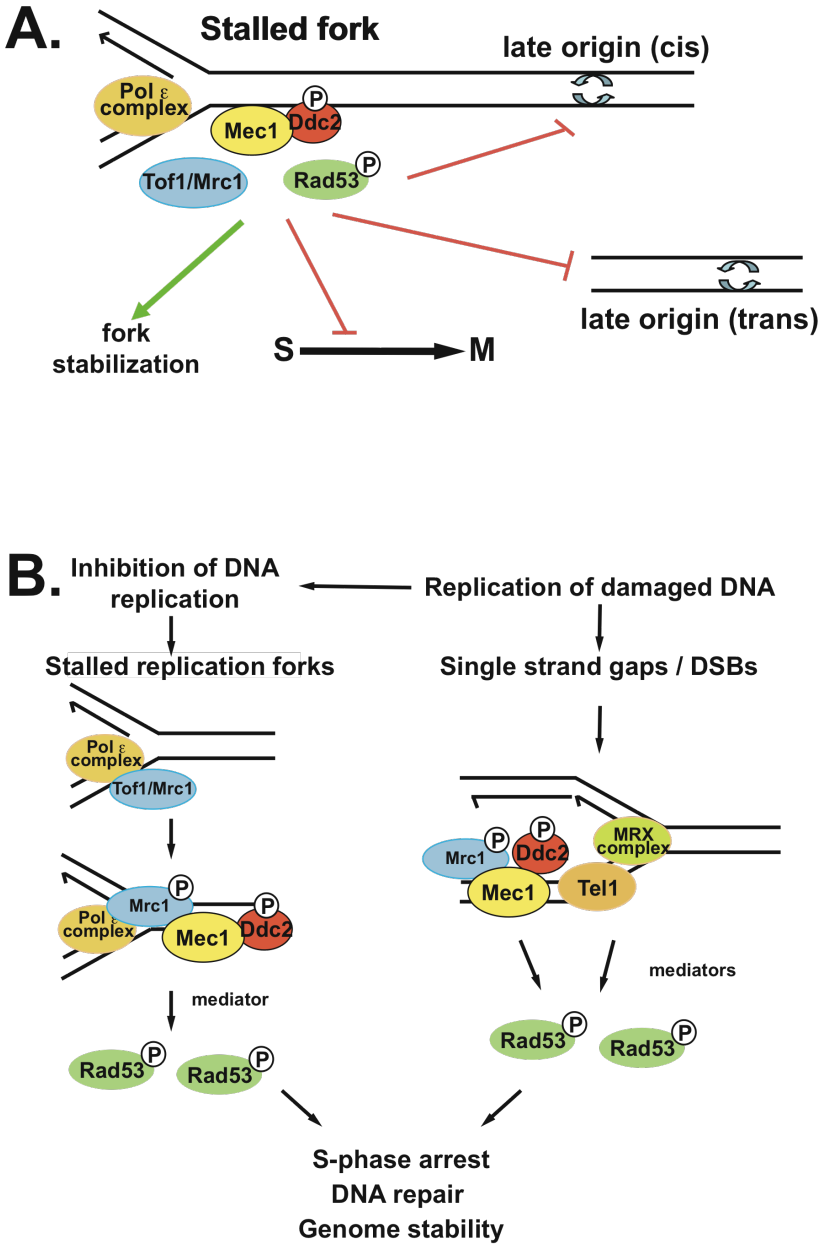

Figure 1.7 Replication fork stalling and the DNA replication checkpoint in budding yeast.
(A) The DNA replication checkpoint is activated after fork stalling or collapse. It acts to stabilize forks, block transition to mitosis and block late origin firing.

(B) Mec1-Ddc2 (ATR-ATRIP in mammals) act to sense the damage and to initiate the DNA replication checkpoint.

1.11.5 DNA-damage tolerance

One mechanism that the cell uses to cope with replication obstacles is the co-called DNA-damage tolerance (DDT) pathway. Unlike the conventional repair pathways described in section 1.1, DTT does not result in the repair of primary lesions; instead, it is concerned with bypassing the lesion so that DNA replication can resume. The existence of such a pathway was first inferred from experiments carried out in budding yeast in the 1980s which suggested that there were specific pathways to allow the replication apparatus to 'bypass' lesions that caused replication fork stalling (di Caprio and Cox, 1981; Prakash, 1981). Budding yeast NER mutants were exposed to UV-radiation, resulting in the formation of DNA photoproducts that could not be repaired. During DNA replication, these unrepaired lesions gave rise to single strand gaps, observed through separation of genomic DNA in an alkaline sucrose gradient. Following recovery, the fragmented genomic lesions were converted to larger molecular weight species, indicating that the single-strand gaps were subsequently filled in (di Caprio and Cox, 1981; Prakash, 1981). DTT operates by two different pathways: 'error-prone' and 'error-free' damage bypass (Barbour and Xiao, 2003; Broomfield et al., 2001; Higgins et al., 1976; Lawrence, 1994; Smirnova and Klein, 2003; Ulrich, 2005). Error-free bypass is not very well understood but is believed to involve a 'template-switch' mechanism that engages recombination proteins (Barbour and Xiao, 2003; Broomfield et al., 2001; Higgins et al., 1976; Lawrence, 1994; Smirnova and Klein, 2003; Ulrich, 2005). Error-prone damage bypass involves DNA synthesis past the lesion by specialized translesion-synthesis (TLS) polymerases.

In budding yeast both pathways have been shown to be mediated by *RAD6* epistasis group of genes (Barbour and Xiao, 2003; Broomfield et al., 2001; Smirnova and Klein, 2003; Ulrich, 2005). DTT has been shown to be under the control of post-translational modification by ubiquitination. Indeed, many of the *RAD6* epistasis group genes encode enzymes of the ubiquitination system (Jentsch et al., 1987; Ulrich, 2005; Ulrich and Jentsch, 2000). The crucial substrate of this pathway is PCNA (Hoege et al., 2002; Moldovan et al., 2007). Different types of ubiquitin modifications that become induced upon DNA damage dictate whether DDT proceeds via the error-prone or the error-free branch. Error-prone DDT is triggered by conjugation of a single ubiquitin moiety (monoubiquitylation) to PCNA at lysine-164 (K164), which involves Rad6 and Rad18 (Hoege et al., 2002; Stelter and Ulrich, 2003). Monoubiquitylated PCNA then recruits TLS polymerases through a direct interaction with their ubiquitin-binding motifs (Bienko et al., 2005; Kannouche et al., 2002; Kannouche and Lehmann, 2006; Kannouche and Lehmann, 2004; Kannouche et al., 2004; Lehmann et al., 2007; Watanabe et al., 2004). TLS polymerases are able to replicate past DNA lesions as they have a more relaxed catalytic core than normal replicative polymerases (Friedberg and Gerlach, 1999; Woodgate, 1999). Because of this, TLS polymerases exhibit low fidelity and this is why translesion synthesis is referred to as error-prone DNA damage bypass (Prakash et al., 2005). The majority of mutations induced by genotoxins are believed to result from mutagenic processing by TLS polymerases (Pages and Fuchs, 2002).

Error-free DDT requires modification of the same residue of PCNA, but by a K63-linked polyubiquitin chain (Hoege et al., 2002). Synthesis of this polyubiquitin chain requires in addition to Rad6 and Rad18 the heterodimeric Ubc13-Mms2 and the ubiquitin ligase

Rad5 (Branzei et al., 2008; Hoege et al., 2002; Ulrich and Jentsch, 2000; Zhang and Lawrence, 2005). Once modified by this polyubiquitin chain, PCNA triggers by an unknown mechanism lesion bypass involving the undamaged template (template switching) and specific repair proteins (Branzei et al., 2006; Giot et al., 1997b). Although the *RAD6* pathway was thought to operate during S-phase, recent work using an inducible system of DNA damage bypass demonstrated that the process is separable from DNA replication (Daigaku et al., 2010; Karras and Jentsch, 2010). PCNA ubiquitination and both TLS and error-free bypass can occur outside of S-phase (Daigaku et al., 2010). This suggests that DNA damage that is left unrepaired in S-phase may cause PCNA to remain associated with gaps in the DNA daughter strand or that PCNA can be re-loaded onto DNA and ubiquitinated outside of replication.

1.12 The role of HR in the response to DNA replication stress

The close connection between DNA replication and recombination was first described in bacteriophage systems in the 1960s (Luder and Mosig, 1982; Mosig, 1987), where it was demonstrated that the D-loop recombination intermediates could be converted into fully functional replication forks (Formosa and Alberts, 1986; Kreuzer, 2000). A similar requirement for HR in rescuing blocked replication was soon after documented in prokaryotes (Khidhir et al., 1985; Rupp and Howard-flanders, 1968; Rupp et al., 1971; Witkin et al., 1987) and, later on, in eukaryotes (Kadyk and Hartwell, 1992; Zou and Rothstein, 1997). It is now thought that HR first evolved precisely to salvage stalled replication forks and complete DNA replication, and it was subsequently employed for other processes in eukaryotes. The role played by HR in re-initiating DNA replication in

an origin-independent manner has become an active area of research and is contributing vastly to our understanding of genome stability.

1.12.1 HR and the rescue of stalled/collapsed replication forks in bacteria

The mechanistic details of the involvement of HR in rescuing replication is best understood in bacteria, where HR has been convincingly shown to play a key role in DNA replication (Courcelle and Hanawalt, 2003; Cox et al., 2000; Kreuzer, 2005). Consistent with this, cells lacking the core recombination protein RecA (eukaryotic RAD51; see Table 1.1) demonstrate a slower rate of DNA replication, and a higher rate of chromosome breakage, than wild type cells (Mao et al., 1989). RecA binds to the single-strand regions generated at a blocked replication fork, thereby sensing that replication is blocked (Roberts et al., 1982; Sassanfar and Roberts, 1990).

Firstly, the bound RecA acts as a transactivator to induce the upregulation of over 40 genes involved in the replication stress response (Courcelle et al., 2001). RecA also acts to maintain the structural integrity of the replication fork itself until replication can resume (Clark and Margulies, 1965; Howard-Flanders et al., 1969). Subsequently, the RecA-ssDNA filament initiates strand exchange to form a D-loop. Another set of proteins use the D-loop for replication fork re-activation. The most important of these is the structure-specific DNA-binding protein PriA (Kogoma et al., 1996; Masai et al., 1994). PriA binds with high affinity to D-loop DNA by recognizing bent DNA at the three-strand junction created by the parental duplex and the 3'end of the invading strand (McGlynn et al., 1997). The 3'-OH of the invading strand is used as the primer for DNA synthesis and PriA loads the DnaB helicase into the displaced strand of the D-loop;

DnaB then recruits DnaG primase, resulting in re-start of DNA synthesis via the DNA Pol III holoenzyme (Lovett, 2003; McGlynn et al., 1997). The subsequent extension of the 3'end by any polymerase requires the prior disassembly of the RecA filament (Lusetti and Cox, 2002). In a parallel mechanism, the PriC protein re-primes replication on the leading strand downstream of the encountered lesion, leaving behind a gap that is repaired by recombination (Heller and Marians, 2006). The importance of recombination in completing DNA replication is demonstrated by the fact that abolishing recombination-mediated fork re-start causes lethality of near lethality in bacteria (Liu et al., 1999; Sandler, 2000).

1.12.2 HR and the rescue of stalled replication forks in budding yeast

Although PriA is not conserved in eukaryotes, several lines of evidence support a crucial role for HR in DNA replication re-start in budding yeast, too. For instance, the viability of several replication and replication checkpoint mutants depends on the recombination process (Giot et al., 1997a, b; Murray et al., 1994). Further, recombination mutants are hypersensitive to agents that block DNA replication, such as MMS and camptothecin – see section 1.6 (Dong and Fasullo, 2003; Fasullo and Dong, 2004; Fasullo et al., 2001). HU-stalled replication forks, however, only require HR for re-start if the checkpoint response is dysfunctional in a way that leads to replication fork collapse (Lopes et al., 2001; Meister et al., 2005).

Establishing the connection between HR and replication fork re-start in a more direct way, recombination intermediates can be observed during replication in both fission and

budding yeast (Segurado et al., 2002; Zou and Rothstein, 1997), including Holliday junctions between sister chromatids at stalled forks (Minca and Kowalski, 2010). In addition, recombination factors have been shown to be indispensable for restarting replication and for the suppression of abnormal structures at stalled forks (Alabert et al., 2009; Minca and Kowalski, 2010).

Importantly, HR plays an active role at stalled forks and it is not merely a consequence of DSBs resulting from replication fork collapse. Indeed, although HR is required for the repair of DSBs and the rescue of stalled replication alike, some genes have been identified in yeast that map into the *RAD52* epistasis group and display sensitivity to agents that block replication forks but not to DSBs. These include complexes such as the Shu1-Psy3-Shu2-Csm2, and support an argument whereby there are context-specific HR proteins that act primarily for replication-fork support (Alabert et al., 2009; Duro et al., 2008; Mankouri et al., 2007; Shor et al., 2005). Furthermore, recent data suggests that the DNA replication checkpoint impedes recombination at DSBs during S-phase by inhibiting resection; at stalled forks, on the other hand, ssDNA is already present and can be used to initiate recombination with the sister chromatid (Alabert et al., 2009). Thus, the replication checkpoint may favour recombination at stalled forks over that at DSBs.

An important HR mechanism employed in rescuing blocked replication forks in yeast is break-induced replication (BIR) (Kraus et al., 2001). BIR is thought to act in a similar way to the PriA-dependent mechanism in bacteria. Indeed, BIR provides an explanation on how recombination can be used to re-start replication in an origin-independent fashion. Recent data have shown that BIR requires almost all factors that are essential for

DNA replication except CDC6 and ORC, both of which are needed specifically for the assembly of the pre-RC at origins of replication (Lydeard et al., 2010). The dependence of BIR on replication factors lends credence to proposals that BIR can function as a *bona fide* replication re-start mechanism in eukaryotes. In agreement with this, BIR has been shown to be important for the lengthening of telomeres in telomerase-deficient cells (Le et al., 1999; Lydeard et al., 2007; McEachern and Haber, 2006; Teng et al., 2000).

Lastly, it is important to note that HR at the replication fork is carefully fine-tuned, since hyper-recombination can adversely affect genome stability. Indeed, the helicases Srs2 and Sgs1 (human BLM) act to prevent the accumulation of recombinogenic structures at damaged replication forks in a manner co-coordinated by sumoylation of PCNA (Branzei et al., 2006).

1.12.3 HR and the rescue of stalled replication forks in mammals

A strong connection between HR and replication has also been observed in mammalian cells. Indeed, agents that block replication fork progression strongly induce HR (Arnaudeau et al., 2001; Lundin et al., 2002; Saleh-Gohari et al., 2005b) and HR has been proposed to support replication fork progression (Daboussi et al., 2008). Like in yeast, HR at stalled forks is likely to be initiated by ssDNA that results from the uncoupling between DNA polymerase and the helicase (Byun et al., 2005; Lopes et al., 2001). In mammals however, these ssDNA stretches are extended by nuclease of MRE11 that is recruited to stalled and collapsed replication fork by PARP1 and PARP2 (Bryant et al., 2009).

RAD51 coats the ssDNA overhangs and invades the homologous molecule, facilitating the formation of a HJ. In a manner similar to fork reactivation in bacteria, RAD51-dependent strand invasion can facilitate replication re-start from the DNA end. It is thought that the recombination tract (if any) that would result from this would be very short (Petermann et al., 2010). Alternatively, recombination intermediates can serve as a substrate for origin-independent replisome loading, in a similar way to what has been described in bacteria (Heller and Marians, 2006). Supporting this notion, biochemical fractionation experiments have shown that, unlike the replicative DNA POL δ, the TLS POL η can initiate DNA synthesis from D-loops (Kawamoto et al., 2005; McIlwraith et al., 2005) and RAD51 may play a role in targeting POL η to the D-loop (Kannouche et al., 2001). Additionally, HR may act after S phase to repair DNA gaps that result from replication fork collapse (Petermann et al., 2010). This would be similar to what has been reported in DT40 cell lines, where DNA structures that bind to activated RPA accumulate during S phase to be resolved during G2 by an HR-dependent mechanism (Su et al., 2008).

It is interesting to note that, like in yeast, a separation between the involvement of HR in DSB repair from that in replication fork re-start has been observed in mammalian cells. Indeed, PARP1 and PARP2 are required for HR stimulated by replication blocks but not by DSBs (Bryant et al., 2009; Yang et al., 2004). Furthermore, the RAD51 paralogue XRCC2 is required for HR at stalled replication forks, but not at DSBs (Mohindra et al., 2004). These observations establish a direct link between replication fork rescue and HR in mammalian cells: the fact that HR pathways responding to replication stress or to

DSBs are genetically distinguishable argues that HR at replication forks is not a mere consequence of DSBs that may result from fork collapse.

1.13 DNA replication and repair in the context of chromatin

The eukaryotic genome is compacted inside the nucleus as chromatin, the building block of which is the nucleosome. The nucleosome contains 146 bp of DNA wrapped around the histone octamer, which contains of a central $(H3\text{-}H4)_2$ tetramer flanked by two H2A-H2B dimers (Luger et al., 1997). Interacting nucleosomes then form what is termed 'higher-order chromatin' (Bassett et al., 2009). The compact chromatin structure poses a challenge to the processes that use DNA as a template. But we also know that chromatin is not a mere way of compacting DNA within the confines of the nucleus: it also carries heritable information in the form of DNA methylation, post-translation modifications on histones and histone variants. These marks affect genome function without alternations in DNA sequence; they are referred to as 'epigenetic marks' and the cumulative information that they carry is termed 'the histone code' (Probst et al., 2009; Strahl and Allis, 2000).

Epigenetic marks are necessary for the maintenance of genome function, including the differential gene expression patterns and the establishment of essential architectural features such as telomeres and centromeres. It is thus vital to viability and proliferation that epigenetic marks are inherited accurately. Thus, the challenge faced by the processes that use DNA as a template within the chromatin context is two-fold: firstly, the chromatin structure has to be disrupted in such way that the machinery can overcome the physical barrier imposed by the nucleosome in order to access template DNA; secondly,

epigenetic marks must be restored following chromatin disruption, so that epigenetic inheritance is not affected. The former is carried out by displacing nucleosomes with respect to DNA (by ATPase chromatin remodelling complexes); the latter challenge is met by histone chaperones acting in concert with histone-modifying complexes.

1.13.1 DNA replication and chromatin dynamics

The destabilization of nucleosomes ahead of the replication fork was first observed in replicating SV40 minichromosomes (Gasser et al., 1996; Sogo et al., 1986). Whether it is due to the passage of the replication machinery itself – in a way reminiscent of RNA POL II transcription (Hodges et al., 2009; Studitsky et al., 1995) – or it is mediated by histone chaperones and ATP-dependent chromatin remodeling enzymes is not yet known. However, several chromatin-remodelling complexes have been implicated in the disruption of chromatin ahead of the replication fork. For instance, the ISWI class of ATP-dependent chromatin remodelling enzymes have been shown to promote replication fork progression in budding yeast (Vincent et al., 2008) and metazoa (Bozhenok et al., 2002; Collins et al., 2002; Hur et al.; Poot et al., 2004). Another chromatin remodelling complex that has been suggested to play a role in DNA eplication is FACT (Facilitates chromatin transcription). FACT has been shown to associate with the replisome in budding yeast (Gambus et al., 2006) and with the MCM complex in human cells (Tan et al., 2006). FACT is thought to remove H2A-H2B dimers; once they have exited from the DNA, the $(H3\text{-}H4)_2$ tetramers can then be removed.

One histone chaperone that has the potential to remove H3/H4 from replicating chromatin is Asf1 (anti-silencing function). Asf1 localizes to replication foci in *Drosophila* S2 cells, but rapidly dissociates when replication is halted in response to hydroxyurea treatment (Schulz and Tyler, 2006). In yeast, Asf1 interacts with the PCNA loader, RFC (replication factor C) and it is required for the integrity of stalled replisomes (Franco et al., 2005). Human ASF1 (which consists of ASF1A and ASF1B) has been shown to bind to the MCM helicase complex via a H3-H4 bridge (Groth et al., 2007a), thus being ideally placed to influence chromatin structure during replication. Arguing for a role for Asf1 in histone disassembly during replication, the ASF1-H3/H4-MCM complex displays a parental distribution of histone post-translational modifications, suggesting that the histones bound to ASF1 have been removed from the parental chromatin (Groth et al., 2007a).

At the wake of the replication fork, chromatin has to be re-assembled on both DNA duplexes and the epigenetic marks need to be transferred onto the newly replicated DNA. Chromatin is reassembled onto newly-replicated DNA as soon as the length of DNA needed to wrap around the core histone octamer has emerged from the replication machinery (Sogo et al., 1986). This includes the re-deposition of evicted (parental) histones as well as the assembly of newly-synthesised histones. Firstly, $(H3\text{-}H4)_2$ tetramers are deposited onto DNA; then two H2A-H2B dimers are deposited. Histone chaperones play key roles as histone acceptors and donors in assisting the re-assembly, as well as disruption, of nucleosomes by controlling the availability of histones at specific sites. One such chaperone is the evolutionarily conserved CAF-1 (**c**hromatin **a**ssembly **f**actor-1) (Glowczewski et al., 2004; Hoek and Stillman, 2003 ; Kamakaka et al., 1996;

Kaufman et al., 1995; Kaufman et al., 1997; Smith and Stillman, 1989; Verreault et al., 1996). CAF-1 is tethered to replication forks via an interaction with PCNA (Krude, 1995; Shibahara and Stillman, 1999). Abolishing its function markedly reduces cell viability, blocks DNA replication and leads to genome instability (Nabatiyan and Krude, 2004; Ye et al., 2003), suggesting that efficient chromatin reassembly behind the replication forks is essential for the progression of the replication fork. In human cells this feedback mechanism may be controlled by the histone chaperone ASF1, which delivers histones to CAF-1 (Galvani et al., 2008; Sanematsu et al., 2006).

ASF1 interacts not only with CAF-1 but also with the MCM replicative helicase complex via a histone H3/H4 bridge (Groth et al., 2007a). By acting as a donor and acceptor of histones and by interacting with the MCM complex ASF1 co-ordinates histone supply and demand with replicative DNA unwinding. When ASF1 is depleted or when its function is compromised by H3-H4 overexpression, DNA unwinding stops and replication fork progression is halted (Groth et al., 2007a). In budding yeast, Asf1 is localized to replication forks via its interaction with replication factor C, acting to promote replication fork integrity (Franco et al., 2005).

The process of replication-coupled chromatin assembly is dependent on histone post-translational modifications. Newly-synthesized histones H3 and H4 have a specific pattern of post-translational acetylation marks, including H4K5Ac, H4K12Ac and H3K9Ac or H3K14Ac (Ling et al., 1996; Loyola et al., 2006; Sobel et al., 1995). Acetylation marks enhance the association of histones with chaperones. In budding yeast, newly-synthesized histone H3 is acetylated on lysine 56 (H3K56Ac) (Masumoto et al.,

2005), a mark dependent on the histone acetyltransferase Rtt109 and Asf1 (Driscoll et al., 2007; Han et al., 2007a; Han et al., 2007b). H3K56Ac acts to recruit H3/H4 dimers to CAF-1 and Rtt106, both of which are poised at DNA replication forks, thereby promoting their assembly onto DNA (Huang et al., 2005; Huang et al., 2007; Li et al., 2008). H3K56Ac is also important for chromatin re-assembly following DNA repair and replication stress (Chen et al., 2008; Driscoll et al., 2007; Han et al., 2007a; Tsubota et al., 2007) and the regulation of its levels is pivotal to the maintenance of genome stability (Celic et al., 2006; Celic et al., 2008). In mammalian cells H3K56Ac has been documented (Das et al., 2009) but its contribution to the process of replication-dependent chromatin assembly is uncertain. Moreover, histone acetylation marks play an important role in what is termed 'chromatin maturation'. Histones are first deposited onto DNA in a random manner to form an irregularly spaced array of nucleosomes. The subsequent action of ATP-dependent chromatin remodelers displaces histone octamers to their optimal positions, which are thought to be determined by a combination of DNA sequence, nearby sequence-specific DNA-binding proteins and electrostatic repulsion from adjacent histone octamers. Histone acetylation provides a looser chromatin conformation, such that nucleosome repositioning during chromatin maturation is facilitated. Acetylation marks are then removed once nucleosomes have assumed their correct positions (Ransom et al., 2010).

Mammalian cells possess different variants of histone H3: H3.1, H3.2 and H3.3 (Hake and Allis, 2006). H3.1 and H3.2 are only expressed during S-phase and are deposited onto DNA only during replication by CAF-1 (Tagami et al., 2004). H3.3 is expressed throughout the cell-cycle and is deposited onto DNA in a replication-independent

manner. After the $(H3\text{-}H4)_2$ tetramer is assembled onto the DNA, a dimer of H2A/H2B is incorporated on either side of the tetramer. This is thought to be carried out by the chaperones FACT and NAP1 (Ransom et al., 2010). Finally, epigenetic inheritance requires the copying of epigenetic marks (notably histone PTMs and DNA methylation) onto newly-assembled nucleosomes. The maintenance of DNA methylation is ensured by the recruitment to the replication fork of DNA-methylating and methyl-binding enzymes (Chuang et al., 1997; Sarraf and Stancheva, 2004). Histone post-translational marks are thought to be copied from nearby parental nucleosomes (Groth et al., 2007b; Probst et al., 2009).

1.13.2 DNA repair and chromatin dynamics

Like in other DNA processes, chromatin dynamics during DNA repair is governed by histone post-translational modifications and nucleosome remodelling, which act in concert to facilitate DNA repair. Of the histone PTMs that are induced upon DNA damage, the phosphorylation of histone H2A in yeast and of histone variant H2AX in metazoan is the most prominent and important one (Downs et al., 2000; Rogakou et al., 1998). Phosphorylation of H2AX occurs in a large domain flanking the DNA lesion – Mb in mammals (Rogakou et al., 1999) and 50 kb in yeast (Shroff et al., 2004) – and is one of the first steps of DNA damage signalling. Phosphorylated H2AX (γ-H2AX) acts as a signal to recruit many other proteins involved in DNA damage signalling and repair, including NBS1 (Kobayashi et al., 2002), MDC1 (Stewart et al., 2003; Stucki et al., 2005) and 53BP1 (Ward et al., 2003). γ-H2AX also recruits cohesins to DSB sites (Ström

et al., 2004; Unal et al., 2004), which promote efficient repair by keeping the DSB ends in close proximity.

Highlighting the importance of H2AX phosphorylation, mutations of the phosphorylatable residue of H2AX lead to genomic instability and sensitivity to all genotoxic agents (Bassing et al., 2003; Celeste et al., 2003; Celeste et al., 2002; Kinner et al., 2008; Srivastava et al., 2009). Another key histone PTM is TIP60-mediated histone H4 acetylation, which has been shown to be required for the recruitment of RAD51 to sites of DNA damage (Murr et al., 2006). In a similar manner, ubiquitination of H2A by the ubiquitin ligase RNF8 leads to the recruitment of repair protein to sites of DNA damage (Doil et al., 2009; Huen et al., 2007; Mailand et al., 2007; Stewart et al., 2009). It is important to note that there is substantial cross-talk between histone PTMs and the other aspect of chromatin dynamics: chromatin remodelling. γ-H2AX, for instance, recruits various chromatin-remodelling complexes to DNA lesions (Morrison et al., 2004; van Attikum et al., 2004). The link between chromatin remodelling and DNA repair was first observed in NER over 30 years ago (Smerdon and Lieberman, 1978), where NER-induced nucleosome rearrangements were shown to be dependent on histone acetylation (Smerdon et al., 1982). The remodelling of chromatin by ATP-dependent chromatin remodelling enzymes at sites of UV damage is now well-documented (Dinant et al., 2008). It is not clear, however, whether histone octamers are simply moved along DNA or they are removed during NER. The degree of chromatin remodelling on DSB sites, on the other hand, is less well agreed upon. It is thought that any dechromatisation at such sites is simply a consequence of end resection (Shroff et al., 2004; Tamburini and Tyler, 2005). On the other hand, the fact that the chromatin remodeler INO80 is required

both for nucleosome disassembly at DSBs and for DNA resection (van Attikum et al., 2007; van Attikum et al., 2004) argues that the two processes are tightly coupled. In any case, histones on resected ssDNA are evicted and replaced by RPA and RAD51 (Dubrana et al., 2007; Tsukuda et al., 2009). More recently, the chromatin remodelling complex has been shown to be recruited to sites of DNA damage by poly(ADP-ribosyl)ation to relax chromatin by sliding nucleosomes (Ahel et al., 2009). Following damage repair, γ-H2AX is dephosphorylated (Keogh et al., 2006) and chromatin is re-assembled in a manner very similar to that during DNA replication.

1.13.3 Chromatin dynamics during DNA replication stress

Excess non-nucleosomal histones accumulate during replication stress (Bonner et al., 1988; Senshu and Ohashi, 1979). This excess of soluble histones has been shown to be toxic, interfering with DNA metabolic processes such as transcription and increasing the rate of mitotic chromosome loss (Meeks-Wagner and Hartwell, 1986). In yeast, the checkpoint kinase Rad53 has been shown to induce the degradation of non-nucleosomal histones following replication stress (Emili et al., 2001; Gunjan and Verreault, 2003). In mammals, ASF1 plays a pivotal role in sequestering excess S-phase histones (Emili et al., 2001; Groth et al., 2005; Hu et al., 2001). Mammalian ASF1a and ASF1b are substrates of the Tousled-like kinases TLK1 and TLK2 (Groth et al., 2003; Silljé and Nigg, 2001). TLK1/2 normally phosphorylate ASF1 in the S phase of the cell cycle; during genotoxic stress TLK1/2 are phosphorylated and inactivated by CHK1, thus preventing ASF1 phosphorylation (Krause et al., 2003).

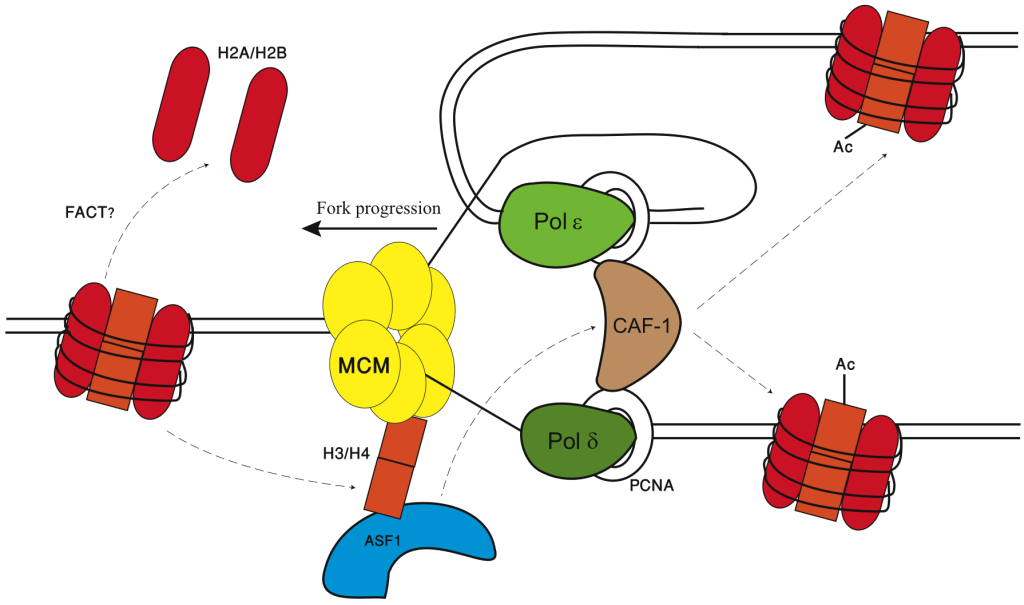

Figure 1.8 Chromatin dynamics at the replication fork.

Nucleosomes ahead of the replication fork are disrupted, perhaps by FACT. ASF1 accepts the evicted histones and donates them to CAF-1 for deposition on the newly-synthesised DNA. This process requires histones to be acetylated. ASF1 interacts with the MCM replicative helicase complex via a histone H3-H4 bridge; its is, thus, ideally placed to co-ordinate histone dynamics with replication fork progression.

The function of Asf1 phosphorylation, however, is not known. It is known, however, that evicted histones become trapped with ASF1 when histone deposition is blocked upon replication arrest (Jasencakova et al., 2010). It is thought that these histones are then made available for deposition when DNA replication recommences. Supporting the importance of maintaining the balance between histone levels and DNA synthesis, depletion of ASF1 impedes S-phase progression in mammals (Groth et al., 2005) and, in yeast, *ASF1* deletion causes replication fork collapse and hypersensitivity to agents that interfere with DNA replication (Le et al., 1997; Tyler et al., 1999).

1.13.4 Plant TONSOKU

The link between genetic and epigenetic stability has also been demonstrated in plants. The *TONSOKU*/*BUSHY1*/*MGOUN3* (*TSK*/*BRU1*/*MGO3*) gene was isolated in three independent screens carried out in *Arabidopsis thaliana*: i) a screen for MMS hypersensitivity; ii) a screen for defective transcriptional silencing; and iii) a screen for mutants with developmental problems (Takeda et al., 2004). *TSK* mutants were shown to be hypersensitive to genotoxic stress and displayed a constitutively activated DNA-damage response (Takeda et al., 2004). Further, despite not being required for DNA methylation, *TSK* was found to be indispensable for proper transcriptional silencing, leading to the hypothesis that TONSOKU maintains appropriate chromatin structure (Takeda et al., 2004). Abolishing TONSOKU function may disrupt chromatin, which could, in its turn, affect DNA replication in a manner similar to CAF-1 mutations in human cells. This is supported by experimental data showing that TSK is expressed in S-phase and its defects arrest cells at the G2/M phase of the cell-cycle (Inagaki et al.,

2006; Suzuki et al., 2005). *TSK* mutants were also isolated in screen for developmental problems. It was shown, indeed, that *TSK* is required for the correct organisation of root apical meristem (RAM) and shoot apical meristem (SAM), which are organised pools of actively-dividing and undifferentiated cells that support adult organogenesis in plants. This is intriguingly reminiscent of the developmental problems caused in vertebrates by mutations in the DNA-damage response. Furthermore, since RAM and SAM contain highly-proliferative cells, it supports a role for *TSK* in DNA replication. The precise mechanism by which *TSK* supports DNA replication-related chromatin assembly is unknown. Since it contains two protein-interaction domains – namely tetracortico-peptide-repeats (TPR) and leucine-rich-repeats (LRR) domains – it is thought that it could act as a scaffold.

1.14 Inducing DNA damage in the laboratory

Our ability to study the cellular response to DNA damage and to replication stress relies on the ability to introduce specific DNA lesions. DSBs, for instance, are induced by ionizing radiation (IR) exposure or by treatment with radiomimetic chemicals. Random energy deposition by IR leads to a wide array of DNA lesions, including DSBs, SSBs and many different types of base damage, though it is widely accepted that that the lesion responsible for the traditional radiobiological effects is the DNA DSB (Ward, 1985, 1995). The DSB caused by IR results from radicals formed in clusters as a result of the non-homogeneous deposition of radiation energy reacting with DNA (Ward, 2002). IR-induced DSBs often contain modified bases at their 3'- and 5'-ends, for example, the majority of these breaks have a 3'-phosphate or 3'-phosphoglycolate (Henner et al.,

1983). Intermediary metabolic products of *Streptomycetes*, including bleomycin, neocarzinostatin and related compounds, induce DSBs directly by attacking specific carbons in deoxyribose, also leaving non-standard end-groups (Henner et al., 1983; Kross et al., 1982).

Over-expressing a specific endonuclease within a eukaryotic cell can induce single, site-specific DSB and the contribution of the various DSB repair pathways to the repair of this break can be assayed. For example, a site-specific DSB can be generated in yeast when the recognition site for the HO (homothallic) endonuclease is inserted in a yeast chromosome (Rudin and Haber, 1988). Recombination reporter substrates have also been designed for integration into mammalian cells, where DSBs can then be introduced by the RAG recombinase or, more commonly, the rare-cutting I-SceI endonuclease (Pierce and Jasin, 2005; Pierce et al., 1999; Weinstock et al., 2006).

Cisplatin is an alkylating-like agent that introduces DNA inter-strand crosslinks (ICLs) and other non-functional adducts (Noll et al., 2006). ICLs prevent the separation of DNA strands, thus blocking DNA replication. Because of its effect on replication, cisplatin targets highly proliferative cells in particular, a characteristic that has been exploited in cancer-treatment (Andreassen and Ren, 2009; McHugh et al., 2001; Sanderson and Shield, 1996).

Another commonly-used laboratory genotoxin is hydroxyurea (HU). HU does not induce DNA damage; instead, it interferes with DNA replication by stalling replication forks

(Rosenkranz and Levy, 1965; Skoog and Nordenskjöld, 1971; Slater, 1973). It acts by inhibiting the enzyme ribonucleotide reductase (RNR), which catalyzes the formation of deoxyribonucleotides from ribonucleotides. This is the rate-limiting step for DNA synthesis, thus HU potently inhibits the progression of DNA replication forks. This inhibition effectively uncouples DNA polymerase from the replicative helicase, leading to the creation of stretches of ssDNA, which in their turn activate replication checkpoint (Elledge, 1996; Lopes et al., 2001; Sogo et al., 2002). Checkpoint kinases activate a pathway that, among others, acts to maintain and increase dNTP levels. Thus, HU treatments help to assess the cellular response to stalled replication forks.

Another laboratory drug that interferes with replication is the alkylating agent methylmethane sulfonate (MMS) (Beranek, 1990; Wyatt and Pittman, 2006). MMS is an electrophilic agent capable of reacting with a number of nucleophilic sites on DNA. Since the N^7 position of guanine and the N^3 position of adenine are the strongest nucleophilic centres on DNA, 7-methylguanine (N^7-MeG) and 3-methyladenine (N^3-MeA) are the predominant adducts from MMS (Wyatt and Pittman, 2006). MMS-induced lesions potently inhibit DNA replication and activate the replication checkpoint (Larson et al., 1985; Tercero and Diffley, 2001). Base excision repair, homologous recombination and DNA damage tolerance pathways all co-operate to facilitate replication fork progression through alkylated DNA (Vazquez et al., 2008).

Topoisomerase inhibitors also interfere with DNA replication. Camptothecin (CPT) is a naturally-occurring alkaloid that inhibits DNA topoisomerase I (TOP1). As described in section 1.10, TOP1 relaxes DNA supercoiling by nicking the DNA and enabling the broken strand to rotate around the TOP1-bound DNA strand (Fig. 1.5). This cleavage

intermediate complex (TOPIcc) is very transient and, once DNA is relaxed, TOP1 quickly reverses the covalent binding to DNA, thereby religating the break (Wang, 2002). Camptothecin binds to and stabilises TOP1cc, thereby forming a ternary complex that cannot progress to the re-ligation step. Thus, camptothecin introduces a nick in the DNA specifically in S-phase cells. The replication machinery collapses upon encountering the nick, creating a DSB. It is important to note that TOP1cc can also be trapped during cellular growth, as demonstrated by the existence of a specific enzyme, TDP1 (tyrosyl-DNA-phosphodiesterase), that cleaves the phosphodiester bond linking the active site tyrosine of eukaryotic type I topoisomerases to DNA (Interthal et al., 2001; Pommier et al., 2006; Pouliot et al., 1999b). Doxorubicin (also referred to as adriamycin) is another naturally-occurring topoisomerase inhibitor (Cutts et al., 2005; Tewey et al., 1984). It inhibits topoisomerase II (TOP2) by trapping a DNA-TOP2 intermediate in a ternary complex in a manner very similar to that of camptothecin (Frederick et al., 1990). Like camptothecin, doxorubicin create a single-strand break specifically during DNA replication, thereby causing replication fork collapse (Pommier, 2006). Because of their selectivity, camptothecin and doxorubicin provide a powerful way to study the factors associated in the cellular response to replication fork collapse.

Increasingly, studying the recruitment of specific proteins to DNA damage sites has been aided by the use of laser micro-irradiation (Limoli and Ward, 1993; Rogakou et al., 1999). Cells are treated with the halogenated nucleotide analogue bromodeoxyuridine (BrdU), so that it is incorporated within the DNA. This sensitizes the DNA in such a way that subsequent laser UVA radiation (generally of wavelengths within the 337–405 nm range) can be absorbed to cause lesions. This technique causes different types of lesions,

including SSBs, DSBs and pyrimidine dimers (Kong et al., 2009). Although this limits its usefulness in dissecting the contribution of various factors to different DNA-damage response pathway, laser micro-irradiation is a powerful way of analysing the kinetics and recruitment of factors to sites of DNA damage.

Chapter II

2 Materials and methods

2.1 Materials

2.1.1 Chemicals and instruments

Protein G-sepharose, HiLoad 26/60 Superdex 200 preparative grade gel filtration column and enhanced chemiluminescence reagent (ECL) were from Amersham Pharmacia Biotech/GE Healthcare (Little Chalfont, Buckinghamshire, U.K.). Molecular biology grade filter pipette tips and PCR tubes were from Axygen Scientific Inc. (CA, U.S.A). Glycerol, methanol, isopropanol, acetic acid, acetone, ethanol, tris(hydroxymethyl)methylamine (Tris), manganese chloride, magnesium acetate, sucrose, sodium orthovanadate, sodium ethylenediaminetetraacetate (EDTA), sodium chloride, sodium dodecyl sulphate (SDS), sodium acetate, and 2-mercaptoethanol (biochemical grade) were from BDH Chemicals Ltd. (Lutterworth, Leics., UK). Centrifuges and rotors were from Beckman Instruments Inc. (Palo Alto, U.S.A.). FACSsafe, FACSclean, FACSrinse, FACScalibur, and BD LSR were from Becton Dickinson (BD Biosciences, San Diego, U.S.A.). Sterilin plates were from Bibby-Sterilin Ltd (Stone, Staffordshire, U.K.). Unstained SDS standards (broad range), gel filtration standards, Mini-Cell tank, cellophane support were from BioRad (Hertfordshire, UK). Spin-X columns were from Corning Incorporated (NY, U.S.A.). Tissue culture plasticware were also from Corning Incorporated (NY, U.S.A.), Greiner (Frickenhausen, Germany) or Nunc (Roskilde, Denmark). Cell scrapers were from Costar (Cambridge,

MA, U.S.A.). Class II microbiological safety cabinet was from Envair (Lancs, U.K.). Biophotometer and UVettes were from Eppendorf (Hamburg, Germany). Acrylamide:bis-acrylamide (40% (w/v) 29:1) solution was from Flowgen Bioscience (Nottingham, U.K.). Nuclease free water, phenol:chloroform:isoamyl alcohol and ammonium formate were from Fluka (Sigma-Aldrich, Poole, Dorset, U.K.). Microcystin-LR was from GIBCO BRL/Life Technologies Inc (Paisley, UK). DMEM, RPMI, McCoy's 5A, Dulbecco's phosphate buffered saline (PBS), heat-inactivated FBS (fetal bovine serum), cell dissociation buffer, penicillin/streptomycin, L-glutamine, trypsin-EDTA without Ca^{2+} or Mg^{2+}, Hepes (1 M, pH 7.4), puromycin, the neomycin analogue G418, TOPO-TA and TOPO-XL cloning kits, agarose (electrophoresis grade), colloidal blue staining kit, pre-cast NuPAGE Novex 4-12% Bis-Tris polyacrylamide gels, NuPAGE 4-12% Tris-Glycine polyacrylamide gels, NuPAGE MOPS running buffer (20x), NuPAGE Tris-Glycine running buffer (10x), NuPAGE LDS Sample Buffer (4x), NuPAGE Transfer Buffer (20x), NuPAGE Tris-Glycine Transfer Buffer (25x), and X-Cell SureLock Mini-Cell electrophoresis system, 1 kbp DNA ladder, protein G Dynabeads were from Invitrogen (Paisley, U.K). Liebovitz's medium was from Gibco. IgG–free BSA was from Jackson Immunoresearch (Suffolk, U.K.). Autoradiography cassettes with intensifying screens and X-ray film for detecting ECL were from Kodak (Liverpool, U.K.). The Konica SRX-101A automatic film processor was from the Konica Corporation (Japan). Cellulose filters (0.22 μm and 0.45 μm), Steriflip columns, and sterile filters (0.22 μm) were from Millipore Ltd. (Norwich, UK). Isopropyl thio-β-D-galactoside (IPTG), geneticin (G418) and dithiothreitol (DTT) were from Melford Laboratories (Ipswich, UK). LEEC CO_2 incubators were from Merck (Dorset, U.K.). Restriction enzymes were from New England Biolabs (Beverly MA, U.S.A.).

Oligonucleotides were synthesised by the Oligonucleotide Synthesis Service (University of Dundee). siRNA oligonucleotides and siMAX Universal Buffer were from MWG Biotech (Germany). Coomassie protein assay reagent (Bradford reagent), bovine serum albumin (BSA) for protein standard determination and HRP-conjugated secondary antibodies were from Pierce (Cheshire, UK). Skimmed milk powder (Marvel) was from Premier Brands (Stafford, UK). Trypsin, RNasin and single stranded herring sperm DNA were from Promega (Southampton, U.K.). QIAGEN Plasmid Mini kit, Maxi kit, RNeasy kit, QIAQuick Gel Extraction kit, HiPerFect siRNA-transfection reagent and Ni^{2+}-nitrilotriacetate (NTA) agarose were from Qiagen (Crawley, U.K.). Acetonitrile (HPLC grade) and trifluoroacetic acid were from Rathburn Chemicals (Walkerburn, U.K.). Polyplus siRNA-transfection reagent was from PolyPlus Transfection (Ilkirch, France). T4 DNA ligase, alkaline phosphatase, RNaseA, High Fidelity and Long Template PCR kits, dithiothreitol (DTT), Polymerase Chain Reaction (PCR) Nucleotide Mix, adenosine 5'-triphosphate, and Complete protease inhibitor cocktail tablets (which inhibit metallo-, aspartyl-, cysteine-, and serine- proteinases) were from Roche (Lewes, UK). Nitrocellulose membranes were from Schleicher and Schuell (Anderman and Co. Ltd., Surrey, UK). Herring sperm DNA, Ponceau S solution, hydroxyurea (HU), methyl methanesulphonate (MMS), camptothecin (CPT), doxorubicin, cisplatin, ampicillin, chloramphenicol, phenol: chloroform: isoamyl alcohol (25:24:1), kanamycin, foetal bovine serum (FBS), dimethyl sulphoxide (DMSO), proteinase K, t-octylphenoxypolyethoxyethanol (Triton) X-100, polyethylene glycol sorbitan monolaurate (Tween-20), Coomassie brilliant blue G-250, bromophenol blue, ammonium persulphate, N,N,N',N',-tetramethylethylenediamine (Temed), iodoacetamide, L-arginine, L-lysine, L-methionine and calf thymus DNA (CT-DNA)

were from Sigma-Aldrich (Poole, U.K.). ClonNAT (nourseothricin) was from Werner BioAgents (Jena, Germany). Vydac C18 reverse phase HPLC column was from The Separations Group (Hesperia, U.S.A.). Neubauer haemacytometer and Giemsa staining solution were from VWR (Leicestershire, U.K.). 3MM chromatography paper was from Whatman International Ltd. (Maidstone, UK). All other chemicals were of the highest purity grade available from Sigma-Aldrich (Poole, Dorset, UK) or from BDH Chemicals Ltd. (Lutterworth, UK).

2.1.2 Peptides

The α-factor yeast mating pheromone peptide (WHWLQLKPGQPMY) was synthesized by Dr Graham Bloomberg (University of Bristol).

2.1.3 Plasmids and oligonucleotides

The plasmids used in the thesis were constructed by Dr Rachel Toth or Thomas Macartney (Cloning Team, DSTT, University of Dundee) unless otherwise indicated. The plasmids and their sources are described in Table 2.1. The sequences of all constructs were verified by the DNA Sequencing Service (University of Dundee) by full sequencing of both strands. All the oligos used in this thesis were generated by the Oligonucleotide Synthesis Service; their sequences are listed in Table 2.2.

Name	Plasmid	Source
pRS416	pRS416	Stratagene
pYES	pYES	Invitrogen
DU11763	pRS416-*MMS1*	Dr. R. Toth
DU11724	pYES2-*MMS22*	Dr. R. Toth
pGHOT	pHO-TRP1-GAL3	Dr. M. Fasullo
pHar001	pYES2-GAL-*RAD51*	Prof. H. Klein
p4399	Replaces *KANMX* with *NAT* after EcoRI digest	Cross (1997)
pJM500	p*SGS1-URA3*	Mullen et al (2000)
pSA22	Disrupts *RAD52* with *TRP1* following SalI digest	Dr. D. Weaver
DU16031	pGEX6P MMS22L G944-T1243 (end)	Dr. R. Toth
DU16032	pGEX6P MMS22L M1-L300	Dr. R. Toth
DU19589	pGEX6PB TONSL M1-E300	T. Macartney
DU19569	pGEX6PB TONSL G1079-L1378 (end)	T. Macartney
DU19382	pcDNA5 frtTO FLAG-MMS22L	T. Macartney
DU13156	pcDNA5frtTO GFP	Dr. M. Deak
DU31100	pcDNA5frtTO GFP-TONSL	Dr. R. Toth
DU31198	pcDNA5 FRT/TO MMS22L-FLAG	T. Macartney
DU33261	pcDNA5frtTO GFP-ASF1A	T. Macartney
DU33262	pcDNA5frtTO GFP-ASF1B	T. Macartney
DU19960	pcDNA5frtTO GFP-TONSL c-NLS 1-470	T. Macartney
DU19968	pcDNA5frtTO GFP-TONSL c-NLS 1-680	T. Macartney
DU19969	pcDNA5frtTO GFP-TONSL c-NLS 1-910	T. Macartney
DU19970	pcDNA5frtTO GFP-TONSL c-NLS 1-1028	T. Macartney
DU33010	pcDNA5frtTO GFP-TONSL c-NLS 1029-1378 (end)	T. Macartney
DU33564	pcDNA5frtTO GFP-TONSL n-NLS 400-700	T. Macartney
DU31232	pSuperior.GFP MMS22L_52	Dr. R. Toth
DU31239	pSuperior.GFP MMS22L_54	Dr. R. Toth
DU31237	pSuperior.GFP TONSL_94	Dr. R. Toth
DU31238	pSuperior.GFP TONSL_96	Dr. R. Toth
ASF1A wt	p-EXPR-OneSTrEP-ASF1A wt	Dr. A. Groth
ASF1A V94R	p-EXPR-OneSTrEP-ASF1A V94R	Dr. A. Groth

Table 2.1 Plasmids used in this thesis.

Name	Oligo	Sequence (5' - 3')	Used to
EDO01	MMS1_fwd_100	GCGAGGCATTACCCGCATATTAT	PCR *MMS1* ORF
EDO02	MMS1_rev_100	GCAATACTCAGAGGAATGATCGAT	PCR *MMS1* ORF
EDO03	MMS1_fwd_200	GCCAGAGATGGGCTCTGCAAAAGA	PCR *MMS1* ORF
EDO04	MMS1_rev_200	CGACGCGTAGCACATTGATCGAGA	PCR *MMS1* ORF
EDO05	MMS22_fwd_100	GGCAGCCAGCTTCTACTCTTTT	PCR *MMS22* ORF
EDO06	MMS22_rev_100	GCTTTTCTTGTTACAGAATTGTAT	PCR *MMS22* ORF
EDO07	MMS22_fwd_200	GCGCATCTGCGTGTAAAA	PCR *MMS22* ORF
EDO08	MMS22_rev_200	CCAACACTGATAGATCTTG	PCR *MMS22* ORF
EDO09	MMS1_fwd_800	CGGTTTTCTTTGGTGGAGC	PCR *MMS22* ORF
EDO10	MMS22_fwd_800	GACTGAATCGCTTTGCCTCT	PCR *MMS22* ORF
EDO11	NAT_rev	GTTGACGTTGGTGACCTCCA	PCR *NATMX* cassette
EDO12	ASF1_fwd_100	GGAATAACTCCAAACAGGTAAGA	PCR *ASF1* ORF
EDO13	ASF1_rev_100	GGACTCGTCCAATTTCTTTTT	PCR *ASF1* ORF
EDO14	ASF1_fwd_200	GGGCGTACAACCGACGATGGAA	PCR *ASF1* ORF
EDO15	ASF1_rev_200	GGAAAATATTACTGCCTTTTATTT	PCR *ASF1* ORF
EDO16	RTT101_fwd_100	GCGTAATGATGAATATGAACAAT	PCR *RTT101* ORF
EDO17	RTT101_rev_100	GGGCTGGACGGATTATAAA	PCR *RTT101* ORF
EDO18	RTT101_fwd_200	GGATGTTCAATATTCCTGATTAAGTAT	PCR *RTT101* ORF
EDO19	RTT101_rev_200	GGACAAGAAAGATAGTTTT	PCR *RTT101* ORF
EDO20	RTT107_fwd_250	GCCGCCCACTTTTCACGCG	PCR *RTT107* ORF
EDO21	RTT107_rev_250	GTGGAATAAATGATTCTACTC	PCR *RTT107* ORF
EDO22	RTT107_fwd_500	GCGGGAACTCCAGGGC	PCR *RTT107* ORF
EDO23	RTT107_rev_500	GTTCTTACTAACGTTAGTAGTTGGC	PCR *RTT107* ORF
EDO24	RTT109_fwd_100	CGCGTTGTAAGCTATAATGGAAAATG	PCR *RTT109* ORF
EDO25	RTT109_rev_100	CCTAGAAAGGTGGCGATCAAGGTA	PCR *RTT109* ORF
EDO26	RTT109_fwd_200	GCTTCTGAGATGCATACAATTACTAA	PCR *RTT109* ORF
EDO27	RTT109_rev_200	CCTACCCTCTTATTTATTGTTCCC	PCR *RTT109* ORF

Table 2.2. Oligoucleotides used in this thesis.

2.1.4 Small interfering (si) RNA oligos

siRNA duplexes with a dTdT overhang at the 3' end were purchased from Dharmacon or MWG Biotech. The sequences of all siRNAs used in this thesis are listed in Table 2.3.

Target protein	siRNA name	siRNA target sequence (5'-3')	Source
non-target	siCTRL	GCGCGCUUUGUAGGAUUCG	MWG
ATR	siATR	GGGAGCCUGUUAGACAAGAU	MWG
MMS22	siMMS22L-52	UCACAAAGUCCUUGGAAUA	MWG
MMS22	siMMS22L-54	GGGAGAAAGCAAAGGAAUU	MWG
TONSL	siTONSL-96	CAGUGUAGCUGAAGAUGAA	MWG
TONSL	siTONSL-98	GGGACAAGUGUGUGGCUGA	MWG
RAD51	siRAD51	GAGCUUGACAAACUACUUC	Dharmacon
ASF1A	siASF1A	AAGUGAAGAAUACGAUCAAGU	MWG
ASF1B	siASF1B	AACAACGAGUACCUCAACCCU	MWG

Table 2.3. siRNAs used in this thesis.

2.1.5 Antibodies

The source and the catalogue numbers of all antibodies employed in this thesis are described in Table 2.4. Antibodies against MMS22L, TONSL and GFP were supplied by the DSTT (University of Dundee). The first or the last 300 amino acids of MMS22L or TONSL fused to GST were expressed in bacteria; these protein fragments were used as antigens for injecting into sheep. The antibody purification protocol is described in section 2.2.1.9. All secondary antibodies purchased were horseradish peroxidase (HP) conjugated.

Antigen	Catalogue number	Source
FLAG (M2)	F3165	Sigma

Rad53 (mixture of yN–19 and yC–19)	sc-6748 and sc-6749	Santa Cruz
Mouse IgG (H+L) (HRP)	31430	Pierce
Rabbit IgG (H+L) (HRP)	31460	Pierce
Sheep IgG (H+L) (HRP)	31480	Pierce
Goat (H+L) (HRP)	31402	Pierce
mouse IgG (H+L) (Alexa Fluor® 488)	A-11001	Invitrogen
sheep IgG (H+L) (Alexa Fluor® 488)	A-11015	Invitrogen
rabbit IgG (H+L) (Alexa Fluor® 647)	A-31573	Invitrogen
rabbit IgG (H+L) (Alexa Fluor®594)	A-11012	Invitrogen
mouse IgG (H+L) (Alexa Fluor®594)	A-11005	Invitrogen
sheep IgG (H+L) (Alexa Fluor®594)	A-11016	Invitrogen
STREP	34850	Qiagen
ASF1A (C6E10)	2990	Cell Signalling Technology
ASFIB (C70E2)	2769	Cell Signalling Technology
GAPDH (14C10)	2118	Cell Signalling Technology
MCM2	610701	BD Transduction Laboratories
MCM6	sc-9843	Santa Cruz
MCM7	sc-46687	Santa Cruz
ATR (N-19)	sc-1887	Santa Cruz
53BP1	A300-272A	Bethyl
γ-H2AX	A300-081A	Bethyl
RAD51 (H92)	sc-8349	Santa Cruz
FITC-conjugated active caspase-3	559341	BD Pharmingen
RPA32	ab16850	Abcam
phosphoRPA32 (S33)	A300-246A	Bethyl
phosphoRPA32 (S4/S8)	A300-245A	Bethyl
MMS22L (N-terminus)	S4110	DSTT
MMS22L (C-terminus)	S4111	DSTT
TONSL (N-terminus)	S775	DSTT
TONSL (C-terminus)	S776	DSTT
GFP	S268B	DSTT
CAF1-p150	A301-481A	Bethyl

Antigen	Catalogue number	Source
CAF1-p60	A301-085A	Bethyl
H3	ab1791	Abcam
H4	ab10158	Abcam
H2A	ab18255	Abcam
H2B	ab1790	Abcam
BLM	A300-110A	Bethyl
FBW7	A301-720A	Bethyl
AND1	A301-141A	Bethyl
MRE11 (12D7)	ab214	Abcam
PCNA (PC10)	sc-56	Santa Cruz
cyclin A (6E6)	sc-56299	Santa Cruz
cyclin E (HE12)	sc-247	Santa Cruz

Table 2.4 Antibodies used in this thesis.

2.1.6 Buffers and solutions

10x DNA loading dye: 1.25% (w/v) xylene cyanol, 1.25% (w/v) bromophenol blue, 0.625% (w/v) SDS, 62.5% (v/v) glycerol

2X HBS: 280 mM NaCl, 1.5 mM Na_2HPO_4, 50 mM HEPES, pH 7.0. Aliquoted and stored at –20°C

Bacterial high-salt wash buffer; 1x PBS, 0.3 M NaCl, 0.5% Triton, 0.1% 2-mercaptoethanol

Bacterial low-salt wash buffer; 1x PBS, 0.15 M NaCl, 0.5% Triton

Bacterial lysis buffer: 1x PBS, 6 mM CHAPS, 0.1% (v/v) 2-mercaptoethanol and one tablet of Complete protease inhibitor cocktail per 50 ml buffer

Coomassie staining solution: 50% (v/v) water, 40% (v/v) methanol, 10% (v/v) acetic acid, 0.2% (w/v) Brilliant Blue (G-250)

Coomassie destain solution: 50% (v/v) water, 40% (v/v) methanol, 10% (v/v) acetic acid

Dialysis buffer: 5 mM Tris/HCl pH 7.4, 10 mM NaCl, 0.02% (v/v) 2-mercaptoethanol, 0.01% (v/v) Triton-X100

98% Formamide loading dye: 98% formamide, 0.005% (w/v) bromophenol blue, 0.005% (w/v) xylene cyanol FF, 10 mM EDTA pH 8.0, stored at -20ºC

FPLC buffer A: 50 mM HEPES/KOH pH 7.4, 50 mM NaCl, 0.1% (v/v) 2-mercaptoethanol, sterile-filtered before use

FPLC buffer B: 50 mM HEPES/KOH pH 7.4, 1 M NaCl, 0.1% (v/v) 2-mercaptoethanol, sterile-filtered before use

Gel filtration buffer: 50 mM Tris/HCl pH 7.4, 1 mM EDTA pH 8.0, 150 mM KCl, 0.1% (v/v) 2-mercaptoethanol, sterile-filtered before use

Glutathione elution buffer: 50 mM Tris/HCl pH 7.4, 0.15 M NaCl, 0.1% (v/v) 2-mercaptoethanol, 50 mM glutathione, pH 7.4

Luria Bertani broth (LB): 1% (w/v) tryptone peptone, 0.5% (w/v) yeast extract, 86 mM NaCl. After autoclaving for 20 minutes, and cooling down to less than 50°C ampicillin (Amp) was added to a final concentration of 50 μg/ml (LB/Amp). LB/Amp plates contained additional 2% (w/v) bacto-agar, and were stored at 4°C

Yeast culture medium YPD (yeast extract peptone dextrose): 1% (w/v) yeast extract, 2% (w/v) peptone, 2% (w/v) dextrose (glucose). YPAD-plates contained additional 2% (w/v) agar

YPAD: YPD + 0.01% (w/v) adenine

Minimal medium (SD (synthetic dextrose) medium): 2% dextrose, 0.67% (w/v) nitrogen base without amino acids and bases (amino acids and bases were supplemented as required: 0.08% (w/v) each of adenine, uracil, tryptophane, histidine, arginine, and methionine, 0.12% (w/v) each of tyrosine and lysine, 0.24% (w/v) leucine, 0.2% (w/v) phenylalanine, and 0.8% (w/v) threonine). SD plates contained additional 2% (w/v) agar.

5-Fluoroorotic acid (FOA) plates: SD plates, 0.1% (w/v) 5-FOA, 0.16% (w/v) uracil plus required amino acids and bases

Canavanine plates: SD plates without arginine but with canavanine (60 µg/ml final concentration).

Plates containing genotoxins or other drugs: methyl methanesulphonate (MMS), camptothecin (CPT), hydroxyurea (HU), G-418 (used at final concentration of 200 µg/ml) or ClonNAT (used at final concentration of 100 µg/ml) were added to the YPAD agar after autoclaving and cooling down to less than 50°C.

Mammalian cell lysis buffer (buffer A): 40 mM HEPES pH 7.4, 120 mM NaCl, 1 mM EDTA, 10 mM sodium pyrophosphate, 50 mM sodium fluoride, 1.5 mM sodium orthovanadate, 1% Triton X-100 and one tablet of complete protease inhibitor cocktail per 50 ml buffer

CSK buffer: 10 mM PIPES pH7, 100mM NaCl, 300mM sucrose, 3mM $MgCl_2$

Phosphate-buffered saline (1x): 137 mM NaCl, 2.7 mM KCl. 4.3 mM Na_2HPO_4, 1.47 mM KH_2PO_4. Adjusted to a final pH of 7.4

Blocking buffer for immunofluorescence: 3% (w/v) IgG-free BSA, PBS, 0.2% (v/v) Tween-20

Proteinase K buffer (2X): 200 mM Tris/HCl, pH7.5, 25 mM EDTA, 300 mM NaCl, 2% (w/v) SDS

Tris-acetate-EDTA (TAE) (1x): 40 mM Tris base, 20 mM glacial acetic acid, 1 mM EDTA, pH 8.0

Tris Buffered Saline (TBS): 50 mM Tris/HCl pH 7.5, 150 mM NaCl

TBS-T: TBS, 0.1% (v/v) Tween 20

Tris-borate-EDTA (TBE) (1x): 89 mM Tris base, 89 mM boric acid, 2 mM EDTA, pH 8.0

Tris-EDTA (TE): 10 mM Tris/HCl pH 8.0, 1 mM EDTA pH 8.0

Tris-glycine sodium dodecyl sulphate electrophoresis buffer: 25 mM Tris base, 192 mM glycine, 0.1% SDS (w/v)

Tris-glycine sodium dodecyl sulphate transfer buffer: 48 mM Tris base, 39 mM Glycine

5 x siMAX Universal Buffer: 30 mM HEPES, 100 mM KCl, 1 mM $MgCl_2$, pH 7.3.

2.1.7 Escherichia coli cells.

Competent *Escherichia coli* (*E. coli*) cells (BL21, Top10 or DH5α) were provided by Dr Mark Peggie (Cloning Team, DSTT, University of Dundee).

2.2 General methods

2.2.1 Determination of protein concentration

Protein concentrations were measured by the Bradford method (Bradford, 1976). A standard curve was prepared according to the manufacturer's protocol, by adding increasing amounts of BSA to a final volume of 0.1 ml with water, and then mixing with 0.9 ml Bradford reagent. The mixture was allowed to stand at room temperature for 5 min. The optical density of the standards was measured at 595 nm (OD_{595}) in 1.5 ml

plastic cuvettes against a reference cuvette containing water (0.1 ml) and Bradford reagent (0.9 ml). This was used to construct a standard curve that was employed to determine protein concentrations of cell lysates. On average the linear range of protein Bradford measurements lies between OD_{595} 0.1 and OD_{595} 0.7. Cell lysates were diluted so that the OD_{595} lay in this range. Bradford measurements were performed in triplicate.

2.2.2 Determination of DNA concentration

The absorbance of DNA in aqueous solutions was measured in a disposable 'UVette' at 260 nm with a Biophotometer, using the OD_{260} of sterile water as zero. The integrity of plasmid DNA was assessed by agarose gel electrophoresis.

2.2.3 DNA sequencing

Sequencing of plasmid DNA and PCR products was performed by The Sequencing Service, School of Life Sciences, University of Dundee, using DYEnamic ET terminator chemistry (Amersham Pharmacia Biotech) on Applied Biosystems automated DNA sequencers. For DNA sequences containing a high GC content (typically > 75%), 10% (v/v) of GC-melt solution (Clontech) was added to the sequencing reaction.

2.2.4 Separation of proteins by sodium dodecyl sulphate (SDS) polyacrylamide gel electrophoresis (PAGE)

Protein samples were denatured in lithium dodecyl sulphate (LDS) sample buffer (1x) and β-mercaptoethanol (β-ME) (10% (v/v)). Samples were boiled at 95°C for 5-10 min

before loading onto SDS-polyacrylamide gels. Two different systems were used for SDS-PAGE: the ATTO system for gel electrophoresis coupled with the BioRad system for electrophoretic transfer, and the NuPAGE electrophoresis (4-12% Bis-Tris or Tris-Glycine gels) and transfer system from Invitrogen. Slab gels for the ATTO system were poured between glass plates using separating gel consisting of 0.375 M Tris-HCl pH 8.8, 0.1% (w/v) SDS, 10% (w/v) acrylamide/0.4% (w/v) N, N'-methylene bisacrylamide and 0.075% (w/v) ammonium persulphate. Polymerisation was initiated by the addition of 0.1% (v/v) N, N, N',N',-tetramethylethylenediamine (TEMED). Isopropanol was then layered carefully over the acrylamide solution and polymerisation allowed to proceed for at least 15 min. The isopropanol was removed and stacking gel comprising 0.125 M Tris-HCl (pH 6.8), 0.1% (w/v) SDS. 3% (w/v) acrylamide/0.08% (w/v) N, N'-methylene bisacrylamide, 0.075% (w/v) ammonium persulphate and 0.1% (v/v) TEMED, was poured onto the separating gel top and a 14-well comb added prior to polymerisation and left to set for at least 10 min. Electrophoresis was performed using ATTO gel electrophoresis buffer at a constant voltage of 200 V for 60-90 min. Pre-cast gels were used for all experiments involving Mass Spectrometry. Invitrogen Bis-Tris gels were run in Novex NuPAGE 3-[N-morpholino] propane sulphonic acid (MOPS) running buffer, and Invitrogen Tris-Glycine gels in Tris-Glycine running buffer at 200 V for 60-90 min.

2.2.5 Staining of protein gels

To visualize proteins after SDS-PAGE, gels were stained in Coomassie stain or Colloidal Blue staining solution for 30 min at room temperature with continual agitation on a rocking platform. Gels were destained with destain solution after Coomassie staining or water after Colloidal Blue staining using several changes of the solution until the background staining was greatly reduced.

2.2.6 Immunoblotting

Protein gels were assembled into a gel-membrane sandwich as described in the manufacturer's protocol. Nitrocellulose membrane was placed on a gel, this assembly was placed between two pieces of filter paper (3MM), and this structure in turn was placed between two sponges. All components were pre-soaked in transfer buffer. This assembly was loaded into a BioRad Mini-Cell tank filled with transfer buffer, and proteins were transferred to nitrocellulose at 100 V for 1 h. The nitrocellulose membranes were blocked in TBS-T containing skimmed milk (5% (w/v)) for 1 h at room temperature. Antibodies were diluted in TBS-T containing skimmed milk (5% (w/v)). Most antibodies were used at a final concentration of 1 μg/ml, and the membranes were incubated with the primary antibodies for approximately 2 h at room temperature. Membranes were washed with TBS-T three times for ten minutes, incubated with secondary antibodies conjugated to horseradish peroxidase (all secondary antibodies used at 1:5000 dilutions in TBS-T containing 5% (w/v) skimmed milk) for 1 h at room temperature. After washing, the blot was developed with enhanced chemiluminescence reagent (ECL). ECL reagents 1 and 2 were mixed in equal volumes and 1 ml of the ECL

reagent mix was added to each blot for 1 min. The membrane was then placed in a clean piece of polythene roll that was cut to fit into an autorad cassette. The membrane was then exposed to Medical X-Ray Film (Konica Minolta) and developed in an automatic processor.

2.2.7 DNA agarose gels

The size and the purity of DNA PCR products and plasmids were verified by agarose gels electrophoresis (1% agarose) containing ethidium bromide (0.2 μg/ml). Gels were submerged in TAE (1x) as running buffer in an agarose gel tank. Typically, 500 ng DNA with DNA loading dye (1x) were loaded onto a gel, and 1 kbp DNA ladder from Invitrogen (800 ng) was used as a standard. Gel tanks were normally run at 80 V for approximately 20 min. DNA/ethidium bromide complexes were visualised using a UV transilluminator.

2.2.8 Antibody generation

Recombinant fragments of portions of MMS22L or TONSL (amino acid residues 1-300 or 944-1243 for MMS22L; 1-300 or 1079-1378 for TONSL) fused to GST were used as antigens for antibody production in sheep (Table 2.5). Both antigens were emulsified in Freund's adjuvant prior to injection. As standard protocol, one pre-immune bleed was taken on the same day as the first injection of antigen. Three more injections, one every 28 days, were administered and blood was taken seven days after the second, third and fourth injections. Antisera were raised in sheep at Scottish National Blood Transfusion Service (Penicuik, U.K.). Typically 750 ml of blood was taken per bleed, yielding 250-

350 ml of serum. Each bleed was allowed to clot overnight at 4^{o}C and, following centrifugation for 60 min at 1500 x g at 4^{o}C, the sheep antiserum was decanted through glass wool and stored at -20^{o}C. For purification, the serum was heated for 20 min at 56°C followed by filtration through a 0.45 µM filter. The anti-serum was diluted 1:1 in 50 mM Tris/HCl pH 7.5 with 2% Triton X-100, and anti-GST antibodies were depleted using a column of GST coupled to activated CH-Sepharose. Flow-through fractions were affinity-purified against the relevant antigen, and antibodies were eluted with 50 mM glycine pH 2.5 and neutralized by dialyzing overnight into PBS. Antibodies were purified by the DSTT antibody production team co-ordinated by H. McLauchlan and J. Hastie (University of Dundee).

2.3 Molecular Biology

2.3.1 Polymerase chain reaction (PCR)

PCR reactions were performed using either the Long Template PCR kit or High Fidelity PCR kit. Yeast genomic DNA or plasmid DNA was used as template DNA, and PCRs were performed according to the manufacturer's instructions, in 50 µl volume including PCR buffer (including $MgSO_4$), sense- and anti-sense primer (2.5 µg/ml each), dNTP mix (25 mM), DNA polymerase, plasmid or genomic DNA (100 ng and 500 ng, respectively) and water. PCR reactions were performed on a Peltier Thermal Cycler (MJ Research) in PCR microcentrifuge (0.2 ml) tubes using the following protocol: 95°C for 3 min, 35 cycles of (94°C for 1 min, 50°C for 1 min, and 72°C for 4 min), followed by an incubation at 72°C for 2 min.

2.3.2 Restriction digests of plasmid or genomic DNA

Restriction digests were performed in 50 µl reaction volumes at 37°C for 1 h (plasmid DNA) or overnight (genomic DNA or PCR products). Restriction enzymes were used according to the manufacturer's instructions. Typically, plasmid DNA (2 µg) or genomic DNA (approximately 50 µg) were digested with the relevant restriction enzyme buffer, water, BSA (at final concentration of 100 µg/ml) and restriction enzyme (generally 1 unit of enzyme per 1 µg of DNA).

2.3.3 Transformation of Escherichia coli cells

For each transformation, competent *E. coli* cells (50 µl) from -80°C glycerol stocks were thawed on ice. Plasmid DNA (approximately 50 ng) was added to the cells, mixed gently, and incubated on ice for 5-20 min. To facilitate the uptake of DNA, cells were heat-shocked by incubating the cells at 42°C for 45 seconds and cells were then placed back on ice for a further 2 min. Bacteria harbouring plasmids with ampicillin-resistance genes were streaked directly onto LB/Amp agar plates. For bacteria harbouring plasmids with chloramphenicol-resistance genes, 1 ml of LB was added to the cells, and the cells were allowed to recover at 37°C for 1 h with shaking before plating onto LB/Cml agar plates. Plates were then incubated overnight at 37°C to allow for colony growth.

2.3.4 Preparation of plasmid DNA from bacteria

To prepare small amounts of plasmid DNA in microgram quantities ('Mini-prep'), DH5α *E. coli* cells were transformed with plasmid DNA, and a single colony was inoculated in 5 ml of LB/Amp or LB/Cml. Transformed cells were grown in LB media containing

appropriate antibiotics to stationary phase by incubation at 37°C overnight in a shaking incubator. After centrifugation, plasmid DNA was extracted from the cell pellet by sequential lysis, precipitation and elution on an automated Qiagen BioRobot 9600 using the QIAsoft 3.0 software program, by the DNA Sequencing Service (University of Dundee). The DNA was eluted in sterile water (100 µl) and typically yielded 100-300 µg/ml plasmid DNA. To prepare larger quantities of plasmid DNA, 'Maxi-preps' were performed using the Qiagen DNA Maxi Kit. A single bacterial colony, transformed with the relevant construct was used to inoculate LB (250 ml) containing the appropriate antibiotic. After an overnight incubation at 37°C, the cells were pelleted by centrifugation at 3,000 rpm for 10 min in a J-6 Beckman centrifuge. Plasmid DNA was purified according to the manufacturer's instructions. Overnight cultures of 250 ml typically yielded 0.5-1 mg plasmid DNA.

2.3.5 Purification of GST-tagged proteins from bacteria

The bacterial expression vector encoding the protein to be purified was transformed into BL21 *E.coli*. A single colony of the transformed bacteria was added to 50 ml LB broth containing 100 µg/ml ampicillin and this was incubated overnight in a rotary shaker at 37°C. The 50 ml starter culture was added to 1000 ml LB with ampicillin and allowed to grow until the optical density (OD) at 600 nM was approximately 0.5. The OD of the culture was tested approximately every half hour and more frequently as the OD approached 0.5. Once the bacteria had reached the required OD, protein expression was induced by the addition of isopropyl β-D-1-thiogalactopyranoside (IPTG).

To maximise protein expression, a pilot experiment was carried out for each new protein to determine the optimal growth duration, temperature and IPTG concentration to be used. Typically, the following conditions would be tested: an overnight induction with 0.1 mM IPTG at 16°C and a three hour induction with 1 mM IPTG at 37°C. The amount of protein expressed under these conditions was compared with that from uninduces bacteria and from induced untransformed bacteria. Following induction, bacteria were harvested by centrifugation in a Beckman J6 rotor at 4000 rpm for 20 min at 4°C. The bacterial pellet was resuspended in bacterial lysis buffer (see section 2.1.6) – 30 ml lysis buffer was used for every litre of original culture. The lysate was aliquoted into 50 ml tubes, snap frozen and stored at -80°C until ready for further processing. The lysate was thawed at 4°C, pooled and sonicated on ice three times for 45 sec each with 1 min resting in between to cool. The lysate was cleared by centrifugation at 26,000 rpm for 20 min 4°C. An aliquot (200 µl) named 'cleared lysate' was saved and denatured to test protein expression. Glutathione 4B Sepharose (GSH-Sepharose) was equilibrated in PBS (stored in ethanol) and 1 ml of beads (settled volume) was prepared for every 500 ml of original culture. The sepharose was added to the cleared lysate and incubated rolling at 4°C for 1 hour in a 50 ml tube. The sepharose beads were pelleted by centrifugation at 3000 rpm for 15 min at 4°C. The supernatant was removed and the sepharose was added to 50 ml tubes, approximately 4 ml settled sepharose per tube. Batch washes were carried out; 4 x 50 ml bacterial high salt wash buffer (section 2.1.4) followed by 4 x 50 ml wash buffer (section 2.1.4). GST-fusion proteins were eluted from GHS-sepharose by adding an equal volume of glutathione elution buffer (section 2.1.4). The eluate was collected and a second elution carried out using 50% of the bead volume.

2.3.6 Cloning

The coding region for human TONSL/NFκBIL2 (NCBI Acc. NM_013432.4 GI:187608776) was amplified from IMAGE consortium EST clone 3628374 using primer 5'-gaggatccatgagcctggagcgcgagcttcgccagctgagc-3' and primer 5'-gtgcggccgctcagaggcgccgaaagaagagcttg-3'. The PCR product was digested with BamH1 and Not1 and ligated into pcDNA5 FRT/TO-GFP (a derivative of pcDNA5 FRT/TO (Invitrogen) that contains the cDNA for GFP just upstream of a multiple cloning site) for expression of the fusion protein GFP-NFκBIL2. A mutation (A714V) originating from the EST was mutated back to alanine using mutagenic primers 5'-cagaggcctctcaggcccatgtcagggtctc-3' and 5'-gagaccctgacatgggcctgagaggcctctg-3'. MMS22L (C6ORF167, NM_198468.2) template was obtained from Origene (pCMV6-XL4 C6ORF167). The coding region was PCR-amplified as a NotI-NotI fragment; a FLAG tag was added to the carboxy terminus of this fragment before being cloned into the mammalian expression vector pcDNA5/FRT/TO (Invitrogen, Flp-In T-REx system) for downstream cell-line generation. PCR was performed using KOD Hot Start Polymerase according to the manufacturers protocols (Novagen) with the addition of 3ul DMSO per 50 μl reaction.

2.4 Yeast methods

2.4.1 Yeast cell culture

All *S. cerevisiae* strains used in this thesis and their sources are described in Table 2.5. Yeast cells were cultured at 30°C either in rich YPAD medium or in minimal medium (either in liquid cultures or on agar plates). Yeast cells on agar plates were stored for up

to four months on agar plates at 4°C.

2.4.2 Preparation of glycerol stocks

For long-term storage, glycerol stocks were prepared of all yeast strains. Approximately, 1 ml from an overnight culture (1x 10^8 cells) was mixed with 1 ml of sterile glycerol (final concentration of 20%). The suspension was slowly frozen and stored at –80°C.

2.4.3 Synchronization of yeast cells in G1 or G2 phases of the cell cycle

For experiments including cell cycle arrest or release, cells in early–log phase (OD_{600} of 0.5) were synchronised in G1 by the addition of α–factor (5 μg/ml) until small unbudded cells accounted for >90% of the cell population. To synchronise cells in G2, nocodazole (15 μg/ml) and DMSO (1%) were added to early–log phase cells until large dumb–bell shaped cells accounted for >90% of the cell population. Release from arrest was achieved by quickly filtering and extensively washing the cells with YPAD before incubation in pre–warmed medium.

2.4.4 Preparation of carrier DNA for yeast transformations

Herring sperm DNA (1 mg) was dissolved in water (200 μl), and an equal volume of phenol:chloroform:isoamyl alcohol (25:24:1) was added. The mixture was centrifuged for 15 min at 13,000 rpm, the upper (aqueous) layer was removed to an Eppendorf tube, and DNA was precipitated by adding sodium acetate (to final concentration of 0.15 M) and isopropanol (to a final concentration of 50% (v/v)). After gentle mixing, tubes were placed at -20°C for 15 min and then centrifuged for 15 min at 4°C. The DNA pellet was

washed with 70% ethanol (0.5 ml per tube) and resuspended in water (0.2 ml). The DNA was precipitated for a second time, washed again with 70% ethanol, and resuspended in water (0.5 ml). The carrier DNA was sonicated (15 sec at 30%), boiled, and the single stranded DNA was frozen away in aliquots and kept at -20°C.

Strain	Genotype	Background	Source
W303-1A	MATa *ade2-1 can1-100 his3-11,15 leu2-3,112 trp1-1 ura3-1 rad5-535*	W303	Thomas & Rothstein (1989)
BY4741	MATa *his3Δ1 leu2Δ0 met15Δ0 ura3Δ0*	BY4741	Euroscarf
EDY1	*mms1Δ::KANMX*	BY4741	Euroscarf
EDY2	*mms22Δ::KANMX*	BY4741	Euroscarf
EDY3	*rad52Δ::KANMX*	BY4741	Euroscarf
EDY4	*asf1Δ::KANMX*	BY4741	Euroscarf
EDY5	*rtt107Δ::KANMX*	BY4741	Euroscarf
EDY6	*rtt101Δ::KANMX*	BY4741	Euroscarf
EDY7	*rtt109Δ::KANMX*	BY4741	Euroscarf
EDY8	*mms1Δ::kanmx::NAT*	BY4741	This thesis
EDY9	*mms22Δ::kanmx::NAT*	BY4741	This thesis
EDY10	*BY4741 mms1Δ::KANMX mms22Δ::kan::NAT*	BY4741	This thesis
DDY053	*mec1Δ::TRP1 sml1-1*	W303	D'Amours & Jackson (2002)
YB163	MATa-*inc ura3-52 his3-Δ200 ade2-101 lys2-801 trp1-Δ1 gal3–trp1::[his3-Δ3'::HOcs his3-Δ5'*	S288c	Fasullo et al. (2001)
YB177	YB163 *rad51Δ::URA3*	YBI63	Fasullo et al. (2001)
EDY11	YB163 *mms1Δ::kanmx::NAT*	YBI63	This thesis

Strain	Genotype	Background	Source
EDY13	YB163 *asf1Δ::KANMX*	YBI63	This thesis
EDY14	YB163 *rtt107Δ::KANMX*	YBI63	This thesis
EDY15	YB163 *rtt101Δ::KANMX*	YBI63	This thesis
EDY16	YB163 *rtt109Δ::KANMX*	YBI63	This thesis
MR966	MATa *ura3-52 leu2-3,112 trp1-289 his1-7*	SK1	Resnick et al. (1984)
MR93-28c	*MATα ura3-52 leu2-3,112 trp1-289 his1-1*	SK1	Resnick et al. (1984)
MR101	MATa/α *MR966/MR93-28c*	MR966/MR93-28c	Miyajima et al. (2000)
EDY17	MR966 *mms1Δ::KANMX*	MR966	This thesis
EDY18	MR93-28c *mms1Δ::kanmx::NAT*	MR93-28c	This thesis
EDY19	MR966 *mms22Δ::KANMX*	MR966	This thesis
EDY20	MR93-28c *mms22Δ::kanmx::NAT*	MR93-28c	This thesis
EDY21	MR101 *mms1Δ::KANMX / mms1Δ::kanmx::NAT*	MR101	This thesis
EDY22	MR101 *mms22Δ::KANMX / mms22Δ::kanmx::NAT*	MR101	This thesis
GA2321	*MATinc-URA3 hml::ADE1 hmr::ADE1 ade3::GALHO*	W303	Luke et al. (2006)
GA2368	GA2321 *rad52Δ::LEU2*	GA2321	Luke et al. (2006)
EDY23	GA2321 *mms1Δ::kanmx::NAT*	GA2321	This thesis
EDY24	GA2321 *mms22Δ::kanmx::NAT*	GA2321	This thesis
EDY25	BY4741 *hho1Δ::KANMX*	BY4741	Euroscarf
EDY26	BY4741 *hho1Δ::KANMX mms1Δ::kan::NAT*	BY4741	This thesis
EDY27	BY4741 *hho1Δ::KANMX mms22Δ::kan::NAT*	BY4741	This thesis
K6745	MATa *ade2-1 trp1-1 can1-100 his3-11,15 leu2::LEU2tetR-GFP ura3::3xURA3tetO112*	W303	Michaelis et al. (1997)
K6751	K6745 *scc1-73::TRP1*	K6745	Michaelis et al. (1997)

Strain	Genotype	Background	Source
EDY29	K6745 *mms1Δ::kanmx::NATMX*	K6745	This thesis
JMY1462	MATa *ade2-1; ade3::hisG; ura3-1; his3-11,15; leu2-3,112; trp1-1; mus81-10::KAN; sgs1-20::HGR; can1-100; RAD5; +pJM500*	W303	Mullen et al (2000)
EDY30	JMY1462 *rad52Δ::TRP1; + pJM500*	JMY1462	This thesis
EDY31	JMY1462 *mms1Δ::kanMX::NAT; + pJM500*	JMY1462	This thesis
EDY32	JMY1462 *mms22Δ::kanMX::NAT; + pJM500*	JMY1462	This thesis
UCC1188	MATa *leu2Δ1 lys2-801 trp1 ura3 hhf1-hht1::LEU2 hhf2-hht2::HIS3 RDN1::URA3,* pMP9 *(LYS2 CEN ARS)-HHF2-HHT2*	BY4705	van Leeuwen et al. (2002)
EDY33	UCC1188 *mms1Δ::KANMX*	UCC1188	This thesis
EDY34	UCC1188 *mms22Δ::KANMX*	UCC1188	This thesis
UCC1369	MATa *ade2::hisG his3Δ200 leu2Δ0 lys2Δ0 met15Δ0 trp1Δ63 ura3Δ0 adh4::URA3-TEL-VIIL ADE2-TEL-VR hhf2-hht2::MET15 hhf1-hht1::LEU2,* pMP9 *(LYS2 CEN ARS)-HHF2-HHT2*	BY4705	van Leeuwen et al. (2002)
EDY35	UCC1369 *mms1Δ::KANMX*	UCC1369	This thesis
EDY36	UCC1369 *mms22Δ::KANMX*	UCC1369	This thesis
UCC7262	MATa *ade2 his3 leu2 lys2 ura3 hhf1-hht1::LEU2 hhf2-hht2::MET15 ADE2-TEL-VR hmr::URA3,* pMP9 *(LYS2 CEN ARS)-HHF2-HHT2*	BY4705	Brachmann et al. (1995)
EDY37	UCC7262 *mms1Δ::KANMX*	UCC7262	This thesis
EDY38	UCC7262 *mms22Δ::KANMX*	UCC7262	This thesis

Strain	Genotype	Background	Source
EDY39	UCC7266 *mms1Δ::KANMX*	UCC7266	This thesis
EDY40	UCC7266 *mms22Δ::KANMX*	UCC7266	This thesis
QZY013	MATa *ade2-101(och) his3Δ300 lys2-801(amb) trp1Δ901 ura3-52 hht1,hhf1::LEU2 hht2,hhf2::HIS3 adh4::URA3-TEL, pFX04 (CEN4/ARS1/TRP1, HHT2 and HHF2 under native promoter control, H3K56G, parent plasmid is pRM200)*	BY4705	van Leeuwen et al. (2002)

Table 2.5. Yeast strains used in this thesis.

Yeast strains from EUROSCARF (EUROpean Sacharomyces Cerevisiae Archive for Functional analysis) were purchased from http://web.uni-franfurt.de/fb15/mikro/euroscarf/index.html.

2.4.5 Transformation of yeast cells

For each transformation, approximately 1x 10^7 cells from an overnight culture were pelleted by centrifugation, and almost all medium was taken off leaving approximately 50 µl medium over the pellet. Carrier DNA (20 µg) was added to the suspension together with plasmid DNA (approximately 2-4 µg) or PCR products (approximately 30 ng). Cells and DNA were mixed and resuspended in PLATE mix (0.5 ml) (40% PEG-3500, 0.1 M lithium acetate, 1x TE) and left at room temperature for 2-4 h (plasmid transformation), or overnight (transformation with gene targeting constructs). Cells were incubated for 10 min at 42°C, washed with sterile water (1 ml), and spread onto selective agar plates that then incubated at 30°C for 3 days. If the selection marker was *KANMX* or *kanmx::NAT*, cells were incubated in YPAD (20 ml) for 2 h, shaking at 200 rpm at 30°C, before plating

cells out onto selective agar plates (to allow transcription of genes required for resistance).

2.4.6 Preparation of yeast genomic DNA

To prepare yeast genomic DNA yeast cells were grown overnight at 30°C in YPAD (10 ml) with shaking at 200 rpm. Cells were harvested by centrifugation at 3,000 rpm for 5 min in an Allegra™6R bench-top centrifuge (Beckman), and the cell pellets were resuspended in lyticase buffer (1 M sorbitol, 0.1 M Na_2EDTA (pH 7.5) containing 0.2 µg/ml lyticase) (0.5 ml) before incubation for 60 min at 37°C. Sphaeroplasts were centrifuged at 12,000 rpm for 1 min in a bench-top centrifuge, resuspended in resuspension buffer (50 mM Tris-Cl (pH 7.4), 20 mM Na2 EDTA) (0.5 ml), and after addition of SDS (20%) (25 µl) the suspension was incubated for 30 min at 65°C. Potassium acetate was added (to a final concentration of 0.2 M) and after incubation for 60 min on ice, DNA was centrifuged for 5 min at 13,000 rpm and the supernatant was transferred into a fresh Eppendorf tube. Isopropanol (to a final concentration of 50% (v/v)) was added, and the mixture was incubated at room temperature for 5 min, after gentle mixing. DNA was pelleted by centrifugation for 10 sec at 13,000 rpm. The air-dried DNA was resuspended in resuspension buffer (0.3 ml), RNase A was added (to a final concentration of 0.5 µg/ml) and incubated for 30 min at 37°C. Sodium acetate was added (to a final concentration of 0.3 M), and the DNA was precipitated by addition of isopropanol (equal volume). DNA was collected by centrifugation and resuspended in water (50 µl). Before storage of the DNA at -20°C, insoluble material was removed by centrifugation for 15 min at 13,000 rpm.

2.4.7 Construction of yeast strains

2.4.7.1 Gene disruption: transformation with linearised plasmids

Strain EDY30 was constructed by transformation of strain JMY1462 with plasmid pSA22 that had been digested with SalI, resulting in the disruption of *RAD52* with *TRP1*. After appropriate selection, positive colonies were tested for disruption of *RAD52* by PCR.

2.4.7.2 Gene disruption: transformation with PCR products

To disrupt or replace gene X in yeast strain Y, strain Y was transformed with an open reading frame that had been amplified of genomic DNA from strain Z by PCR. After appropriate selection, positive colonies were tested for disruption or replacement of gene X by PCR. The primers used for PCR verification amplified a larger region that encompasses the one covered by the initial amplification.

Strains EDY17, EDY33, EDY35, EDY37 and EDY39 were constructed by transformation of strains MR966, UCC188, UCC1369, UCC7262 and UCC7266 respectively with *KANMX*-disrupted *MMS1*, amplified by PCR from genomic DNA of strain EDY01, using oligos EDO01 and EDO02. Strains EDY19, EDY34, EDY36, EDY38, EDY36 and EDY40 were constructed by transformation of strains MR966, K6745, UCC188, UCC1369, UCC7262 and UCC7266 respectively with *KANMX*-disrupted *MMS22*, amplified by PCR from genomic DNA of strain EDY02, using oligos EDO05 and EDO06. Strains EDY11, EDY18, EDY26, EDY29 and EDY31 were constructed by transformation of strains YB163, MR93-28c, EDY25, K6745 and

JMY1462 *kanmx::NAT*- disrupted *MMS1*, amplified by PCR from genomic DNA of strain EDY08, using oligos EDO01 and EDO02. Strains EDY12, EDY20, EDY10, EDY27 and EDY32 were constructed by transformation of strains YB163, MR93-28c, EDY01, EDY25 and JMY1462 with *kanmx::NAT*- disrupted *MMS22*, amplified by PCR from genomic DNA of strain EDY09, using oligos EDO05 and EDO06. Strains EDY13, EDY14, EDY15 and EDY16 were constructed by transforming strain YB163 with *kanmx::*-disrupted *ASF1*, *RTT107*, *RTT101* or *RTT109*, respectively. The latter were PCR-amplified from genomic DNA of strains EDY04, EDY05, EDY06 or EDY07, respectively, using oligo pairs EDO012 and EDY13 for *ASF1*, EDO016 and EDY17 for *RTT101*, EDO020 and EDY21 for *RTT107*, and EDO024 and EDY25 for *RTT109*. Strain EDY21 was constructed by mating strains EDY17 and EDY18. Strain EDY22 was constructed by mating strains EDY19 and EDY20.

2.4.7.3 Marker swapping by transformation with targeting constructs

To swap selection marker X in yeast strain Y, strain Y was transformed with a targeting construct that had been digested with relevant restriction enzymes to release the targeting sequence (plasmids are listed in Table 2.1). After appropriate selection, positive colonies were tested for gene X disruption by PCR. Strains EDY08 and EDY09 were constructed by transformation of strains EDY01 and EDY02 respectively with plasmid p4399 which had been digested with EcoRI, to swap the *KANMX* marker cassette with a *kanmx::NAT* marker cassette.

2.4.8 DNA-damage sensitivity assays

The sensitivity of a yeast strain to different genotoxins was determined by spotting a dilution series of a strain onto agar plates with or without genotoxins (the concentrations of MMS, CPT and HU varied depending on the experiment) and evaluating the growth rates after 3 days growth at 30°C. For dilution series a stock of OD_{600} of 0.6 was prepared in water (100 µl). This stock was further diluted three times in a 1 in 10 ratio. Each dilution (5 µl) was spotted onto YPAD agar plates.

2.4.9 Measurement of spontaneous mutation rates

The frequency of forward mutations at the *CAN1* gene locus was determined by the rate of appearance of canavanine-resistant colonies that grew on selective minimal medium plates lacking Arg but containing canavanine (60 µg/ml) (for example Stelter and Ulrich, 2003). Canavanine resistance is caused by inactivation of the *CAN1* gene – encoding an arginine permease that facilitates the uptake of both L-arginine and its analogue L-canavanine (Gocke and Manney, 1979). Canavanine is toxic to cells probably because it disrupts polyamine biosynthesis. The inactivation of the permease by mutation prevents canavanine from entering the cell and renders cells canavanine resistant (Gocke and Manney, 1979). Cultures were grown to stationary phase for 24 h in minimal medium lacking Arg. The OD600 of cells was measured, and from the same culture, in parallel, approximately 2x 10^7 cells were plated onto canavanine plates and 2x 10^2 cells onto YPAD plates. The colonies were counted after incubation at 30°C for 3 days. To calculate spontaneous mutation rates, the number of canavanine resistant colonies per ml culture was divided by the number of colony forming units (on YPAD) per ml culture.

Mutation rates represent the average from three independent triplicate experiments, and the relative rate is calculated from the fold increase or decrease in mutation rate in comparison to the wild type strain.

2.4.10 Measurement of sister chromatid exchange frequency

Strains containing two *his3* fragments, *his3-Delta5'* and *his3-Delta3'* (Fig. 3.5A) were used to measure unequal SCE (uSCE) frequencies by the rate of *HIS3+* recombinants (Dong and Fasullo, 2003). Cells were grown in YPAD to mid–log phase before being treated with MMS (0.02%) or CPT (10 μg/ml) for 3 h. Alternatively, cells were treated with 180 Gy of ionizing radiation. For measuring uSCE induced by an HO endonuclease-induced DSB, cells were transformed with a plasmid expressing HO endonuclease under a galactose-inducible promoter (see Table 2.1). After growth for 24 h in media containing raffinose as the sole carbon source, cells were grown for 4 h in media containing either glucose (to repress HO expression) or galactose (to induce HO expression) as the sole carbon source. After these treatments, approximately 1x 10^6 cells were plated onto minimal medium plates lacking His, and 2.5x 10^2 cells were plated onto YPAD plates. The colonies were counted after incubation at 30°C for 3 days. The rate of SCE is expressed as the number of HIS+ colonies per colony forming unit (on YPAD) and represents the average from three independent triplicate experiments.

2.4.11 Measurement of interchromosomal recombination frequency

The diploid MR101 strain contains the *HIS1* gene deletion fragments *his1-1* and *his1-7* in homologous chromosomes (Fig. 3.8A). Interchromosomal recombination between the

heteroalleles leads to the restoration of histidine prototrophy. Cells were grown in YPAD to mid-log phase and then MMS was added to the indicated concentrations. Approximately $4x10^6$ cells were plated on SC-HIS and 400 cells on YPAD. Colonies were counted after incubation at 30^oC for 3 days. The rate of interchromosomal recombination is expressed as the number of HIS^+ colonies per colony forming unit (on YPAD) and represents the average from at least three independent experiments.

2.4.12 Measurement of HRD-mediated DSB repair

This assay makes use of strain GA2321. In this strain the silent mating-type loci *HML* and *HMR* are deleted, an HO-inducible site is introduced in the MAT locus and the HO endonuclease is placed under the galactose-inducible promoter *GAL1,10*. Further, a non-cleavable copy of the *MAT* locus (*MATinc*) is introduced on chromosome V. For a schematic of the assay see Figure 3.10A. When cells are grown in media containing galacatose as the only carbon source, the HO endonuclease is expressed; HO introduces a DSB at the recognition site at the MAT locus on chromosome III. In HR-proficient the DSB is repaired by HR with the MATinc locus on chromosome V, thus allowing cells to survive. In HR-deficient cells, the DSB cannot be repaired and, consequently, cells cannot survive in galactose-containing media. This assay has been described previously (Luke et al., 2006).

2.4.13 Assaying sister chromatid cohesion

To test the role of *MMS1* and *MMS22* in cohesion, a microscopy-based assay was used as described previouslt (Michaelis et al., 1997). *MMS1* or *MMS22* were deleted in a strain

containing a 3x(112 *tetO*) array integrated into the *URA3* locus, 35 kbp away from the centromere on the left arm of chromosome V – strain K6754 from Prof. Kim Nasmyth (Michaelis et al., 1997). This strain also expresses the tet repressor-GFP (tetR-GFP) fusion protein (integrated into the *LEU2* locus). Binding of the fusion protein to the tet operators enabled the visualization of the *ura3*::3x *URA3tetO 112* locus. Cells were grown logarithmically in YPAD medium and then arrested in G2/M phase by synchronising first in G1 by incubating with 5 μg/ml of alpha factor for 90 min, followed by release by incubating in the presence of 15 μg/ml nocodazole for 2 h at 30 °C. Cells were treated with 0.033% MMS and then fixed by incubation with an equal volume of 4% paraformaldehyde (in PBS) for 30 min, washed twice with 0.01M phosphate buffer pH 6.6 (K_2HPO_4 and KH_2PO_4) and resuspended in 50 μl of phosphate buffer for cohesion assessment. For every sample, 100 cells were analyzed.

2.4.14 Assaying transcriptional silencing

Silencing of a *URA3* reporter gene integrated at telomere VII-L, *HML*, *HMR* or rDNA was examined by growth of cells on media containing 5-fluoroorotic acid (5-FOA). Cells with silent *URA3* are resistant to 5-FOA, but cells expressing *URA3* are sensitive to 5-FOA due to conversion of 5-FOA into toxic 5-fluorouracil. Early log phase cells were collected and spotted in a 10-fold dilution series onto plates with synthetic complete (SC) media lacking or containing 0.1% 5-FOA. Then the plates were incubated at 30°C for 2-3 days before being photographed. In addition, to quantitate the efficiency of transcriptional silencing, approximately 400 cells were plated on SC media and $4x10^6$ cells on SC media containing FOA. Colonies were counted after incubation at 30^oC for

2-3 days. The efficiency of silencing is expressed as the number of FOA-resistant colonies per colony forming unit (on SC without FOA) and represents the average from at least three independent experiments.

2.4.15 Preparation of yeast cell extract

Cells were grown to mid–log phase in liquid cultures (on average 10 ml) at 30°C shaking at 200 rpm. Cells (approximately 20 x 10^7) were harvested by centrifugation at 3,000 rpm for 5 min at 4°C and were resuspended in TCA (0.5 ml) (20%). After addition of an equal volume of glass beads, cells were lysed by bead beating for 1 min at maximum speed. The TCA lysates were taken off the beads and centrifuged at 13,000 rpm for 5 min. Protein pellets were resuspended in sample buffer (0.2 ml LDS sample buffer that had been adjusted to 0.3 M Tris, pH 8.8). Samples were boiled for 10 min, and approximately 5-10 µl of the TCA lysates were loaded onto gels for western blot analysis.

2.5 Mammalian cell-culture methods

2.5.1 Mammalian tissue culture

All media and buffers used for tissue culture were pre-warmed to 37ºC prior to use and all procedures were carried out under aseptic conditions compliant with biological safety Category-2 regulations. Unless otherwise indicated, the cells were cultured and maintained at 37ºC in a 5 % CO_2 water-saturated incubator. The cells were grown until 80-90 % confluency before splitting for routine maintenance.

2.5.2 Human Embryo Kidney 293 (HEK293) cells

HEK293 cells were purchased from the European Tissue Culture Collection. They were cultured in 150 cm^2 flasks (for routine passaging) or 10 cm dishes (for experiments) in DMEM supplemented with 10 % (v/v) foetal bovine serum (FBS) and 1 % (v/v) penicillin/streptomycin solution. For passaging of cells, the culture medium was aspirated, cells were washed once with sterile Dulbecco's phosphate buffered saline (PBS) and 2 ml of sterile trypsin/EDTA added per flask. Cells were returned to the 37ºC incubator for 5 min. After cells detached from the surface of the flask, they were resuspended to a final volume of 10 ml in complete medium and the clumps of cells broken by passing through a narrow-bore pipette several times. 2 ml of cell suspension was used to seed a 150 cm^2 flask to maintain stocks in 25 ml of complete medium. For experiments, 1 ml of cell suspension was used to seed a 10 cm dish in 10 ml of complete medium.

2.5.3 HeLa cells

HeLa cells were passaged in the same manner as HEK293 cells (section 2.2.4.1). HeLa cells were used in microscopy experiments due to their large size and easily discernable cytoplasm and nucleus. They also adhere more firmly making them particularly suitable for microscopy-based experiments.

2.5.4 U2OS cells

U2OS cells were passaged in the same manner as HEK293 cells (section 2.2.4.1). U2OS cells were used in microscopy experiments due to their large nuclei. They were also used for cell-cycle experiments due to their relatively slow proliferation rate.

2.5.5 Cell freezer stocks

Cell stocks were stored at -196°C in liquid nitrogen; when necessary, growing cells were frozen down to ensure a constant supply. Cells to be frozen for storage were allowed to grow to 90 % confluence; after washing with PBS, trypsin was added to detach cells. Harvested cells were then washed, to remove trypsin, in an excess of normal growth media by centrifugation at 800 rpm for 5 min. The supernatant was removed and after tapping the tube to loosen up the pellet, cells were resuspended in cryogenic storage media (50 % FCS, 10 % DMSO, 40 % DMEM). Cells were resuspended so that 1 ml cryogenic storage media contained the same number of cells that would have been passaged into a new dish. Aliquots of cell suspension (1 ml) were stored in 1.5 ml cryogenic screw top vials (Corning) at -80°C in an insulated box for 24 h, before transfer to the liquid nitrogen cell freezer. This is because, to ensure viability during storage at -196°C, cells must be allowed to cool at a rate slow enough to allow the cells time to dehydrate but fast enough to prevent excessive dehydration damage. A cooling rate of -1°C to -3°C per minute is satisfactory for most animal cell cultures. Larger cells or cells having less permeable membranes may require a slower freezing rate since their dehydration takes longer.

2.5.6 Transient transfection of cells

2.5.6.1 Transfection of HEK293 and HeLa cells

A modified calcium phosphate precipitation method was used to transiently transfect HEK293 or HeLa cells with plasmid DNA. All solutions were formulated in MilliQ-water and sterile-filtered through 0.22 μm pore-size syringe filters. Confluent HEK293 cells were trypsinised as described in section 2.2.2.1 and approximately $4x10^6$ cells per plate were seeded onto ten 10 cm dishes. The cells were allowed to adhere to the plates and recover from the trypsinisation process for 24 h before transfection. For transfection experiments, plasmid DNA was purified using the Qiagen Plasmid Maxi kit (section 2.2.10.3) For each 10 cm dish to be transfected, the indicated amount of plasmid DNA (typically 10 μg) was made up to 50 μl with MilliQ-water in a sterile tube. To this, $CaCl_2$-$2H_2O$ was added to a final concentration of 122 mM, sterile H_2O was added to 500 μl and the solution was mixed by tapping. The DNA/$CaCl_2$ mixture was added dropwise with constant mixing to 500 μl of 2XHBS Buffer. The resulting solution was left for 30 min at room temperature to induce the precipitation of DNA/$CaCl_2$ complexes before pipetting the final 1 ml solution drop-wise onto a 10 cm dish. The cells were then incubated in a 37°C, incubator for 16-20 h before cell lysis. In certain cases (i.e. for larger DNA constructs) 48 h incubation after transfection was required for optimum protein expression.

2.5.6.2 Transfection of U2OS cells

U2OS cells were transiently transfected with GeneJuice (Novagen) according to manufacturers protocol. Confluent U2OS cells were trypsinised as described for HEK293 cells in section 2.2.2.1, and approximately $4x10^6$ cells per plate were seeded onto ten 10 cm dishes. Cells were transfected 18 hrs after initial seeding. For transfection experiments in a 10 cm plate, GeneJuice reagent (30 μl) was added to 1 ml of FBS- and antibiotic-free DMEM medium in a sterile tube. This mixture was agitated gently and left at room temperature for 5 min, at which point plasmid DNA (5 or 10 μg, as indicated) was added. After gently mixing the solution was left at room temperature for 10 min. The mixture was then added dropwise to the cells which were incubated at 37°C in 5 % CO_2.

For the measurement of homologous recombination, as decribed in section 2.2.4.22, U2OS cells were transfected with I-SceI DNA using PEI or with siRNA using DharmaFect (Dharmacon) reagent. The transfections took place in a well of a 96-well plate. For Dharmafect transfection, 1 μl of 2 μM siRNA was diluted in 9 μl OptiMEM (Invitrogen) and 0.1 μl DharmaFect was diluted in 9.9 μl OptiMEM and both solutions were incubated for 5 min before being mixed together and incubated for a further 20 min. The 20 μl solution was added to U2OS cells in antibiotic free DMEM in a well of a 96-well plate. PEI (Sigma-Aldrich) was dissolved in Milli-Q water to make a 100 mg/ml solution then diluted to 1 mg/ml with Milli-Q water and the pH was adjusted to 7.2. DNA vector to be transfected (0.2 μg) was diluted in 50 μl OptiMEM and then 0.25 μg of PEI was added. The solution was mixed and incubated for 20 min before being added to cells in one well of a 96-well dish in 100 μl antibiotic-free DMEM.

2.5.6.3 siRNA transfection

siRNA oligos were received in lyophilised form and were resuspended to a final concentration of 100 μM in siMAX Universal Buffer provided by the manufacturer. 30-40% confluent cells growing in 10cm dishes were transfected with 25 nM of siRNA (MWG Biotech, Germany). For HEK293 cells HBS.$CaCl_2$ was used (see above). For HeLa cells HiPerFect (Qiagen) was used according to manufacturer's protocol. Briefly, siRNA was diluted in 0.5 ml DMEM and then 0.1 ml of HiPerFect was added dropwise; the mixture was vortexed and then incubated for 10 min at room temperature before being added dropwise to a 10 cm dish of cells. For U2OS cells, Interferin (Polyplus) was used according to manufacturer's protocol. Briefly, siRNA was diluted in 0.5 ml DMEM and then 0.1 ml of Interferin was added dropwise; the mixture was vortexed and allowed to incubate for 10 min at room temperature before being added dropwise to a 10 cm dish of cells. After siRNA transfection, cells were incubated at 37°C for 48–60 h, as indicated. The oligo sequences and their sources are listed in table 2.3.

2.5.7 Construction of stable cell-lines

FLP-In T-Rex cells were purchased from Invitrogen. These were used to make cell lines stably expressing FLAG-MMS22L and GFP-TONSL. These cells were passaged as described in section 2.2.2.1 except that media was supplemented with 100 μg/ml zeocin (Invitrogen) to select for the maintenance of the FLP recombination target (FRT) sites and 15 μg/ml blasticidin (Invitrogen) to select for the maintenance of the tetracycline repressor sequence. A schematic diagram illustrating the process of making a stable cell line by this method is shown in fig 2.1. Cells were split into 10 cm dishes containing

DMEM and 24 h later they were transfected using the modified calcium phosphate method as described in section 2.2.3.1 with 1 μg of pcDNA FRT/TO FLAG-MMS22L or pcDNA FRT/TO GFP-TONSL and 9 μg of pOGG44 plasmid from Invitrogen. pOGG44 expresses the FLP recombinase which allows site specific recombination of the sequence of interest. After 48 h, the medium was removed from the cells and replaced with DMEM supplemented with 15 μg/ml blasticidin and 50 μg/ml hygromycin-B. Hygromycin-B was used to select for the integration of the sequence of interest present on the pcDNA plasmid. This media was refreshed every 48 h until colonies began to appear that were visible to eye (approximately 10 days). Drug-resistant colonies were trypsined according to the procedure described in section 2.2.2.1 and "pooled" into one 6 cm plate. The "pooled" colonies were then expanded in media supplemented with blasticidin and hygromycin-B. Cell lines were tested for expression of FLAG-MMS22L or GFP-TONSL by the addition of tetracycline at 1 μg/ml 24 h prior to lysis and subsequent western blotting.

2.5.8 Genotoxin treatments of human cells

Cells were treated with a variety of genotoxins at a range of concentrations as indicated. Doxorubicin, cisplatin and camptothecin were dissolved in DMSO to make 1 M stock solutions, stored at -20 ^{o}C. Hydroxyurea was dissolved in Milli-Q water to make 1 M stock solutions, stored at -20 ^{o}C. Ionising radiation was delivered using a ^{137}Cs radiation source at a delivery rate of 3 Gy/min.

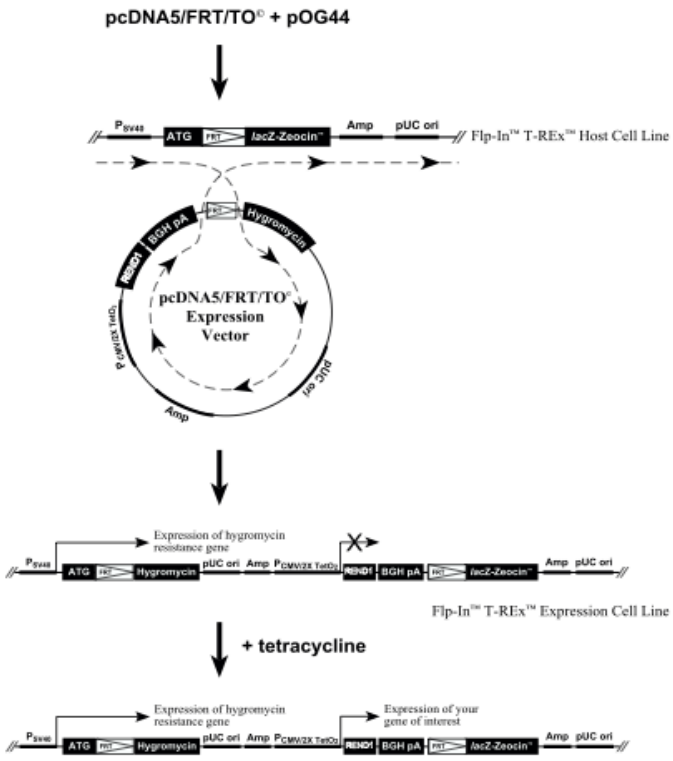

Figure 2.1 Schematic diagram of tetracycline-inducible MMS22L- or TONSL-expressing cell lines (adapted from Invitrogen).

A diagram illustrating the main features of the Flp-In T-rex parental cell line and the pcDNA5 FRT/TO plasmid containing FLAG-MMS22L or GFP-TONSL. Parental cells contain an FRT recombination site and a zeocin resistance gene. pcDNA5 FTR/TO plasmids contain an FRT site and a hygromycin B resistance gene lacking a promoter and ATG initiating codon. FLP recombinase expressed from pOG44 plasmid mediates a homologous recombination event between the FRT sites. Insertion of the pcDNA5 FRT/TO plasmid into the genome brings the SV40 promoter and initiation codon into proximity and frame with the hygromycin-B resistance gene and inactivates the zeocin resistance gene. Expression of epitope-tagged MMS22L or TONSL is controlled by a human cytomegalovirus promoter in which two tandem copies of the tet operator sequence have been insterted. In the absence of tetracycline, the Tet repressor binds to the tet operator sequences and represses transcription of FLAG-MMS22L or GFP-TONSL.

2.5.9 Clonogenic survival assay

HEK293 cells in 10cm dishes were transfected (using HBS.$CaCl_2$) with control siRNA or siRNAs specifically targeting MMS22L, TONSL or ATR. After 48 h, cells were split and seeded into 10 cm dishes at approximately 4000 cells per dish. Cells were allowed to adhere overnight before they were irradiated using a ^{137}Cs radiation source at the indicated doses. Alternatively, cells were incubated with the indicated doses of cisplatin, doxorubicin, camptothecin, methylmethanesulfonate or hydroxyurea for 24h. Cells were subsequently incubated in fresh medium. Between ten and fourteen days later, dishes were washed, fixed and stained with 20% Giemsa solution, and the number of colonies on each plate was counted. Results were normalized to plating efficiencies.

2.5.10 Construction of cell-growth curve after MMS22L or TONSL depletion

After being incubated with siRNA for 48 h, cells were trypsinised as described in section 2.2.2.1, resuspended in 15 ml media and mixed well. An aliquot (200 μl) was taken, diluted one in two with Trypan Blue dye and pipetted carefully (avoiding the introduction of any air bubbles) into a haemocytometer chamber. Trypan Blue dye allowed visualization of dead cells. Live cells within a 0.1 mm area, delimited by a double line (9 small squares) were counted. This count total is equivalent to the number of 1 x 10^4 cells per 1 ml of sample being counted. Cells were then seeded into 10 cm dishes at 30 x 10^4 cells per 1 ml of medium and allowed to adhere for 16 h at which point the first count was performed (day one). Every 24 h from the first count on day one a cell count was done as described. The experiment was carried out in triplicate.

2.5.11 Lysis of cells under native conditions

Plates were placed on ice and the media was aspirated. The cells were washed gently in ice-cold PBS. Ice-cold lysis buffer was added, the cells were scraped and the lysate was placed in a suitable tube. The lysate was centrifuged at 13,000 rpm for 12 min at 4°C (Eppendorfs) and the supernatant transferred to a clean Eppendorf. The lysates were snap frozen in liquid nitrogen and stored at -80°C.

2.5.12 Lysis of cells under native conditions with DSP crosslinker

Where indicated, the reversible crosslinker dithiobis succinimidyl propionate (DSP) was added fresh and dropwise to the lysis buffer. Plates were placed on ice and the media was aspirated. The cells were washed gently in ice-cold PBS. Ice-cold lysis buffer was added, the cells were scraped and the lysate was placed in a suitable tube. The lysate was placed on ice for 30 min, and then Tris-HCl pH 7.4 was added at a final concentration of 0.2 mM to quench the crosslinking action. The lysate was placed on ice for a further 30 min, at which point it was centrifuged at 13,000 rpm for 12 min at 4°C and the supernatant transferred to a clean Eppendorf tube. The lysates were used for immunoprecipitation experiments immediately.

2.5.13 Lysis of HEK293 suspension cells for protein analysis

Logarithmycally growing HEK293 suspension cells were spun down, and an equal volume of 2x cell pellet lysis buffer (section 2.1.4) was added to the cell pellet and mixed by vortexing. Cells were then broken open using a Dounce homogeniser at 4°C. Cells

were then left on ice for 20 min before centrifugation at 20,000 rpm for 45 min. Supernatant was carefully removed and transferred to a clean tube. The lysates were snap frozen in liquid nitrogen and stored at -80°C.

2.5.14 Immunoprecipitation

2.5.14.1 Conjugation of antibodies to Protein-G sepharose

Generally, 1 µg of antibody was conjugated to 10 µl Protein-G Sepharose (PGS). The required volume of PGS was washed 3 times in PBS then re-adjusted to the original volume before addition of the antibodies. The antibody/PGS mixture was mixed on a platform shaker for 2h at 4°C, the beads were washed 3 times with PBS and were stored in their original volume of PBS at 4°C.

2.5.14.2 Immunoprecipitation of protein from native cell-lysates

Generally 1 µg coupled antibody was used for 1 mg extract protein. For large-scale protein interaction studies, 1 µg antibody was used for 5 mg cell extract protein. The antibody-bead conjugate was incubated with cell extract for 2 h at 4°C on a shaking platform or a roller depending on the size of the tube used. The supernatant was removed and the beads washed three times with 1 ml of wash buffer. This was followed by a wash with ice-cold PBS. The immunoprecipitate was denatured in LDS sample buffer, heated at 95°C for 5 min and then subjected to SDS-PAGE (section 2.2.1.5 and 2.2.1.6).

2.5.14.3 Small-scale immunoprecipitation of protein from native cell-lysates

Generally 2 μg coupled antibody or 10 μl FLAG-M2 beads or 10 μl of settled GFP-TRAP beads was used per 3 mg extract. The antibody-bead conjugate was incubated with cell extract for 1 h at 4 °C on a shaking platform or a roller depending on the size of the tube used. The supernatant was removed and the beads washed four times with 500 μl of lysis buffer. Immunoprecipitates were denatured in LDS sample buffer and heated at 95 °C for 5 min. The supernatant was then removed and subjected to SDS-PAGE.

2.5.14.4 Immunoprecipitation of protein from native cell-lysates for large-scale purification

Generally, 100 μl FLAG-M2 beads or 100 μl GFP-TRAP beads was used for each 40 mg extract protein. For FLAG-M2 immunoprecipitation the lysate was first subjected to pre-clearing by incubating with 100 μl agarose beads alone for 30 min at 4 °C on a shaking platform or on a rolling platform depending on the size of the tube used. The supernatant was then used for FLAG immunoprecipitation. The antibody-bead conjugate was incubated with cell extract for 1 h at 4°C on a shaking platform or a roller depending on the size of the tube used. The supernatant was removed and the beads washed four times with 2 ml of lysis buffer. The immunoprecipitate was denatured in an equal volume of 0.5 X LDS sample buffer, heated at 95 °C for 5 min. The suernatant was removed and concentrated by speed-vac to reduce the volume 2-4 fold to an approximate volume of 50 μl before SDS-PAGE.

2.5.15 Mass-spectrometric identification of proteins associated with FLAG-MMS22L or GFP-TONSL

Large-scale immunoprecipitations were carried out as described in section 2.2.4.13.4 and the immunoprecipitate subjected to SDS-PAGE before trypsin digestion of the gel slices.

2.5.15.1 In-gel digestion of proteins for mass spectrometry

To minimise keratin and other exogenous contaminations, all manipulations of gels for mass spectrometry analysis were prepared under a laminar flow hood. Protein bands were excised from a colloidal Coomassie stained gel using a sterile scalpel. Gel pieces were washed with 0.5 ml each of 50% acetonitrile/water, 0.1 M NH_4HCO_3 and 50% acenotrile/50 mM NH_4HCO_3. All washes were performed on a Vibrax shaking platform for 10 min. All liquid was removed between washes. Proteins were then reduced with 10 mM DTT in 0.1 M NH_4HCO_3 (45 min, 65 ^oC) and alkylated with 50 mM iodoacetamide in 0.1 M NH_4HCO_3 (30 min, room temperature). Gel pieces were then repeatedly washed with 0.1 M NH_4HCO_3 and 50% acenotrile/50 mM NH_4HCO_3. Once colourless, the gel pieces were shunk with 0.3 ml acetonitrile for 15 min, the acetonitrile was then then removed and a speed-vac was used to dry the gel pieces. Gel pieces were then swollen in 25 mM triethylammonium bicarbonate with 5 μg/ml of trypsin and incubated over-night at 30^oC on a shaker. After 12 h an equivalent volume of acetonitrile was added to the digest and incubated for a further 15 min. The supernatants were transferred to a clean tube and concentrated to dryness by Speed Vac. Meanwhile 100 μl 50% acetonitrile/2.5% formic acid was added to the gel pieces. This second extraction was combined with the dried first extract. The samples were stored at -20^oC.

2.5.15.2 Mass spectrometry

Liquid chomatography-mass spectrometry (LC-MS) analysis was performed by Dr. David Campbell and Dr. Robert Gourlay. The reconstituted tryptic peptides were injected on to a Dionex 3000 nano liquid chomatography system coupled to a Thermo-Electron LTQ-orbitrap mass spectrometer. Data files (raw files) were converted to MSM files which were then submitted to the in house Mascot server. The data was searched against the IPI-Human database with the oxidation of methionine as a variable modification. Peptide tolerance was 20 ppm for precursor ions and 1.0 Da for fragment ions (MSMS tolerance).

2.5.16 Gel filtration of whole cell extracts of HEK293 cells

Gel filtration samples were a kind gift from Dr Mary Gardiner.

The AKTA Explorer was operated according to manufacturers instructions using Unicorn 4.1 software. All buffers, lysates and markers were sterile-filtered before loading onto the column. The Hiload™ 26/60 Superdex™ 200 preparative grade column was attached and equilibrated overnight with three column volumes of gel filtration buffer (buffer composition is detailed in section 2.1.4). Four 500 ml HEK293 suspension cell cultures were grown to a confluency of 2 million cells per ml (cell number was counted using a haemocytometer, section 2.2.5). Two of the flasks were left untreated, and two were exposed to IR (20 Gy) and allowed to recover for 1 h before washing in PBS. Native lysis buffer (6 ml) containing microcystin was then added to the cell pellet. Lysates were snap-frozen before centrifugation and stored at -80°C until required. The lysates were thawed on ice and cleared by centrifuged at 15,000 g for 30 min. The supernatant was

sterile-filtered on 0.22 μm Steriflip columns and the protein concentration of each lysate was estimated (section 2.2.1.1.). Equal amounts (90 mg, 10 ml) of each protein lysate were loaded onto the Superdex column. Between runs the column was washed through with two column volumes of buffer. Fractions of 1 ml (200) were collected at a flow-rate of 1.5 ml/min. Molecular weight markers from BioRad with added Dextran blue were resuspended in water and were run after the lysates. The void volume of the column is 100 ml (Dextran Blue (2000 kDa) is the marker for the void volume). The 670 kDa marker (thyroglobulin) eluted in fractions 117-129. The 158 kDa marker (bovine gamma globulin) eluted in fractions 165-180. Fractions from 98 to 288 were transferred to Eppendorfs and snap-frozen. 100 μl of every third fraction from 99 to 207 was denatured in LDS sample buffer, boiled for 5 min at 95°C and 5 μl of each denatured fraction was subjected to western blot analysis.

2.5.17 Immunologocal detection of activated caspase-3 by flow cytometry

Cells were seeded onto 3.5 cm dishes at 50% confluency (section 2.2.2.1 for details on exact procedure) and incubated for approximately 16 h to re-adhere to dishes before IR treatment (10Gy). Following treatment, cells were harvested at indicated time-points using standard trypsinisation as described in section 2.2.2.1. To ensure inclusion of any apoptotic cells that had become detached from the bottom of the dish, media was removed and any unattached cells in the media were retrieved by centrifugation and added to the trypsinised cells. The cells were washed once in PBS that had been pre-warmed to 37°C and resuspended in 1% (w/v) paraformaldehyde (1 ml). Cells were then incubated at 37°C for 30 min, collected by centrifugation at 1000 rpm for 5 min, washed

once in PBS and then centrifuged again. Cells were then re-suspended in 70% (v/v) ethanol with mixing during resuspension. Samples were then stored at -20°C for up to two weeks. For antibody staining, samples were brought to room temperature and washed twice in PBS with 1% BSA (w/v) (PBS-BSA). The cell number was adjusted to approximately 5 x 10^5 cells/ml and these cells were collected by centrifugation. Antibody stock solution (20 µl) was added to 100 µl of PBS-BSA and this was added to each cell pellet. Samples were mixed and left in the dark, at room temperature, for 20 min. Cells were then washed once in PBS-BSA (1 ml) and re-suspended in 300 µl of the same buffer before being analysed on a Beckman FACS Calibur Flow Cytometer. Live cells were gated on the flow cytometer using Linear FSC-H and Linear SSC-H and active caspase-3 was detected as Log FL1-H.

2.5.18 Cell-cycle analysis of flow cytometry

Cells were seeded onto 10 cm dishes at 50% confluency. Cells were transfected with siRNA (see section *2.2.4.6.3*) and, after 36 h, cells were harvested using standard trypsinisation as described in section 2.2.2.1, washed once in PBS that had been pre-warmed to 37°C and then resuspended in ice-cold 70% (v/v) ethanol with vortexing during addition. Samples were then stored at -20°C until required. When required, samples were brought to room temperature and washed twice in PBS with 1% (w/v) BSA before resuspension in PBS (300 µl) containing propidium iodide (50 µg/ml), ribonuclease A (50 µg/ml) and TritonX-100 (0.1% v/v). Samples were then incubated at room temperature for 20 min in the dark before analysis by flow cytometry on a Beckman FACS Calibur Flow Cytometer detecting Lin FSC-H, Lin SSC-H and DNA as

Lin FL2-H. FL2-W and FL2-A were used to distinguish single cells. Cell numbers in different cell cycle stages were measured on FlowJo using the Watson Paradigm model.

2.5.19 Indirect immunofluorescence

HeLa or U2OS cells were grown on 13 mm diameter glass coverslips in 6 cm dishes. Cells were washed twice gently with ice-cold PBS before fixation with ice-cold methanol on ice for 10 min. Alternatively, cells were fixed with 2% paraformaldehyde for 10 minutes at room temperature. After fixation, cells were permeabilised with 0.2% Triton X-100 in phosphate–buffered saline for 10 min at room temperature. After several washes in PBS, cells were incubated in blocking solution (section 2.1.6) for 1 h. Coverslips were then incubated with primary antibodies (1 μg/ml) in blocking solution for 1h at room temperature, or for 16 h at 4^{o}C where indicated. After extensive washing in PBS–T (section 2.1.6) coverslips were incubated with secondary antibodies (2 μg/ml) conjugated to FITC, Cy5 or Texas Red for 1h at room temperature. Coverslips were washed thoroughly in PBS–T and mounted on glass slides. Before covering with a cover slip cells were stained with DAPI for 5 min. Slides were viewed using a Deltavision microscope and images were deconvolved after acquisition.

2.5.20 Indirect immunofluorescence with pre-extraction

HeLa or U2OS cells were grown on 13 mm diameter glass coverslips. Cells were washed twice gently with ice-cold PBS before treatment on ice for 5 min with ice-cold 0.2% triton X-100. Cells were then washed three times with ice-cold PBS before fixation in

4% paraformaldehyde for 10 minutes at room temperature and permeabilisation with 0.5% Triton in phosphate–buffered saline for 10 min at room temperature. From here the protocol proceeds as for immunofluorescence without pre-extraction.

For PCNA immunofluorescence, cells were washed in CSK buffer (section 2.1.6), extracted with CSK + 0.5% Triton X-100 for 5min on ice, and rinsed with cold CSK and cold PBS before fixation with 4% paraformaldehyde for 10 min on ice. Protease inhibitor (Roche) was included in the buffers. Subsequently, cells were washed with cold PBS and fixed with ice-cold methanol for 10 min at -20^{o}C. Cells were re-hydrated with cold PBS and immunofluroescence was performed as described above

2.5.21 Laser micro-irradiation

For the generation of localized damage in cellular DNA by exposure to an ultraviolet-A laser beam, cells were plated on glass-bottomed dishes (Willco-Wells) and pre-sensitized with 10 μM 5-bromo-2'-deoxyuridine (BrdU) in phenol red-free medium (Liebovitz's medium) for 24 h at 37°C (Bekker-Jensen et al., 2006; Limoli and Ward, 1993; Lukas et al., 2003). Laser micro-irradiation was performed by using an Olympus IX70 microscope equipped with a 37°C heating stage and a 406 nm laser diode (6 mW). The time of cell exposure to the laser beam was 200 ms (fast scanning mode). Laser settings were chosen that generate a detectable damage response restricted to the laser path in a pre-sensitization-dependent manner without noticeable cytotoxicity. Imaging of live cells was done on the same microscope, using an exposure time of 100 ms. Imaging of fixed cells was done as described above.

2.5.22 Measurement of I-SceI-induced homologous recombination with the DR-GFP reporter

A schematic diagram illustrating the principle of the assay is shown in figure 2.2. U2OS cells harbouring a copy of the DR-GFP recombination reporter (Jasin, 1996), were transfected with 20 nM siRNA, at a density of 8000 cells per 80 μl antibiotic free DMEM, in one well of a 96-well plate, using DharmaFect. Around 24 h post-transfection, a further 150 μl DMEM/well was added. After 24 h, 0.2 μg I-SceI vector was transfected into the cells using PEI (transfections were performed as described in section 2.2.3.1). The media was removed from cells and fresh media added, 24 h post PEI transfection. After 24 h, cells were trypsinized and re-suspended in 100 μl PBS and GFP fluorescence (a measure of successful homologous recombination) was measured by FACS analysis. Live cells were gated on the flow cytometer using forward scatter and side scatter parameters (linear scale), and green fluorescence was detected in the FL2-H channel.

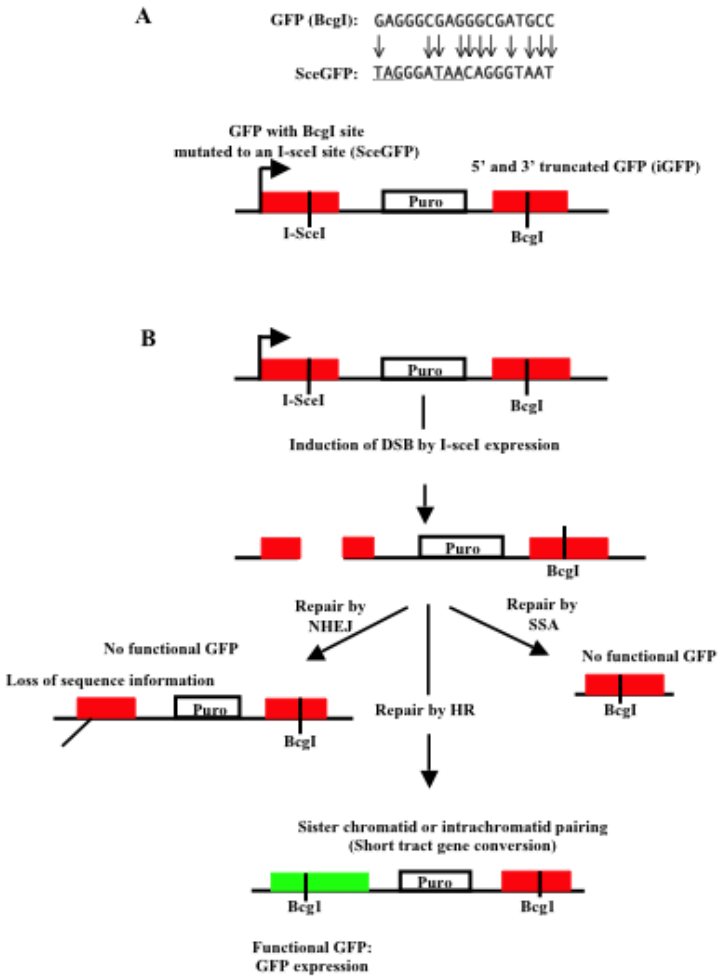

Figure 2.2 Schematic diagram illustrating the principles of the DR-GFP reporter assay. **A.** The DR-GFP recombination reporter used in this study contains a GFP gene (SceGFP) modified to contain an I-SceI cutting site and in-frame termination codons (underlined). Downstream of the SceGFP gene is iGFP, a 5' and 3' truncated GFP gene. **B.** After expression of I-SceI in cells containing the DR-GFP reporter, repair of the DSB can proceed though HR, NHEJ, or SSA. Only a short tract gene conversion will result in restoration of a functional GFP gene.

Chapter III

3 Budding yeast *MMS1* and *MMS22* promote homologous recombination after replication stress

3.1 Introduction

MMS1 and *MMS22* were isolated in a screen for mutants hypersensitive to MMS (Prakash and Prakash, 1977). Mutations in these genes are synthetic lethal with mutations in *MCM10*, a gene essential for the initiation of DNA replication (Araki et al., 2003). *MMS1* and *MMS22* have also been shown to interact genetically with *RTT107/ESC4* (Pan et al., 2006), a gene that has been shown to play an important role in the response to stalled DNA replication (Rouse, 2004). These studies suggested that *MMS1* and *MMS22* are involved in responding to perturbations during DNA replication. I set out to investigate this possibility.

3.2 Results

3.2.1 Cells lacking MMS1 or MMS22 are hypersensitive specifically to agents that perturb replisome progression

I first tested the sensitivity of *mms1Δ* and *mms22Δ cells* to a wide variety of genotoxins: UV light (which causes pyrimidine dimers), hydroxyurea (HU, which slows replisome progression by inhibiting the dNTP supply), methyl methanesulfonate (MMS, which alkylates DNA, thereby causing replisome stalling), camptothecin (CPT, which introduces DNA single-strand breaks, thereby causing replisome collapse) and ionising radiation (IR, which causes DNA DSBs at all phases of the cell cycle) (section 1.14).

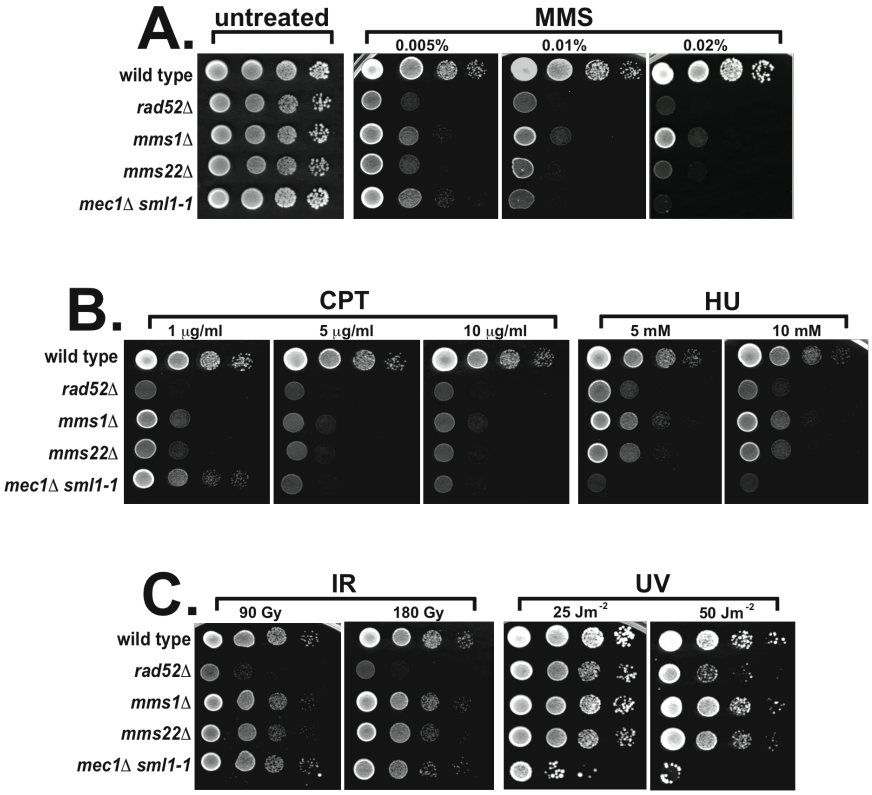

Figure 3.1 Sensitivity of cells lacking *MMS1* or *MMS22* to genotoxins.

(A-C) Strains BY4741 (wild type), *rad52Δ*, *mms1Δ*, *mms22Δ* or *mec1Δsml1-1* were grown to saturation in liquid culture; ten-fold serial dilutions were spotted on YPAD agar and left untreated or exposed to the indicated doses of IR or UV. Alternatively, cells were spotted onto YPAD agar plates containing MMS, CPT or HU at the indicated concentrations. Cells were subsequently incubated at 30^{o}C for 3 days.

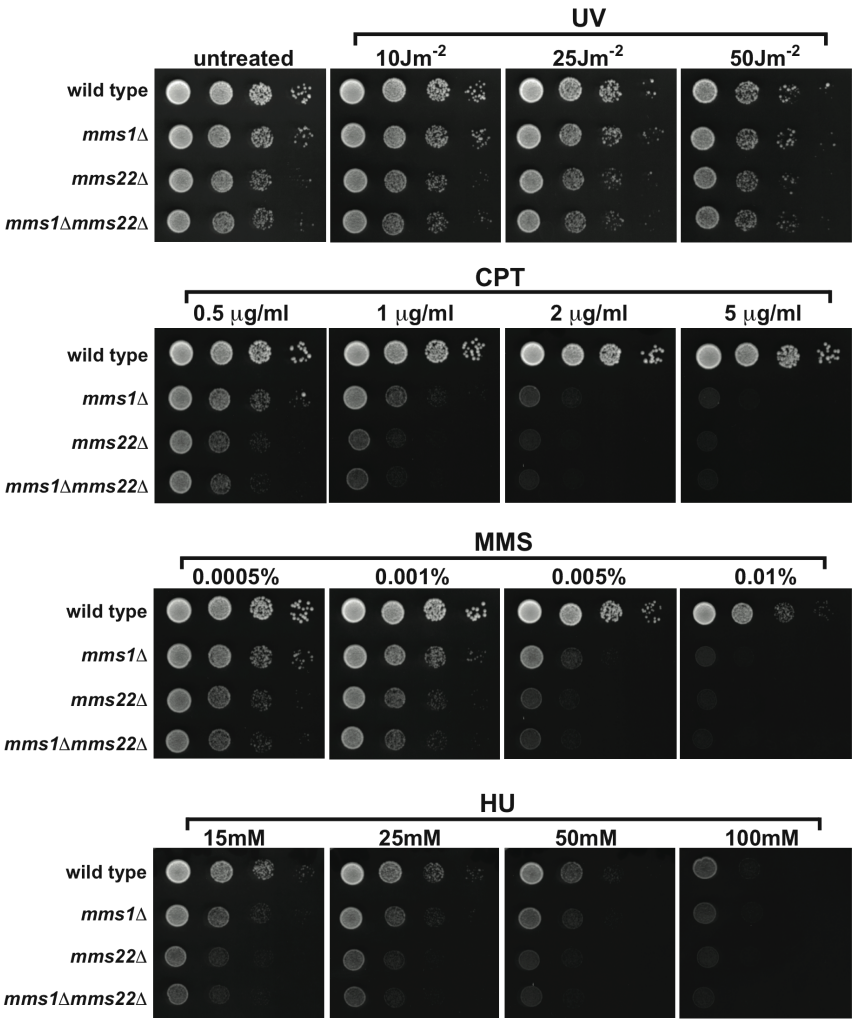

Figure 3.2 *MMS1* and *MMS22* act in the same pathway.

Strains BY4741 (wild type), *mms1Δ*, *mms22Δ* or *mms1Δ mms22Δ* were grown to saturation in liquid culture; ten-fold serial dilutions were spotted on YPAD agar and left untreated or exposed to the indicated doses of UV. Alternatively, cells were spotted onto YPAD agar plates containing MMS, CPT or HU. Cells were subsequently incubated at 30^{o}C for 3 days.

Cells lacking *MMS1* or *MMS22* showed a high degree of hypersensitivity to MMS, camptothecin, and were mildly hypersensitive to HU. These cells were not more sensitive to UV or IR than wild-type cells (Fig. 3.1). This spectrum of genotoxins sensitivity is usually indicative of a defect in DNA damage responses during S phase, and suggests that *MMS22* and *MMS1* play important and, perhaps, general roles in the response to perturbed replisomes. Consistent with a previous report (Araki et al., 2003), cells lacking both *MMS1* and *MMS22* were not more sensitive to CPT, MMS and HU than cells lacking either gene (Fig. 3.2), suggesting that the two genes act in the same pathway with respect to the response to stalled replisomes.

3.2.2 Cells lacking MMS1 or MMS22 are defective in recovering from MMS-induced replisome stalling

I wished to know if the hypersensitivity of *mms1Δ* and *mms22Δ* strains to agents that block replication fork progression was due to an inability to recover from replication fork stalling or collapse. When DNA replication is blocked the DNA replication checkpoint, which involves the Mec1 and Rad53 checkpoint kinases, is activated (Tercero and Diffley, 2001; Tercero et al., 2003). Rad53, after being phosphorylated by Mec1, orchestrates the response to replication stress, which involves stabilization of stalled replisomes, inhibition of late origin firing and repair of DNA lesions (section 1.11.4) (Lopes et al., 2001; Pellicioli et al., 1999; Tercero and Diffley, 2001; Tercero et al., 2003). Once cells have recovered from replisome stalling or collapse, Rad53 is de-phosphorylated and cells can resume DNA replication. Thus, monitoring Rad53 phosphorylation status is a convenient way to analyse recovery from replisome stalling.

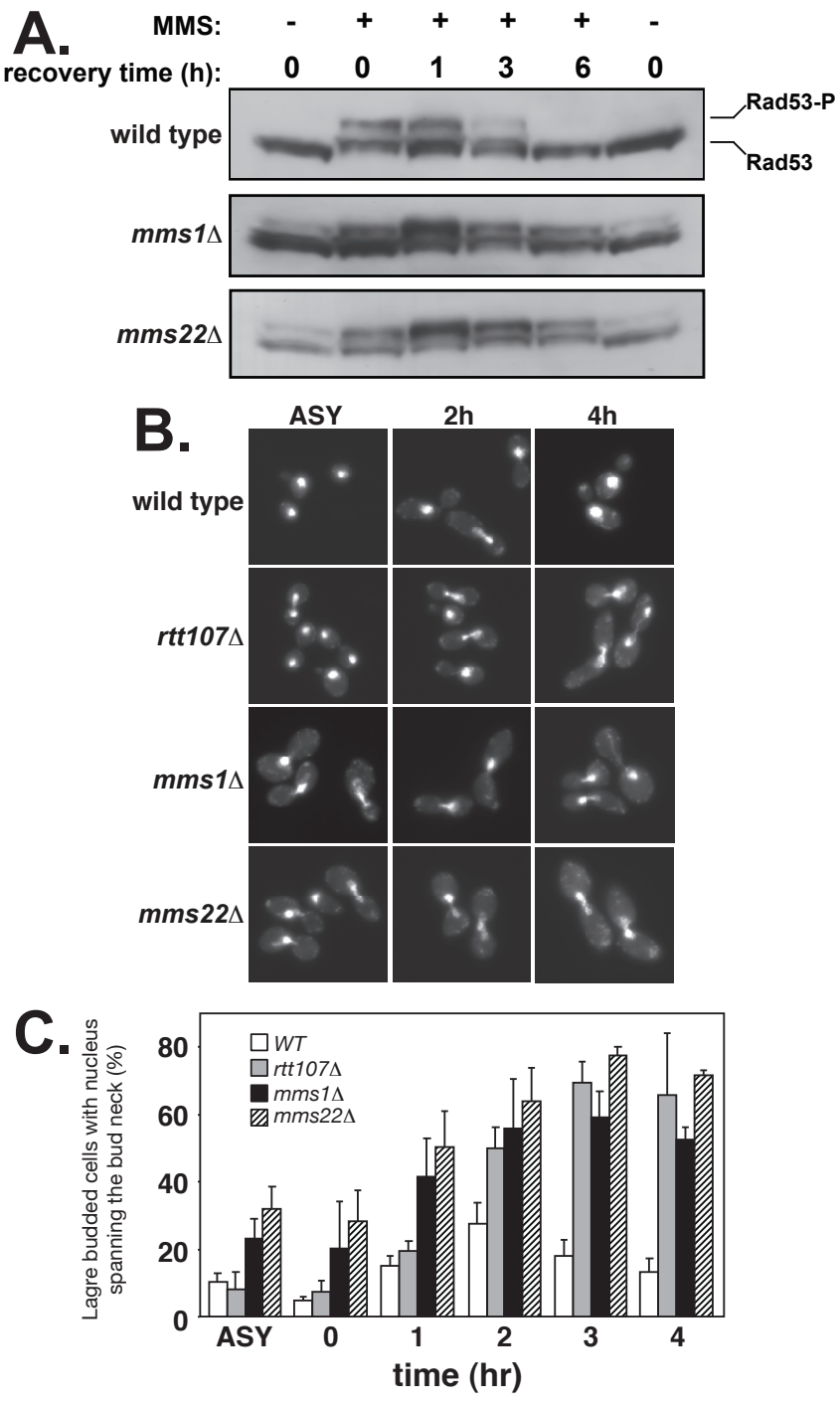
A.
MMS: - + + + + -
recovery time (h): 0 0 1 3 6 0
wild type
mms1Δ
mms22Δ
Rad53-P
Rad53
B.
ASY
2h
4h
wild type
rtt107Δ
mms1Δ
mms22Δ
C.
Lagre budded cells with nucleus spanning the bud neck (%)
WT
rtt107Δ
mms1Δ
mms22Δ
0
20
40
60
80
ASY
0
1
2
3
4
time (hr)

Figure 3.3 Cells lacking *MMS1* or *MMS22* show defects in recovery from MMS.
(A) Cells were grown to mid-log phase in liquid culture, arrested in G1 with α-factor and released from arrest into fresh medium containing 0.033% (v/v) MMS at 30°C. After 60 min, cells were filtered and washed extensively (MMS was quenched with sodium thiosulfate). Cells were then incubated in YPAD and after the times indicated, cells were lysed and extracts were subjected to immunoblotting with anti-Rad53p antibodies.
(B, C) Nuclear morphology during recovery from MMS was monitored. Cells grown to mid-log phase in liquid culture were treated with 0.03% (v/v) MMS for 1 h, at which point the cells were harvested and washed. Cells were then incubated in media lacking MMS, sampled at the indicated times and stained with DAPI to examine nuclear morphology. DAPI images are shown (A) and the percentage of cells with a large bud and an elongated nucleus spanning the bud neck is plotted (B).

To investigate the involvement of *MMS1* and *MMS22* in the recovery from replication stress, cells were arrested in G1 and released into S-phase in the presence of MMS; this led to phosphorylation and activation of Rad53, as judged by electrophoretic mobility shift after immunoblotting. When cells were washed free of MMS, Rad53 phosphorylation declined to basal levels after 6 h (Fig. 3.3A). In cells lacking either *MMS22* or *MMS1*, however, Rad53 phosphorylation was observed even preceding genotoxins treatment. Treatment of *mms1Δ* or *mms22Δ* cells with MMS caused the levels of phosphorylated Rad53 to increase further. When cells were washed free of MMS, Rad53 phosphorylation remained high at 6 h post-recovery, in contrast to wild type cells (Fig. 3.3A). It is interesting to note that *mms22Δ* cells have higher levels of Rad53 activation, both before MMS treatment and following recovery (Fig. 3.3A).

Previous work has pointed to the genetic interactions between *MMS1/MMS22* and other genes that have been shown to be required for recovery after replisome stalling: *RTT107, RTT101, RTT109* and *ASF1* (Collins et al., 2007b; Pan et al., 2006; Roberts et al., 2006; Rouse, 2004). Further, *rtt107*Δ cells show an anaphase-like delay during the recovery process (Roberts et al., 2006; Rouse, 2004). To determine if this is the case in cells lacking *MMS1* or *MMS22*, Jessica Vaisica and Grant Brown examined nuclear morphology of *mms22Δ* and *mms1Δ* cells during recovery from MMS. Cells were stained with the DNA-binding dye DAPI; within 1 h of MMS removal, wild type, *mms22Δ* and *mms1Δ* strains accumulated large-budded cells with a single nucleus indicative of cells that are in G2 (Fig. 3.3B, C). Wild-type cells proceeded through mitosis, as evidenced by the decrease in large-budded cells at 2 and 3 h. In contrast *mms22Δ*, *mms1Δ* and *rtt107Δ* strains continued to accumulate in G2/M, with an elongated nucleus spanning the bud

neck (Fig. 3.3B, C). This morphology was similar to that exhibited by cells with dicentric chromosomes, which delay at mid-anaphase (Yang et al., 1997). These results reinforce the notion that recovery from MMS-induced damage is defective in *mms22Δ* and *mms1Δ* mutants and show that these mutants accumulate in anaphase during recovery. These data agree with previous reports that even in asynchronous populations of *mms22Δ*, there is an elevated incidence of cells that appear to be stuck in anaphase (Baldwin et al., 2005), consistent with the elevated level of phosphorylated Rad53 (Fig. 3A). This suggests that *MMS1* and *MMS22* play a role during an unchallenged S-phase.

3.2.3 Analysis of spontaneous mutation rates in cells lacking MMS1 or MMS22

The sensitivity of *mms1Δ* and *mms22Δ* deletion strains to agents that block replisome progression could be due to a defect in DNA lesion bypass. DNA lesion bypass is divided into two branches: the error-free pathway and the translesion synthesis (TLS, error-prone) pathway (see section 1.11.5). TLS is responsible for spontaneous mutations, and abolishing TLS leads to a decrease in mutation rates. Abolishing the error-free pathway, on the other hand, causes an increase in mutation rates because of a compensatory increase in TLS. I tested the involvement of *MMS1* and *MMS22* in TLS by measuring mutation rates in cells lacking *MMS1* or *MMS22*. To this end, the rate of forward mutation in the *CAN1* gene was measured. Canavanine is toxic to cells with functional *CAN1* gene, because the Can1 arginine permease facilitates the uptake of canavanine, an arginine analogue that probably disrupts polyamine biosynthesis; the inactivation of *CAN1* by spontaneous mutation prevents canavanine from entering the cells, thereby rendering them canavanine-resistant (Gocke and Manney, 1979). As shown

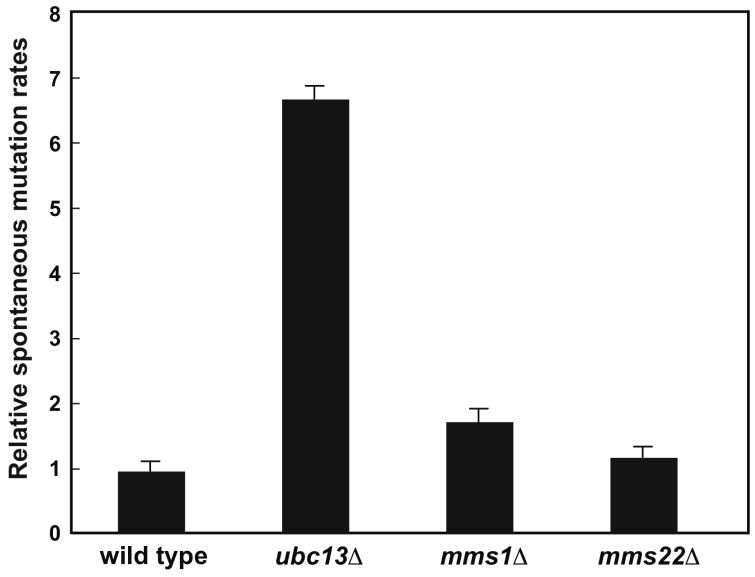

Figure 3.4 Analysis of the spontaneous mutation rate in *mms1Δ* and *mms22Δ* cells.
Spontaneous forward mutation rates at the *CAN1* gene locus were determined for strains BY4741 (wild type), *ubc13Δ*, *mms1Δ* and *mms22Δ* as described in section 2.2.3.4. Relative rates are shown compared to the wild-type strain. The data at each point represents the mean ± S.E.M. from three independent experiments.

in Fig. 3.4, deletion of *UBC13*, which is required for the error-free pathway, caused an increase in mutation rates. However, the spontaneous mutation rates in *MMS1* and *MMS22* were similar to wild type ones (Fig. 3.4), arguing against a role for *MMS1* and *MMS22* in the DNA lesion bypass pathway.

3.2.4 MMS1 and MMS22 are required for sister-chromatid exchange induced by replication fork blockage

Cells use recombination between sister chromatids to restart stalled forks leading to sister chromatid exchanges (SCEs) (Zou and Rothstein, 1997). Studies using genetic assays have reported a substantial increase in SCE following replisome stalling. Consistent with this, abolishing SCE (e.g. by deleting *RAD51*) causes hypersensitivity to genotoxins that arrest replication forks (Fasullo et al., 2005a; Fasullo et al., 2005b; Fasullo et al., 2001). Based on this well-established link, I decided to assay SCE in strains lacking *MMS1* and *MMS22*. To this end, I used a genetic assay developed by Fasullo and colleagues (Fasullo et al., 2001) to assay the frequency of unequal SCE (uSCE) before and after genotoxic insult. In this assay a yeast strain (strain YB163) harbouring a uSCE reporter cassette is used. His^+ recombinants are formed as a result of uSCE involving two truncated *his3* fragments at the *TRP1* locus (see Fig. 3.5A for a description of the assay) (Fasullo et al., 2001). Equal sister chromatid exchange events are genetically silent and, thus, cannot be measured by this assay.

MMS1 or *MMS22* were disrupted in the YB163 background. The frequency of spontaneous uSCE (i.e. preceding genotoxic insult) in cells lacking *MMS1* or *MMS22*

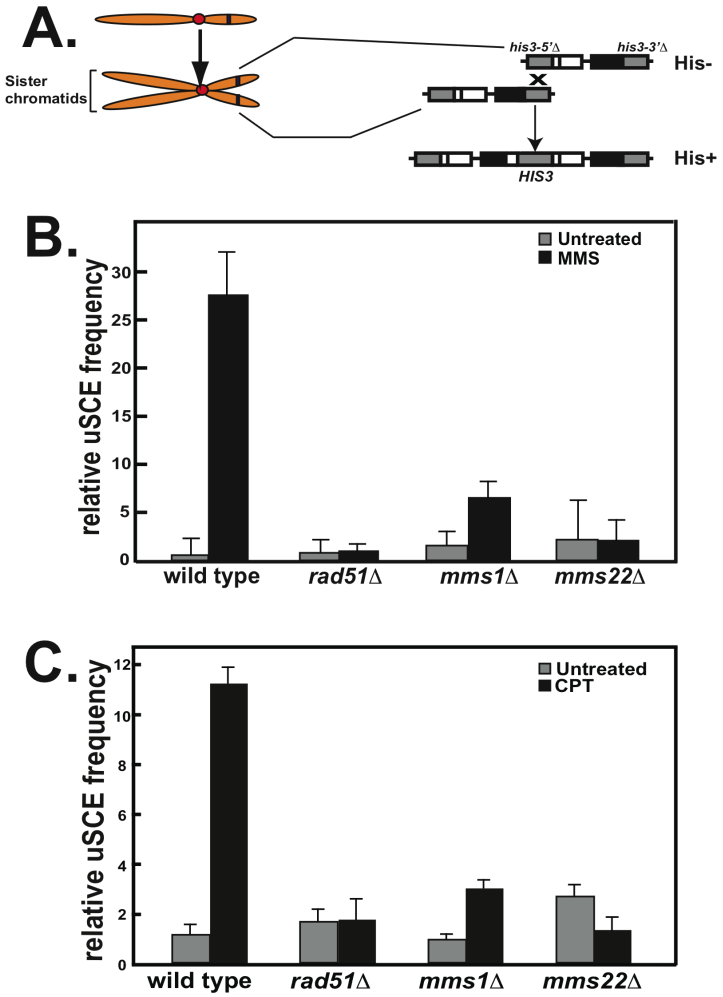

Figure 3.5 *MMS1* and *MMS22* are required for uSCE stimulated by agents that block replisome progression.

(A) Schematic diagram of the assay used to measure unequal SCE, modified from Dong and Fasullo, 2003.

(B) Cultures of wild-type (YB163), *rad51*Δ (YB177), *mms1*Δ (EDY11) or *mms22*Δ (EDY12) cells were grown to mid-log phase at which point MMS (0.02%, v/v) was added, or cells were left untreated. uSCE was then measured as described in section 2.2.3.5. The data are represented as uSCE frequencies relative to untreated wild-type cells (this value approximately 1.2×10^{-5}; relative uSCE = 1). The data at each point represents the mean ± S.E.M. from at least three independent experiments.

(**C**) Same as B, except that camptothecin (CPT; 10 µg/ml) was used instead of MMS.

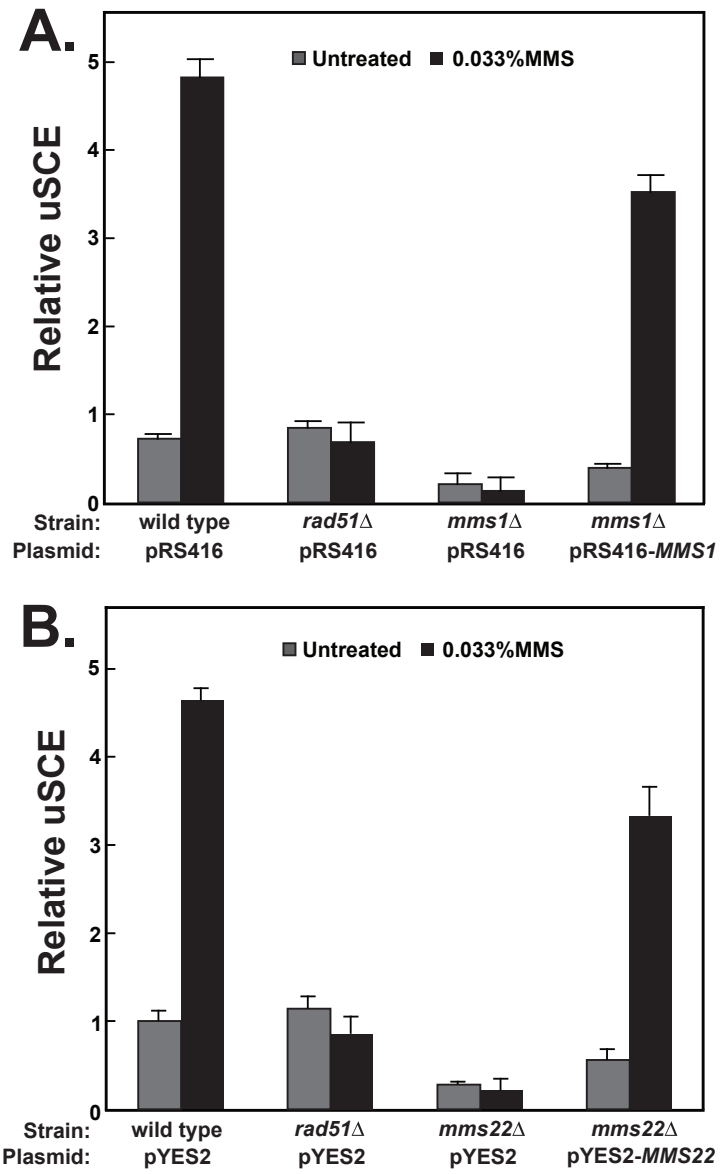

Figure 3.6 *MMS1* and *MMS22* are required for uSCE stimulated by agents that block replisome progression.

Cultures of wild-type (YB163), *rad51*Δ (YB177), *mms1*Δ (EDY11) or *mms22*Δ (EDY12) cells were transformed with the indicated plasmids expressing wild-type *MMS1* **(A)** or *MMS22* **(B)**. Cells were grown to mid-log phase at which point MMS (0.033%, v/v) was added, or cells were left untreated. uSCE was then measured as described in section 2.2.3.5. The data are represented as uSCE frequencies relative to untreated wild-type cells. The data at each point represents the mean ± S.E.M. from at least three independent experiments.

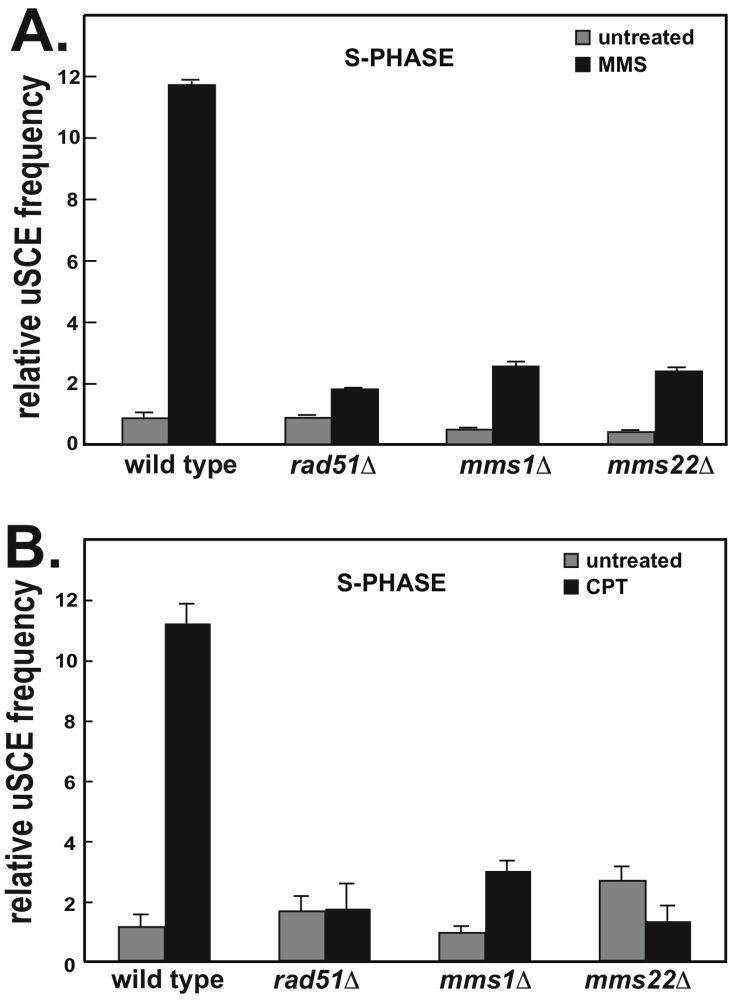

Figure 3.7 *MMS1* and *MMS22* are required for uSCE induced by replication fork blockage in S phase.

Cells were synchronised in G1 with α-factor. Cells were then released from α-factor arrest in the presence of MMS **(A)** or CPT **(B)**. uSCE frequency was measured as in Fig 3.5.

was indistinguishable from wild-type cells. Treatment of wild-type cells with MMS or CPT caused a ~30-fold increase in uSCE frequency. However, uSCE scarcely increased in strains lacking *MMS1* or *MMS22* (Fig. 3.5B, C). Expressing *MMS1* or *MMS22* from plasmids in the respective deletion strains rescued the uSCE defect (Fig. 3.6). To confirm that the effects of MMS on HR occurred in S-phase, cells were synchronised in G1 with alpha-factor and released from G1 into S-phase in the presence of MMS. After 45 min, cells were washed free of MMS and uSCE was measured. As shown in Fig. 3.7, cells lacking *MMS22* or *MMS1* showed a marked defect in MMS-induced HR during S-phase.

3.2.5 MMS22 and MMS1 are required for inter-allelic HR stimulated by agents that stall replisomes

HR occurs not only between sister chromatids but also between homologous chromosomes in diploid cells. To measure the frequency of recombination between homologous chromosomes I used a diploid yeast strain carrying the *HIS1* deletion fragments *his1-1/his1-7* on chromosomes V (Fig. 3.8A) (Ogiwara et al., 2007; Ui et al., 2007). Heteroallelic recombination between the two fragments restores the *HIS1* locus, thus leading to histidine prototrophy. Spontaneous heteroallelic recombination was elevated 3-fold and 5-fold, respectively, in *mms1*Δ and *mms22*Δ cells compared with wild-type cells (Fig. 3.8B). The frequency of heteroallelic recombination increased robustly in wild-type cells after MMS treatment, in a dose-dependent manner, but this was much less pronounced in cells lacking *MMS1* and *MMS22* (Fig. 3.8B). Thus, *MMS1* and *MMS22* are required for recombination between homologous chromosomes, as well as between sister chromatids, when replisome progression is perturbed.

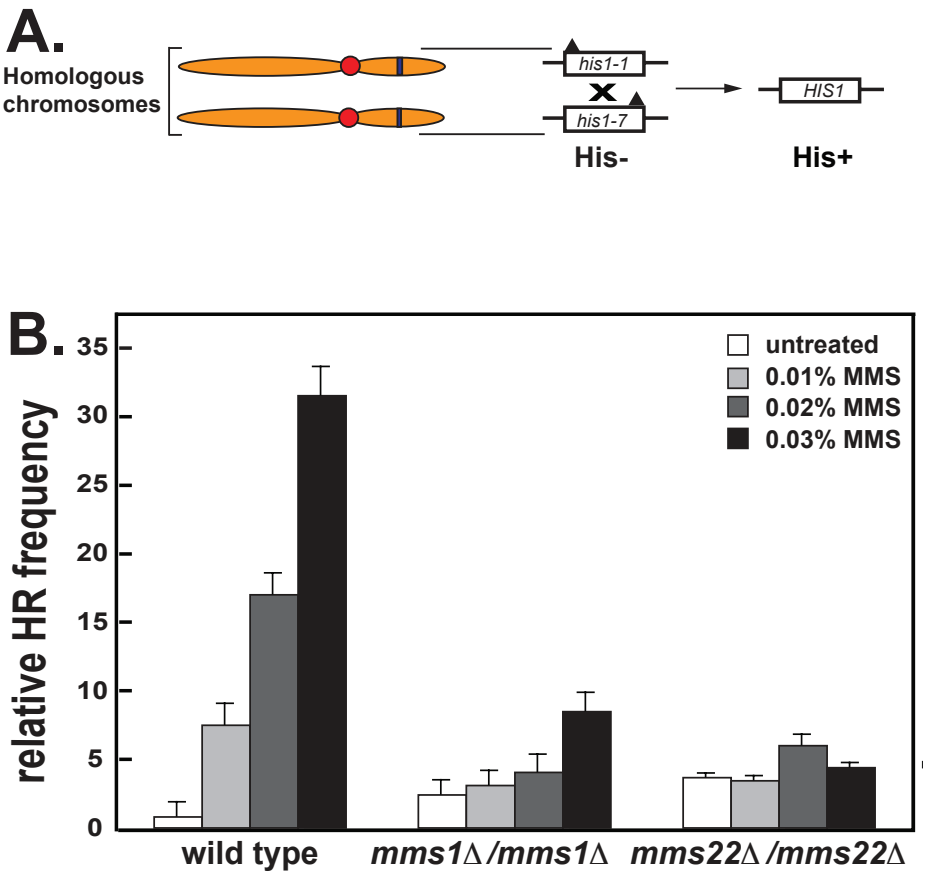

Figure 3.8 *MMS1* and *MMS22* are required for interchromosomal HR.

(A) Schematic diagram of the assay used to measure inter-chromosomal recombination.

(B) Wild-type diploid cells MR101, *mms1*Δ/*mms1*Δ (EDY21) and *mms22*Δ/*mms22*Δ (EDY22) were treated for 60 min with MMS at the indicated concentrations (v/v). HR was measured as described in section 2.2.3.6. The data are represented as HR frequencies relative to the untreated wild-type cells (this value was approximately 1.6×10^{-5}; relative uSCE = 1). The data at each point represents the mean ± S.E.M. from at least three independent experiments.

3.2.6 MMS1 and MMS22 are not required for HR induced by DSBs

In addition to rescuing stalled replication forks, HR is a major pathway for the repair of DSBs. I next investigated if *MMS1* and *MMS22* are required for repair of HR induced by DSBs. To address this question, cells harbouring the uSCE reporter (depicted in Fig. 3.5A) were transformed with a plasmid bearing the HO endonuclease gene under the control of a galactose-inducible promoter that cleaves at a HO restriction site between the two truncated *his3* alleles (Fig. 3.9A). Induction of the HO nuclease with galactose caused a strong increase in HR that required Rad51, consistent with previous reports (Fasullo et al., 2001). However, neither *MMS22* nor *MMS1* were required for DSB-induced uSCE (Fig. 3.9B). Consistent with this, uSCE induced by ionising radiation (IR)-induced DSBs did not require *MMS22* or *MMS1* (Fig. 3.9D). This is in agreement with the finding that cells lacking *MMS22* or *MMS1* are not more sensitive to IR than wild-type cells (Fig. 3.1C). It could be argued that *MMS22* and *MMS1* do respond to double-strand breaks, but only during S-phase, for example at collapsed replication forks. To test this, cells were synchronised in G1 and released into S-phase under conditions where the HO endonuclease was switched on. Although Rad51 was required for uSCE induced the HO-induced DSB in S-phase, *MMS22* and *MMS1* were not (Fig. 3.9C).

To further assess the involvement of *MMS1* and *MMS22* in HR-mediated DSB repair I used an additional assay (Frank-Vaillant and Marcand, 2002; Luke et al., 2006). In this assay a strain is used where an HO-inducible site is introduced between the silent mating-type loci and the HO endonuclease is placed under the galactose-inducible promoter *GAL1,10*, thus ensuring that the DSB is induced only when cells are grown in galactose-

containing media. Further, the mating-type loci *HML* and *HMR* are deleted, and the HO-induced DSBs are repaired by HR between the MAT locus on chromosome III and a non-cleavable copy of the *MAT* locus (*MATinc*) on chromosome V, thus allowing cells to survive when HO is induced (Fig. 3.10A). *RAD52* disruption rendered cells extremely sensitive to induction of HO cleavage of *MAT*. *MMS1* or *MMS22* disruption caused a slight decrease in cell viability when HO was induced but the effect was much less pronounced than that seen in *rad52*Δ cells (Fig. 3.10B, C). This confirms the conclusions drawn from the previous experiments that *MMS1* and *MMS22* are not required for HR at DSBs. Taken together these data indicate that DSBs are unlikely to be the primary substrate of *MMS22* and *MMS1*-dependent uSCE, and that their involvement in HR is specific to stalled- or collapsed-fork situations.

3.2.7 HR induced by MMS requires ASF1, RTT101, RTT109 but not RTT107

Two-dimensional hierarchical clustering of genetic interactions (Collins et al., 2007b) showed that *MMS22* and *MMS1* clustered closely with genes known to respond to stalled replisomes: *RTT101, RTT107, RTT109* and *ASF1*. The possible involvement of these genes in HR was also investigated. Cells lacking *RTT101, RTT109* and *ASF1* all showed a marked defect in MMS-induced HR similar to that seen in cells lacking *MMS1* (Fig. 3.11A), whereas HR induced by HO-induced DBSs did not require any of these genes (Fig. 3.11B). MMS-induced HR in cells lacking *RTT107* was not significantly different from wild type cells, consistent with a previous report (Rouse, 2004). It was previously shown that *RTT101* and *ASF1* are not required for repair of HO-induced DSBs (Luke et

al., 2006; Ramey et al., 2004). The data presented in this section indicate that *RTT101* is required for HR at blocked replisomes.

3.2.8 MMS1 and MMS22 are unlikely to act by remodelling higher-order chromatin

Eukaryotic DNA is compacted by association with four core histone proteins to form the nucleosome; nucleosomes are further compacted by association with linker histones to form higher-order chromatin (section 1.13) (Graziano et al., 1994). Judging from the genetic interactions between *MMS1/MMS22* and factors involved in chromatin remodeling (Collins et al., 2007b; Pan et al., 2006), I hypothesized that *MMS1* and *MMS22* may facilitate HR by modifying higher-order chromatin. The linker histone H1 (yeast Hho1) has been shown to suppress HR induced by replisome blockage or DSBs (Downs et al., 2003). If *MMS1* and *MMS22* promote HR by relaxing higher-order chromatin, deleting *HHO1* in *mms1*Δ and *mms22*Δ cells should restore HR, thus alleviating the hypersensitivity to DNA-damaging agents. To test this, I disrupted *MMS1* or *MMS22* in an *hho1*Δ deletion strain. The double mutants (*hho1*Δ*mms1*Δ and *hho1*Δ*mms22*Δ) show similar levels of sensitivity to DNA-damaging agents as the single mutants (*mms1*Δ and *mms22*Δ) (Fig. 3.12). This suggests that *MMS1* and *MMS22* are unlikely to facilitate HR by remodelling higher-order chromatin structures. The possibility remains, however, that *MMS1* and *MMS22* remodel chromatin at the nucleosome level.

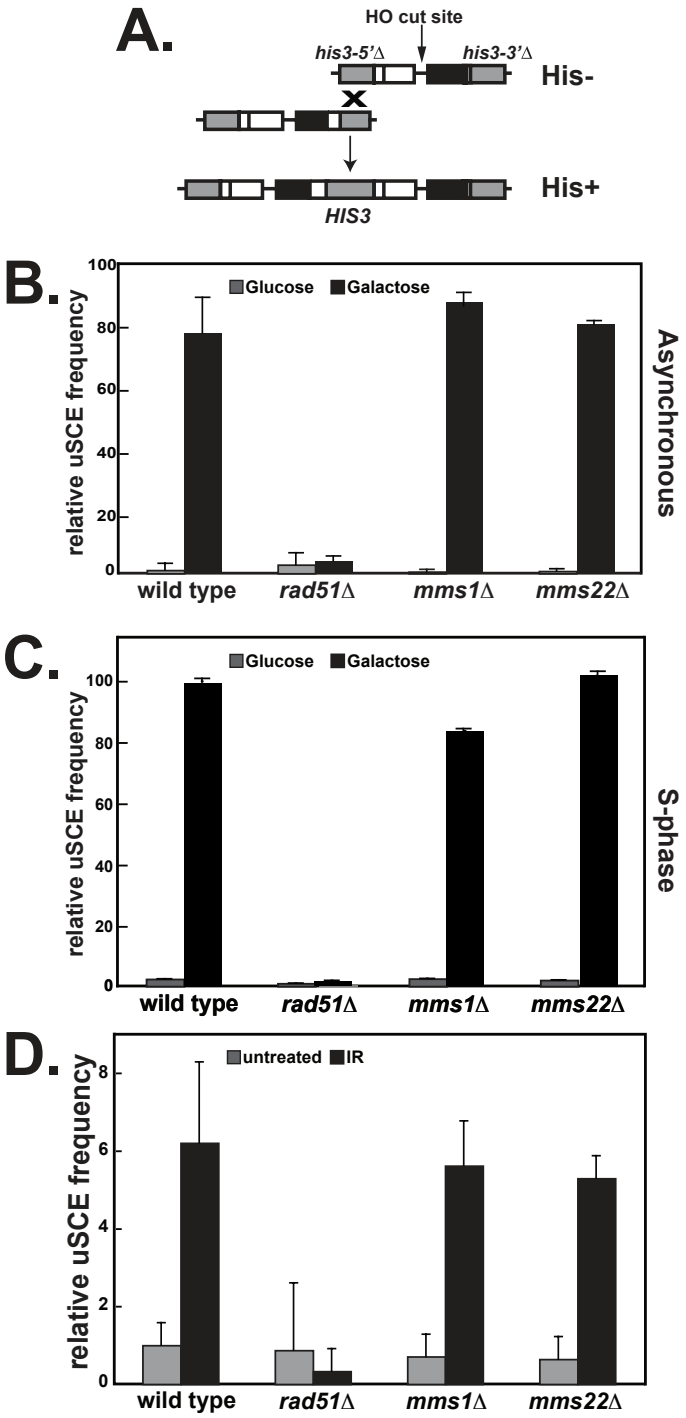
A.
HO cut site
his3-5'Δ
his3-3'Δ
His-
His+
HIS3
B.
Glucose
Galactose
relative uSCE frequency
Asynchronous
wild type
rad51Δ
mms1Δ
mms22Δ
C.
Glucose
Galactose
relative uSCE frequency
S-phase
wild type
rad51Δ
mms1Δ
mms22Δ
D.
untreated
IR
relative uSCE frequency
wild type
rad51Δ
mms1Δ
mms22Δ

Figure 3.9 *MMS1* and *MMS22* are not required for uSCE induced by DSBs.
(A) Schematic diagram of the assay used to measure HO endonuclease-stimulated uSCE.
(B) HO-induced uSCE frequencies in wild-type (YB163), *rad51*Δ (YB177), *mms1*Δ (EDY11) or *mms22*Δ (EDY12) cells transformed with plasmid pGHOT-*TRP1*-*GAL3* were determined as described in section 2.2.3.5. Glucose represses HO expression, galactose induces HO expression.
(C) Same B, except that cells were treated with 180 Gy of ionising radiation (IR).
(D) Same as B, except that the HO endonuclease was induced in cultures that were synchronised at the G1 phase of the cell cycle. Cells were subsequently synchronously released into S-phase in galactose-containing media for 4 h. Cells were plated, incubated and counted as described.
The data at each point represents the mean ± S.E.M. from at least three independent experiments.

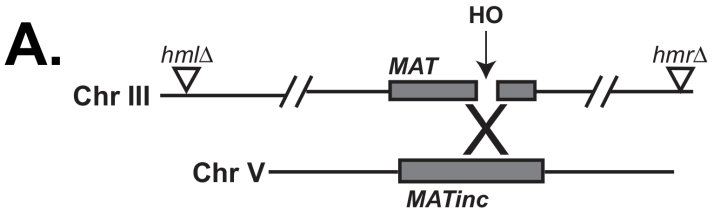
A.
HO
hmlΔ
MAT
hmrΔ
Chr III
Chr V
MATinc

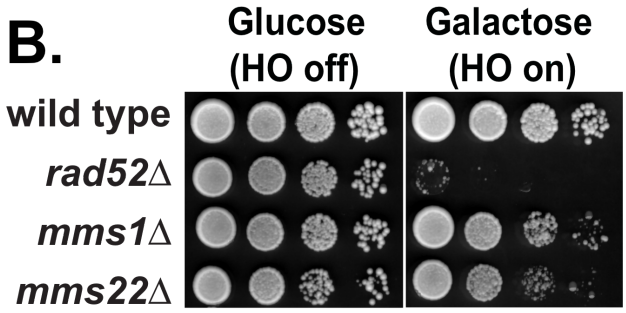
B.
Glucose
(HO off)
Galactose
(HO on)
wild type
rad52Δ
mms1Δ
mms22Δ

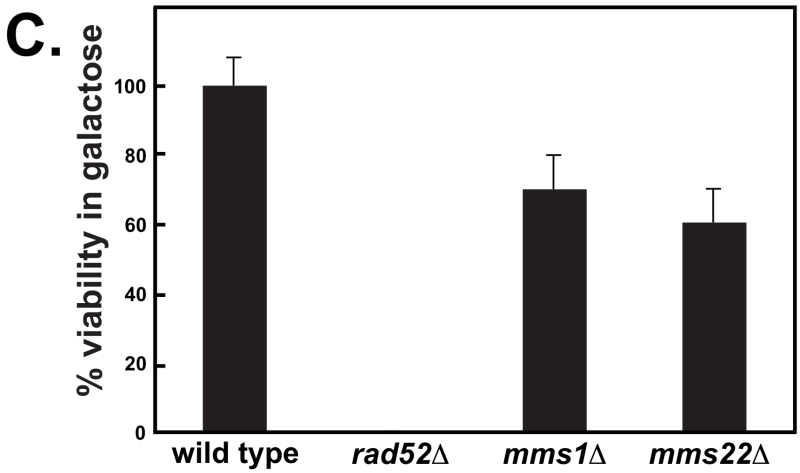
C.
% viability in galactose
100
80
60
40
20
0
wild type
rad52Δ
mms1Δ
mms22Δ

Figure 3.10 *MMS1* and *MMS22* are not required for uSCE induced by DSBs.
(A) Schematic diagram of strain GA2321 used to assay repair of a HO-induced DSB at *MAT* locus. Both *HML* and *HMR* have been deleted and a non-cleavable copy of the *MAT* locus has been integrated on chromosome V.

(B) Wild-type (GA2321), *mms1*Δ (EDY23), *mms22*Δ (EDY24) and *rad52*Δ (GA2368) strains were grown in YPAD, before being filtered, washed extensively and resupsended in raffinose-containing media. Cells were then grown to saturation before being spotted in ten-fold serial dilutions on plates containing glucose or galactose as the sole carbon source. Cells were grown for 3 days at 30^{o}C.

(C) Approximately 200 cells of the indicated strains – wild-type (GA2321), *mms1*Δ (EDY23), *mms22*Δ (EDY24) and *rad52*Δ (GA2368) – were plated on media containing galactose (HO ON) or glucose (HO OFF). Colonies were counted after an incubation of 3 days at 30°C. The data are represented as the ratio of the colonies growing on galactose-containing media to those growing on glucose-containing media. The data at each point represents the mean ± S.E.M. from at least three independent experiments.

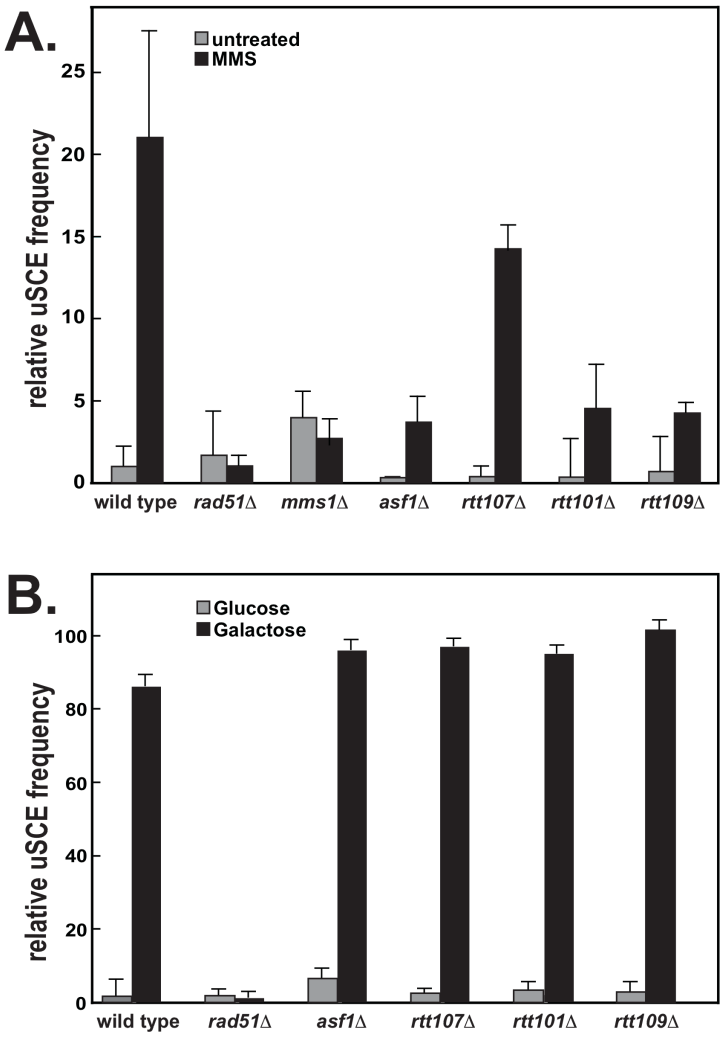

Figure 3.11 *RTT101*, *RTT109* and *ASF1* are specifically required for uSCE induced by replisome blockage.

(A) The strains indicated (all in the YB163 genetic background) were grown to mid-log phase and MMS (0.02%, v/v) was added for 45 min. uSCE was measured as described in section 2.2.3.5. The data at each point represents the mean ± S.E.M. from at least three independent experiments.

(B) The strains indicated (all in the YB163 genetic background), transformed with plasmid pGHOT-*TRP1*-*GAL3*, were grown to mid-log phase and incubated with either glucose (to repress HO) or galactose (to induce HO) for 2 h. uSCE was measured as described in section 2.2.3.5. The data at each point represents the mean ± S.E.M. from at least three independent experiments.

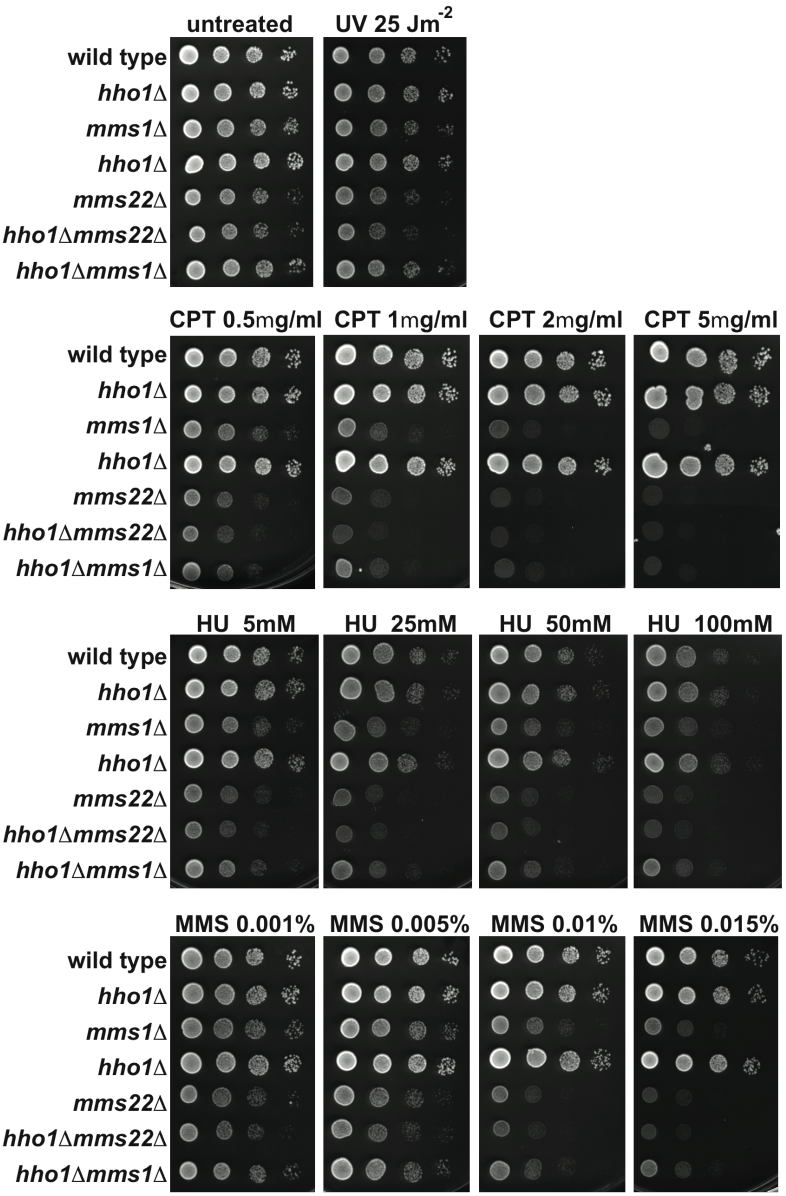

Figure 3.12 *MMS1* and *MMS22* are unlikely to act by remodelling higher-order chromatin. Strains BY4741 (wild type), *rad52Δ*, *mms1Δ*, *mms22Δ*, *hho1Δmms1Δ*, *hho1Δmms22Δ* were grown to saturation in liquid culture; ten-fold serial dilutions were spotted on YPAD agar and left untreated or exposed to UV. Alternatively, cells were spotted onto YPAD agar plates containing MMS, CPT or HU. Cells were subsequently incubated at 30^{o}C for 3days.

3.2.9 MMS1 and MMS22 are not required for global sister chromatid cohesion

The exchange of genetic information between sister chromatids requires that they be held together in a process referred to as cohesion. Recent research has highlighted the importance of cohesion establishment for SCE induced by DNA damage and replisome blockage (Ogiwara et al., 2007; Sjögren and Nasmyth, 2001; Sjögren and Ström, 2010; Ström et al., 2004). I tested the possible involvement of *MMS1* and *MMS22* in cohesion using fluorescence microscopy. An assay devised by Prof. Kim Nasmyth and colleagues (Michaelis et al., 1997) makes use of the binding of the bacterial tetR (tetracycline repressor) protein to tetO (tetracycline operator) DNA (Fig. 3.13). I obtained a strain that expresses tetR-GFP and where a tetO DNA array has been inserted in chromosome VI. In the G2 phase of the cell cycle the sister chromatids are held close together, as are the tetO arrays therein. The fluorescent tetR-GFP will bind to both arrays, but because of their physical proximity, a single fluorescent spot would be observed. If cohesion is defective, however, the chromatids are not held close together, and thus the tetO arrays will be further apart, so two spots are seen (Fig. 3.13). In a strain deficient for the cohesion factor *SCC1* (Uhlmann et al., 1999), two fluorescent spots were observed in the vast majority of cells (Fig. 3.14). As expected, in wild-type cells only one spot was seen, showing that cohesion is normal (Fig. 3.14). *MMS1* or *MMS22* deletion did not affect cohesion – the proportion of cells with one bright spot was not lower than in the wild-type (Fig. 3.14). I therefore conclude that *MMS1* and *MMS22* are not required for sister chromatid cohesion at a global level. It should be noted that this assay only measures sister-chromatid cohesion at the site of the tetO array. However, *MMS1* and *MMS22* may enhance sister-chromatid cohesion locally near stalled or collapsed replication forks.

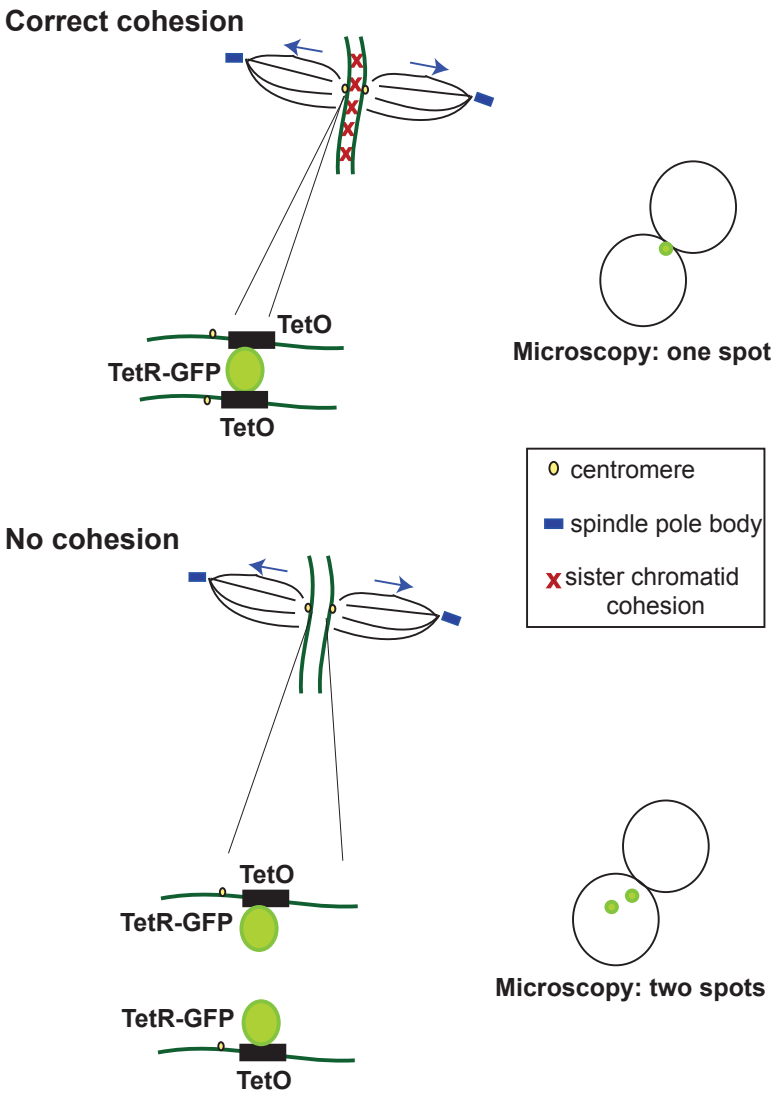

Figure 3.13 Schematic of the assay used to monitor sister chromatid cohesion.
Bacterial tetO DNA arrays were inserted 35 kbp away from the centromere on the left arm of chromosome V. The yeast strain also expresses a GFP-tagged tetR protein (tetR-GFP) that binds to the tetO arrays. During correct cohesion the tetO DNA arrays are held in close proximity, thus only one fluorescent spot is observed. If cohesion is dysfunctional, however, the tetO arrays are far apart, so that two distinct fluorescent spots are observed.

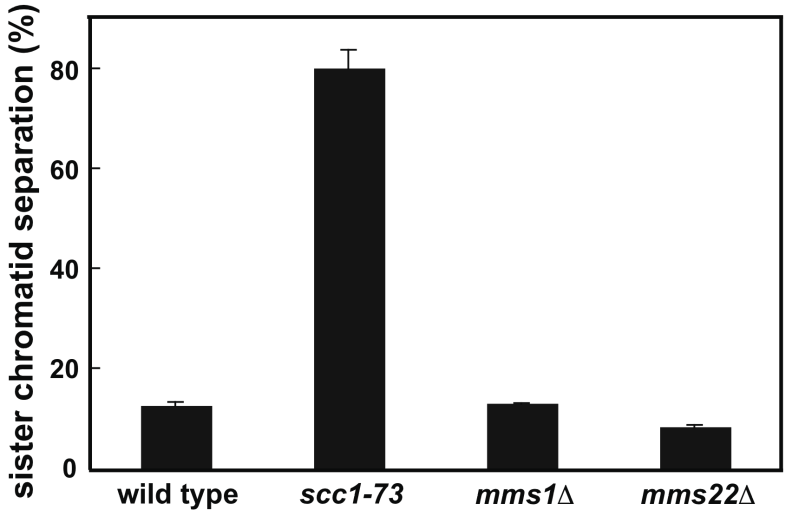

Figure 3.14 *MMS1* and *MMS22* are not required for global sister chromatid cohesion. Wild-type cells, cohesion-deficient (*scc1-73*) cells or cells lacking *MMS1* or *MMS22* were arrested in G2/M phase before being treated with 0.033% MMS. Cells were then fixed, sonicated, concentrated by short centrifugation, and immobilized on a slide. Cells were then visualized using light and fluorescence microscopy. Cells were divided into those that contained one tetR-GFP spot (cohesion) or two (separation). The graph represents the percentage of cells counted that show separation, i.e. no cohesion. At least 100 cells were counted for each strain.

3.2.10 The effect of overexpressing Rad51 in cells lacking MMS1 or MMS22

One of the first steps of HR involves the recruitment of the core recombinase Rad51 (the homologue of bacterial RecA) onto ssDNA generated via nucleolytic processing of DSBs or ssDNA that is associated with stalled or damaged DNA replication forks (San Filippo et al., 2008). I considered the hypothesis that *MMS1* and *MMS22* could be involved in the recruitment of Rad51 recombinase to sites of stalled forks. If *mms1*Δ and *mms22*Δ cells were defective in the formation of Rad51 foci, over-expressing Rad51 would rescue the phenotype of the deletion cells. Rad51 was over-expressed using a plasmid harbouring *RAD51* under the control of a galactose-inducible promoter (a kind gift of Prof. Hannah Klein). Thus, Rad51 was expressed at low levels in glucose-containing media and at high levels in galactose-containing media. The over-expression of Rad51 did not alleviate the hypersensitivity of *mms1*Δ or *mms22*Δ cells to any of the genotoxins tested (Fig. 3.15). Overexpressing Rad51 in a *rad51*Δ deletion strain restored the wild-type phenotype. Therefore, it is unlikely that *MMS1* and *MMS22* are involved in the recruitment of Rad51 or the subsequent nucleoprotein filament formation.

3.2.11 Investigating further the role of MMS1 and MMS22 in HR

To investigate further the role of *MMS1* and *MMS22* in HR, I took two approaches. The first involved genetics. When the *SGS1* helicase is deleted in combination with *MUS81*, the accumulation of recombination intermediates reaches a threshold that is lethal to the cell (Ii and Brill, 2005). An *sgs1*Δ*mus81*Δ strain is kept viable with a plasmid harbouring wild-type *SGS1* and expressing the *URA3* gene.

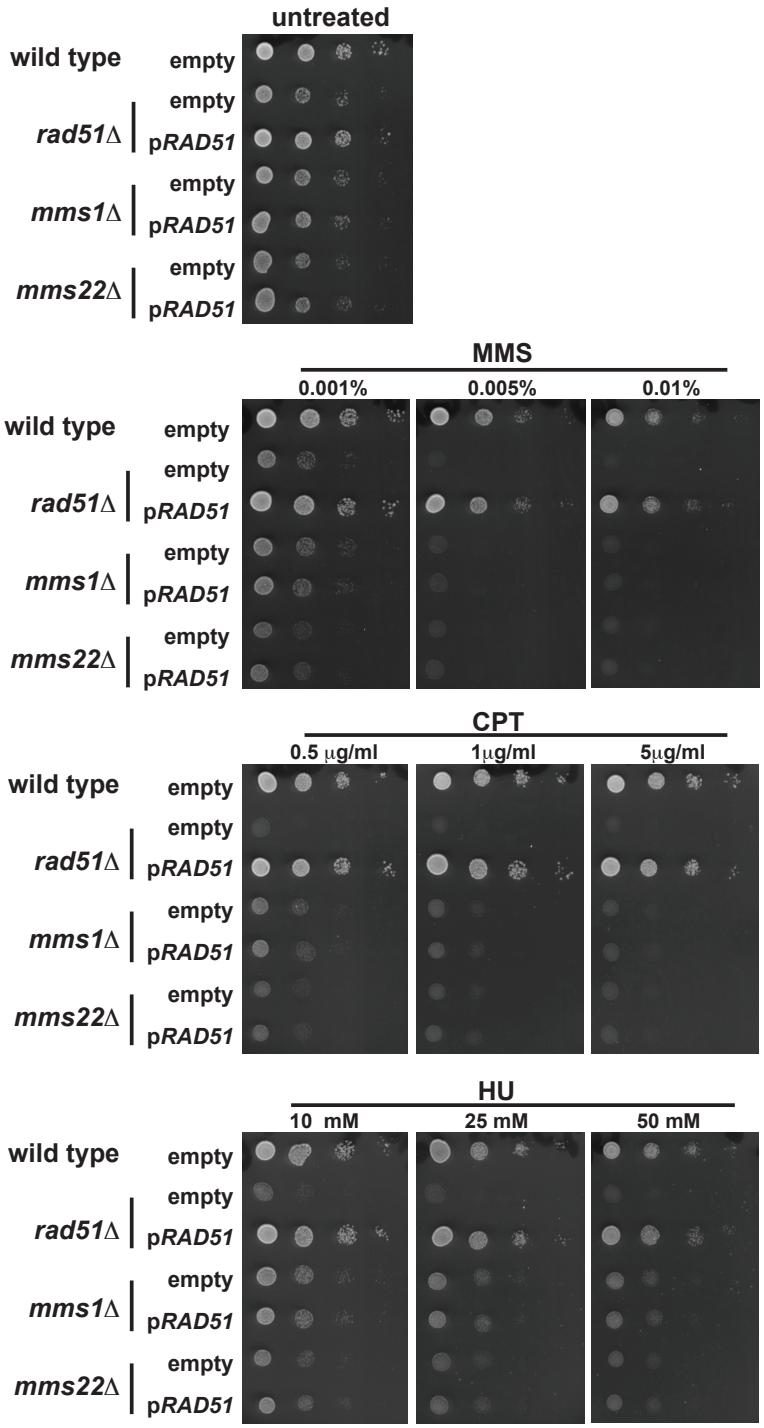

Figure 3.15 The effect of deleting *MMS1* or *MMS22* on the recruitment of the core recombinase Rad51.

Cells were transformed with an empty plasmid or one harbouring *RAD51* under the control of a galactose-inducible promoter. Serial dilutions of the indicated cells were spotted on plates with galactose as the carbon source. Cells were grown at 30^{o}C for 5 days.

When cells are grown in 5'-FOA-containing media, the product of the *URA3* gene is toxic, thus the plasmid is forced out of the cell, leading to the death of *sgs1*Δ*mus81*Δ cells. If, however, the core recombinase *RAD52* is also deleted, no recombination intermediates accumulate, thus cells can lose the *SGS1*-bearing plasmid and still remain viable (Fig. 3.16). Strains *sgs1*Δ*mus81*Δ*mms1*Δ and *sgs1*Δ*mus81*Δ*mms22*Δ triple mutants were, like *sgs1*Δ*mus81*Δ, inviable (Fig. 3.16). This suggests that *MMS1* and *MMS22* are unlikely to be involved in the early steps of HR.

In the second approach HR intermediates in cells lacking *MMS1* or *MMS22* were analysed. These can be visualised by two-dimensional (2D) DNA gel electrophoresis, where replication intermediates are separated both according to size – by running DNA in the first dimension at low voltage over a long time – and shape – by running DNA in the second dimension at high voltage over a short time (see Fig. 3.17A for a schematic). 2D gel electrophoresis has been widely used to characterise replication intermediates as well as aberrant structures that arise during disrupted DNA replication (Friedman and Brewer, 1995). Using this technique, it has been shown that the RecQ helicase *SGS1* is required for the resolution of HR intermediates – indeed, in its absence, *RAD51*-dependent X-structures accumulate (Liberi et al., 2005). As it can be seen in Fig. 10, X-molecules persist in *sgs1*Δ cells but not in *mms1*Δ or *mms22*Δ cells. Two-dimensional gel analysis showed that X-structures persisted in the *sgs1*Δ*mms1*Δ and *sgs1*Δ*mms22*Δ strains just as they persisted in the *sgs1*Δ strain[·]. I can conclude that *MMS1* and *MMS22* are unlikely to be required for processing HR intermediates.

[·] Two-dimensional gel analysis performed by Dr. Hocine Mankouri in Ian Hickson's lab, Oxford. The necessary strains for the experiments were prepared by me.

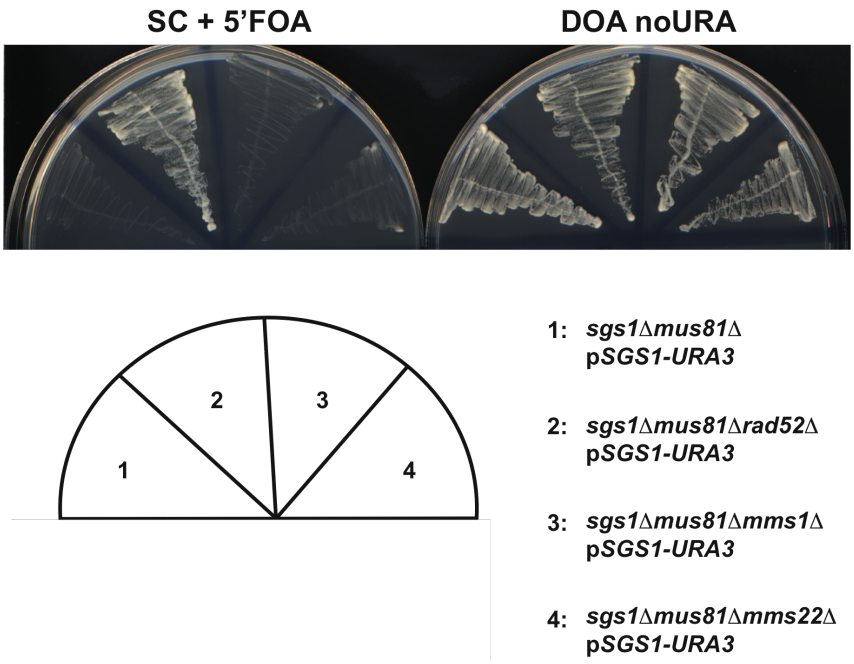

Figure 3.16 Investigating further the role of *MMS1* and *MMS22* in HR – A.

The indicated strains were streaked on media without uracil (thus maintaining pSGS1) or in 5-FOA media (thus shuffling pSGS1 out of cells). Cells were grown at 30^{o}C for three days.

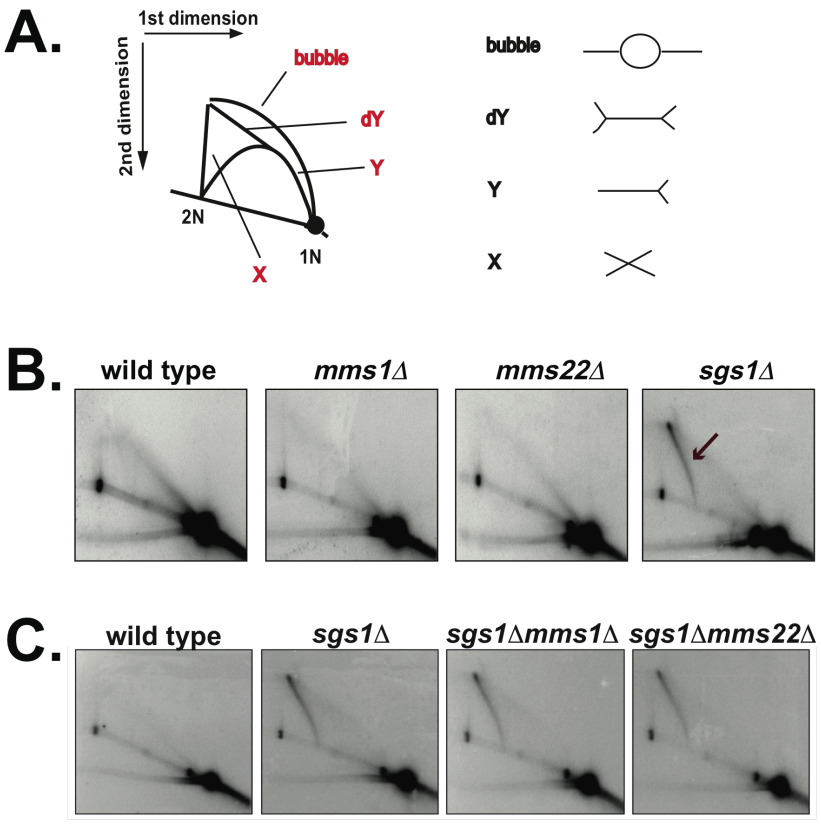

Figure 3.17 Investigating further the role of *MMS1* and *MMS22* in HR – B.

(A) Detection of DNA replication intermediates by 2D gel electrophoresis.

(B) Wild-type, *mms1Δ, mms22Δ* and *sgs1Δ* cells were released from G1 arrest into fresh medium containing 0.033% MMS. After 180 min, genomic DNA was isolated and digested with the restriction enzyme NcoI. Subsequently, the digested DNA was run in two dimensions. DNA samples were analyzed with a probe for the early-firing ARS305 replication origin. The arrowhead indicates the position of MMS-induced persistent X-molecules.

(C) The double mutant strains were treated in the same way as those described above.

3.2.12 MMS1 and MMS22 are not required for transcriptional silencing

Genetic studies have shown that *MMS1* and *MMS22* interact with factors involved in the acetylation of histone H3 on lysine56 (H3K56Ac) (Collins et al., 2007a; Pan et al., 2006). Lending support to this observation, data presented in section 3.2.8 show that, like *MMS1* and *MMS22*, two factors required for H3K56 acetylation – the acetyltransferase *RTT109* and the histone chaperone *ASF1* – are required for HR induced specifically by replisome stalling. *MMS1* and *MMS22* have been shown not to be required for H3K56 acetylation per se (Collins et al., 2007b). One process for which H3K56Ac has been shown to be required is the establishment of chromatin conformation that favours transcriptional silencing at loci that include the rDNA locus, telomeres and the silent mating-type loci (*HML* and *HMR*) (Xu et al., 2007). Transcriptional silencing at these loci can be assayed by using the reporter gene *URA3* inserted at the locus of interest (see Fig. 3.18, upper panel). If the reporter gene is silenced, cells can grow in the presence of 5-FOA; if it is not, as is the case with cells expressing the H3K56G point mutant, *URA3* is transcribed and 5-FOA kills the cells. The deletion of *MMS1* or *MMS22* did not affect the transcription status of the reporter gene at silent loci (Fig. 3.18). Thus, *MMS1* and *MMS22* are not involved in the H3K56Ac-dependent transcriptional silencing. In agreement with this, a recent screen identified *RTT109* and *ASF1*, but not *MMS1* or *MMS22*, as genes required for silencing, (Raisner and Madhani, 2008).

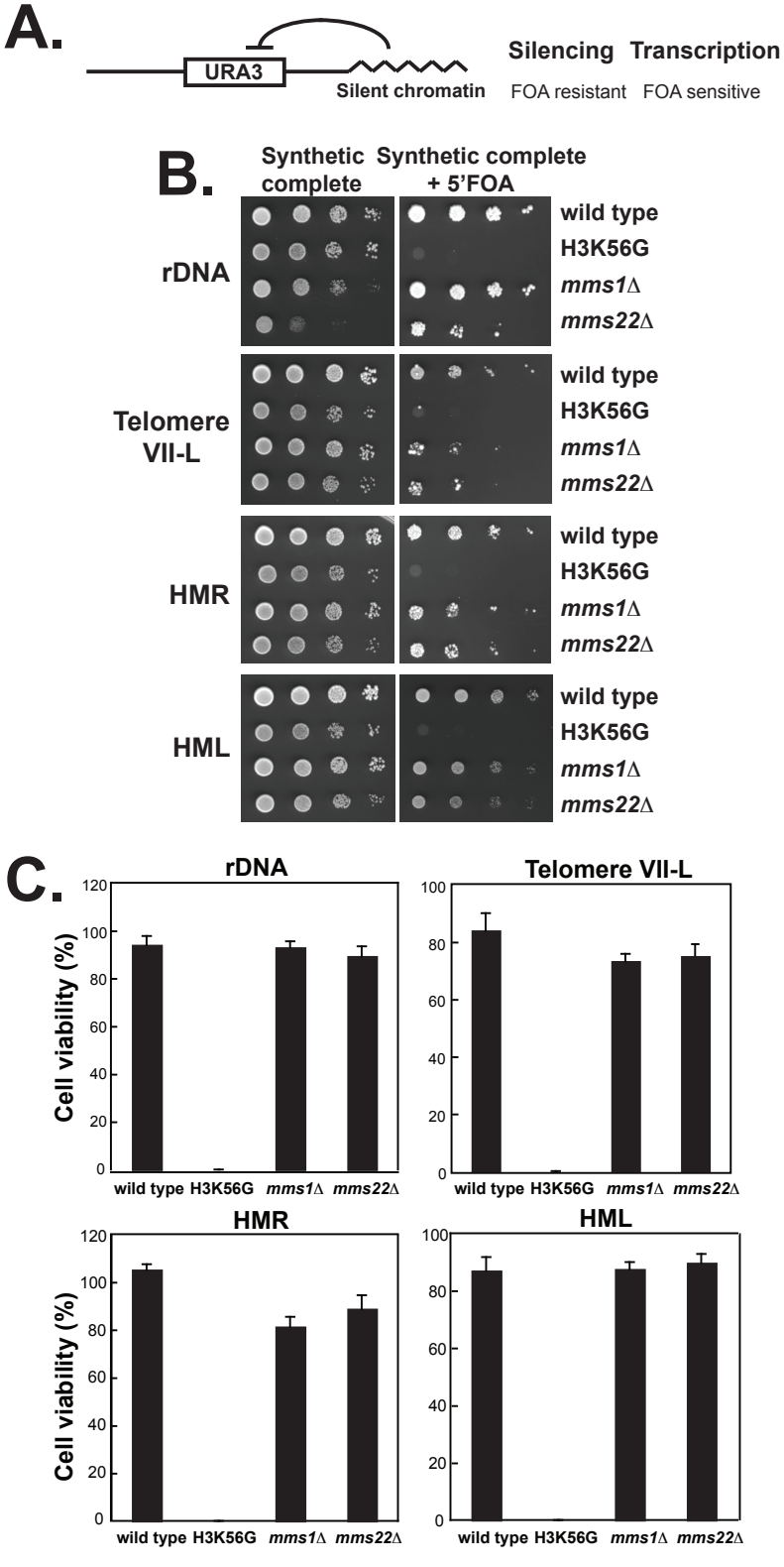
A.
URA3
Silent chromatin
Silencing
Transcription
FOA resistant
FOA sensitive
B.
Synthetic complete
Synthetic complete + 5'FOA
rDNA
Telomere VII-L
HMR
HML
wild type
H3K56G
mms1Δ
mms22Δ
C.
rDNA
Telomere VII-L
HMR
HML
Cell viability (%)
wild type
H3K56G
mms1Δ
mms22Δ

Figure 3.18 *MMS1* and *MMS22* are not required for transcriptional silencing.
(A) The *URA3* reporter gene is inserted in different loci (see B). If the silent chromatin structure is assembled correctly, the reporter gene is silenced and cells are resistant to 5-FOA, a chemical that is toxic to cells expressing the *URA3* gene product. If the gene is not silenced, such as in the H3K56G point mutants, cells die in the presence of 5-FOA in the medium.
(B) Serial dilutions of the indicated strains were spotted on plates as shown and grown at 30^{o}C for three days.
(C) 200 cells were plated on synthetic complete media with or without 5-FOA. Cell viability is expressed as the percentage of the ratio between cells grown with 5-FOA and those grown in the absence of 5-FOA.

3.3 Discussion

The data presented in this chapter show that in the budding yeast *Saccharomyces cerevisiae* Mms22 and Mms1 are required for HR induced specifically DNA replication blocks. In the absence of *MMS1* or *MMS22*, stalled or collapsed replication forks cannot recover, leading to a G_2/M arrest and persistent DNA damage checkpoint activation (Fig. 3.3). Consistent with this, Philip Pasero and colleagues have demonstrated the requirement for *MMS1* and *MMS22* in recovery from replication blockage in a more direct way by DNA combing analysis of single chromosome fibers (Zaidi et al., 2008). It is likely that *MMS1* and *MMS22* are also required during an unperturbed S phase since deletion of these genes leads to constitutive hyperactivation of the DNA damage response and G_2/M arrest even in the absence of genotoxic insult (Fig. 3.3). This is consistent with the observation that *S. pombe mms22Δ* cells show an elevated level of Rad22 (budding yeast Rad52) foci and a high proportion of elongated cells, indicative of spontaneous DNA damage (Dovey et al., 2009; Dovey and Russell, 2007). It is interesting to note that although *MMS1* and *MMS22* act in the same pathway (Fig. 3.2; Pan et al., 2006; Collins et al., 2007), *mms22Δ* cells seem to be slightly more sensitive than *mms1Δ* cells to genotoxins (Fig. 3.1) and have higher levels of hyper-phosphorylated Rad53 (Fig. 3.3A). The significance of this is not clear, but it may point to *MMS22* playing an additional, *MMS1*-independent role in the response to perturbed DNA replication.

Further, *MMS1* and *MMS22* deletions are synthetic lethal with mutations in genes essential for DNA replication such as *MCM10* (Araki et al., 2003) and *DNA2* (Budd et

al., 2005). This suggests that *MMS1* and *MMS22* rescue replication forks that stall or collapse spontaneously during normal S phase. Data presented in this chapter suggest that *MMS1* and *MMS22* rescue stalled or collapsed replisomes by promoting HR. At present, the precise molecular roles of Mms22 and Mms1 in promoting HR are not clear. However, the defect in MMS-induced HR in *mms22Δ* or *mms1Δ* cells is as severe as that seen in *rad51*Δ cells so whatever the molecular functions of Mms22 and Mms1 at blocked replisomes, they appear to be fundamentally important for HR.

Since *MMS22* and *MMS1* are not required for HR induced by DSBs it is unlikely that these proteins act as core recombinases regulating the transactions central to HR. Consistent with this, I found that over-expressing Rad51 did not rescue the hypersensitivity of *mms1Δ* and *mms22Δ* strains to agents that block replication forks (Fig. 3.15). Moreover, another study has reported higher levels of Rad52 foci in *mms1Δ* and *mms22Δ* cells (Alvaro et al., 2007). Genetic and 2D gel analyses showed that *MMS1* and *MMS22* are not required for the formation or processing of recombination intermediates that are detected by 2D gel electrophoresis (Fig. 3.16 and Fig. 3.17). I also tested whether *MMS1* and *MMS22* facilitate HR by promoting sister-chromatid cohesion. Whilst I found no evidence for the two genes being involved in establishing cohesion at the tested site (Fig. 3.14), I cannot exclude that they may aid cohesion locally at stalled or collapsed forks. This will be difficult to test, since the current laboratory genotoxins induce replication fork stalling and collapse stochastically.

One clue to the function of *MMS1* and *MMS22* in promoting HR may be provided by their genetic interactions. *MMS1* and *MMS22* have been shown to interact genetically

with other factors required for genome stability: the histone chaperone Asf1, the histone acetyltransferase Rtt109 and the cullin Rtt101 (Collins et al., 2007b; Pan et al., 2006; Zaidi et al., 2008). I found that these factors are also required for HR induced specifically by replication blocks (Fig. 3.11). In this light, it is possible that the effect of *MMS22* and *MMS1* deletion on HR when replisomes stall is caused by perturbation of chromatin configuration. These proteins somehow enable HR to take place in the complicated milieu of stalled replisomes. Mms22 and Mms1 could in principle recognize some protein or DNA found at sites of replisome stalling or could bind to DSBs when stalled replisomes collapse. However, uSCE induced by a single DSB in S-phase cells does not require *MMS22* or *MMS1* (Fig. 3.9D) and so it is unlikely that DSBs are the trigger for these proteins. *MMS22* interacts with the cullin *RTT101* indirectly via *MMS1* in a DNA-damage dependent manner as part of an SCF-like complex (Zaidi et al., 2008). Since all three proteins are required for HR induced by replication blocks, it is tempting to suggest that they could facilitate HR by ubiquitinating yet-unidentified factors, thereby remodeling stalled/collapsed replisomes in a way that may favour HR. It will be interesting to see if any of these factors localise at stalled replisomes and what the hierarchy of recruitment is, and if acetylation of H3K56 is required for their localization.

The role of HR in rescuing replication has been studied in detail in bacteria (Cox et al., 2000; Michel, 2000; Michel et al., 2004; Possoz et al., 2006) and its importance has become apparent in eukaryotes (Alvaro et al., 2007; Branzei and Foiani, 2010; Budd et al., 2005; Daboussi et al., 2008; Moynahan and Jasin, 2010; Rothstein et al., 2000). Data presented in this chapter show that HR can be regulated differentially at DSBs and at sites of blocked replication, in agreement with published reports (section 1.12.2) (Alabert

et al., 2009; Duro et al., 2008; Mankouri et al., 2007; Shor et al., 2005). It will be interesting to understand the mechanisms that underlie this regulation.

Studies in the fission yeast *Schizosaccharomyces pombe* demonstrate that *MMS1* and *MMS22* have evolutionarily conserved roles in the response to blocked DNA replication. Indeed, *S. pombe* Mms1 and Mms22 have been shown to maintain genomic integrity during replication (Dovey et al., 2009; Dovey and Russell, 2007). Further, *S. pombe* Mms22 forms foci in response to camptothecin-treatment that co-localise with Rad22 (budding yeast Rad52) (Dovey and Russell, 2007), pointing to an HR-related role of Mms22 in the repair of collapsed replication forks.

The fundamental importance of *MMS1* and *MMS22* in HR-mediated replication fork rescue, and their conservation between two distantly-related yeasts, prompted me to look for their mammalian homologues. The human counterpart of yeast *MMS22* and its roles in the DNA–damage response are discussed in Chapter 4.

Chapter IV

4 Identification of human MMS22L and TONSL, two novel factors that facilitate homologous recombination

4.1 Introduction

The previous chapter discussed the importance of budding yeast Mms1 and Mms22 in HR-mediated replication fork rescue. Since HR is a highly conserved process in evolutionary terms, I asked whether yeast Mms1 and Mms22 have homologues in humans. In this chapter I describe the identification of C6ORF167 (MMS22L), a previously-uncharacterised protein, as a putative orthologue of yeast Mms22. I show that MMS22L and the MMS22L-interacting protein NFκBIL2 (TONSL) play an important role in HR by promoting the recruitment of the core recombinase RAD51 to sites of DNA damage.

4.2 Results

4.2.1 Identification of a putative human orthologue of yeast Mms22

Given the important role of Mms22 in responding to perturbations during DNA replication in yeasts (discussed in chapter 3), I reasoned that this protein is likely to be evolutionarily conserved. To investigate this possibility, I searched for Mms22–like proteins in higher eukaryotes with the help of Luis Sanchez-Pulido and Chris Ponting (University of Oxford). BLAST searches with full–length budding yeast Mms22 failed to reveal orthologues, but iterative similarity searches with *Schizosaccharomyces pombe*

Mms22 identified remote orthologues in animals with statistically significant E–values for sequence similarity, including the human hypothetical protein C6ORF167 (Fig. 4.1). Multiple sequence alignments defined a single evolutionarily conserved region spanning residues 373–535 in C6ORF167 that corresponds to residues 781-920 in budding yeast (indicated by purple ovals in Fig. 4.1). This conserved region is devoid of obvious structural or catalytic motifs, and it is the only region of similarity in Mms22 orthologues (Fig. 4.1). There are no reports on C6ORF167 except for a large-scale proteomic study which identified ASF1B as a C6ORF167–interacting protein (Ewing et al., 2007). This is reminiscent of the genetic interaction of *MMS22* with *ASF1* in budding yeast (Collins et al., 2007). Based on the similarity between C6ORF167 and yeast Mms22, we decided to characterize C6ORF167, to which we refer to hereafter as MMS22L (Mms22–like).

4.2.2 Identification of MMS22L-interacting proteins

In order to understand the cellular roles of MMS22L, I sought to identify MMS22L-interacting proteins. A plasmid expressing MMS22L fused to an N-terminal FLAG tag in a tetracycline-inducible manner was stably integrated in HEK293 cells (Fig. 4.2A). After inducing expression by incubating with tetracycline for 24 h, cells were lysed in the presence of the reversible crosslinker dithiobis succinimidyl propionate (DSP). Lysates were subjected to immunoprecipitation using FLAG antibody conjugated to M2 agarose. After extensive washing, precipitates were treated with dithiotheitol (DTT) to reverse DSP crosslinks.

Figure 4.1 Identification of MMS22L.

Upper panel. Schematic representation of Mms22 orthologues from the species indicated. Multiple sequence alignments defined an evolutionarily conserved region, spanning residues 373-535 in C6ORF167, and residues 781-920 in budding yeast Mms22, illustrated as a purple oval. *Lower panel.* Alignment of the only conserved region in the orthologues of yeast Mms22. The coloring scheme indicates average BLOSUM62 score (correlated to amino acid conservation): red (greater than 3), violet (between 3 and 1.5) and light yellow (between 1.5 and 0.3). Green cylinders represent α–helical regions. Full species names and the relevant Uniprot protein identification codes are: Human, *Homo sapiens* Q6ZRQ5; Mouse, *Mus musculus* B1AUR6; Opossum, *Monodelphis domestica* UPI0000F2C0F8; Chicken, *Gallus gallus* UPI0000ECC9F6; Xenopus, *Xenopus tropicalis* B2GUQ6; Nematostella, *Nematostella vectensis* JGI genome & FGENESH; Trichoplax, *Trichoplax adhaerens* JGI genome & FGENESH; Aedes, *Aedes aegypti* Q0IEY5; Culex, *Culex quinquefasciatus* B0W570; Anopheles, *Anopheles gambiae* A7UR11; Fly, *Drosophila melanogaster* D0Z773. Fungal sequences: Aspor, *Aspergillus oryzae* Q2UF57; Pencw, *Penicillium chrysogenum* B6GX21; Ajecn, *Ajellomyces capsulata* A6R2B1; Neucr, *Neurospora crassa* Q96U00; Fission yeast, *Schizosaccharomyces pombe* O14207; Budding yeast, *Saccharomyces cerevisiae* Q06164.

Subsequently, precipitates were eluted from the agarose beads by boiling in LDS sample buffer containing β-mercaptoethanol (β-ME) and eluates were subjected to SDS-PAGE. A strong band corresponding to FLAG-MMS22L was observed in precipitates from cells expressing FLAG-MMS22L, but not from parental HEK293 cells (Fig. 4.2B). Mass fingerprinting of FLAG-MMS22L precipitates indentified the largely-uncharacterised protein NFκB inhibitor-like 2 (NFκBIL2) as an interacting partner of MMS22L (Table 4.1). NFκBIL2 was so named based on a remote similarity to the NFκB inhibitor protein IκB (Ray et al., 1995). However, it does not appear to be part of the extended IκB gene family (Norman and Barton, 2000). Computational sequence analysis of NFκBIL2 (Fig. 4.3A) demonstrated that it is the human homologue of plant TONSOKU, which has been shown to be involved in the cellular response to perturbed DNA replication and the maintenance of silent chromatin (Takeda et al., 2004). This prompted me to re-name NFκBIL2 as TONSL (TONSOKU-Like). TONSL contains several different sets of modular domains that could be involved in protein-protein interactions: tetratricopeptide repeats (TPR), ankyrin repeats (ANK) and leucine-rich repeats (LRR) (Fig. 4.3, p.177). It also contains a novel ubiquitin-like fold (UBL) containing homo-oligomerization surfaces (Feng et al., 2007) (Fig. 4.4, p.178).

In order to confirm the interaction between MMS22L and TONSL, antibodies were raised against MMS22L and TONSL. In cell extracts, the anti-MMS22L and anti-TONSL antibodies each recognized a band around the predicted molecular weights of MMS22L (144 kDa) and TONSL (153 kDa), respectively; each band disappeared when cells were transfected with MMS22L- or TONSL-specific siRNA (Fig. 4.10A, p.190).

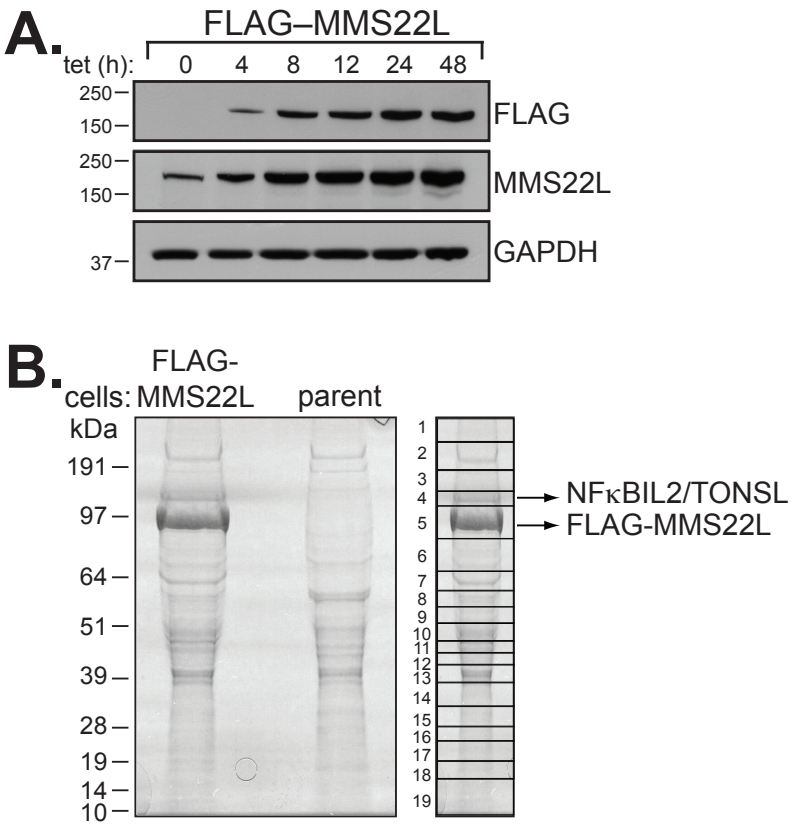

Figure 4.2 Stable expression of FLAG–MMS22L.

(A) Plasmids pcDNA5.1–FRT–TO (Invitrogen), expressing MMS22L with an N–terminal FLAG tag (under the control of tetracycline–inducible promoter were stably integrated at the FRT sites in HEK293 Flp–In cells (Invitrogen) according to the manufacturer's instructions. Cells were incubated with tetracycline for the times indicated and lysed. Extracts were subjected to SDS–PAGE followed by western blotting with indicated antibodies.

(B) HEK293 Flp–In cells that stably express MMS22L fused to an N–terminal FLAG tag under the control of a tetracycline–inducible promoter were incubated with tetracycline for 24 h and lysed. Extracts of these cells or parent HEK293 cells were subjected to immunoprecipitation with FLAG agarose beads and precipitates were subjected to SDS–PAGE. The gel was fixed and stained with Colloidal Blue (left panel). The gel lane containing MMS22L–associated proteins was cut into slices, as indicated (right panel), and the proteins were digested with trypsin before mass spectrometric fingerprinting.

Band no.	Accession number	Protein name	Molecular mass (Da)	No. of peptides	Mascot score
3	Q96HA7	NFκBIL2	153001	41	795
4	Q96HA7	NFκBIL2	153001	239	4405
4	Q14683	SMC1A	143771	2	125
4	Q92878	RAD50	183291	4	89
5	Q6ZRQ5	C6orf167	144106	603	14406
5	Q6PJL0	PARP1	113811	3	30
5	P49736	MCM2	102516	2	37
5	Q96HA7	NFκBIL2	153001	17	249
6	Q6PJL0	PARP1	113811	36	538
6	P33991	MCM4	97068	8	140
6	Q96HA7	NFκBIL2	153001	11	139
6	P49736	MCM2	102516	20	280
6	P11387	TOP1	91125	8	80
7	Q96HA7	NFκBIL2	153001	25	266
8	Q6IC76	XRCC6	70084	4	117
8	P11940	PABPC1	70854	25	450
9	P11940	PABPC1	70854	21	415
9	Q13310	PABPC4	71080	8	324
9	Q6IC76	XRCC6	70084	33	710
10	Q96HA7	NFκBIL2	153001	9	318
12	Q9H2B0	NAP1L1	45631	8	286
14	P11940	PABPC1	37987	10	469

Table 4.1 FLAG-MMS22L-associated proteins identified by mass spectrometry.

I used the antibodies to immunoprecipitate endogenous MMS22L and TONSL from HEK293 cells. Endogenous TONSL was detected in anti-MMS22L immunoprecipitates, but not in precipitates with an antibody against an unrelated protein (GFP, 'IgG') (Fig. 4.5, p.180). Similarly, MMS22L was detected in anti-TONSL immunoprecipitates (Fig. 4.5). Since cells were lysed in the presence of ethidium bromide, I can exclude the possibility that the MMS22L-TONSL interaction is mediated by DNA.

4.2.3 Identification of TONSL-interacting proteins

The presence of multiple protein-interaction domains in TONSL prompted me to search for TONSL-interacting proteins. A plasmid expressing TONSL fused to an N-terminal GFP tag under the control of a tetracycline-inducible promoter was stably integrated in HEK293 cells (Fig. 4.6A, p.181); as a control, another HEK293 cell line was created stably expressing GFP only. After inducing expression of GFP-TONSL or GFP, cell extracts were subjected to immunoprecipitation with GFP-Trap beads. A strong band corresponding to GFP-TONSL was observed in anti-GFP precipitates from these cells, but not from cells expressing GFP only (Fig. 4.6B, p.181). Mass fingerprinting of GFP-TONSL precipitates confirmed an interaction with MMS22L and also indentified the histone chaperones ASF1A and ASF1B and the MCM replicative helicases as interactors (Table 4.2, p.182). These interactions were confirmed by immunoblotting (Fig. 4.7A, p.184). Size exclusion chromatography of HEK293 cell extracts showed that TONSL co-elutes with MMS22L in a large complex of around 2 MDa. Further MMS22L and TONSL co-elute with ASF1A and with a small portion of MCM2 (Fig. 4.7B, p.184).

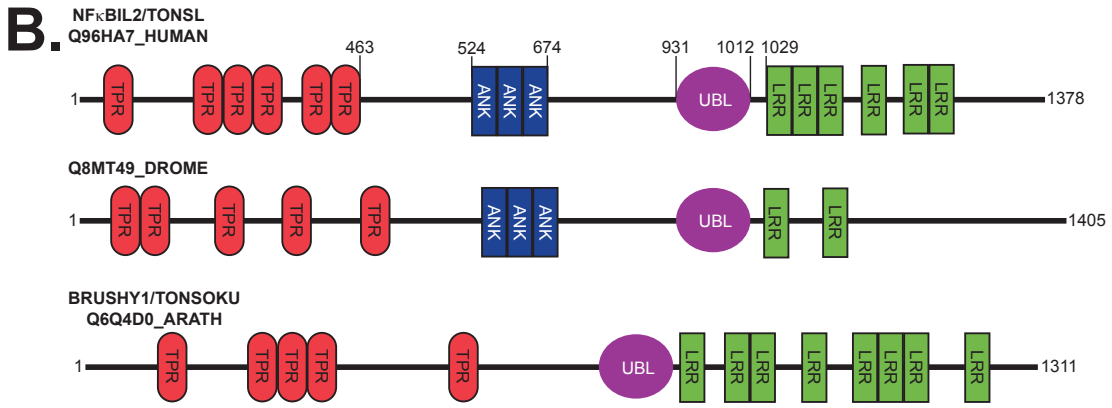

Figure 4.3 Bioinformatic analysis of TONSL.

(A) Representative multiple sequence alignment of TONSOKU orthologues. The amino acid colouring scheme indicates average BLOSUM62 scores (which are correlated with amino acid conservation) for each alignment column: cyan (greater than 3), blue (between 3 and 1.5) and grey (between 1.5 and 0.5). Tetratricopeptide repeats (TPR) region, ankyrin repeats region, PB1 ubiquitin-like domain [PMID: 17476308, PMID: 12906794, PMID: 11796218] and Leucine-Rich repeats (LRR) region are boxed in red, blue, violet and green, respectively. Locations of the repeats (TPR, ankyrin and LRR) are according to predictions from Pfam and SMART family databases [PMID: 19920124, PMID: 14681379], supplemented by REP web server analysis [PMID: 10772867]. Sequences are named with their UniProt identifiers [PMID: 19843607]. **(B)** Schematic representation of the domain architecture of *Homo sapiens* NFκBIL2/TONSL from *Homo sapiens* and TONSOKU/BRUSHY1 from *Arabidopsis thaliana* (ARATH). The UniProt identifier and the relevant species name for each protein is indicated.

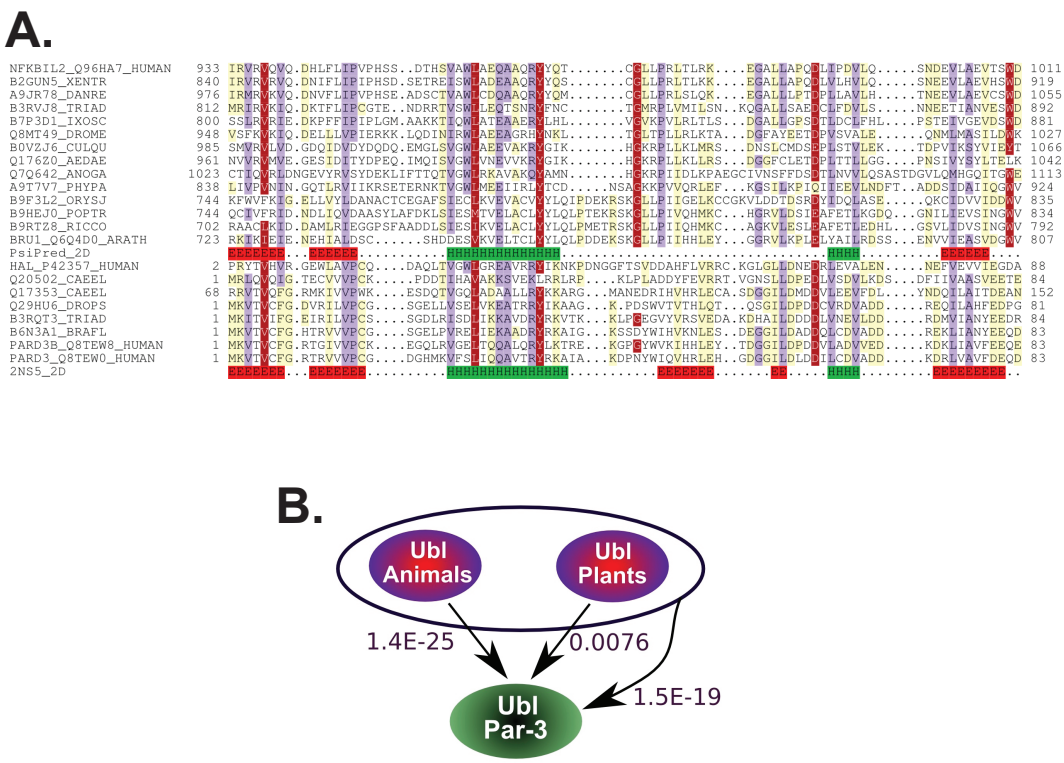

Figure 4.4 The ubiquitin-like domain of TONSL.

(A) Representative multiple sequence alignment of the PB1 ubiquitin-like domain common to TONSOKU homologous proteins, HAL (Histidine Ammonia Lyase) family and PAR-3 family. Sequences are named with their UniProt identifiers [PMID: 19843607]. "PsiPred_2D" indicates the secondary-structure prediction for the PB1 ubiquitin-like domain of TONSOKU homologous proteins. Secondary-structure predictions were performed with PsiPred [PMID:10493868]. "2NS5_2D" indicates the known secondary structure of the N-terminal PB1 ubiquitin-like Par-3 domain [PMID: 17476308]. Alpha-helices and beta-strands are indicated by "H" and "E" letters, respectively.

(B) Values correspond to global profile-versus-profile comparison *E*-Values (HHpred) [PMID: 15980461] between the PB1 ubiquitin-like domain of TONSOKU homologous proteins (in plants and animals) and the N-terminal PB1 ubiquitin-like Par-3 domain. Arrows indicate the profile search direction.

Inhibition of DNA replication triggers accumulation of H3 and MCMs in ASF1 immunoprecipitates, and this may reflect the storage of excess histones H3.1–H4 that build up when histone deposition is blocked (Groth et al., 2005; Jasencakova et al., 2010). In this light, exposure of cells to hydroxyurea or camptothecin caused an increase in the amount of MMS22L and TONSL in immunoprecipitates of STREP–tagged ASF1B stably expressed in HeLa cells (Fig. 4.8A, p.185). It was also previously reported that a mutated version of ASF1A, V94A, that abrogates binding to H3–H4 dimers results in loss of MCM subunits and other partners from ASF1A immunoprecipitates (Jasencakova et al., 2010). In this light, we found that the ASF1A V94A mutant does not co–immunoprecipitate with GFP–TONSL (Fig. 4.8B, p. 185), suggesting that TONSL interacts indirectly with ASF1 and, possibly, MCMs.

4.2.4 Mapping TONSL interaction domains

Next, I attempted to determine which domains of TONSL interact with its various partners by immunoprecipitating from cells expressing GFP-tagged fragments of TONSL (Fig. 4.9A, p.187). Fragments of TONSL lacking the leucine-rich repeat (LRR) region of the carboxy-terminus (GFP-TONSL 1-1028) could not interact with MMS22L, whereas the LLR region alone (GFP-TONSL 1029-1071) interacted with MMS22L in a manner indistinguishable from full-length TONSL (Fig. 4.9B). Thus the C–terminal LRR region of TONSL is necessary and sufficient for its interaction with MMS22L. In contrast, ASF1A/B, MCM2 and MCM6 could not interact with the LRR region of TONSL (Fig. 4.9B). Instead these proteins interacted only with TONSL fragments that had the ankyrin repeat domain (Fig. 4.9B, C). Taken together these data suggest that TONSL acts as a

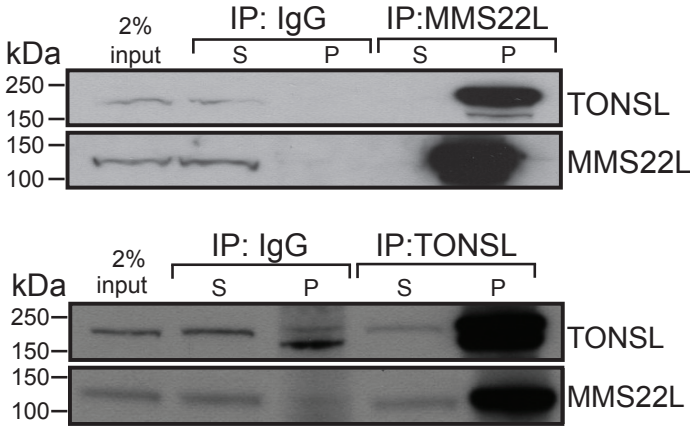

Figure 4.5 Confirmation of MMS22L-TONSL interaction.

HEK293 cells were lysed in the presence of ethidium bromide (50 μg/ml) and extracts were subjected to immunoprecipitation with antibodies raised against MMS22L (top panels), TONSL (bottom panels) or GFP ("IgG"). Precipitates were subjected to western blotting with the indicated antibodies. S, supernatant; P, pellet.

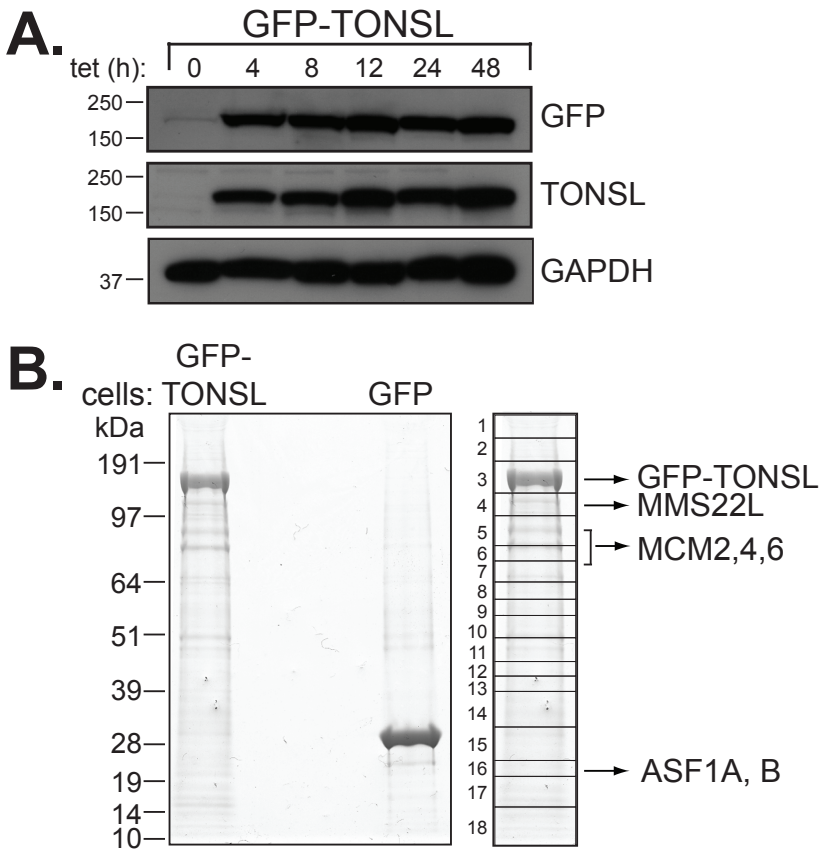

Figure 4.6. Stable expression of GFP-TONSL.

(A) Plasmids pcDNA5.1–FRT–TO (Invitrogen), expressing TONSL with an N–terminal GFP tag (under the control of tetracycline–inducible promoter were stably integrated at the FRT sites in HEK293 Flp–In cells (Invitrogen) according to the manufacturer's instructions. Cells were incubated with tetracycline for the times indicated and lysed. Extracts were subjected to SDS–PAGE followed by western blotting with indicated antibodies.

(B) HEK293 Flp–In cells that stably express GFP only or TONSL fused to an N–terminal GFP tag under the control of a tetracycline–inducible promoter were incubated with tetracycline for 24 h and lysed. Extracts were subjected to immunprecipitation with GFP–Trap beads and TONSL–associated proteins were identified as described for MMS22L in Fig. 4.2.

Band no.	Accession number	Protein name	Molecular mass (Da)	No. of peptides	Mascot score
3	Q96HA7	NFκBIL2	153001	544	10641
4	Q6ZRQ5	C6orf167	144106	37	849
5	P49736	MCM2	102516	22	559
5	Q6PJL0	PARP1	113811	7	150
6	P33991	MCM4	97068	4	129
6	Q14566	MCM6	57412	2	106
14	Q15365	PCBP1	37987	16	297
14	Q15366	PCBP2	38597	10	264
15	Q15365	PCBP1	37987	4	96
17	Q9Y294.1	ASF1A	23125	2	134
18	Q9NVP2.1	ASF1B	22761	2	96

Table 4.2 GFP-TONSL-associated proteins identified by mass spectrometry.

scaffold protein, with MMS22L binding at the C terminus, and ASF1A/B and the MCM complex binding, possibly via histones H3 and H4, to the N terminus (Fig. 4.20, p.217).

4.2.5 Depletion of MMS22L and TONSL causes a constitutive DNA damage response

Yeast cells lacking Mms22 show elevated levels of spontaneous DNA damage and defects in cell cycle progression (Dovey et al., 2009; Duro et al., 2008) and this prompted me to carry out similar investigations in human cells depleted of MMS22L or TONSL. In order to do this, cells were transfected with siRNAs specific for MMS22L or TONSL. Strikingly, depletion of endogenous MMS22L from HEK293 cells with two separate siRNAs reduced the level of endogenous TONSL protein and depletion of TONSL decreased levels of MMS22L (Fig. 4.10A, p.190). This implies that MMS22L stability depends on TONSL and *vice versa*. Caution must therefore be exercised when interpreting cellular consequences of depleting MMS22L or TONSL. Since both proteins are depleted when siRNA duplexes targeting either protein are used, conclusions can only be drawn on the effects of depleting both proteins together.

Depletion of MMS22L or TONSL caused a pronounced decrease in the rate of cell proliferation (Fig. 4.10B), which is likely due to DNA damage. Consistent with this idea, depletion of MMS22L or TONSL was accompanied by increased apoptosis judged by an increase in the levels of activated caspase–3 (Fig. 4.10C, D). Furthermore, depletion of MMS22L or TONSL caused an increase in the number of cells with spontaneous 53BP1 and γ-H2AX (Fig. 4.11A-C, p.192) subnuclear foci, both markers of DSBs.

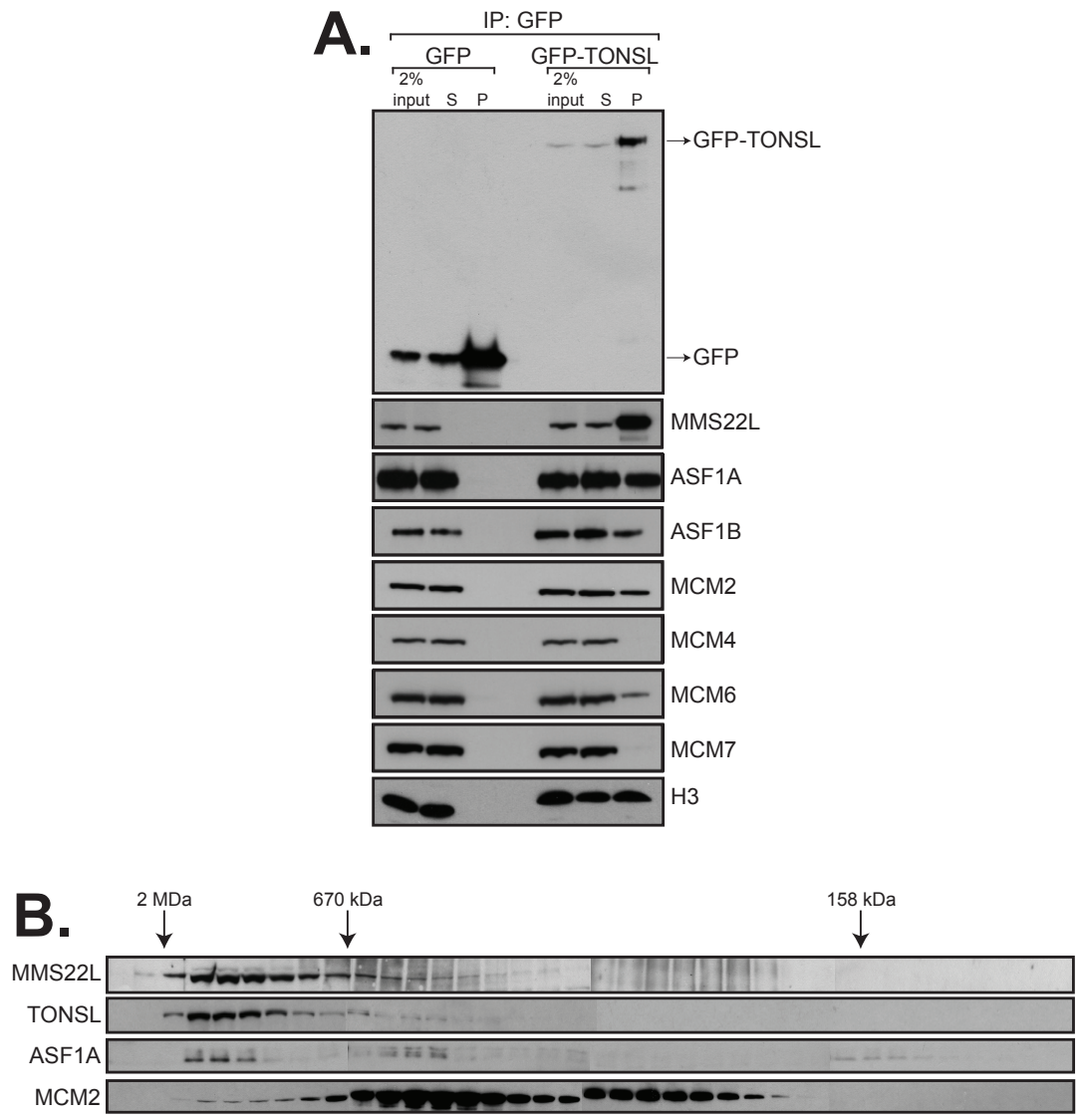

Figure 4.7 Confirmation of TONSL protein interactions.

(A) Extracts of cells expressing GFP or GFP–TONSL were subjected to immunoprecipitation with GFP–Trap beads. Precipitates were subjected to western blotting with the indicated antibodies. I, input; S, supernatant; P, pellet.

(B) Extracts of HEK293 cells were analyzed by size exclusion chromatography on a HiLoad 26/60 Superdex 200 column in buffer containing 0.2 M NaCl, and every third fraction was denatured and analyzed by western blotting with the indicated antibodies. The elution positions of Dextran blue (2 MDa), thyroglobulin (670 kDa), and bovine γ-globulin (158 kDa) are shown.

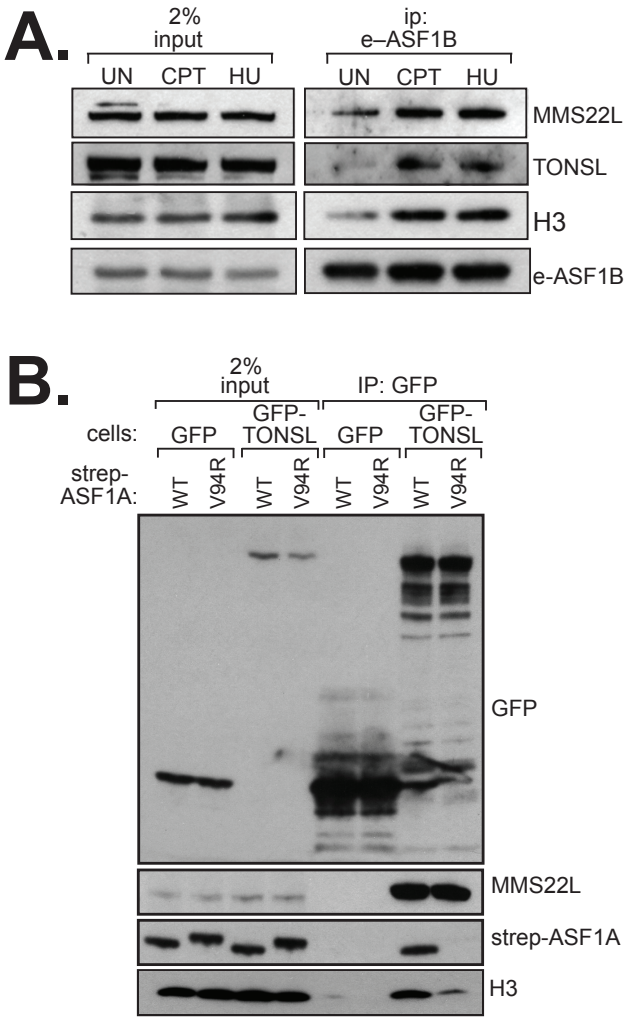

Figure 4.8 TONSL and ASF1 interact via a histone bridge.

(A) HeLa S3 cells stably expressing STREP–tagged ASF1B were treated with or without camptothecin (20 nM) or HU (3 mM) for 1.5 hours as indicated. Or left untreated ("UN"). Nuclear extracts were prepared and complexes were isolated with anti–STREP tag matrix and eluted with biotin. Precipitates were subjected to western blotting with the indicated antibodies. **(B)** Cells stably expressing GFP, or GFP–TONSL were transiently transfected with plasmids expressing STREP–tagged ASF1A wild type or V94R. Cell extracts were subjected to immunoprecipitation with GFP–Trap beads and precipitates were subjected to western blotting with the indicated antibodies. "Input" shows western blotting of whole cell extracts.

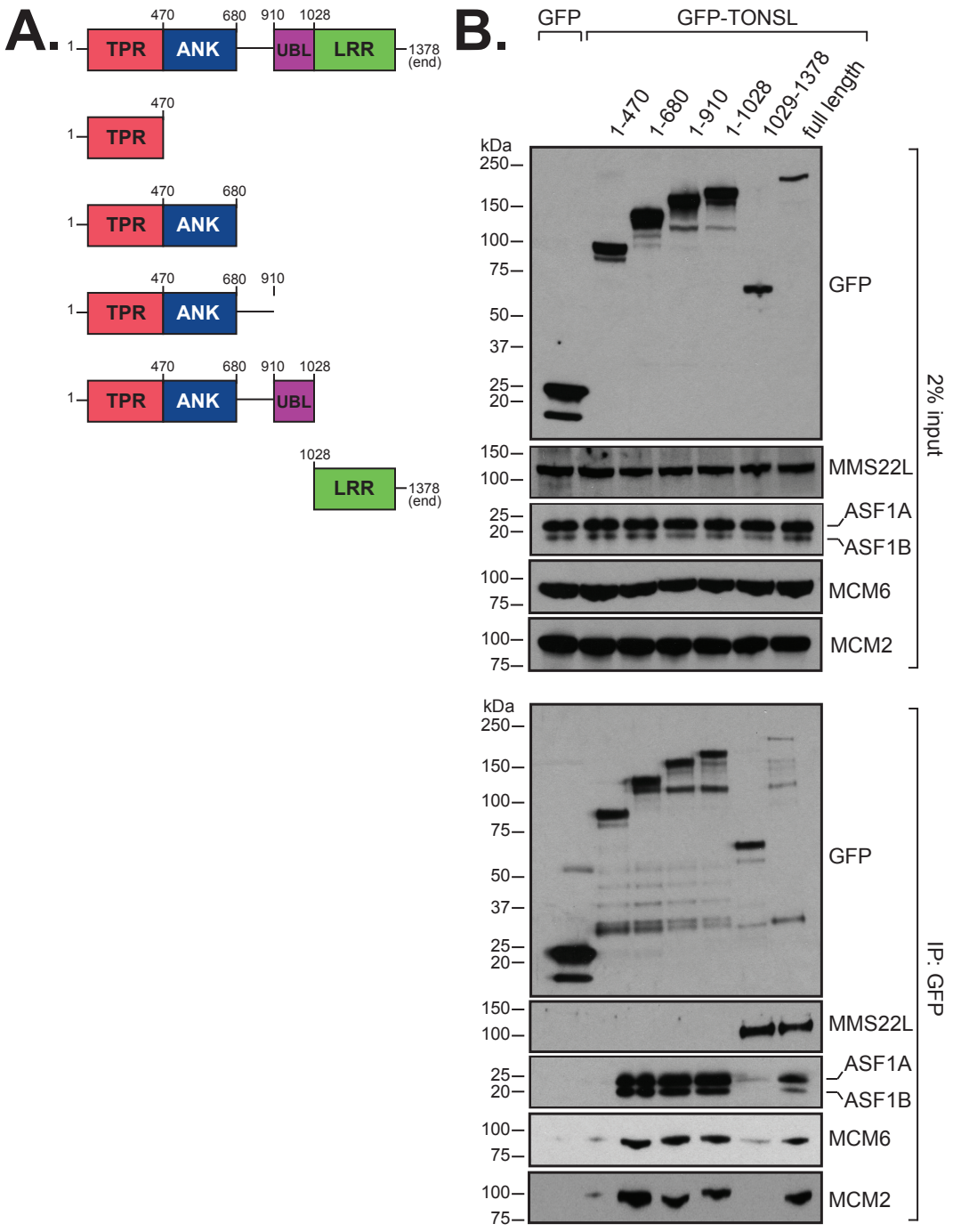
A.
1
470
680
910
1028
1378
(end)
TPR
ANK
UBL
LRR
B.
GFP
GFP-TONSL
1-470
1-680
1-910
1-1028
1029-1378
full length
kDa
250
150
100
75
50
37
25
20
GFP
MMS22L
ASF1A
ASF1B
MCM6
MCM2
2% input
IP: GFP

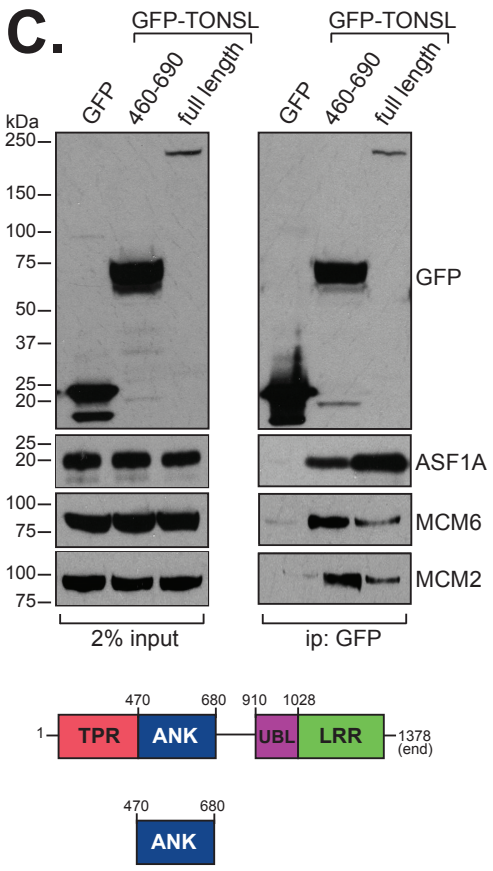

Figure 4.9 Mapping TONSL interactions.

(A) Schematic diagram of full length TONSL and TONSL deletion fragments. All deletion fragments were fused to a synthetic nuclear localization signal and GFP. TONSL domain boundaries are denoted by amino acid numbers.

(B) HEK293 cells were transiently transfected with plasmids expressing GFP, full length TONSL fused to GFP, or the indicated TONSL fragments fused to GFP. Cell extracts were subjected to immunoprecipitation with GFP–Trap beads and precipitates were subjected to western blotting with the indicated antibodies. “Input” shows western blotting of whole cell extracts.

(C) Same as (B).

I could estimate that depletion of MMS22L or TONSL caused a 2.5–3 fold increase in spontaneous DSBs (Fig. 4.11B, C, p.192). I next wished to investigate if these DSBs occur specifically in S–phase cells. To this end, I depleted MMS22L or TONSL and co-stained cells against S-phase cyclins and 53BP1. Cyclin E levels peak at the G1/S transition, whereas cyclin A levels peak at S/G2. I observed that more than 80% of cells with more than five 53BP1 foci were cyclin A-positive and cyclin E-negative (Fig. 4.11D-F). This suggests that depletion of MMS22L or TONSL causes DNA damage as cells pass through S–phase. Consistent with this, FACS analysis revealed that depletion of MMS22L or TONSL caused cells to accumulate at G2/M phase of the cell cycle, similarly to plant TONSOKU and yeast MMS22 mutants (Fig. 4.12, p.195). Taken together, these data suggest that TONSL and MMS22L are required to prevent DNA damage during DNA replication.

4.2.6 MMS22L and TONSL are required for cellular resistance to agents that cause replication fork collapse

I speculated that the spontaneous DNA damage observed in cells depleted of MMS22L or TONSL during DNA replication is caused by replication fork collapse. This prompted me to test if depletion of MMS22L or TONSL sensitized cells to agents that cause fork collapse, such as DNA topoisomerase inhibitors. Camptothecin is a TOP1 inhibitor that induces nicks in the genome and doxorubicin is a TOP2 inhibitor that causes S–phase–associated DSBs (section 1.14) (Pommier, 2006). Cells depleted of MMS22L or TONSL showed pronounced hypersensitivity to camptothecin and to doxorubicin (Fig. 4.13, p.197).

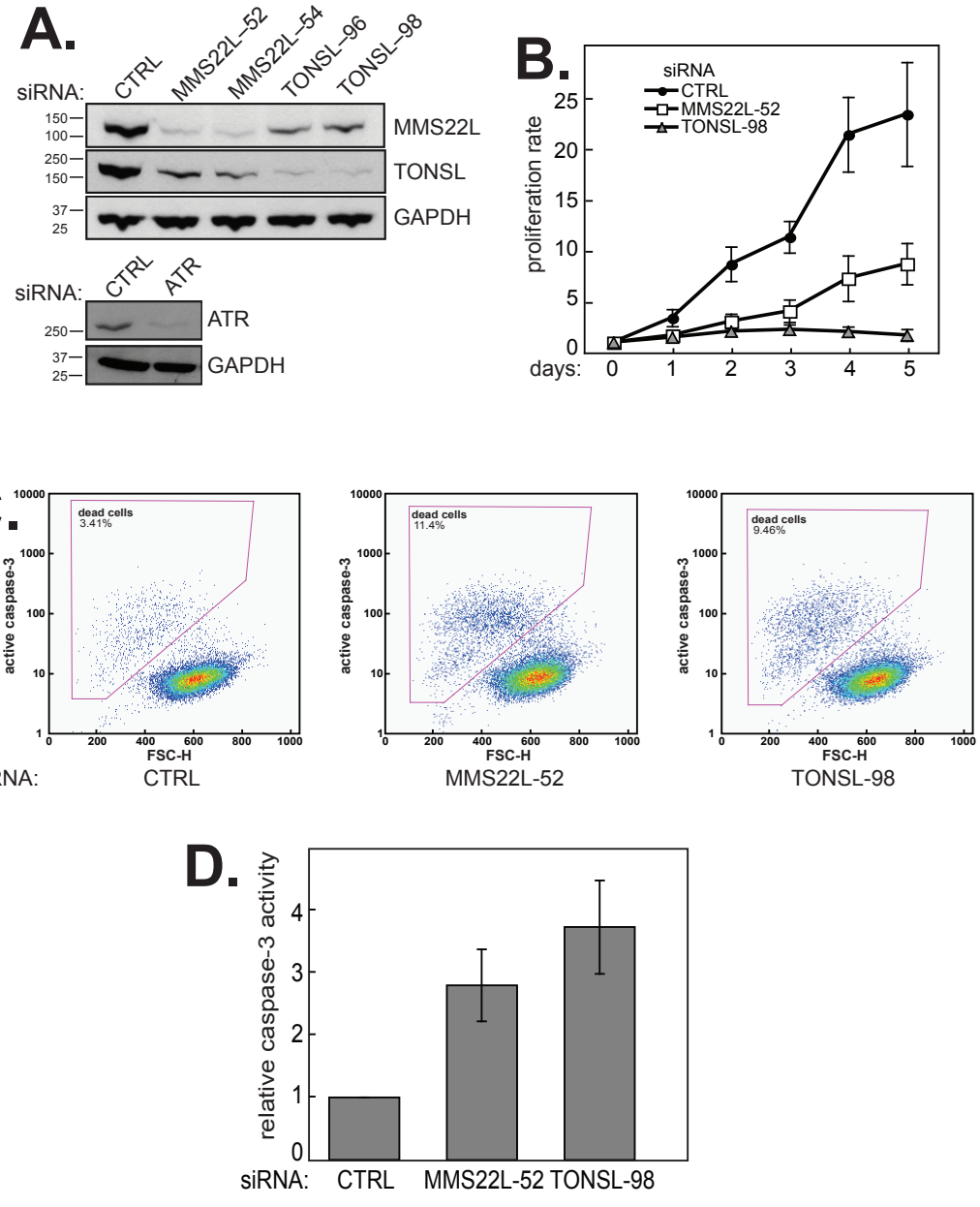
A.
siRNA:
CTRL
MMS22L–52
MMS22L–54
TONSL–96
TONSL–98
150
100
250
150
37
25
MMS22L
TONSL
GAPDH
siRNA:
CTRL
ATR
250
37
25
ATR
GAPDH
B.
siRNA
CTRL
MMS22L-52
TONSL-98
proliferation rate
25
20
15
10
5
0
days:
0
1
2
3
4
5
C.
dead cells
3.41%
dead cells
11.4%
dead cells
9.46%
active caspase-3
10000
1000
100
10
1
0
200
400
600
800
1000
FSC-H
siRNA:
CTRL
MMS22L-52
TONSL-98
D.
relative caspase-3 activity
4
3
2
1
0
siRNA:
CTRL
MMS22L-52
TONSL-98

Figure 4.10 MMS22L and TONSL depletion causes slow proliferation and increased apoptosis.

(A) HEK293 cells were transfected with control siRNA (CTRL), ATR–specific siRNA or two different siRNAs specifically targeting MMS22L (siRNAs 52 or 54) or TONSL (siRNAs 96 or 98). After 48 h, cell extracts were subjected to immunoblotting with the indicated antibodies. **(B)** HEK293 cells were transfected with control siRNA (CTRL) or siRNA specifically targeting MMS22L (52) or TONSL (98). After 48 h, cells were split and growth rate was assessed by counting cell number each day, relative to day 0. Each data point represents the average ± SEM from three independent experiments.

(C) HeLa cells were transfected with control siRNA (CTRL) or siRNA specifically targeting MMS22L (52) or TONSL (98). After 72h cells were fixed and were incubated with a FITC–conjugated antibody specific for the activated form of caspase–3, detected by flow cytometry. **(D)** The proportion of active caspase-3 positive cells was determined in cells treated with control siRNA (CTRL), or siRNA specific for MMS22L (52) or TONSL (98). Average values ± SEM from three independent experiments are shown.

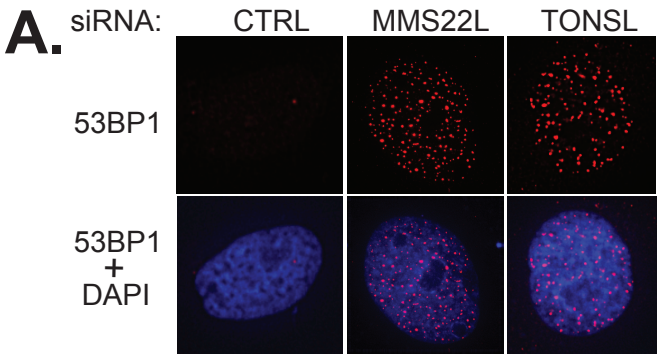

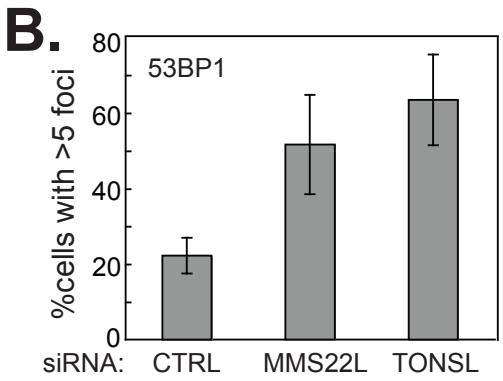

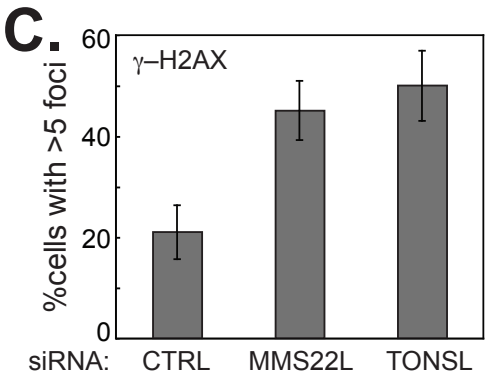

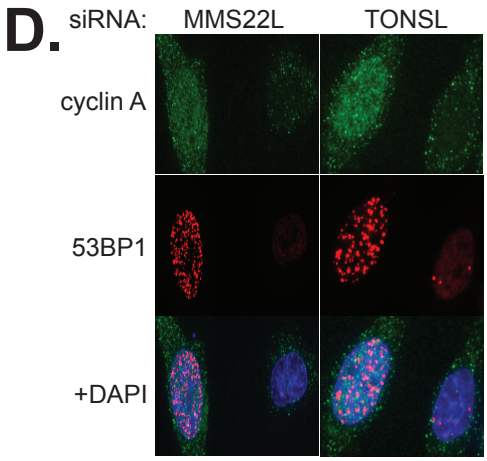

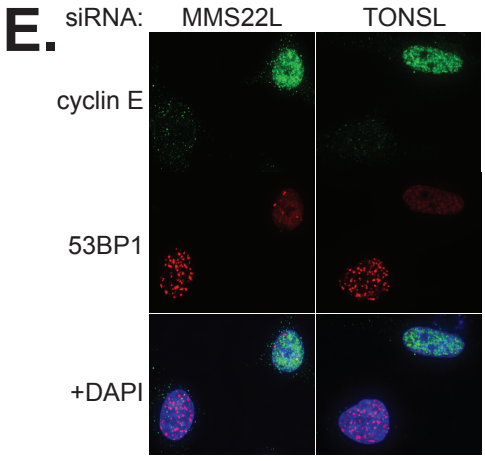

F.

	%cyclin A-positive cells	%cyclin E-positive cells
siMMS22L	91.8 ± 2.2	5.2 ± 0.5
siTONSL	91.5 ± 1.2	7.3 ± 0.9

Figure 4.11 MMS22L and TONSL prevent spontaneous DNA damage.

(A) HeLa cells transfected with control siRNA (CTRL) or siRNA targeting MMS22L (52) or TONSL (98) were grown on glass coverslips. Cells were fixed, permeabilized, washed, and immunofluorescence was carried out to visualize 53BP1 foci.

(B) The proportion of cells in each population with more than five 53BP1 foci was determined in cells treated with control siRNA (CTRL), or siRNA specific for MMS22L (52) or TONSL (98). Average values ± SEM from three independent experiments are shown.

(C) Same as B except that γ-H2AX foci were quantitated.

(D) As in (A), except cyclin A was also visualized.

(E) As in (A), except cyclin E was also visualized.

(F) Quantitation of 53BP1-positive cells stained with either cyclin A or cyclin E.

These cells were also sensitive to high concentrations of the DNA alkylating agent MMS that are probably sufficient to cause replication fork collapse (Fig. 4.13, p.197). Depletion of MMS22L or TONSL did not sensitize cells to hydroxyurea (which inhibits fork progression), ionizing radiation (which causes DSBs) or cisplatin (which induces DNA crosslinks) (Fig. 4.13A). In contrast, depletion of the ATR protein kinase sensitized cells to all of these agents (Fig. 4.13). Similar survival data with camptothecin and hydroxyurea were obtained using alternative MMS22L and TONSL siRNAs (Fig. 4.13B). These data suggest that MMS22L and TONSL are required for cellular responses to collapsed replication forks.

4.2.7 MMS22L and TONSL accumulate at perturbed replication forks and at DNA damage sites

Many DNA repair proteins are recruited into subnuclear 'foci' at sites of damaged replication forks. I wanted to determine if also MMS22L and TONSL are recruited into nuclear foci at damaged replication forks. In most untreated cells GFP–TONSL showed a diffuse staining pattern (Fig. 4.14A, p.198). Exposure of cells to HU or CPT resulted in a ~4-fold increase in the number of cells with >5 GFP–TONSL foci, and endogenous MMS22L formed foci that co–localized with GFP–TONSL (Fig. 4.14A, B). In a fraction of these cells, ASF1A also formed subnuclear foci that co–localized with GFP–TONSL (Fig. 4.14C, p.199).

In order to test if GFP–TONSL foci correspond to distressed replication forks, I examined the co–localization of GFP–TONSL with PCNA. Before staining cells with

antibodies, soluble nucleoplasmic proteins were extracted to aid visualization of chromatin–bound proteins. In around 70% of cells treated with HU or camptothecin that had GFP–TONSL foci, these foci co–localized with endogenous PCNA (Fig. 4.14D, p.199). In these cells, PCNA showed a punctate staining pattern consisting of small foci, characteristic of PCNA staining in early S–phase (Fig. 4.14D) (Dimitrova et al., 2002). In cells where PCNA staining was predominantly perinuclear, characteristic of mid–S–phase, GFP–TONSL had a diffuse staining pattern that did not co–localize with PCNA (Fig. 4.14D). I next investigated the binding of GFP–TONSL to sites of DNA damage induced by laser micro-irradiation. As shown in Fig. 4.15A (p.201), MMS22L and TONSL co–localized at sites of laser micro–irradiation–induced DNA damage and in these experiments MMS22L and TONSL co–localized with γ-H2AX. Taken together, these experiments show that MMS22L and TONSL localize to perturbed replication forks and at sites of DNA damage. I also examined the ability of TONSL fragments (Fig. 4.15B) to localize at sites of laser–induced DNA damage. Only TONSL fragments that had the ankyrin repeat domain localized at laser stripes (Fig. 4.15B). For example TONSL 1–470 corresponding to the TPR repeats showed a diffuse localization after nuclear micro–irradiation, whereas TONSL 1–680 corresponding to the TPR repeats plus the ankyrin repeats colocalized with γ-H2AX at sites of laser–induced DNA damage (Fig. 4.15B, p.201). These data suggest that the ankyrin repeats recruits TONSL to sites of DNA damage.

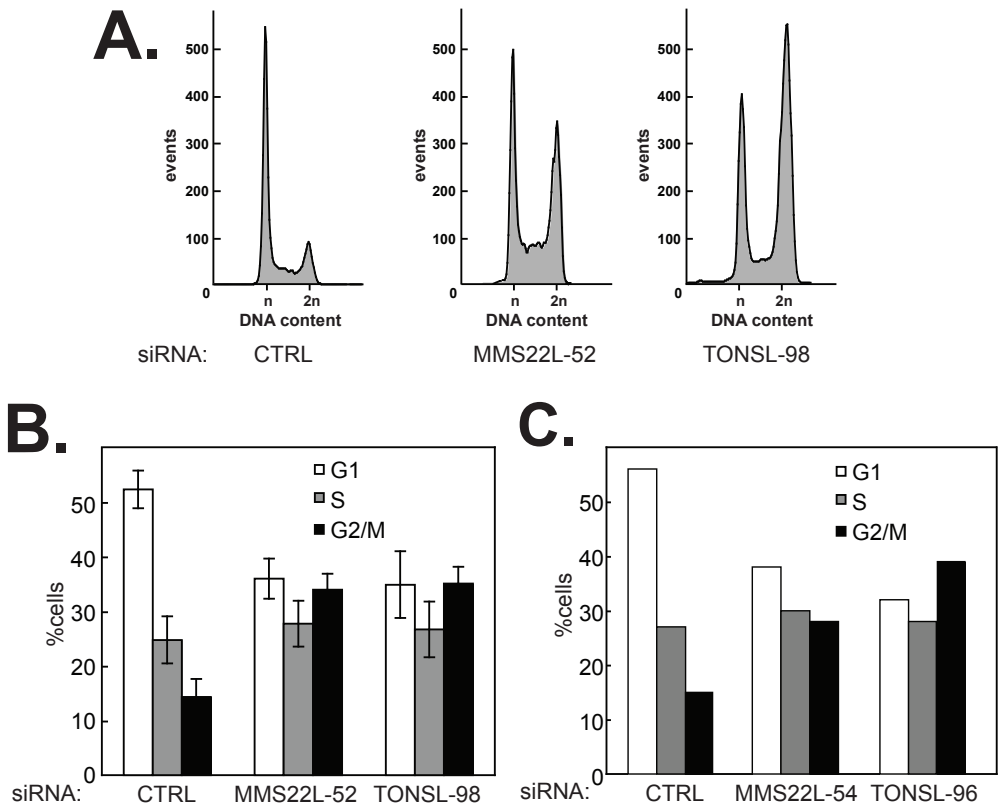

Figure 4.12 Depletion of MMS22L or TONSL affects cell cycle progression.

(A) U2OS cells were transfected with control siRNA (CTRL) or siRNA specifically targeting MMS22L (52) or TONSL (98). Representative flow-cytometry measurements of propidium iodide stained cells are shown.

(B) Watson-Paradigm program was used to model the distribution of cells into different phases of the cell cycle. The averages ± SEM from three independent experiments are shown.

(C) As in (B), except that the alternative siRNA oligos were used to target MMS22L and TONSL (54 and 96, respectively).

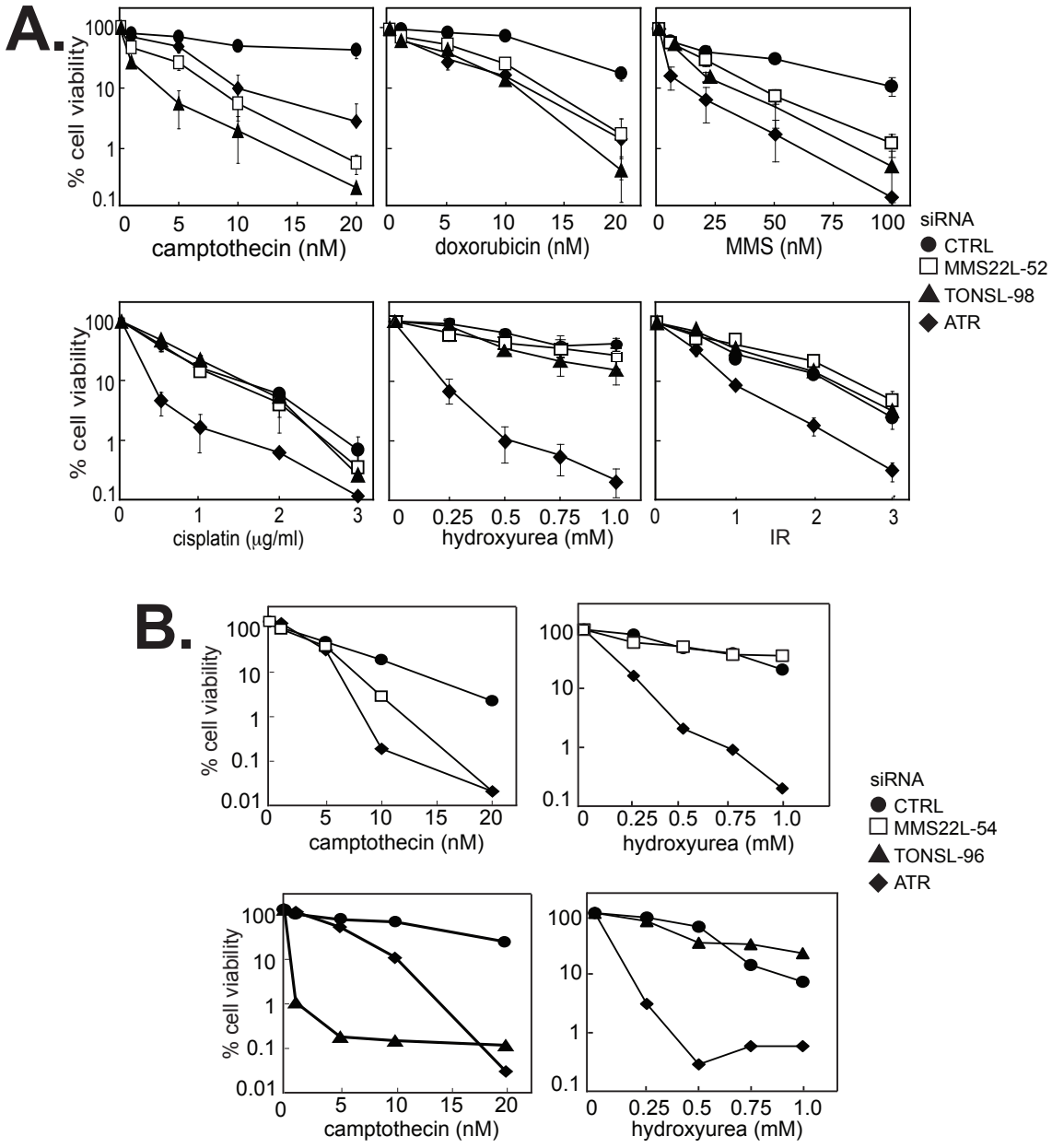
A.
% cell viability
100
10
1
0.1
0
5
10
15
20
camptothecin (nM)
doxorubicin (nM)
0
25
50
75
100
MMS (nM)
siRNA
CTRL
MMS22L-52
TONSL-98
ATR
cisplatin (μg/ml)
0
1
2
3
hydroxyurea (mM)
0
0.25
0.5
0.75
1.0
IR
B.
% cell viability
100
10
1
0.1
0.01
camptothecin (nM)
hydroxyurea (mM)
siRNA
CTRL
MMS22L-54
TONSL-96
ATR

Figure 4.13 Analysis of genotoxin sensitivity in cells depleted of MMS22L and TONSL.

(A) Cells were transfected with the relevant siRNA for 48 h and cells were split and seeded in 10 cm dishes (5000 cells/dish). Clonogenic survival assays were carried out with the genotoxins indicated. For each siRNA, cell viability of untreated cells is defined as 100%. Each data point represents an average ± standard error of the mean (SEM).

(B) As in (A), except that the alternative siRNA oligos were used to target MMS22L and TONSL (54 and 96, respectively).

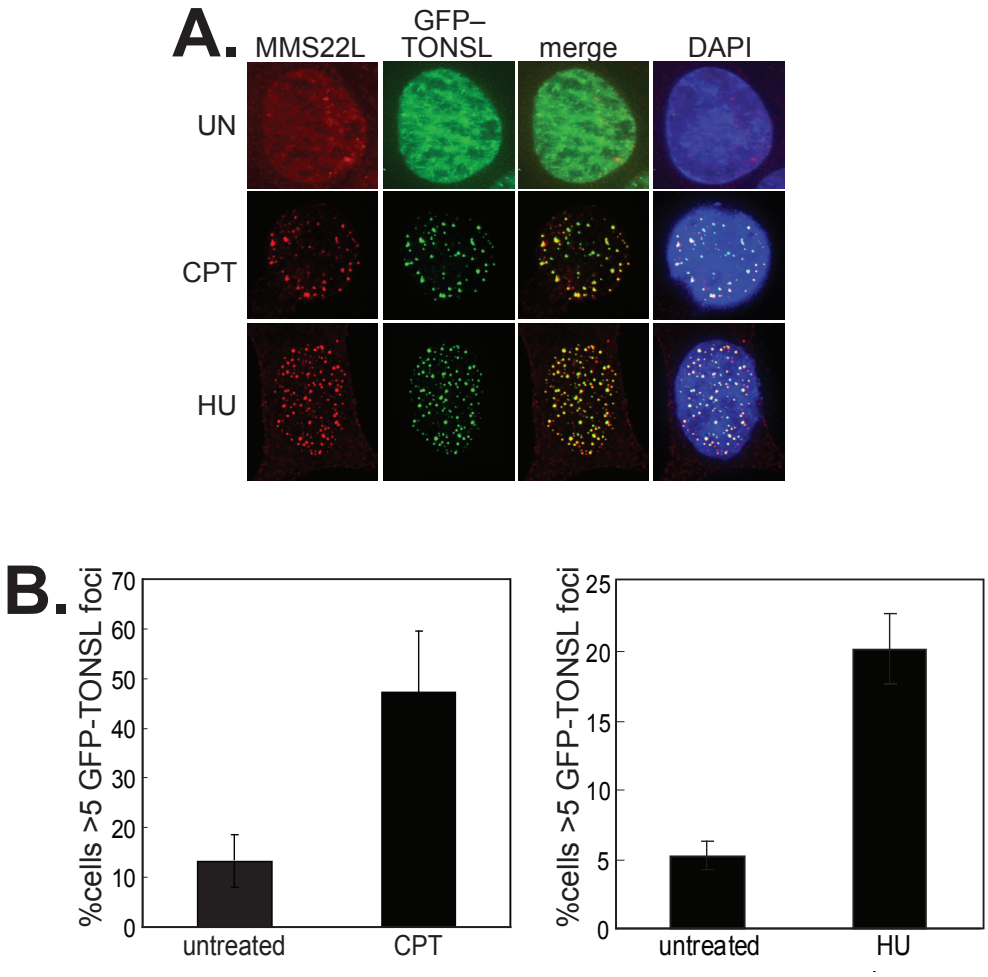
A.
MMS22L
GFP–
TONSL
merge
DAPI
UN
CPT
HU
B.
%cells >5 GFP-TONSL foci
70
60
50
40
30
20
10
0
untreated
CPT
%cells >5 GFP-TONSL foci
25
20
15
10
5
0
untreated
HU

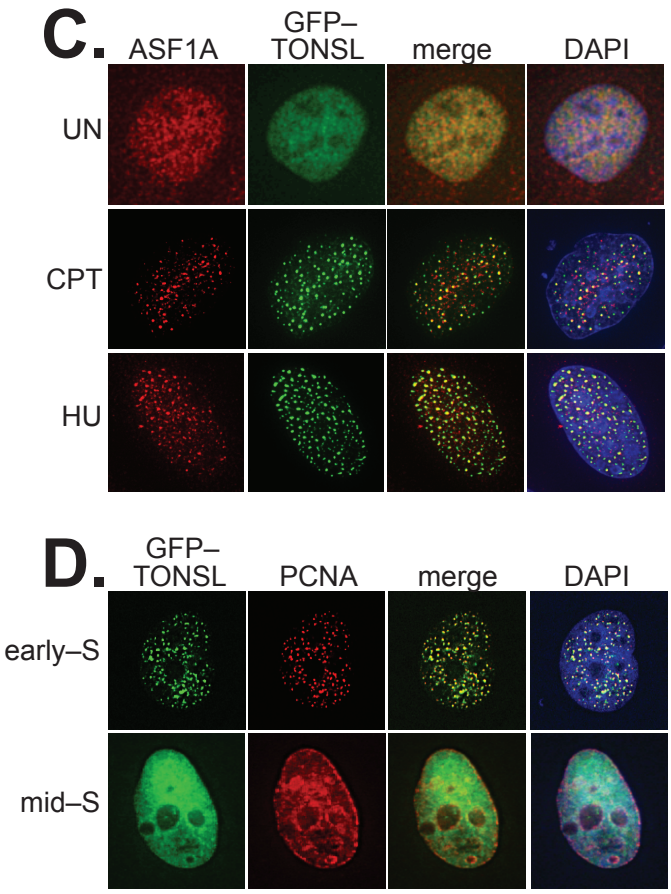

Figure 4.14 MMS22L and TONSL form subnuclear foci.

(A) U2OS cells stably expressing GFP–TONSL were treated, or not, with 20 nM camptothecin for 15 h or 2 mM HU for 24 h. Cells were fixed and stained with antibodies against MMS22L. MMS22L was detected in the TRITC channel and GFP was detected in the FITC channel.

(B) The number of cells with >5 GFP–TONSL foci was quantitated. Each data point represents an average ± standard error of the mean (SEM).

(C) Same as B except that cells were stained with antibodies against ASF1A.

(D) U2OS cells stably expressing GFP–TONSL were exposed to 2 mM HU for 24 h and cells were fixed and subjected to pre–extraction to remove soluble nuclear proteins. Cells were fixed and stained with antibodies against PCNA. PCNA was detected in the TRITC channel and GFP was detected in the FITC channel. Early S–phase cells are classified by small punctate, pan–nuclear PCNA foci, whereas mid–S–phase cells have perinuclear PCNA.

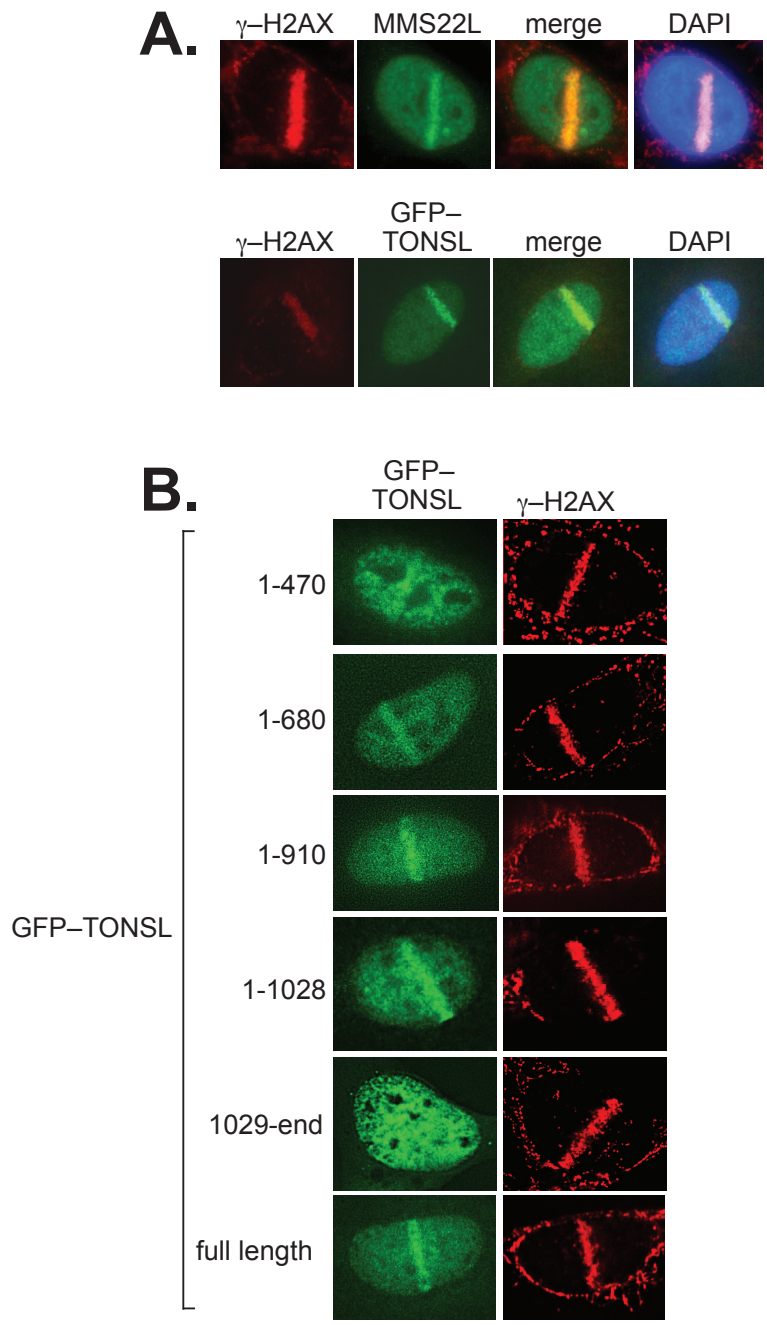
A.
γ–H2AX
MMS22L
merge
DAPI
γ–H2AX
GFP–
TONSL
merge
DAPI
B.
GFP–
TONSL
γ–H2AX
GFP–TONSL
1-470
1-680
1-910
1-1028
1029-end
full length

Figure 4.15 TONSL and MMS22L are recruited to sites of laser-induced DNA damage.

(A) U2OS cells stably expressing GFP–TONSL were laser micro–irradiated; after 10 min cells were fixed, permeabilised and immunofluorescence was performed with antibodies against MMS22L and γ-H2AX (top panels). Alternatively, cells were stained with antibodies against γ-H2AX (bottom panels) and secondary antibodies conjugated to AlexaFluor594. In this case, γ-H2AX was detected in the TRITC channel and GFP was detected in the FITC channel.

(B) U2OS cells were transiently transfected with plasmids expressing GFP, full length TONSL fused to GFP, or the indicated TONSL fragments fused to GFP. Cells were laser micro–irradiated; after 15 min cells were fixed, permeabilised and immunofluorescence was performed with antibodies against γ-H2AX.

4.2.8 MMS22L or TONSL are required for efficient homologous recombination

The hypersensitivity of cells depleted of MMS22L or TONSL to agents that cause replisome collapse suggested that these proteins are required to repair broken replication forks. Because HR is an important mechanism for fork rescue, and because yeast Mms22 is required for HR induced by agents that block replisomes (Duro et al., 2008), we next tested the involvement of MMS22L and TONSL in HR. Formation of the RAD51 nucleoprotein filament on resected DNA ends is an important early event in HR that is necessary for strand invasion (Fig. 4.20). We examined formation of RAD51 foci in cells exposed to camptothecin. Depletion of MMS22L or TONSL reduced the number of camptothecin-treated cells with >9 RAD51 foci by approximately 50% and 70% respectively compared with control siRNA (Fig. 4.16A, B). These data suggested that the ability of RAD51 to load onto resected DNA ends is compromised in cells depleted of MMS22 or TONSL. Depletion of MMS22L or TONSL did not affect the appearance of γ-H2AX foci after exposure of cells to camptothecin (Fig. 4.16C) and I therefore conclude that the reduction in RAD51 foci in cells depleted of MMS22L or TONSL is not due to a defect in the formation of DSBs. RAD51 protein expression was unaffected by depletion of MMS22L or TONSL (Fig. 4.16D).

The loading of RAD51 on to DSBs requires DSB resection to generate a 3' ssDNA overhang to which RAD51 binds (section 1.7.2) (San Filippo et al., 2008). In this light, the defect in RAD51 loading in cells depleted of MMS22L or TONSL could be explained by a defect in DSB resection. ssDNA generated by resection is coated with the replication protein A (RPA) heterotrimer that is important for DNA replication and repair

(Sakaguchi et al., 2009). I therefore analysed RPA foci after exposure of cells to camptothecin to assess DSB resection. It was reported that depletion of CtIP, a protein that is required for end resection, prevents formation of camptothecin–induced RPA foci (Huertas and Jackson, 2009). Therefore RPA focus formation is a reliable readout of resection in camptothecin–treated cells. I found that MMS22L or TONSL depletion did not prevent camptothecin–induced RPA focus-formation. Around 80% of cells treated with control siRNA, TONSL siRNA or MMS22L siRNA had >9 RPA foci after exposure to camptothecin (Fig. 4.17A, B). In most cells treated with control siRNA, camptothecin–induced RPA foci disappeared during recovery and, after 96 h, only 24% of cells had >9 RPA foci (Fig. 4.17A, B). Intriguingly, RPA foci did not decline in cells depleted of MMS22L or TONSL. Even after 96 h of recovery from exposure to camptothecin, almost 80% of cells depleted of MMS22L or TONSL had >9 RPA foci (Fig. 4.17A, B). These data suggest that MMS22L and TONSL are required for the displacement of RPA by RAD51 on resected DNA ends at collapsed replication forks (Fig. 4.20B). This is likely to be through indirect mechanisms, since I did not detect any interaction between TONSL and a variety of HR factors, including RAD51 (Fig. 4.17C).

HR is important not just for fork rescue but also for DSB repair. In this light, cells depleted of MMS22L or TONSL showed a reduction of 44% and 66%, respectively, in the number of cells with >9 IR–induced RAD51 foci compared with control siRNA (Fig. 4.18A). In order to assess DSB–induced HR directly, we used a reporter system in U2OS cells to measure HR frequency. In this system, an 18 bp sequence recognized by the I-*Sce*I meganuclease is placed between tandem mutant copies of GFP (Pierce et al., 1999). HR between these two copies generates a wild-type GFP.

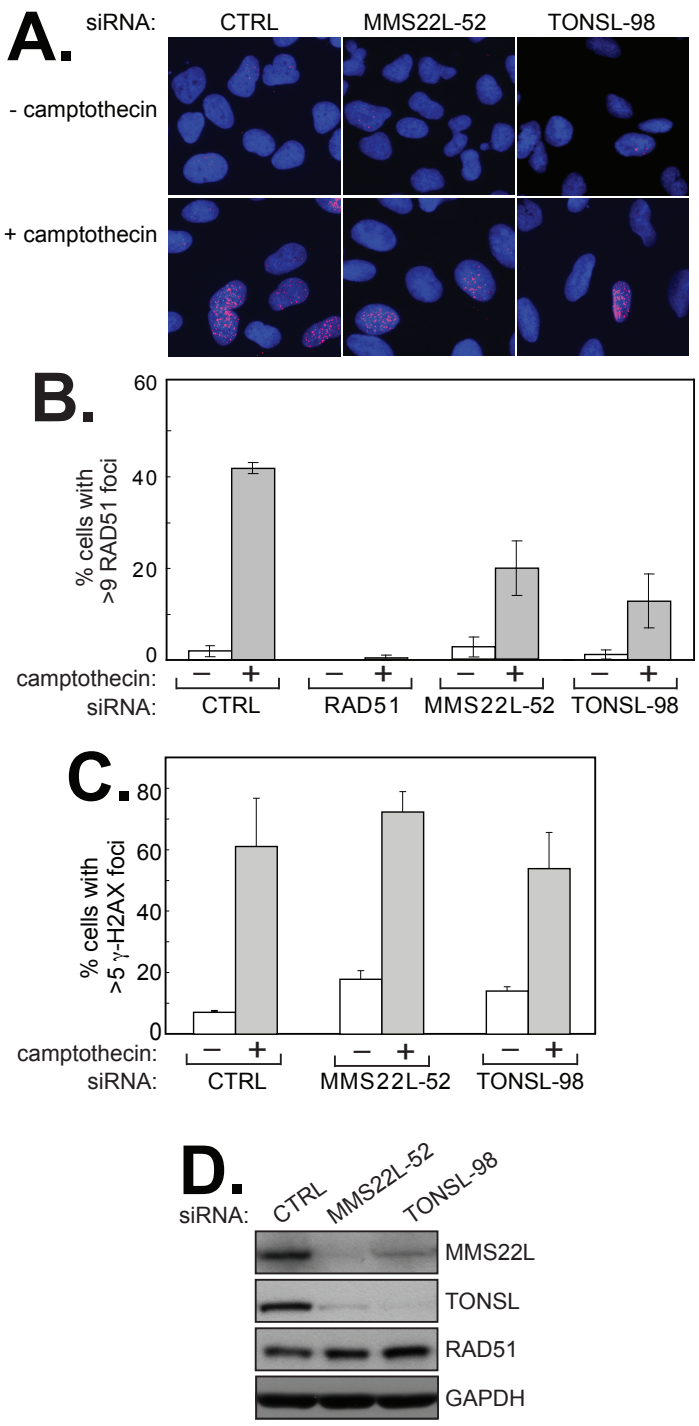
A.
siRNA:
CTRL
MMS22L-52
TONSL-98
- camptothecin
+ camptothecin
B.
% cells with >9 RAD51 foci
60
40
20
0
camptothecin:
siRNA:
CTRL
RAD51
MMS22L-52
TONSL-98
C.
% cells with >5 γ-H2AX foci
80
60
40
20
0
camptothecin:
siRNA:
CTRL
MMS22L-52
TONSL-98
D.
siRNA:
CTRL
MMS22L-52
TONSL-98
MMS22L
TONSL
RAD51
GAPDH

Figure 4.16 MMS22L and TONSL are required RAD51 loading.

(A) U2OS cells transfected with control siRNA (CTRL), or siRNA specific for MMS22L (52), TONSL (98) or RAD51 were treated with camptothecin (50 nM) for 24 h. Cells were fixed and stained with antibody against RAD51. Representative images are shown.

(B) The number of cells with >9 RAD51 foci after camptothecin treatments was counted. Each timepoint was analysed in triplicate and each datapoint represents the average ± SEM.

(C) MMS22L or TONSL depletion does not affect the level damage induced by camptothecin. Cells were treated as in (A) and then stained with antibodies recoginising γ-H2AX.

(D) MMS22L or TONSL depletion does not affect RAD51 protein levels. Lysates from cells transfected with control siRNA (CTRL), or siRNA specific for MMS22L (52), TONSL (98) were subjected to immunoblotting with the indicated antibodies.

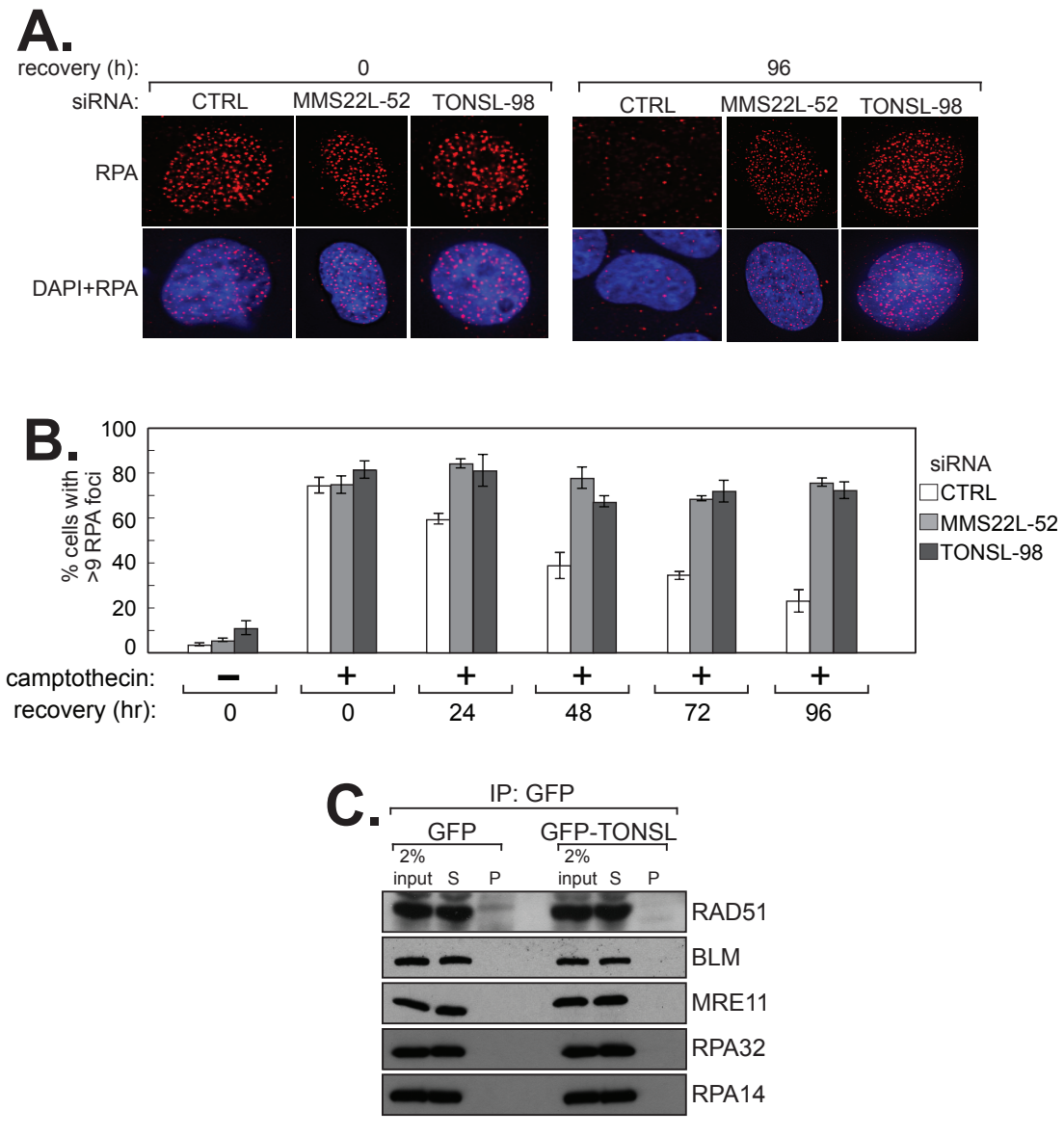
A.
recovery (h):
0
96
siRNA:
CTRL
MMS22L-52
TONSL-98
CTRL
MMS22L-52
TONSL-98
RPA
DAPI+RPA
B.
% cells with >9 RPA foci
100
80
60
40
20
0
siRNA
CTRL
MMS22L-52
TONSL-98
camptothecin:
recovery (hr):
0
0
24
48
72
96
C.
IP: GFP
GFP
GFP-TONSL
2%
input
S
P
2%
input
S
P
RAD51
BLM
MRE11
RPA32
RPA14

Figure 4.17 RPA foci persist in cells depleted of MMS22L and TONSL.

(A) U2OS cells transfected with control siRNA (CTRL), MMS22L siRNA (52) or TONSL siRNA (98) were treated with camptothecin (20 nM) for 24 h and then allowed to recover for the times indicated. RPA foci were then detected by indirect immunofluorescence. A representative experiment is shown.

(B) Quantitiation of RPA foci during recovery from exposure of U2OS cells to camptothecin. The number of cells with >9 RPA foci was counted. Each timepoint was analysed in triplicate and each datapoint represents the average ± SEM.

(C) Extracts of cells expressing GFP or GFP–TONSL were subjected to immunoprecipitation with GFP–Trap beads. Precipitates were subjected to western blotting with the indicated antibodies. I, input; S, supernatant; P, pellet.

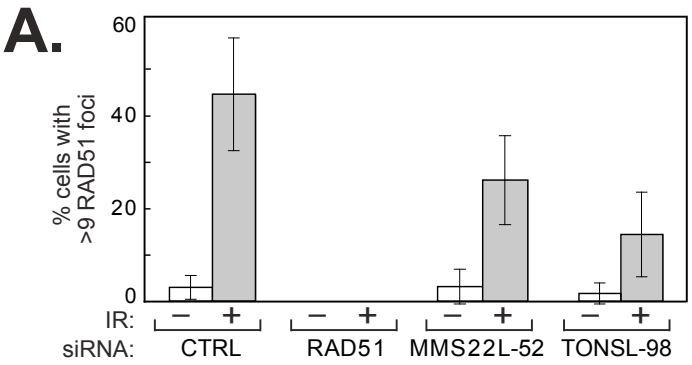
A.
% cells with >9 RAD51 foci
60
40
20
0
IR:
siRNA:
CTRL
RAD51
MMS22L-52
TONSL-98

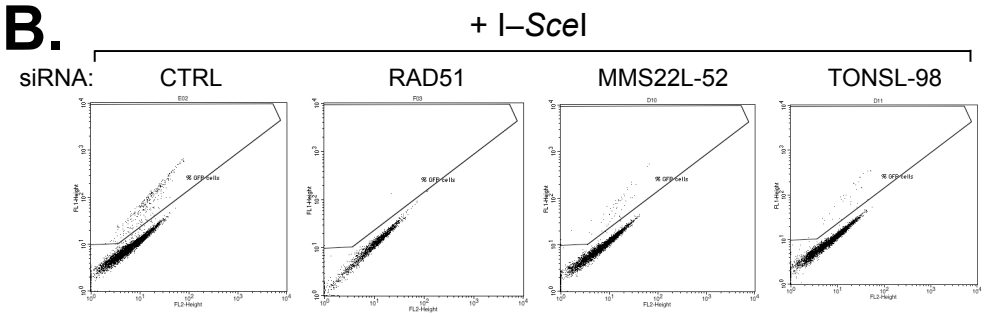
B.
+ I–SceI
siRNA:
CTRL
RAD51
MMS22L-52
TONSL-98

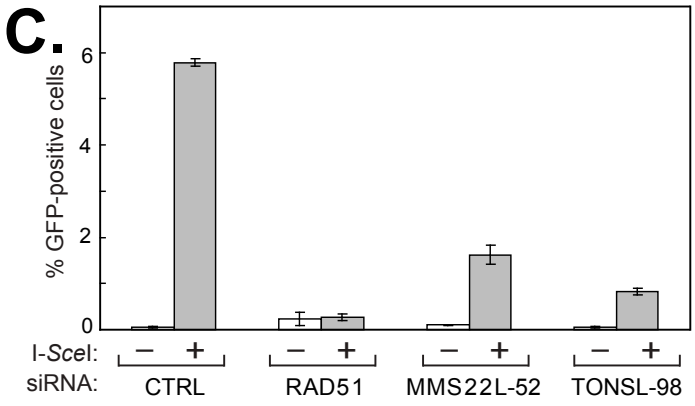
C.
% GFP-positive cells
6
4
2
0
I-SceI:
siRNA:
CTRL
RAD51
MMS22L-52
TONSL-98

Figure 4.18 MMS22L and TONSL are required for efficient HR.

(A) The number of cells with >9 RAD51 foci after IR treatments was counted. Each timepoint was analysed in triplicate and each datapoint represents the average ± SEM.

(B) U2OS cells harboring a GFP–based HR reporter were transfected with control siRNA (CTRL) or siRNAs specifically targeting RAD51, TONSL (98), or MMS22L (52) and later transfected with a plasmid expressing I-SceI or with an empty vector. A further 24 h later, cells were tested for GFP expression by FACS analysis. Representative flow cytometry measurements are shown.

(C) The frequency of HR in cells transfected with the various siRNAs was calculated relative to cells transfected with control siRNA. Each data point represents the average ± standard deviation from three independent experiments.

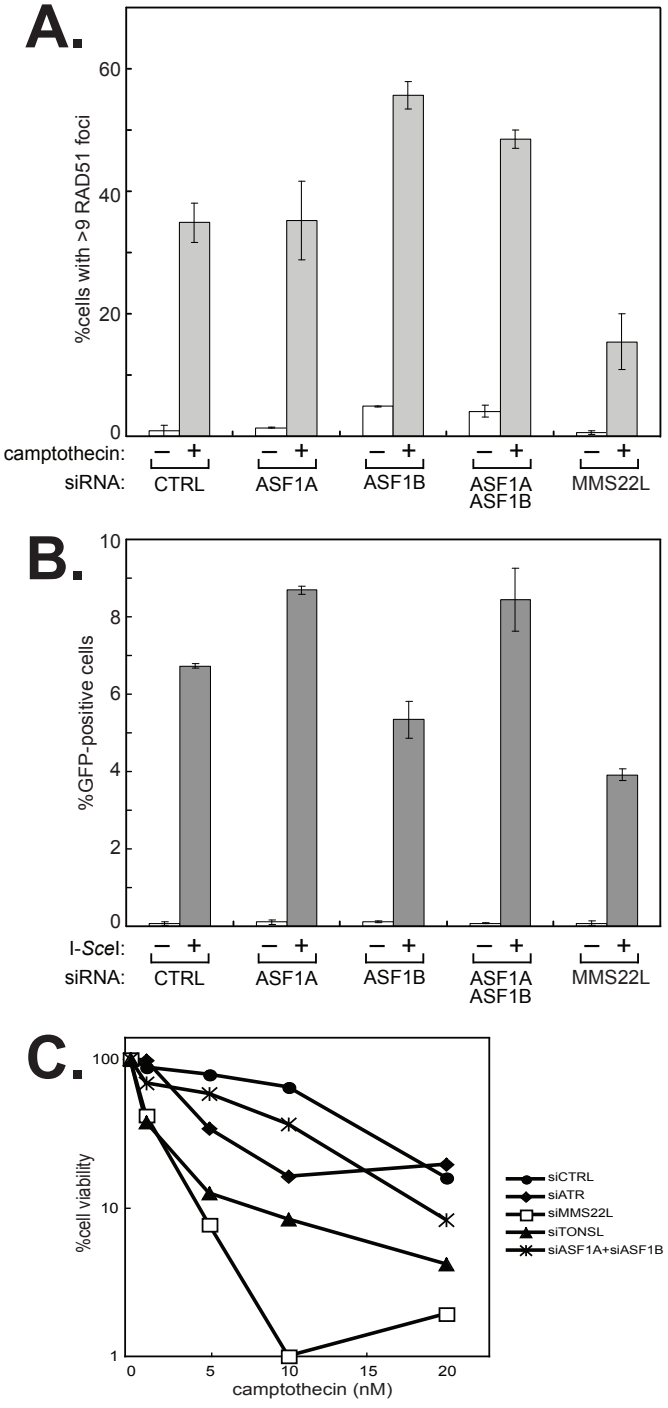
A.
%cells with >9 RAD51 foci
60
40
20
0
camptothecin:
– +
siRNA:
CTRL
ASF1A
ASF1B
ASF1A
ASF1B
MMS22L
B.
%GFP-positive cells
10
8
6
4
2
0
I-SceI:
siRNA:
CTRL
ASF1A
ASF1B
ASF1A
ASF1B
MMS22L
C.
%cell viability
100
10
1
0
5
10
15
20
camptothecin (nM)
siCTRL
siATR
siMMS22L
siTONSL
siASF1A+siASF1B

Figure 4.19 ASF1A and ASF1B depletion does not affect HR or survival after replication stress.

(A) U2OS cells transfected with control siRNA (CTRL), or siRNAs specifically targeting ASF1A, ASF1B or both ASF1A and ASF1B for 24 h. The number of cells with >9 RAD51 foci was counted. Each timepoint was analysed in triplicate and each datapoint represents the average ± SEM.

(B) U2OS cells harboring a GFP–based HR reporter were transfected with control siRNA (CTRL) or siRNAs specifically targeting ASF1A, ASF1B or both ASF1A and ASF1B. Cells were later transfected with a plasmid expressing I-SceI or with an empty vector. A further 24 h later, cells were tested for GFP expression by FACS analysis.

(C) Cells were transfected with the relevant siRNA for 48 h and cells were split and seeded in 10 cm dishes (5000 cells/dish). Clonogenic survival assays were carried out with the genotoxins indicated. For each siRNA, cell viability of untreated cells is defined as 100%. Each data point represents an average ± standard error of the mean (SEM).

open reading frame, and functional GFP expression can be detected by FACS analysis. As shown in Fig. 4.18B and C, depletion of RAD51 completely abolished I-*Sce*I-induced HR and depletion of MMS22L or TONSL reduced the efficiency by 70% and 80% respectively. It is interesting to note that depleting ASF1A and ASF1B by siRNA singly or in combination had little effect on I-*Sce*I-induced HR (Fig. 4.19A) or on the formation of camptothecin–induced RAD51 foci (Fig. 4.19B). Furthermore, depletion of both ASF1A and ASF1B from HEK293 cells causes only very weak sensitivity to camptothecin or doxorubicin (Fig. 4.19C). Taken together, these data indicate that MMS22L and TONSL promote HR by facilitating the replacement of RPA with RAD51 on ssDNA overhangs generated by DSB resection. This appears to be independent of ASF1.

4.3 Discussion

In this chapter I identify C6ORF167/MMS22L as a putative human orthologue of yeast Mms22. In support of this, I observed important functional similarities between MMS22L and yeast Mms22: depletion of MMS22L from human cells, like Mms22 deletion in budding and fission yeast, causes slow proliferation, increased spontaneous DNA damage, sensitivity to camptothecin and defects in HR. However, there are important differences between human MMS22L and yeast Mms22. Firstly, MMS22L depletion in human cells does not cause sensitivity to HU, whereas *mms22*Δ yeast mutants are hypersensitive to this agent. Secondly, no TONSL orthologue could be found in yeast. Further, budding yeast Mms22 is thought to be part of an SCF–type E3 ubiquitin ligase (Zaidi et al., 2008), but we could not detect any of the known

components of human SCF complexes in MMS22L or TONSL immunoprecipitates. However, since fission yeast Mms22 also does not appear to interact with cullins, this aspect may not be evolutionarily conserved.

MMS22L interacts with TONSL, which appears to be the human orthologue of plant TONSOKU. *Arabidopsis* TONSOKU was identified in a screen for "fasciation" (*fas*) mutants that have disorganized meristems (Suzuki et al., 2004), regions of very rapid cell proliferation. Other *fas* mutants correspond to subunits of chromatin assembly factor 1 (CAF-1) (Kaya et al., 2001) and AtMRE11 (Bundock and Hooykaas, 2002). TONSOKU mutations cause sensitivity to genotoxins, elevated intra–chromosomal recombination and, like CAF-1 mutants, this is accompanied by loss of transcriptional silencing (Takeda et al., 2004). TONSOKU mutations also cause arrest at G2/M (Suzuki et al., 2005). Taken together these findings suggest that TONSOKU is required to prevent DNA damage in S–phase by modulating chromatin. The data presented in this study indicate that depleting TONSL – or its partner MMS22L – from human cells causes similar defects to those noted for TONSOKU mutants. These phenotypic similarites, together with similarity in domain organization suggest that TONSL is the functional equivalent of TONSOKU in human cells.

GFP–TONSL accumulates at replication forks in cells treated with HU or camptothecin but it is not yet clear how these proteins are recruited there. I only observed co–localization of GFP–TONSL with PCNA in early–S–phase cells, and it is not yet clear why. It is interesting to note that ASF1 is also present in some of these GFP–TONSL foci. As well as localizing at replication forks, TONSL and MMS22L localize at sites of

laser–induced DNA damage. However, neither ASF1A nor ASF1B localized detectably at laser stripes (data not shown). Perhaps only a small pool of ASF1A and ASF1B localize at sites of laser-induced DNA damage. Alternatively, it might be that the ASF1 only cooperates with MMS22L and TONSL at perturbed replication forks. However, depleting ASF1A and ASF1B does not cause the severe camptothecin sensitivity or HR defects seen in cells depleted of TONSL or MMS22L. Thus, if ASF1A and ASF1B do cooperate with MMS22L and TONSL in responses to perturbed DNA replication, there must be redundancy with other factors that remain to be identified. In plants, TONSOKU protects genome stability in S-phase and TONSOKU mutations such as *bru1* cause DNA damage and cause a phenotype similar to mutations in subunits of CAF1 (Suzuki et al., 2004; Takeda et al., 2004). On this basis, it is possible that TONSOKU remodels perturbed replication forks to facilitate their repair. It is possible that TONSL and MMS22L function in an analogous manner in human cells.

TONSL and MMS22L are required for efficient HR and this appears to reflect a role in facilitating the replacement of RPA with RAD51 on resected DNA ends. In cells depleted of MMS22L or TONSL, DSBs formed after exposure to camptothecin are resected normally, judged by formation of RPA foci, but strikingly these RPA do not disappear during recovery. This is accompanied by decreased loading of RAD51. These findings suggest that MMS22L and TONSL somehow influence the replacement of RPA with RAD51 on resected DNA ends. So how might MMS22L and TONSL facilitate replacement of RPA with RAD51? It has also been reported that displacement of RPA from DNA during HR is influenced by checkpoint signalling (Sleeth et al., 2007) although I did not detect checkpoint defects in cells depleted of MMS22L or TONSL.

Work from many labs has shown that mediator proteins such as RAD52, BRCA2 and RAD51 paralogues act to physically displace RPA by directly binding to RPA and ssDNA (San Filippo et al., 2008). *In vitro*, the RAD52 mediator protein interacts specifically with ssDNA–RPA complexes to facilitate RAD51 nucleoprotein filament assembly (Jackson et al., 2002; Mcllwraith and West, 2008; New et al., 1998; Shinohara and Ogawa, 1998). Although yeast *RAD52*–deleted cells show severe HR defects and DNA damage sensitivity, RAD52–deficient vertebrate cells show only minor defects in HR (de Vries et al., 2005; Rijkers et al., 1998). This is probably because of the existence of alternative mediators such as the RAD51 paralogues RAD51B and RAD51C and the BRCA2 tumour suppressor (San Filippo et al., 2008). BRCA2 is a RAD51 reservoir that regulates the assembly of presynaptic filaments (San Filippo et al., 2008).

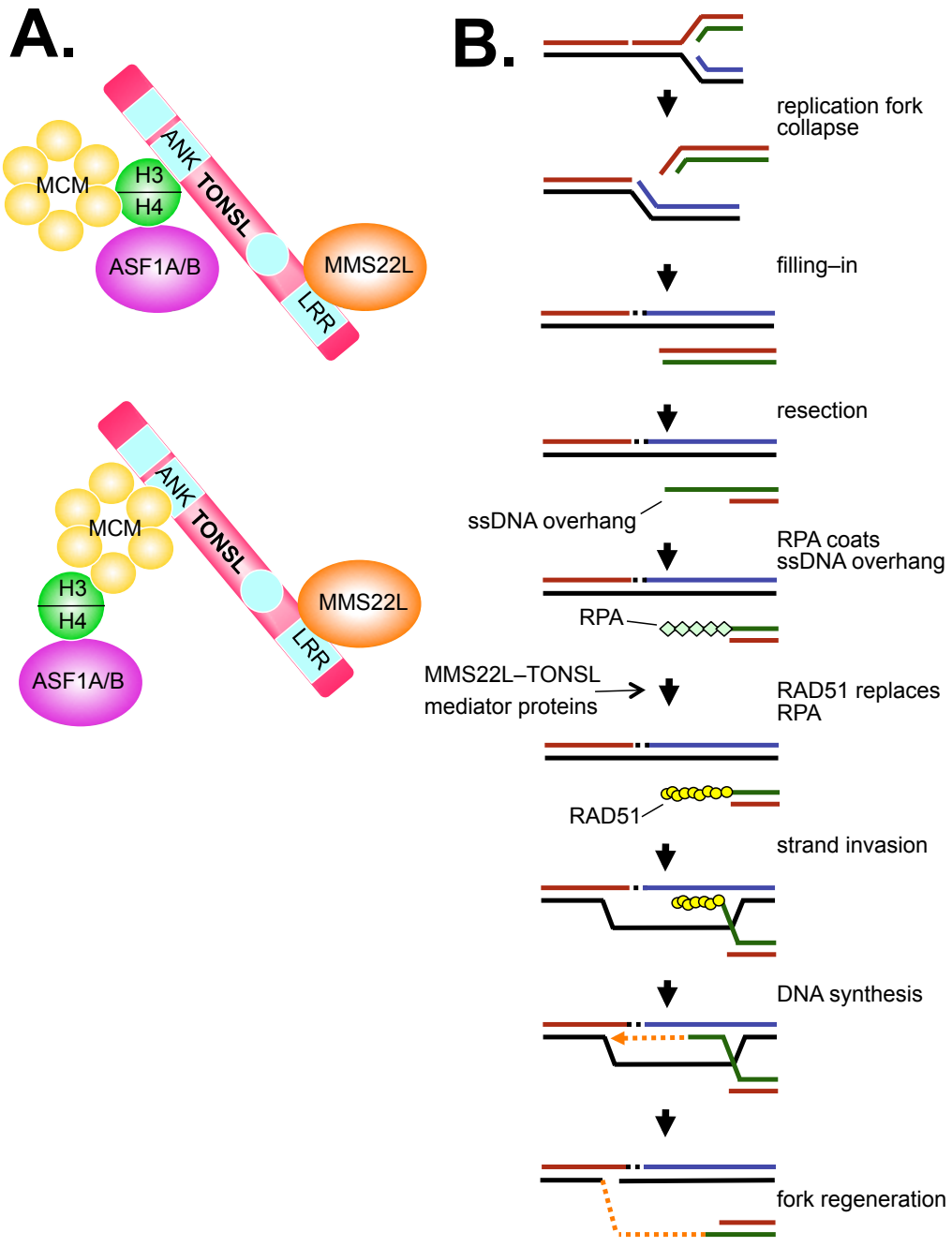
A.
MCM
H3
H4
ASF1A/B
ANK
TONSL
LRR
MMS22L
MCM
H3
H4
ASF1A/B
ANK
TONSL
LRR
MMS22L
B.
replication fork collapse
filling–in
resection
ssDNA overhang
RPA coats ssDNA overhang
RPA
MMS22L–TONSL mediator proteins
RAD51 replaces RPA
RAD51
strand invasion
DNA synthesis
fork regeneration

Figure 4.20 Model for the role of MMS22L and TONSL at collapsed replisomes

(A) Schematic diagram of TONSL as a scaffolding factor. MMS22L binds to the LRR region of TONSL. The ANK repeat region of TONSL is required for the interaction of TONSL with H3, MCMs, and ASF1A/B. The ASF1A V94A mutant, which abrogates binding to H3-H4 dimers and to MCM subunits, does not interact with TONSL. This suggests that TONSL interacts indirectly with ASF1, through binding either directly to histones (upper panel) or the MCM complex (lower panel).

(B) Replication through a nick in DNA backbone would lead to one–ended DSBs as a result of replisome collapse. The nick in the DNA backbone can be filled in and ligated resulting in a template ready for strand invasion. The one–ended DSB is resected, in an MMS22L/TONSL–independent manner, by nuclease(s) that have not yet been identified. Resection generates a ssDNA 3' overhang that is coated by RPA. The initiation of HR requires that RAD51 displace RPA to form the RAD51 nucleoprotein filament required for strand invasion. This step is also regulated by RAD52 and BRCA2. In cells depleted of MMS22L or TONSL, camptothecin–induced RPA foci persist, and the formation of RAD51 foci is hindered. Therefore, it appears that MMS22L and TONSL are required for the replacement of RPA with RAD51 on resected DNA ends to enable HR. Ultimately, HR regenerates an intact replication fork from which DNA replication can continue.

4.4 Future work

The data presented in this chapter suggest that human MMS22L and TONSL promote recombination at collapsed forks by facilitating RAD51 loading at resected DNA ends. Elucidating the molecular mechanism of the precise role of MMS22L and TONSL in HR is the next challenge of this project. MMS22L and TONSL may act by enhancing the activity of HR mediator proteins such as BRCA2 and the RAD51 paralogues. A way to test this hypothesis would be to monitor foci formation of HR mediator proteins after DNA damage. Alternatively, it might be that this complex facilitates RPA displacement directly so that BRCA2 can load RAD51 and this could be addressed by *in vitro* reconstitution experiments.

Since MMS22L and TONSL lack any discernible enzymatic domains, it is likely that they accomplish their role by acting as scaffold proteins. The ubiquitin-like (UBL) domain of TONSL is particularly interesting. Although our mass spectrometric analysis did not identify any interactions with any components of the ubiquitin proteasome pathway, we cannot exclude the presence of these interactions under certain conditions, e.g. during replication stress. The UBL domains of other proteins have been shown to target interacting proteins to the 26S proteasome pathway. I did not observe an interaction between TONSL and the proteasome, or a significant increase in the stability of TONSL-interacting proteins upon TONSL depletion. Thus, I favour the idea that the UBL domain interacts with ubiquitinated proteins to fulfil another role, perhaps in recruiting ubiquitinated proteins to sites of stalled replication.

The interaction of MMS22L and TONSL with histone H3 and the histone chaperones ASF1A and ASF1B points to an involvement in DNA replication-coupled chromatin dynamics. Data from experiments performed in plants clearly show an involvement of the *A. thaliana* TONSL homologue (TONSOKU) in chromatin dynamics. Perhaps MMS22L and TONSL are required for certain histone post-translational modifications that are induced during replication stress. These modifications could act to remodel perturbed replication forks in a way that promotes mediator recruitment. Alternatively, MMS22L and TONSL may interact with modified histones to initiate downstream events. Answering these questions will help our understanding not only of chromatin dynamics during replication stress, but also of the cellular mechanisms for maintaining epigenetic stability.

The data presented in this chapter strongly suggest that MMS22L and TONSL play a role during unchallenged S phase, a role that may be linked to their involvement in chromatin dynamics, as mentioned above. It is important to see whether MMS22L and TONSL affect the replication fork progression by using DNA combing analysis measuring the rate of BrdU incorporation in cells depleted of MMS22L and TONSL.

Given the well-established link between cancer and defective homologous recombination (notably BRCA1 and BRCA2) it would be interesting to test cancer patients for MMS22L and TONSL mutations. If there are, indeed, patients with such mutations, camptothecin may be an advantageous chemotherapy treatment, given the remarkable camptothecin hypersensitivity of MMS22L- and TONSL-depleted cells.

The most striking phenotype of TONSOKU mutants in plants is its defect in apical meristem development. A defect in the highly proliferative meristem tissues highlights the role that TONSOKU, like TONSL in humans, plays during DNA replication. DNA damage and repair pathways have been linked to developmental defects in humans, too. Perhaps mutations in MMS22L and TONSL also cause developmental abnormalities. Again, screening patients for MMS22L and TONSL mutations would shed light on this. It would be interesting to know whether such defects would be caused by disruptions in chromatin dynamics.

References

Abraham, R.T. (2001). Cell cycle checkpoint signaling through the ATM and ATR kinases. Genes Dev *15*, 2177-2196.

Abraham, R.T. (2004). PI 3-kinase related kinases: 'big' players in stress-induced signaling pathways. DNA Repair (Amst) *3*, 883-887.

Admire, A., Shanks, L., Danzl, N., Wang, M., Weier, U., Stevens, W., Hunt, E., and Weinert, T. (2006). Cycles of chromosome instability are associated with a fragile site and are increased by defects in DNA replication and checkpoint controls in yeast. Genes & Development *20*, 159-173.

Ahel, D., Horejsi, Z., Wiechens, N., Polo, S.E., Garcia-Wilson, E., Ahel, I., Flynn, H., Skehel, M., West, S.C., Jackson, S.P.*, et al.* (2009). Poly(ADP-ribose)-dependent regulation of DNA repair by the chromatin remodeling enzyme ALC1. Science *325*, 1240-1243.

Ahnesorg, P., Smith, P., and Jackson, S.P. (2006). XLF interacts with the XRCC4-DNA ligase IV complex to promote DNA nonhomologous end-joining. Cell *124*, 301-313.

Akkari, Y.M.N., Bateman, R.L., Reifsteck, C.A., Olson, S.B., and Grompe, M. (2000). DNA replication is required to elicit cellular responses to psoralen-induced DNA interstrand cross-links. Molecular and Cellular Biology *20*, 8283-8289.

Al-Minawi, A.Z., Saleh-Gohari, N., and Helleday, T. (2008). The ERCC1/XPF endonuclease is required for efficient single-strand annealing and gene conversion in mammalian cells. Nucleic Acids Res *36*, 1-9.

Alabert, C., Bianco, J.N., and Pasero, P. (2009). Differential regulation of homologous recombination at DNA breaks and replication forks by the Mrc1 branch of the S-phase checkpoint. EMBO J *28*, 1131-1141.

Alani, E., Subbiah, S., and Kleckner, N. (1989). The yeast RAD50 gene encodes a predicted 153-kDa protein containing a purine nucleotide-binding domain and two large heptad-repeat regions. Genetics *122*, 47–57.

Alcasabas, A.A., Osborn, A.J., Bachant, J., Hu, F., Werler, P.J., Bousset, K., Furuya, K., Diffley, J.F., Carr, A.M., and Elledge, S.J. (2001). Mrc1 transduces signals of DNA replication stress to activate Rad53. Nat Cell Biol *3*, 958-965.

Allen, J.B., Zhou, Z., Siede, W., Friedberg, E.C., and Elledge, S.J. (1994). The SAD1/RAD53 protein kinase controls multiple checkpoints and DNA damage-induced transcription in yeast. Genes & Development *8*, 2401-2415.

Alvaro, D., Lisby, M., and Rothstein, R. (2007). Genome-Wide Analysis of Rad52 Foci Reveals Diverse Mechanisms Impacting Recombination. PLoS Genet *3*, e228.

Andegeko, Y., Moyal, L., Mittelman, L., Tsarfaty, I., Shiloh, Y., and Rotman, G. (2001). Nuclear retention of ATM at sites of DNA double strand breaks. J Biol Chem *276*, 38224-38230.

Andersen, S.L., Bergstralh, D.T., Kohl, K.P., LaRocque, J.R., Moore, C.B., and Sekelsky, J. (2009). Drosophila MUS312 and the vertebrate ortholog BTBD12 interact with DNA structure-specific endonucleases in DNA repair and recombination. Mol Cell *35*, 128-135.

Andreassen, P.R., and Ren, K. (2009). Fanconi anemia proteins, DNA interstrand crosslink repair pathways, and cancer therapy. Curr Cancer Drug Targets *9*, 101-117.

Anglana, M., Apiou, F., Bensimon, A., and Debatisse, M. (2003). Dynamics of DNA Replication in Mammalian Somatic Cells: Nucleotide Pool Modulates Origin Choice and Interorigin Spacing. Cell *114*, 385-394.

Aparicio, O.M., Weinstein, D.M., and Bell, S.P. (1997). Components and Dynamics of DNA Replication Complexes in S. cerevisiae: Redistribution of MCM Proteins and Cdc45p during S Phase. Cell *91*, 59-69.

Araki, Y., Kawasaki, Y., Sasanuma, H., Tye, B.K., and Sugino, A. (2003). Budding yeast mcm10/dna43 mutant requires a novel repair pathway for viability. Genes to Cells *8*, 465-480.

Arnaudeau, C., Helleday, T., and Jenssen, D. (1999). The RAD51 protein supports homologous recombination by an exchange mechanism in mammalian cells. Journal of Molecular Biology *289*, 1231-1238.

Arnaudeau, C., Lundin, C., and Helleday, T. (2001). DNA double-strand breaks associated with replication forks are predominantly repaired by homologous recombination involving an exchange mechanism in mammalian cells. Journal of Molecular Biology *307*, 1235-1245.

Aylon, Y., Liefshitz, B., and Kupiec, M. (2004). The CDK regulates repair of double-strand breaks by homologous recombination during the cell cycle. EMBO J *23*, 4868-4875.

Azvolinsky, A., Giresi, P.G., Lieb, J.D., and Zakian, V.A. (2009). Highly Transcribed RNA Polymerase II Genes Are Impediments to Replication Fork Progression in Saccharomyces cerevisiae. Molecular Cell *34*, 722-734.

Bae, J.B., Mukhopadhyay, S.S., Liu, L., Zhang, N., Tan, J., Akhter, S., Liu, X., Shen, X., Li, L., and Legerski, R.J. (2008). Snm1B/Apollo mediates replication fork collapse and S Phase checkpoint activation in response to DNA interstrand cross-links. Oncogene *27*, 5045-5056.

Baldwin, E.L., Berger, A.C., Corbett, A.H., and Osheroff, N. (2005). Mms22p protects Saccharomyces cerevisiae from DNA damage induced by topoisomerase II. Nucleic Acids Research *33*, 1021-1030.

Banin, S., Moyal, L., Shieh, S., Taya, Y., Anderson, C.W., Chessa, L., Smorodinsky, N.I., Prives, C., Reiss, Y., Shiloh, Y.*, et al.* (1998). Enhanced phosphorylation of p53 by ATM in response to DNA damage. Science *281*, 1674-1677.

Bankmann, M., Prakash, L., and Prakash, S. (1992). Yeast RAD14 and human xeroderma pigmentosum group A DNA-repair genes encode homologous proteins. Nature *355*, 555-558.

Barbour, L., and Xiao, W. (2003). Regulation of alternative replication bypass pathways at stalled replication forks and its effects on genome stability: a yeast model. Mutat Res *532*, 137-155.

Bartek, J., Lukas, C., and Lukas, J. (2004). Checking on DNA damage in S phase. Nat Rev Mol Cell Biol *5*, 792-804.

Bartkova, J., Rezaei, N., Liontos, M., Karakaidos, P., Kletsas, D., Issaeva, N., Vassiliou, L.-V.F., Kolettas, E., Niforou, K., Zoumpourlis, V.C*., et al.* (2006). Oncogene-induced senescence is part of the tumorigenesis barrier imposed by DNA damage checkpoints. Nature *444*, 633-637.

Bassett, A., Cooper, S., Wu, C., and Travers, A. (2009). The folding and unfolding of eukaryotic chromatin. Current Opinion in Genetics & Development *19*, 159-165.

Bassing, C.H., Suh, H., Ferguson, D.O., Chua, K.F., Manis, J., Eckersdorff, M., Gleason, M., Bronson, R., Lee, C., and Alt, F.W. (2003). Histone H2AX: A Dosage-Dependent Suppressor of Oncogenic Translocations and Tumors. Cell *114*, 359-370.

Batzer, M.A., and Deininger, P.L. (2002). Alu repeats and human genomic diversity. Nat Rev Genet *3*, 370-379.

Baudat, F., Manova, K., Yuen, J.P., Jasin, M., and Keeney, S. (2000). Chromosome Synapsis Defects and Sexually Dimorphic Meiotic Progression in Mice Lacking Spo11. Molecular Cell *6*, 989-998.

Beard, W.A., and Wilson, S.H. (2000). Structural design of a eukaryotic DNA repair polymerase: DNA polymerase beta. Mutat Res *460*, 231-244.

Bekker-Jensen, S., Lukas, C., Kitagawa, R., Melander, F., Kastan, M.B., Bartek, J., and Lukas, J. (2006). Spatial organization of the mammalian genome surveillance machinery in response to DNA strand breaks. The Journal of Cell Biology *173*, 195-206.

Bell, S.P., and Stillman, B. (1992). ATP-dependent recognition of eukaryotic origins of DNA replication by a multiprotein complex. Nature *357*, 128-134.

Bentley, N.J., Holtzman, D.A., Flaggs, G., Keegan, K.S., DeMaggio, A., Ford, J.C., Hoekstra, M., and Carr, A.M. (1996). The Schizosaccharomyces pombe rad3 checkpoint gene. Embo J *15*, 6641-6651.

Beranek, D. (1990a). Distribution of methyl and ethyl adducts following alkylation with monofunctional alkylating agents. Mutation Research *231*, 22-30.

Beranek, D.T. (1990b). Distribution of methyl and ethyl adducts following alkylation with monofunctional alkylating agents. Mutat Res *231*, 11-30.

Bermejo, R., Capra, T., Gonzalez-Huici, V., Fachinetti, D., Cocito, A., Natoli, G., Katou, Y., Mori, H., Kurokawa, K., Shirahige, K.*, et al.* (2009). Genome-Organizing Factors Top2 and Hmo1 Prevent Chromosome Fragility at Sites of S phase Transcription. Cell *138*, 870-884.

Bermejo, R., Doksani, Y., Capra, T., Katou, Y.-M., Tanaka, H., Shirahige, K., and Foiani, M. (2007). Top1- and Top2-mediated topological transitions at replication forks ensure fork progression and stability and prevent DNA damage checkpoint activation. Genes & Development *21*, 1921-1936.

Bienko, M., Green, C.M., Crosetto, N., Rudolf, F., Zapart, G., Coull, B., Kannouche, P., Wider, G., Peter, M., Lehmann, A.R.*, et al.* (2005). Ubiquitin-binding domains in Y-family polymerases regulate translesion synthesis. Science *310*, 1821-1824.

Blankley, R.T., and Lydall, D. (2004). A domain of Rad9 specifically required for activation of Chk1 in budding yeast. J Cell Sci *117*, 601-608.

Blow, J.J., and Dutta, A. (2005a). Preventing re-replication of chromosomal DNA. Nat Rev Mol Cell Biol *6*, 476-486.

Blow, J.J., and Dutta, A. (2005b). Preventing re-replication of chromosomal DNA. Nat Rev Mol Cell Biol *6*, 476-486.

Blow, J.J., and Ge, X.Q. (2009). A model for DNA replication showing how dormant origins safeguard against replication fork failure. EMBO Rep *10*, 406-412.

Blow, J.J., and Tada, S. (2000). Cell cycle. A new check on issuing the licence. Nature *404*, 560-561.

Bolderson, E., Tomimatsu, N., Richard, D.J., Boucher, D., Kumar, R., Pandita, T.K., Burma, S., and Khanna, K.K. (2010). Phosphorylation of Exo1 modulates homologous recombination repair of DNA double-strand breaks 10.1093/nar/gkp1164. Nucl Acids Res *38*, 1821-1831.

Bonilla, C.Y., Melo, J.A., and Toczyski, D.P. (2008). Colocalization of Sensors Is Sufficient to Activate the DNA Damage Checkpoint in the Absence of Damage. Molecular Cell *30*, 267-276.

Bonner, W.M., Wu, R.S., Panusz, H.T., and Muneses, C. (1988). Kinetics of accumulation and depletion of soluble newly synthesized histone in the reciprocal regulation of histone and DNA synthesis. Biochemistry *27*, 6542-6550.

Bosco, G., and Haber, J.E. (1998). Chromosome Break-Induced DNA Replication Leads to Nonreciprocal Translocations and Telomere Capture. Genetics *150*, 1037-1047.

Boskovic, J., Coloma, J., Aparicio, T., Zhou, M., Robinson, C.V., Mendez, J., and Montoya, G. (2007). Molecular architecture of the human GINS complex. EMBO Rep *8*, 678-684.

Bouwman, P., Aly, A., Escandell, J.M., Pieterse, M., Bartkova, J., van der Gulden, H., Hiddingh, S., Thanasoula, M., Kulkarni, A., Yang, Q.*, et al.* (2010). 53BP1 loss rescues

BRCA1 deficiency and is associated with triple-negative and BRCA-mutated breast cancers. Nat Struct Mol Biol *17*, 688-695.

Bowers, J.L., Randell, J.C.W., Chen, S., and Bell, S.P. (2004). ATP Hydrolysis by ORC Catalyzes Reiterative Mcm2-7 Assembly at a Defined Origin of Replication. Molecular Cell *16*, 967-978.

Bozhenok, L., Wade, P.A., and Varga-Weisz, P. (2002). WSTF-ISWI chromatin remodeling complex targets heterochromatic replication foci. EMBO J *21*, 2231-2241.

Bradford, M.M. (1976). A rapid and sensitive method for the quantitation of microgram quantities of protein utilising the principle of protein-dye binding. Anal Biochem *72*, 248-254.

Branzei, D., and Foiani, M. (2010). Maintaining genome stability at the replication fork. *11*, 208-219.

Branzei, D., Sollier, J., Liberi, G., Zhao, X., Maeda, D., Seki, M., Enomoto, T., Ohta, K., and Foiani, M. (2006). Ubc9- and Mms21-Mediated Sumoylation Counteracts Recombinogenic Events at†Damaged Replication Forks. Cell *127*, 509-522.

Branzei, D., Vanoli, F., and Foiani, M. (2008). SUMOylation regulates Rad18-mediated template switch. Nature *456*, 915-920.

Brewer, B.J., and Fangman, W.L. (1987). The localization of replication origins on ARS plasmids in S. cerevisiae. Cell *51*, 463-471.

Brewer, B.J., and Fangman, W.L. (1988). A replication fork barrier at the 3' end of yeast ribosomal RNA genes. Cell *55*, 637-643.

Broomfield, S., Hryciw, T., and Xiao, W. (2001). DNA postreplication repair and mutagenesis in Saccharomyces cerevisiae. Mutat Res *486*, 167-184.

Brown, E.J., and Baltimore, D. (2000). ATR disruption leads to chromosomal fragmentation and early embryonic lethality. Genes Dev *14*, 397-402.

Brown, E.J., and Baltimore, D. (2003). Essential and dispensable roles of ATR in cell cycle arrest and genome maintenance. Genes Dev *17*, 615-628.

Brush, G.Ä., Morrow, D.Ä., Hieter, P., and Kelly, T.Ä. (1996). The ATM homologue MEC1 is required for phosphorylation of replication protein A in‚Äâyeast. Proceedings of the National Academy of Sciences of the United States of America *93*, 15075-15080.

Bryant, H.E., Petermann, E., Schultz, N., Jemth, A.-S., Loseva, O., Issaeva, N., Johansson, F., Fernandez, S., McGlynn, P., and Helleday, T. (2009). PARP is activated at stalled forks to mediate Mre11-dependent replication restart and recombination. EMBO J *28*, 2601-2615.

Budd, M.E., Tong, A.H.Y., Polaczek, P., Peng, X., Boone, C., and Campbell, J.L. (2005). A Network of Multi-Tasking Proteins at the DNA Replication Fork Preserves Genome Stability. PLoS Genet *1*, e61.

Bulavin, D.V., Higashimoto, Y., Popoff, I.J., Gaarde, W.A., Basrur, V., Potapova, O., Appella, E., and Fornace, A.J., Jr. (2001). Initiation of a G2/M checkpoint after ultraviolet radiation requires p38 kinase. Nature *411*, 102-107.

Bundock, P., and Hooykaas, P. (2002). Severe developmental defects, hypersensitivity to DNA-damaging agents, and lengthened telomeres in Arabidopsis MRE11 mutants. Plant Cell *14*, 2451-2462.

Bunting, S.F., CallÈn, E., Wong, N., Chen, H.-T., Polato, F., Gunn, A., Bothmer, A., Feldhahn, N., Fernandez-Capetillo, O., Cao, L.*, et al.* (2010). 53BP1 Inhibits Homologous Recombination in Brca1-Deficient Cells by Blocking Resection of DNA Breaks. Cell *141*, 243-254.

Buonomo, S.C.B. (2010). Heterochromatin DNA replication and Rif1. Exp Cell Res *316*, 1907-1913.

Burgers, P.M. (1991). Saccharomyces cerevisiae replication factor C. II. Formation and activity of complexes with the proliferating cell nuclear antigen and with DNA polymerases delta and epsilon. Journal of Biological Chemistry *266*, 22698-22706.

Byun, T.S., Pacek, M., Yee, M.-c., Walter, J.C., and Cimprich, K.A. (2005). Functional uncoupling of MCM helicase and DNA polymerase activities activates the ATR-dependent checkpoint. Genes & Development *19*, 1040-1052.

Canman, C.E., Lim, D.S., Cimprich, K.A., Taya, Y., Tamai, K., Sakaguchi, K., Appella, E., Kastan, M.B., and Siliciano, J.D. (1998). Activation of the ATM kinase by ionizing radiation and phosphorylation of p53. Science *281*, 1677-1679.

Cann, K.L., and Hicks, G.G. (2007). Regulation of the cellular DNA double-strand break response. Biochem Cell Biol *85*, 663-674.

Carr, A.M. (2002). DNA structure dependent checkpoints as regulators of DNA repair. DNA Repair (Amst) *1*, 983-994.

Casper, A.M., Nghiem, P., Arlt, M.F., and Glover, T.W. (2002). ATR Regulates Fragile Site Stability. Cell *111*, 779-789.

Celeste, A., Difilippantonio, S., Difilippantonio, M.J., Fernandez-Capetillo, O., Pilch, D.R., Sedelnikova, O.A., Eckhaus, M., Ried, T., Bonner, W.M., and Nussenzweig, A. (2003). H2AX haploinsufficiency modifies genomic stability and tumor susceptibility. Cell *114*, 371-383.

Celeste, A., Petersen, S., Romanienko, P.J., Fernandez-Capetillo, O., Chen, H.T., Sedelnikova, O.A., Reina-San-Martin, B., Coppola, V., Meffre, E., Difilippantonio, M.J., *et al.* (2002). Genomic instability in mice lacking histone H2AX. Science *296*, 922-927.

Celic, I., Masumoto, H., Griffith, W.P., Meluh, P., Cotter, R.J., Boeke, J.D., and Verreault, A. (2006). The Sirtuins Hst3 and Hst4p Preserve Genome Integrity by Controlling Histone H3 Lysine 56 Deacetylation. Current Biology *16*, 1280-1289.

Celic, I., Verreault, A., and Boeke, J.D. (2008). Histone H3 K56 Hyperacetylation Perturbs Replisomes and Causes DNA Damage. Genetics *179*, 1769-1784.

Cha, R.S., and Kleckner, N. (2002a). ATR homolog Mec1 promotes fork progression, thus averting breaks in replication slow zones. Science *297*, 602-606.

Cha, R.S., and Kleckner, N. (2002b). ATR Homolog Mec1 Promotes Fork Progression, Thus Averting Breaks in Replication Slow Zones 10.1126/science.1071398. Science *297*, 602-606.

Chabes, A., Georgieva, B., Domkin, V., Zhao, X., Rothstein, R., and Thelander, L. (2003). Survival of DNA Damage in Yeast Directly Depends on Increased dNTP Levels Allowed by Relaxed Feedback Inhibition of Ribonucleotide Reductase. Cell *112*, 391-401.

Chan, T.A., Hermeking, H., Lengauer, C., Kinzler, K.W., and Vogelstein, B. (1999). 14-3-3Sigma is required to prevent mitotic catastrophe after DNA damage. Nature *401*, 616-620.

Chappell, C., Hanakahi, L.A., Karimi-Busheri, F., Weinfeld, M., and West, S.C. (2002). Involvement of human polynucleotide kinase in double-strand break repair by non-homologous end joining. Embo J *21*, 2827-2832.

Chehab, N.H., Malikzay, A., Appel, M., and Halazonetis, T.D. (2000). Chk2/hCds1 functions as a DNA damage checkpoint in G(1) by stabilizing p53. Genes Dev *14*, 278-288.

Chehab, N.H., Malikzay, A., Stavridi, E.S., and Halazonetis, T.D. (1999). Phosphorylation of Ser-20 mediates stabilization of human p53 in response to DNA damage. Proc Natl Acad Sci U S A *96*, 13777-13782.

Chen, C.-C., Carson, J.J., Feser, J., Tamburini, B., Zabaronick, S., Linger, J., and Tyler, J.K. (2008a). Acetylated Lysine 56 on Histone H3 Drives Chromatin Assembly after Repair and Signals for the Completion of Repair. Cell *134*, 231-243.

Chen, M., Pan, Z.Q., and Hurwitz, J. (1992). Studies of the cloned 37-kDa subunit of activator 1 (replication factor C) of HeLa cells. Proceedings of the National Academy of Sciences of the United States of America *89*, 5211-5215.

Chen, Z., Yang, H., and Pavletich, N.P. (2008b). Mechanism of homologous recombination from the RecA–ssDNA/dsDNA structures. Nature *453*, 489-494.

Christina, B., Sibyll, P., Elisabeth, K., Heinz-Peter, N., and Frank, G. (2007). Interactions of human Cdc45 with the Mcm2-7 complex, the GINS complex, and DNA polymerases delta and epsilon during S phase. Genes to Cells *12*, 745-758.

Chuang, L.S.H., Ian, H.-I., Koh, T.-W., Ng, H.-H., Xu, G., and Li, B.F.L. (1997). Human DNA-(Cytosine-5) Methyltransferase-PCNA Complex as a Target for p21WAF1. Science *277*, 1996-2000.

Cimprich, K.A., Shin, T.B., Keith, C.T., and Schreiber, S.L. (1996). cDNA cloning and gene mapping of a candidate human cell cycle checkpoint protein. Proc Natl Acad Sci U S A *93*, 2850-2855.

Ciosk, R., Zachariae, W., Michaelis, C., Shevchenko, A., Mann, M., and Nasmyth, K. (1998). An ESP1/PDS1 complex regulates loss of sister chromatid cohesion at the metaphase to anaphase transition in yeast. Cell *93*, 1067-1076.

Clark, A., and Margulies, A. (1965). Isolation and characterization of recombination-deficient mutants of Escherichia coli K12. Proc Natl Acad Sci USA *53*, 451–459.

Cleaver, J.E. (1968). Defective repair replication of DNA in xeroderma pigmentosum. Nature *218*, 652-656.

Cleaver, J.E. (1969). Xeroderma pigmentosum: a human disease in which an initial stage of DNA repair is defective. Proc Natl Acad Sci U S A *63*, 428-435.

Cliby, W.A., Roberts, C.J., Cimprich, K.A., Stringer, C.M., Lamb, J.R., Schreiber, S.L., and Friend, S.H. (1998). Overexpression of a kinase-inactive ATR protein causes sensitivity to DNA-damaging agents and defects in cell cycle checkpoints. Embo J *17*, 159-169.

Cobb, J.A., Schleker, T., Rojas, V., Bjergbaek, L., Tercero, J.A., and Gasser, S.M. (2005). Replisome instability, fork collapse, and gross chromosomal rearrangements arise synergistically from Mec1 kinase and RecQ helicase mutations. Genes Dev *19*, 3055-3069.

Cohen-Fix, O., and Koshland, D. (1997). The anaphase inhibitor of Saccharomyces cerevisiae Pds1p is a target of the DNA damage checkpoint pathway. Proc Natl Acad Sci U S A *94*, 14361-14366.

Collins, N., Poot, R.A., Kukimoto, I., García-Jiménez, C., Dellaire, G., and Varga-Weisz, P.D. (2002). An ACF1−ISWI chromatin-remodeling complex is required for DNA replication through heterochromatin. Nature Genetics *32*, 627 - 632.

Collins, S.R., Miller, K.M., Maas, N.L., Roguev, A., Fillingham, J., Chu, C.S., Schuldiner, M., Gebbia, M., Recht, J., Shales, M*., et al.* (2007a). Functional dissection of protein complexes involved in yeast chromosome biology using a genetic interaction map. Nature *446*, 806-810.

Collins, S.R., Miller, K.M., Maas, N.L., Roguev, A., Fillingham, J., Chu, C.S., Schuldiner, M., Gebbia, M., Recht, J., Shales, M*., et al.* (2007b). Functional dissection of protein complexes involved in yeast chromosome biology using a genetic interaction map. *446*, 806-810.

Collins, S.R., Miller, K.M., Maas, N.L., Roguev, A., Fillingham, J., Chu, C.S., Schuldiner, M., Gebbia, M., Recht, J., Shales, M*., et al.* (2007c). Functional dissection of protein complexes involved in yeast chromosome biology using a genetic interaction map. Nature *446*, 806-810.

Cortes Ledesma, F., El Khamisy, S.F., Zuma, M.C., Osborn, K., and Caldecott, K.W. (2009). A human 5'-tyrosyl DNA phosphodiesterase that repairs topoisomerase-mediated DNA damage. Nature *461*, 674-678.

Cortez, D., Guntuku, S., Qin, J., and Elledge, S.J. (2001). ATR and ATRIP: partners in checkpoint signaling. Science *294*, 1713-1716.

Costa, R.M., Chigancas, V., Galhardo Rda, S., Carvalho, H., and Menck, C.F. (2003). The eukaryotic nucleotide excision repair pathway. Biochimie *85*, 1083-1099.

Costanzo, V., Robertson, K., Ying, C.Y., Kim, E., Avvedimento, E., Gottesman, M., Grieco, D., and Gautier, J. (2000). Reconstitution of an ATM-dependent checkpoint that inhibits chromosomal DNA replication following DNA damage. Mol Cell *6*, 649-659.

Costanzo, V., Shechter, D., Lupardus, P.J., Cimprich, K.A., Gottesman, M., and Gautier, J. (2003). An ATR- and Cdc7-Dependent DNA Damage Checkpoint that Inhibits Initiation of DNA Replication. Molecular Cell *11*, 203-213.

Courcelle, J., and Hanawalt, P.C. (2003). RECA-DEPENDENT RECOVERY OF ARRESTED DNA REPLICATION FORKS. Annual Review of Genetics *37*, 611-646.

Courcelle, J., Khodursky, A., B, B.P., Brown, P., and Hanawalt, P. (2001). Comparative gene expression profiles following UV exposure in wild-type and SOS-deficient Escherichia coli. Genetics *158*, 41-64.

Cox, M.M., Goodman, M.F., Kreuzer, K.N., Sherratt, D.J., Sandler, S.J., and Marians, K.J. (2000). The importance of repairing stalled replication forks. Nature *404*, 37-41.

Craven, R.J., and Petes, T.D. (2000). Involvement of the checkpoint protein Mec1p in silencing of gene expression at telomeres in Saccharomyces cerevisiae. Mol Cell Biol *20*, 2378-2384.

Critchlow, S.E., Bowater, R.P., and Jackson, S.P. (1997). Mammalian DNA double-strand break repair protein XRCC4 interacts with DNA ligase IV. Current biology *7*, 588-598.

Critchlow, S.E., and Jackson, S.P. (1998). DNA end-joining: from yeast to man. Trends in Biochemical Sciences *23*, 394-398.

Cuadrado, M., Martinez-Pastor, B., Murga, M., Toledo, L.I., Gutierrez-Martinez, P., Lopez, E., and Fernandez-Capetillo, O. (2006). ATM regulates ATR chromatin loading in response to DNA double-strand breaks. J Exp Med *203*, 297-303.

Cummings, C.J., and Zoghbi, H.Y. (2000). Fourteen and counting: unraveling trinucleotide repeat diseases. Hum Mol Genet *9*, 909-916.

Cutts, S.M., Nudelman, A., Rephaeli, A., and Phillips, D.R. (2005). The Power and Potential of Doxorubicin-DNA Adducts. IUBMB Life *57*, 73-81.

Daboussi, F., Courbet, S., Benhamou, S., Kannouche, P., Zdzienicka, M.Z., Debatisse, M., and Lopez, B.S. (2008a). A homologous recombination defect affects replication-fork progression in mammalian cells. Journal of Cell Science
J Cell Sci *121*, 162-166.

Daboussi, F., Courbet, S., Benhamou, S., Kannouche, P., Zdzienicka, M.Z., Debatisse, M., and Lopez, B.S. (2008b). A homologous recombination defect affects replication-fork progression in mammalian cells. Journal of Cell Science
J Cell Sci *121*, 162-166.

Dahmann, C., Diffley, J.F.X., and Nasmyth, K.A. (1995). S-phase-promoting cyclin-dependent kinases prevent re-replication by inhibiting the transition of replication origins to a pre-replicative state. Current Biology *5*, 1257-1269.

Dai, Q.H., and Liu, X. (2000). DNA interstrand cross-link induced by estrogens as well as their complete and synergic carcinogenesis. Chinese Science Bulletin *45*, 2125-2130.

Daigaku, Y., Davies, A.A., and Ulrich, H.D. (2010). Ubiquitin-dependent DNA damage bypass is separable from genome replication. Nature.

Das, C., Lucia, M.S., Hansen, K.C., and Tyler, J.K. (2009). CBP/p300-mediated acetylation of histone H3 on lysine 56. Nature.

Dasika, G.K., Lin, S.C., Zhao, S., Sung, P., Tomkinson, A., and Lee, E.Y. (1999). DNA damage-induced cell cycle checkpoints and DNA strand break repair in development and tumorigenesis. Oncogene *18*, 7883-7899.

Davies, O.R., and Pellegrini, L. (2007). Interaction with the BRCA2 C terminus protects RAD51-DNA filaments from disassembly by BRC repeats. Nat Struct Mol Biol *14*, 475-483.

Davis, A.P., and Symington, L.S. (2004). RAD51-Dependent Break-Induced Replication in Yeast
10.1128/MCB.24.6.2344-2351.2004. Mol Cell Biol *24*, 2344-2351.

de la Loza, M.C.D., Wellinger, R.E., and Aguilera, A. (2009). Stimulation of direct-repeat recombination by RNA polymerase III transcription. DNA Repair *8*, 620-626.

de Vries, F.A.T., Zonneveld, J.B.M., van Duijn-Goedhart, A., Roodbergen, M., Boei, J., van Buul, P.P.W., Essers, J., van Steeg, H., Van Zeeland, A.A., van Benthem, J.*, et al.* (2005). Inactivation of RAD52 aggravates RAD54 defects in mice but not in Schizosaccharomyces pombe. DNA Repair *4*, 1121-1128.

DeGregori, J. (2002). The genetics of the E2F family of transcription factors: shared functions and unique roles. Biochim Biophys Acta *1602*, 131-150.

Desany, B.A., Alcasabas, A.A., Bachant, J.B., and Elledge, S.J. (1998). Recovery from DNA replicational stress is the essential function of the S-phase checkpoint pathway. Genes Dev *12*, 2956-2970.

Deshpande, A.M., and Newlon, C.S. (1996). DNA replication fork pause sites dependent on transcription. Science *272*, 1030-1033.

di Caprio, L., and Cox, B.S. (1981). DNA synthesis in UV-irradiated yeast. Mutat Res *82*, 69-85.

Di Micco, R., Fumagalli, M., Cicalese, A., Piccinin, S., Gasparini, P., Luise, C., Schurra, C., Garre, M., Giovanni Nuciforo, P., Bensimon, A.*, et al.* (2006). Oncogene-induced senescence is a DNA damage response triggered by DNA hyper-replication. Nature *444*, 638-642.

Dianov, G.L., and Parsons, J.L. (2007). Co-ordination of DNA single strand break repair. DNA Repair (Amst) *6*, 454-460.

Dijkwel, P.A., Wang, S., and Hamlin, J.L. (2002). Initiation Sites Are Distributed at Frequent Intervals in the Chinese Hamster Dihydrofolate Reductase Origin of Replication but Are Used with Very Different Efficiencies. Mol Cell Biol *22*, 3053-3065.

Dimitrova, D.S., Prokhorova, T.A., Blow, J.J., Todorov, I.T., and Gilbert, D.M. (2002). Mammalian nuclei become licensed for DNA replication during late telophase. Journal of Cell Science *115*, 51-59.

Dinant, C., Houtsmuller, A., and Vermeulen, W. (2008). Chromatin structure and DNA damage repair. Epigenetics & Chromatin *1*, 9.

Dip, R., Camenisch, U., and Naegeli, H. (2004). Mechanisms of DNA damage recognition and strand discrimination in human nucleotide excision repair. DNA Repair (Amst) *3*, 1409-1423.

Doe, C.L., Ahn, J.S., Dixon, J., and Whitby, M.C. (2002). Mus81-Eme1 and Rqh1 involvement in processing stalled and collapsed replication forks. J Biol Chem *277*, 32753-32759. Epub 32002 Jun 32725.

Doil, C., Mailand, N., Bekker-Jensen, S., Menard, P., Larsen, D.H., Pepperkok, R., Ellenberg, J., Panier, S., Durocher, D., Bartek, J.*, et al.* (2009). RNF168 binds and amplifies ubiquitin conjugates on damaged chromosomes to allow accumulation of repair proteins. Cell *136*, 435-446.

Dong, Z., and Fasullo, M. (2003). Multiple recombination pathways for sister chromatid exchange in Saccharomyces cerevisiae: role of RAD1 and the RAD52 epistasis group genes. Nucl Acids Res *31*, 2576-2585.

Donovan, S., Harwood, J., Drury, L.S., and Diffley, J.F.X. (1997). Cdc6p-dependent loading of Mcm proteins onto pre-replicative chromatin in‚Äâbudding‚Äâyeast. Proceedings of the National Academy of Sciences of the United States of America *94*, 5611-5616.

Dornan, D., Shimizu, H., Perkins, N.D., and Hupp, T.R. (2003). DNA-dependent acetylation of p53 by the transcription coactivator p300. J Biol Chem *278*, 13431-13441.

Dovey, C.L., Aslanian, A., Sofueva, S., Yates Iii, J.R., and Russell, P. (2009). Mms1-Mms22 complex protects genome integrity in Schizosaccharomyces pombe. DNA Repair *8*, 1390-1399.

Dovey, C.L., and Russell, P. (2007). Mms22 Preserves Genomic Integrity During DNA Replication in Schizosaccharomyces pombe. Genetics *177*, 47-61.

Downs, J.A., Allard, S., Jobin-Robitaille, O., Javaheri, A., Auger, A., Bouchard, N., Kron, S.J., Jackson, S.P., and Cote, J. (2004). Binding of chromatin-modifying activities to phosphorylated histone H2A at DNA damage sites. Mol Cell *16*, 979-990.

Downs, J.A., Kosmidou, E., Morgan, A., and Jackson, S.P. (2003). Suppression of Homologous Recombination by the Saccharomyces cerevisiae Linker Histone. Molecular Cell *11*, 1685-1692.

Downs, J.A., Lowndes, N.F., and Jackson, S.P. (2000). A role for Saccharomyces cerevisiae histone H2A in DNA repair. Nature *408*, 1001-1004.

Driscoll, R., Hudson, A., and Jackson, S.P. (2007). Yeast Rtt109 Promotes Genome Stability by Acetylating Histone H3 on Lysine 56 10.1126/science.1135862. Science *315*, 649-652.

Dronkert, M.L., and Kanaar, R. (2001). Repair of DNA interstrand cross-links. Mutat Res *486*, 217-247.

Drury, L.S., Perkins, G., and Diffley, J.F.X. (2000). The cyclin-dependent kinase Cdc28p regulates distinct modes of Cdc6p proteolysis during the budding yeast cell cycle. Current Biology *10*, 231-240.

Dubrana, K., van Attikum, H., Hediger, F., and Gasser, S.M. (2007). The processing of double-strand breaks and binding of single-strand-binding proteins RPA and Rad51 modulate the formation of ATR-kinase foci in yeast. J Cell Sci *120*, 4209-4220.

Dueber, E.L.C., Corn, J.E., Bell, S.D., and Berger, J.M. (2007). Replication Origin Recognition and Deformation by a Heterodimeric Archaeal Orc1 Complex. Science *317*, 1210-1213.

Duro, E., Vaisica, J.A., Brown, G.W., and Rouse, J. (2008). Budding yeast Mms22 and Mms1 regulate homologous recombination induced by replisome blockage. DNA Repair *7*, 811-818.

Durocher, D., Taylor, I.A., Sarbassova, D., Haire, L.F., Westcott, S.L., Jackson, S.P., Smerdon, S.J., and Yaffe, M.B. (2000). The molecular basis of FHA domain:phosphopeptide binding specificity and implications for phospho-dependent signaling mechanisms. Mol Cell *6*, 1169-1182.

Early, A., Drury, L.S., and Diffley, J.F. (2004). Mechanisms involved in regulating DNA replication origins during the cell cycle and in response to DNA damage. Philos Trans R Soc Lond B Biol Sci *359*, 31-38.

el-Deiry, W.S., Tokino, T., Velculescu, V.E., Levy, D.B., Parsons, R., Trent, J.M., Lin, D., Mercer, W.E., Kinzler, K.W., and Vogelstein, B. (1993). WAF1, a potential mediator of p53 tumor suppression. Cell *75*, 817-825.

El-Khamisy, S.F., Saifi, G.M., Weinfeld, M., Johansson, F., Helleday, T., Lupski, J.R., and Caldecott, K.W. (2005). Defective DNA single-strand break repair in spinocerebellar ataxia with axonal neuropathy-1. Nature *434*, 108-113.

Eliasson, R., and Reichard, P. (1978). Primase initiates Okazaki pieces during polyoma DNA synthesis. Nature *272*, 184-185.

Elledge, S.J. (1996). Cell Cycle Checkpoints: Preventing an Identity Crisis. Science *274*, 1664-1672.

Elliott, B., Richardson, C., and Jasin, M. (2005). Chromosomal Translocation Mechanisms at Intronic Alu Elements in Mammalian Cells. Molecular Cell *17*, 885-894.

Emili, A., Schieltz, D.M., Yates Iii, J.R., and Hartwell, L.H. (2001). Dynamic Interaction of DNA Damage Checkpoint Protein Rad53 with Chromatin Assembly Factor Asf1. Molecular Cell *7*, 13-20.

Esashi, F., Christ, N., Gannon, J., Liu, Y., Hunt, T., Jasin, M., and West, S.C. (2005). CDK-dependent phosphorylation of BRCA2 as a regulatory mechanism for recombinational repair. Nature *434*, 598-604.

Ewing, R.M., Chu, P., Elisma, F., Li, H., Taylor, P., Climie, S., McBroom-Cerajewski, L., Robinson, M.D., O'Connor, L., Li, M.*, et al.* (2007). Large-scale mapping of human protein-protein interactions by mass spectrometry. Mol Syst Biol *3*.

Fairman, M.P., and Stillman, B. (1988). Cellular factors required for multiple stages of SV40 DNA replication in vitro. Embo J *7*, 1211-1218.

Falck, J., Coates, J., and Jackson, S.P. (2005). Conserved modes of recruitment of ATM, ATR and DNA-PKcs to sites of DNA damage. Nature *434*, 605-611.

Falck, J., Mailand, N., Syljuasen, R.G., Bartek, J., and Lukas, J. (2001). The ATM-Chk2-Cdc25A checkpoint pathway guards against radioresistant DNA synthesis. Nature *410*, 842-847.

Falck, J., Petrini, J.H., Williams, B.R., Lukas, J., and Bartek, J. (2002). The DNA damage-dependent intra-S phase checkpoint is regulated by parallel pathways. Nat Genet *30*, 290-294.

Fangman, W.L., Hice, R.H., and Chlebowicz-Sledziewska, E. (1983). ARS replication during the yeast S phase. Cell *32*, 831-838.

Fasullo, M., and Dong, Z. (2004). Genetic Control of Sister Chromatid Recombination: The Role of Radiation Repair (RAD) Genes. Current Genomics *5*, 123-136.

Fasullo, M., Dong, Z., Sun, M., and Zeng, L. (2005a). Saccharomyces cerevisiae RAD53 (CHK2) but not CHK1 is required for double-strand break-initiated SCE and DNA

damage-associated SCE after exposure to X rays and chemical agents. DNA Repair (Amst) *4*, 1240-1251.

Fasullo, M., Dong, Z., Sun, M., and Zeng, L. (2005b). Saccharomyces cerevisiae RAD53 (CHK2) but not CHK1 is required for double-strand break-initiated SCE and DNA damage-associated SCE after exposure to X rays and chemical agents. DNA Repair *4*, 1240-1251.

Fasullo, M., Giallanza, P., Dong, Z., Cera, C., and Bennett, T. (2001). Saccharomyces cerevisiae rad51 Mutants Are Defective in DNA Damage-Associated Sister Chromatid Exchanges but Exhibit Increased Rates of Homology-Directed Translocations. Genetics *158*, 959-972.

Fekairi, S., Scaglione, S., Chahwan, C., Taylor, E.R., Tissier, A., Coulon, S., Dong, M.-Q., Ruse, C., Yates III, J.R., Russell, P.*, et al.* (2009a). Human SLX4 Is a Holliday Junction Resolvase Subunit that Binds Multiple DNA Repair/Recombination Endonucleases. Cell *138*, 78-89.

Fekairi, S., Scaglione, S., Chahwan, C., Taylor, E.R., Tissier, A., Coulon, S., Dong, M.Q., Ruse, C., Yates, J.R., 3rd, Russell, P.*, et al.* (2009b). Human SLX4 is a Holliday junction resolvase subunit that binds multiple DNA repair/recombination endonucleases. Cell *138*, 78-89.

Feng, W., Wu, H., Chan, L.-N., and Zhang, M. (2007). The Par-3 NTD adopts a PB1-like structure required for Par-3 oligomerization and membrane localization. EMBO J *26*, 2786-2796.

Fernandez-Capetillo, O., Chen, H.T., Celeste, A., Ward, I., Romanienko, P.J., Morales, J.C., Naka, K., Xia, Z., Camerini-Otero, R.D., Motoyama, N.*, et al.* (2002). DNA damage-induced G2-M checkpoint activation by histone H2AX and 53BP1. Nat Cell Biol *4*, 993-997.

Fien, K., and Stillman, B. (1992). Identification of replication factor C from Saccharomyces cerevisiae: a component of the leading-strand DNA replication complex. Mol Cell Biol *12*, 155-163.

Fishel, R. (1998). Mismatch repair, molecular switches, and signal transduction. Genes Dev *12*, 2096-2101.

Flott, S., Alabert, C., Toh, G.W., Toth, R., Sugawara, N., Campbell, D.G., Haber, J.E., Pasero, P., and Rouse, J. (2007). Phosphorylation of Slx4 by Mec1 and Tel1 Regulates the Single-Strand Annealing Mode of DNA Repair in Budding Yeast 10.1128/MCB.00135-07. Mol Cell Biol *27*, 6433-6445.

Formosa, T., and Alberts, B.M. (1986). DNA synthesis dependent on genetic recombination: Characterization of a reaction catalyzed by purified bacteriophage T4 proteins. Cell *47*, 793-806.

Fortini, P., Pascucci, B., Belisario, F., and Dogliotti, E. (2000). DNA polymerase {beta} is required for efficient DNA strand break repair induced by methyl methanesulfonate but not by hydrogen peroxide. Nucl Acids Res *28*, 3040-3046.

Franco, A.A., Lam, W.M., Burgers, P.M., and Kaufman, P.D. (2005). Histone deposition protein Asf1 maintains DNA replisome integrity and interacts with replication factor C. Genes & Development *19*, 1365-1375.

Frank, K.M., Sekiguchi, J.M., Seidl, K.J., Swat, W., Rathbun, G.A., Cheng, H.-L., Davidson, L., Kangaloo, L., and Alt, F.W. (1998). Late embryonic lethality and impaired V (D)J recombination in mice lacking DNA ligase IV. Nature *396*, 173-177.

Frank-Vaillant, M., and Marcand, S. (2002). Transient Stability of DNA Ends Allows Nonhomologous End Joining to Precede Homologous Recombination. Molecular Cell *10*, 1189-1199.

Frederick, C., Williams, L., Ughetto, G., Marel, G.v.d., Boom, J.v., Rich, A., and Wang, A. (1990). Structural comparison of anticancer drug-DNA complexes: adriamycin and daunomycin. Biochemistry *29*, 2538–2549.

Frei, C., and Gasser, S.M. (2000). The yeast Sgs1p helicase acts upstream of Rad53p in the DNA replication checkpoint and colocalizes with Rad53p in S-phase-specific foci. Genes Dev *14*, 81-96.

Freudenreich, C.H., Kantrow, S.M., and Zakian, V.A. (1998). Expansion and Length-Dependent Fragility of CTG Repeats in Yeast. Science *279*, 853-856.

Friedberg, E.C., and Gerlach, V.L. (1999). Novel DNA polymerases offer clues to the molecular basis of mutagenesis. Cell *98*, 413-416.

Friedberg, E.C., Walker, G. C., Siede, W., Wood, R. D., Schultz, R. A., and Ellenberger, T. (2006). DNA Repair and Mutagenesis. ASM Press, Washington, DC.

Friedman, K., and Brewer, B. (1995). Analysis of replication intermediates by two-dimensional agarose gel electrophoresis. *Meth Enzymol 262*, 613-627.

Frosina, G., Fortini, P., Rossi, O., Carrozzino, F., Raspaglio, G., Cox, L.S., Lane, D.P., Abbondandolo, A., and Dogliotti, E. (1996). Two pathways for base excision repair in mammalian cells. J Biol Chem *271*, 9573-9578.

Galvani, A., Courbeyrette, R., Agez, M., Ochsenbein, F., Mann, C., and Thuret, J.-Y. (2008). In Vivo Study of the Nucleosome Assembly Functions of ASF1 Histone Chaperones in Human Cells. Mol Cell Biol *28*, 3672-3685.

Gambus, A., Jones, R.C., Sanchez-Diaz, A., Kanemaki, M., van Deursen, F., Edmondson, R.D., and Labib, K. (2006). GINS maintains association of Cdc45 with MCM in replisome progression complexes at eukaryotic DNA replication forks. Nat Cell Biol *8*, 358-366.

Gasser, R., Koller, T., and Sogo, J.M. (1996). The Stability of Nucleosomes at the Replication Fork. Journal of Molecular Biology *258*, 224-239.

Gaudier, M., Schuwirth, B.S., Westcott, S.L., and Wigley, D.B. (2007). Structural Basis of DNA Replication Origin Recognition by an ORC Protein. Science *317*, 1213-1216.

Ge, X.Q., Jackson, D.A., and Blow, J.J. (2007). Dormant origins licensed by excess Mcm2-7 are required for human cells to survive replicative stress. Genes Dev *21*, 3331-3341.

Gilbert, C.S., Green, C.M., and Lowndes, N.F. (2001). Budding yeast Rad9 is an ATP-dependent Rad53 activating machine. Mol Cell *8*, 129-136.

Giot, L., Chanet, R., Simon, M., Facca, C., and Faye, G. (1997a). Involvement of the yeast DNA polymerase δ in DNA repair in vivo. Genetics *146*, 1239-1251.

Giot, L., Chanet, R., Simon, M., Facca, C., and Faye, G. (1997b). Involvement of the yeast DNA polymerase δ in DNA repair in vivo. Genetics *146*, 1239-1251.

Glowczewski, L., Waterborg, J.H., and Berman, J.G. (2004). Yeast Chromatin Assembly Complex 1 Protein Excludes Nonacetylatable Forms of Histone H4 from Chromatin and the Nucleus. Mol Cell Biol *24*, 10180-10192.

Gocke, E., and Manney, T.R. (1979). Expression of radiation-induced mutations at the arginine permease (CAN1) locus in Saccharomyces cerevisiae. Genetics *91*, 53-66.

Goldberg, M., Stucki, M., Falck, J., D'Amours, D., Rahman, D., Pappin, D., Bartek, J., and Jackson, S.P. (2003). MDC1 is required for the intra-S-phase DNA damage checkpoint. Nature *421*, 952-956.

Gottlieb, T.M., and Jackson, S.P. (1993). The DNA-dependent protein kinase: requirement for DNA ends and association with Ku antigen. Cell *72*, 131-142.

Gravel, S., Chapman, J.R., Magill, C., and Jackson, S.P. (2008). DNA helicases Sgs1 and BLM promote DNA double-strand break resection 10.1101/gad.503108. Genes & Development *22*, 2767-2772.

Grawunder, U., Wilm, M., Wu, X., Kulesza, P., Wilson, T.E., Mann, M., and Lieber, M.R. (1997). Activity of DNA ligase IV stimulated by complex formation with XRCC4 protein in mammalian cells. Nature *388*, 492-495.

Grawunder, U., Zimmer, D., Fugmann, S., Schwarz, K., and Lieber, M.R. (1998). DNA Ligase IV Is Essential for V(D)J Recombination and DNA Double-Strand Break Repair in Human Precursor Lymphocytes. Molecular Cell *2*, 477-484.

Graziano, V., Gerchman, S.E., Schneider, D.K., and Ramakrishnan, V. (1994). Histone H1 is located in the interior of the chromatin 30-nm filament. Nature *368*, 351–354.

Greenfeder, S.A., and Newlon, C.S. (1992). Replication forks pause at yeast centromeres. Molecular and Cellular Biology *12*, 4056-4066.

Griffiths, D.J., Barbet, N.C., McCready, S., Lehmann, A.R., and Carr, A.M. (1995). Fission yeast rad17: a homologue of budding yeast RAD24 that shares regions of sequence similarity with DNA polymerase accessory proteins. Embo J *14*, 5812-5823.

Grimme, J.M., Honda, M., Wright, R., Okuno, Y., Rothenberg, E., Mazin, A.V., Ha, T., and Spies, M. (2010). Human Rad52 binds and wraps single-stranded DNA and mediates annealing via two hRad52-ssDNA complexes. Nucl Acids Res *38*, 2917-2930.

Groth, A., Corpet, A., Cook, A.J.L., Roche, D., Bartek, J., Lukas, J., and Almouzni, G. (2007a). Regulation of Replication Fork Progression Through Histone Supply and Demand. Science *318*, 1928-1931.

Groth, A., Lukas, J., Nigg, E.A., Sillje, H.H.W., Wernstedt, C., Bartek, J., and Hansen, K. (2003). Human Tousled like kinases are targeted by an ATM- and Chk1-dependent DNA damage checkpoint. EMBO J *22*, 1676-1687.

Groth, A., Ray-Gallet, D., Quivy, J.-P., Lukas, J., Bartek, J., and Almouzni, G. (2005a). Human Asf1 Regulates the Flow of S Phase Histones during Replicational Stress. Molecular Cell *17*, 301-311.

Groth, A., Ray-Gallet, D., Quivy, J.P., Lukas, J., Bartek, J., and Almouzni, G. (2005b). Human Asf1 regulates the flow of S phase histories during replicational stress. Molecular Cell *17*, 301-311.

Groth, A., Rocha, W., Verreault, A., and Almouzni, G. (2007b). Chromatin Challenges during DNA Replication and Repair. Cell *128*, 721-733.

Gu, J., Lu, H., Tippin, B., Shimazaki, N., Goodman, M.F., and Lieber, M.R. (2007). XRCC4:DNA ligase IV can ligate incompatible DNA ends and can ligate across gaps. EMBO J *26*, 1010-1023.

Gu, Y., Seidl, K.J., Rathbun, G.A., Zhu, C., Manis, J.P., van der Stoep, N., Davidson, L., Cheng, H.-L., Sekiguchi, J.M., Frank, K.*, et al.* (1997). Growth Retardation and Leaky SCID Phenotype of Ku70-Deficient Mice. *7*, 653-665.

Gunjan, A., and Verreault, A. (2003). A Rad53 kinase-dependent surveillance mechanism that regulates histone protein levels in S. cerevisiae. Cell *115*, 537-549.

Haber, J.E. (1998). MATING-TYPE GENE SWITCHING IN SACCHAROMYCES CEREVISIAE. Annual Review of Genetics *32*, 561-599.

Haber, J.E. (1999). DNA recombination: the replication connection. Trends in Biochemical Sciences *24*, 271-275.

Haber, J.E. (2006). Transpositions and translocations induced by site-specific double-strand breaks in budding yeast. DNA Repair
Mechanisms of chromosomal translocation *5*, 998-1009.

Hakansson, P., Hofer, A., and Thelander, L. (2006). Regulation of Mammalian Ribonucleotide Reduction and dNTP Pools after DNA Damage and in Resting Cells. Journal of Biological Chemistry *281*, 7834-7841.

Hake, S.B., and Allis, C.D. (2006). Histone H3 variants and their potential role in indexing mammalian genomes: The ‚ÄúH3 barcode hypothesis‚Äù. Proceedings of the National Academy of Sciences *103*, 6428-6435.

Han, J., Zhou, H., Horazdovsky, B., Zhang, K., Xu, R.-M., and Zhang, Z. (2007a). Rtt109 Acetylates Histone H3 Lysine 56 and Functions in DNA Replication. Science *315*, 653-655.

Han, J., Zhou, H., Li, Z., Xu, R.-M., and Zhang, Z. (2007b). Acetylation of Lysine 56 of Histone H3 Catalyzed by RTT109 and Regulated by ASF1 Is Required for Replisome Integrity
10.1074/jbc.M702496200. J Biol Chem *282*, 28587-28596.

Hanada, K., Budzowska, M., Davies, S.L., van Drunen, E., Onizawa, H., Beverloo, H.B., Maas, A., Essers, J., Hickson, I.D., and Kanaar, R. (2007). The structure-specific endonuclease Mus81 contributes to replication restart by generating double-strand DNA breaks. Nat Struct Mol Biol *14*, 1096-1104.

Hanada, K., Budzowska, M., Modesti, M., Maas, A., Wyman, C., Essers, J., and Kanaar, R. (2006). The structure-specific endonuclease Mus81-Eme1 promotes conversion of interstrand DNA crosslinks into double-strands breaks. Embo J *25*, 4921-4932.

Harfe, B.D., and Jinks-Robertson, S. (2000). Mismatch repair proteins and mitotic genome stability. Mutat Res *451*, 151-167.

Harfst, E., Cooper, S., Neubauer, S., Distel, L., and Grawunder, U. (2000). Normal V(D)J recombination in cells from patients with Nijmegen breakage syndrome. Molecular Immunology *37*, 915-929.

Hartwell, L., and Weinert, T. (1989). Checkpoints: controls that ensure the order of cell cycle events. Science *246*, 629-634.

Helleday, T. (2003). Pathways for mitotic homologous recombination in mammalian cells. Mutat Res *532*, 103-115.

Heller, R.C., and Marians, K.J. (2006). Replication fork reactivation downstream of a blocked nascent leading strand. Nature *439*, 557-562.

Helt, C.E., Cliby, W.A., Keng, P.C., Bambara, R.A., and O'Reilly, M.A. (2005). Ataxia telangiectasia mutated (ATM) and ATM and Rad3-related protein exhibit selective target specificities in response to different forms of DNA damage. J Biol Chem *280*, 1186-1192.

Henner, W.D., Rodriguez, L.O., Hecht, S.M., and Haseltine, W.A. (1983). gamma Ray induced deoxyribonucleic acid strand breaks. 3' Glycolate termini. J Biol Chem *258*, 711-713.

Henriques, J.A.P., Brozmanova, J., and Brendel, M. (1997). Role of PSO genes in the repair of photoinduced interstrand cross-links and photooxidative damage in the DNA of the yeast Saccharomyces cerevisiae. Journal of Photochemistry and Photobiology B: Biology *39*, 185-196.

Herrmann, G., Lindahl, T., and Schar, P. (1998). Saccharomyces cerevisiae LIF1: a function involved in DNA double-strand break repair related to mammalian XRCC4. EMBO J *17*, 4188-4198.

Higgins, N.P., Kato, K., and Strauss, B. (1976). A model for replication repair in mammalian cells. J Mol Biol *101*, 417-425.

Hisao, M., and Ken-Ichi, A. (2002). Cdc7 kinase complex: A key regulator in the initiation of DNA replication. Journal of Cellular Physiology *190*, 287-296.

Hodges, C., Bintu, L., Lubkowska, L., Kashlev, M., and Bustamante, C. (2009). Nucleosomal Fluctuations Govern the Transcription Dynamics of RNA Polymerase II. Science *325*, 626-628.

Hoege, C., Pfander, B., Moldovan, G.-L., Pyrowolakis, G., and Jentsch, S. (2002). RAD6-dependent DNA repair is linked to modification of PCNA by ubiquitin and SUMO. Nature *419*, 135-141.

Hoeijmakers, J.H. (2001). Genome maintenance mechanisms for preventing cancer. Nature *411*, 366-374.

Hoek, M., and Stillman, B. (2003). Chromatin assembly factor 1 is essential and couples chromatin assembly to DNA replication in vivo 10.1073/pnas.1635158100 Proceedings of the National Academy of Sciences of the United States of America *100* 12183-12188

Hoffmann, E.R., and Borts, R.H. (2004). Meiotic recombination intermediates and mismatch repair proteins. Cytogenet Genome Res *107*, 232-248.

Howard-Flanders, P., Theriot, L., and Stedeford, J.B. (1969). Some Properties of Excision-defective Recombination-deficient Mutants of Escherichia coli K-12. J Bacteriol *97*, 1134-1141.

Hu, F., Alcasabas, A.A., and Elledge, S.J. (2001). Asf1 links Rad53 to control of chromatin assembly. Genes Dev *15*, 1061-1066.

Hua, X.H., and Newport, J. (1998). Identification of a Preinitiation Step in DNA Replication That Is Independent of Origin Recognition Complex and cdc6, but Dependent on cdk2. The Journal of Cell Biology *140*, 271-281.

Huang, M., Zhou, Z., and Elledge, S.J. (1998). The DNA Replication and Damage Checkpoint Pathways Induce Transcription by Inhibition of the Crt1 Repressor. Cell *94*, 595-605.

Huang, S., Zhou, H., Katzmann, D., Hochstrasser, M., Atanasova, E., and Zhang, Z. (2005). Rtt106p is a histone chaperone involved in heterochromatin-mediated silencing. Proceedings of the National Academy of Sciences of the United States of America *102*, 13410-13415.

Huang, S., Zhou, H., Tarara, J., and Zhang, Z. (2007). A novel role for histone chaperones CAF-1 and Rtt106p in heterochromatin silencing. EMBO J *26*, 2274-2283.

Huen, M.S.Y., Grant, R., Manke, I., Minn, K., Yu, X., Yaffe, M.B., and Chen, J. (2007). RNF8 Transduces the DNA-Damage Signal via Histone Ubiquitylation and Checkpoint Protein Assembly. Cell *131*, 901-914.

Huertas, P., Cortes-Ledesma, F., Sartori, A.A., Aguilera, A., and Jackson, S.P. (2008). CDK targets Sae2 to control DNA-end resection and homologous recombination. Nature *455*, 689-692.

Huertas, P., and Jackson, S.P. (2009). Human CtIP Mediates Cell Cycle Control of DNA End Resection and Double Strand Break Repair. Journal of Biological Chemistry *284*, 9558-9565.

Hur, S.-K., Park, E.-J., Han, J.-E., Kim, Y.-A., Kim, J.-D., Kang, D., and Kwon, J. Roles of human INO80 chromatin remodeling enzyme in DNA replication and chromosome segregation suppress genome instability. Cellular and Molecular Life Sciences *67*, 2283-2296.

Ii, M., and Brill, S. (2005). Roles of SGS1 , MUS81 , and RAD51 in the repair of lagging-strand replication defects in Saccharomyces cerevisiae. Current Genetics *48*, 213-225.

Im, J.-S., Ki, S.-H., Farina, A., Jung, D.-S., Hurwitz, J., and Lee, J.-K. (2009). Assembly of the Cdc45-Mcm2-7-GINS complex in human cells requires the Ctf4/And-1, RecQL4, and Mcm10 proteins. Proceedings of the National Academy of Sciences *106*, 15628-15632.

Inagaki, S., Suzuki, T., Ohto, M.-a., Urawa, H., Horiuchi, T., Nakamura, K., and Morikami, A. (2006). Arabidopsis TEBICHI, with Helicase and DNA Polymerase Domains, Is Required for Regulated Cell Division and Differentiation in Meristems. Plant Cell *18*, 879-892.

Interthal, H., Pouliot, J.J., and Champoux, J.J. (2001). The tyrosyl-DNA phosphodiesterase Tdp1 is a member of the phospholipase D superfamily. Proc Natl Acad Sci U S A *98*, 12009-12014.

Ip, S.C.Y., Rass, U., Blanco, M.G., Flynn, H.R., Skehel, J.M., and West, S.C. (2008). Identification of Holliday junction resolvases from humans and yeast. Nature *456*, 357-361.

Ira, G., Pellicioli, A., Balijja, A., Wang, X., Fiorani, S., Carotenuto, W., Liberi, G., Bressan, D., Wan, L., Hollingsworth, N.M.*, et al.* (2004). DNA end resection,

homologous recombination and DNA damage checkpoint activation require CDK1. Nature *431*, 1011-1017.

Ivanov, E.L., and Haber, J.E. (1995). RAD1 and RAD10, but not other excision repair genes, are required for double-strand break-induced recombination in Saccharomyces cerevisiae. . Mol Cell Biol *15*, 2245–2251.

Ivessa, A.S., Lenzmeier, B.A., Bessler, J.B., Goudsouzian, L.K., Schnakenberg, S.L., and Zakian, V.A. (2003). The Saccharomyces cerevisiae helicase Rrm3p facilitates replication past nonhistone protein-DNA complexes. Mol Cell *12*, 1525-1536.

Ivessa, A.S., Zhou, J.-Q., Schulz, V.P., Monson, E.K., and Zakian, V.A. (2002). Saccharomyces Rrm3p, a 5' to 3' DNA helicase that promotes replication fork progression through telomeric and subtelomeric DNA. Genes & Development *16*, 1383-1396.

Jachymczyk, W.J., Borstel, R.C., Mowat, M.R.A., and Hastings, P.J. (1981). Repair of interstrand cross-links in DNA of Saccharomyces cerevisiae requires two systems for DNA repair: The RAD3 system and the RAD51 system. Molecular and General Genetics MGG *182*, 196-205.

Jackson, D., Dhar, K., Wahl, J.K., Wold, M.S., and Borgstahl, G.E.O. (2002). Analysis of the human replication protein A : Rad52 complex: Evidence for crosstalk between RPA32, RPA70, Rad52 and DNA. Journal of Molecular Biology *321*, 133-148.

Jasencakova, Z., Scharf, A.N.D., Ask, K., Corpet, A., Imhof, A., Almouzni, G., and Groth, A. (2010). Replication Stress Interferes with Histone Recycling and Predeposition Marking of New Histones. Molecular Cell *37*, 736-743.

Jasin, M. (1996). Genetic manipulation of genomes with rare-cutting endonucleases. Trends Genet *12*, 224-228.

Jazayeri, A., Falck, J., Lukas, C., Bartek, J., Smith, G.C., Lukas, J., and Jackson, S.P. (2006). ATM- and cell cycle-dependent regulation of ATR in response to DNA double-strand breaks. Nat Cell Biol *8*, 37-45.

Jentsch, S., McGrath, J.P., and Varshavsky, A. (1987). The yeast DNA repair gene RAD6 encodes a ubiquitin-conjugating enzyme. Nature *329*, 131-134.

Jiricny, J. (2006). The multifaceted mismatch-repair system. Nat Rev Mol Cell Biol *7*, 335-346.

Jowsey, P.A., Doherty, A.J., and Rouse, J. (2004). hPTIP facilitates ATM-mediated activation of p53 and promotes cellular resistance to ionising radiation. J Biol Chem.

Kadyk, L.C., and Hartwell, L.H. (1992). Sister Chromatids Are Preferred Over Homologs as Substrates for Recombinational Repair in Saccharomyces cerevisiae. Genetics *132*, 387-402.

Kamakaka, R.T., Bulger, M., Kaufman, P.D., Stillman, B., and Kadonaga, J.T. (1996). Postreplicative chromatin assembly by Drosophila and human chromatin assembly factor 1. Mol Cell Biol *16*, 810-817.

Kanaar, R., and Cozzarelli, N.R. (1992). Roles of supercoiled DNA structure in DNA transactions. Current Opinion in Structural Biology *2*, 369-379.

Kannouche, P., Broughton, B.C., Volker, M., Hanaoka, F., Mullenders, L.H., and Lehmann, A.R. (2001). Domain structure, localization, and function of DNA polymerase eta, defective in xeroderma pigmentosum variant cells. Genes Dev *15*, 158-172.

Kannouche, P., Fernandez de Henestrosa, A.R., Coull, B., Vidal, A.E., Gray, C., Zicha, D., Woodgate, R., and Lehmann, A.R. (2002). Localization of DNA polymerases eta and iota to the replication machinery is tightly co-ordinated in human cells. Embo J *21*, 6246-6256.

Kannouche, P., and Lehmann, A. (2006). Localization of y-family polymerases and the DNA polymerase switch in mammalian cells. Methods Enzymol *408*, 407-415.

Kannouche, P.L., and Lehmann, A.R. (2004). Ubiquitination of PCNA and the polymerase switch in human cells. Cell Cycle *3*, 1011-1013.

Kannouche, P.L., Wing, J., and Lehmann, A.R. (2004). Interaction of human DNA polymerase eta with monoubiquitinated PCNA: a possible mechanism for the polymerase switch in response to DNA damage. Mol Cell *14*, 491-500.

Karras, G.I., and Jentsch, S. (2010). The RAD6 DNA Damage Tolerance Pathway Operates Uncoupled from the Replication Fork and Is Functional Beyond S Phase. Cell *141*, 255-267.

Kastan, M.B., and Bartek, J. (2004). Cell-cycle checkpoints and cancer. Nature *432*, 316-323.

Kato, R., and Ogawa, H. (1994). An essential gene, ESR1, is required for mitotic cell growth, DNA repair and meiotic recombination in Saccharomyces cerevisiae. Nucleic Acids Res *22*, 3104-3112.

Kaufman, P.D., Kobayashi, R., Kessler, N., and Stillman, B. (1995). The p150 and p60 subunits of chromatin assemblyfactor I: A molecular link between newly synthesized histones and DNA replication. Cell *81*, 1105-1114.

Kaufman, P.D., Kobayashi, R., and Stillman, B. (1997). Ultraviolet radiation sensitivity and reduction of telomeric silencing in Saccharomyces cerevisiae cells lacking chromatin assembly factor-I. Genes Dev *11*, 345-357.

Kawabe, T. (2004). G2 checkpoint abrogators as anticancer drugs. Mol Cancer Ther *3*, 513-519.

Kawamoto, T., Araki, K., Sonoda, E., Yamashita, Y.M., Harada, K., Kikuchi, K., Masutani, C., Hanaoka, F., Nozaki, K., Hashimoto, N.*, et al.* (2005). Dual Roles for DNA Polymerase [eta] in Homologous DNA Recombination and Translesion DNA Synthesis. Molecular Cell *20*, 793-799.

Kaya, H., Shibahara, K., Taoka, K., Iwabuchi, M., Stillman, B., and Araki, T. (2001). FASCIATA genes for chromatin assembly factor-1 in Arabidopsis maintain the cellular organization of apical meristems. Cell *104*, 131-142.

Keeney, S., Baudat, F., Angeles, M., Zhou, Z.-H., Copeland, N.G., Jenkins, N.A., Manova, K., and Jasin, M. (1999). A Mouse Homolog of the Saccharomyces cerevisiae Meiotic Recombination DNA Transesterase Spo11p. Genomics *61*, 170-182.

Keeney, S., Giroux, C.N., and Kleckner, N. (1997). Meiosis-Specific DNA Double-Strand Breaks Are Catalyzed by Spo11, a Member of a Widely Conserved Protein Family. Cell *88*, 375-384.

Keogh, M.-C., Kim, J.-A., Downey, M., Fillingham, J., Chowdhury, D., Harrison, J.C., Onishi, M., Datta, N., Galicia, S., Emili, A.*, et al.* (2006). A phosphatase complex that dephosphorylates [gamma]H2AX regulates DNA damage checkpoint recovery. Nature *439*, 497-501.

Khanna, K.K., and Jackson, S.P. (2001). DNA double-strand breaks: signaling, repair and the cancer connection. Nat Genet *27*, 247-254.

Khidhir, M.A., Casaregola, S., and Holland, I.B. (1985). Mechanism of transient inhibition of DNA synthesis in ultraviolet-irradiated E. coli: Inhibition is independent of recA whilst recovery requires RecA protein itself and an additional, inducible SOS function. Molecular and General Genetics MGG *199*, 133-140.

Kinner, A., Wu, W., Staudt, C., and Iliakis, G. (2008). {gamma}-H2AX in recognition and signaling of DNA double-strand breaks in the context of chromatin. Nucl Acids Res *36*, 5678-5694.

Klungland, A., and Lindahl, T. (1997). Second pathway for completion of human DNA base excision-repair: reconstitution with purified proteins and requirement for DNase IV (FEN1). Embo J *16*, 3341-3348.

Knipscheer, P., Raschle, M., Smogorzewska, A., Enoiu, M., Ho, T.V., Scharer, O.D., Elledge, S.J., and Walter, J.C. (2009). The Fanconi anemia pathway promotes replication-dependent DNA interstrand cross-link repair. Science *326*, 1698-1701.

Knott, S.R.V., Viggiani, C.J., Tavare, S., and Aparicio, O.M. (2009). Genome-wide replication profiles indicate an expansive role for Rpd3L in regulating replication

initiation timing or efficiency, and reveal genomic loci of Rpd3 function in Saccharomyces cerevisiae. Genes & Development *23*, 1077-1090.

Kobayashi, J., Antoccia, A., Tauchi, H., Matsuura, S., and Komatsu, K. (2004). NBS1 and its functional role in the DNA damage response. DNA Repair
BRIDGE OVER BROKEN ENDS - The Cellular Response to DNA Breaks in Health and Disease *3*, 855-861.

Kobayashi, J., Tauchi, H., Sakamoto, S., Nakamura, A., Morishima, K.-i., Matsuura, S., Kobayashi, T., Tamai, K., Tanimoto, K., and Komatsu, K. (2002). NBS1 Localizes to [gamma]-H2AX Foci through Interaction with the FHA/BRCT Domain. Current Biology *12*, 1846-1851.

Kobayashi, T., and Horiuchi, T. (1996). A yeast gene product, Fob1 protein, required for both replication fork blocking and recombinational hotspot activities. Genes to Cells *1*, 465-474.

Kogoma, T., Cadwell, G.W., Barnard, K.G., and Asai, T. (1996). The DNA replication priming protein, PriA, is required for homologous recombination and double-strand break repair. Journal of Bacteriology *178*, 1258-1264.

Kong, X., Mohanty, S.K., Stephens, J., Heale, J.T., Gomez-Godinez, V., Shi, L.Z., Kim, J.-S., Yokomori, K., and Berns, M.W. (2009). Comparative analysis of different laser systems to study cellular responses to DNA damage in mammalian cells. Nucl Acids Res, gkp221.

Koniaras, K., Cuddihy, A.R., Christopoulos, H., Hogg, A., and O'Connell, M.J. (2001). Inhibition of Chk1-dependent G2 DNA damage checkpoint radiosensitizes p53 mutant human cells. Oncogene *20*, 7453-7463.

Kraus, E., Leung, W.-Y., and Haber, J.E. (2001a). Break-induced replication: A review and an example in budding yeast. Proceedings of the National Academy of Sciences of the United States of America *98*, 8255-8262.

Kraus, E., Leung, W.-Y., and Haber, J.E. (2001b). Break-induced replication: A review and an example in budding yeast
10.1073/pnas.151008198. Proceedings of the National Academy of Sciences of the United States of America *98*, 8255-8262.

Krause, D.R., Jonnalagadda, J.C., Gatei, M.H., Sillje, H.H., Zhou, B.-B., Nigg, E.A., and Khanna, K. (2003). Suppression of Tousled-like kinase activity after DNA damage or replication block requires ATM, NBS1 and Chk1. Oncogene *22*, 5927-5937.

Kreuzer, K.N. (2000). Recombination-dependent DNA replication in phage T4. Trends in Biochemical Sciences *25*, 165-173.

Kreuzer, K.N. (2005). INTERPLAY BETWEEN DNA REPLICATION AND RECOMBINATION IN PROKARYOTES. Annual Review of Microbiology *59*, 43-67.

Krishna, T.S.R., Kong, X.-P., Gary, S., Burgers, P.M., and Kuriyan, J. (1994). Crystal structure of the eukaryotic DNA polymerase processivity factor PCNA. Cell *79*, 1233-1243.

Krogh, B.O., and Symington, L.S. (2004). RECOMBINATION PROTEINS IN YEAST. Annual Review of Genetics *38*, 233-271.

Krokan, H.E., Nilsen, H., Skorpen, F., Otterlei, M., and Slupphaug, G. (2000). Base excision repair of DNA in mammalian cells. FEBS Lett *476*, 73-77.

Kross, J., Henner, W.D., Hecht, S.M., and Haseltine, W.A. (1982). Specificity of deoxyribonucleic acid cleavage by bleomycin, phleomycin, and tallysomycin. Biochemistry *21*, 4310-4318.

Krude, T. (1995). Chromatin Assembly Factor 1 (CAF-1) Colocalizes with Replication Foci in HeLa Cell Nuclei. Experimental Cell Research *220*, 304-311.

Kumagai, A., Lee, J., Yoo, H.Y., and Dunphy, W.G. (2006). TopBP1 activates the ATR-ATRIP complex. Cell *124*, 943-955.

Kumar, R., Bourbon, H.-M., and de Massy, B. (2010). Functional conservation of Mei4 for meiotic DNA double-strand break formation from yeasts to mice. Genes & Development *24*, 1266-1280.

Kumiko, H., Tsutomu, K., Shigenori, I., Masumi, H., Takashi, H., and Hisaji, M. (2003). Fate of DNA replication fork encountering a single DNA lesion during *oriC* plasmid DNA replication *in vitro*. Genes to Cells *8*, 437-449.

Labib, K. (2010). How do Cdc7 and cyclin-dependent kinases trigger the initiation of chromosome replication in eukaryotic cells? Genes & Development *24*, 1208-1219.

Labib, K., and Hodgson, B. (2007). Replication fork barriers: pausing for a break or stalling for time? EMBO Rep *8*, 346-353.

Labib, K., Tercero, J., eacute, A., Diffley, J.F., nbsp, and X (2000). Uninterrupted MCM2-7 Function Required for DNA Replication Fork Progression. Science *288*, 1643-1647.

Langston, L.D., and O'Donnell, M. (2006). DNA replication: keep moving and don't mind the gap. Mol Cell *23*, 155-160.

Larson, K., Sahm, J., Shenkar, R., and Strauss, B. (1985). Methylation-induced blocks to in vitro DNA replication. Mutation Research/Fundamental and Molecular Mechanisms of Mutagenesis *150*, 77-84.

Lawley, P.D., and Phillips, D.H. (1996). DNA adducts from chemotherapeutic agents. Mutat Res *355*, 13-40.

Lawrence, C. (1994). The RAD6 DNA repair pathway in Saccharomyces cerevisiae: what does it do, and how does it do it? Bioessays *16*, 253-258.

Le, S., Davis, C., Konopka, J.B., and Sternglanz, R. (1997). Two New S-Phase-Specific Genes from Saccharomyces cerevisiae. Yeast *13*, 1029-1042.

Le, S., Moore, J.K., Haber, J.E., and Greider, C.W. (1999). RAD50 and RAD51 Define Two Pathways That Collaborate to Maintain Telomeres in the Absence of Telomerase. Genetics *152*, 143-152.

Lee, J., Kumagai, A., and Dunphy, W.G. (2007). The Rad9-Hus1-Rad1 checkpoint clamp regulates interaction of TopBP1 with ATR. J Biol Chem *282*, 28036-28044.

Lehman, J.A., Hoelz, D.J., and Turchi, J.J. (2008). DNA-Dependent Conformational Changes in the Ku Heterodimer‚Ä†. Biochemistry *47*, 4359-4368.

Lehmann, A.R., Niimi, A., Ogi, T., Brown, S., Sabbioneda, S., Wing, J.F., Kannouche, P.L., and Green, C.M. (2007). Translesion synthesis: Y-family polymerases and the polymerase switch. DNA Repair (Amst) *6*, 891-899.

Lei, M., Kawasaki, Y., and Tye, B.K. (1996). Physical interactions among Mcm proteins and effects of Mcm dosage on DNA replication in Saccharomyces cerevisiae. Mol Cell Biol *16*, 5081-5090.

Li, F., Chen, J., Solessio, E., and Gilbert, D.M. (2003). Spatial distribution and specification of mammalian replication origins during G1 phase. The Journal of Cell Biology *161*, 257-266.

Li, F., Dong, J., Pan, X., Oum, J.-H., Boeke, J.D., and Lee, S.E. (2008a). Microarray-Based Genetic Screen Defines SAW1, a Gene Required for Rad1/Rad10-Dependent Processing of Recombination Intermediates. Molecular Cell *30*, 325-335.

Li, Q., Zhou, H., Wurtele, H., Davies, B., Horazdovsky, B., Verreault, A., and Zhang, Z. (2008b). Acetylation of Histone H3 Lysine 56 Regulates Replication-Coupled Nucleosome Assembly. Cell *134*, 244-255.

Li, X., Zhang, X.-P., Solinger, J.A., Kiianitsa, K., Yu, X., Egelman, E.H., and Heyer, W.-D. (2007). Rad51 and Rad54 ATPase activities are both required to modulate Rad51-dsDNA filament dynamics. Nucl Acids Res *35*, 4124-4140.

Liang, F., Han, M., Romanienko, P.J., and Jasin, M. (1998). Homology-directed repair is a major double-strand break repair pathway in mammalian cells. Proc Natl Acad Sci U S A *95*, 5172-5177.

Liberi, G., Maffioletti, G., Lucca, C., Chiolo, I., Baryshnikova, A., Cotta-Ramusino, C., Lopes, M., Pellicioli, A., Haber, J.E., and Foiani, M. (2005). Rad51-dependent DNA structures accumulate at damaged replication forks in sgs1 mutants defective in the yeast ortholog of BLM RecQ helicase. Genes Dev *19*, 339-350.

Lieber, M.R. (1997). The FEN-1 family of structure-specific nucleases in eukaryotic DNA replication, recombination and repair. Bioessays *19*, 233-240.

Lieber, M.R. (2010). The Mechanism of Double-Strand DNA Break Repair by the Nonhomologous DNA End-Joining Pathway. Annu Rev Biochem.

Limoli, C.L., and Ward, J.F. (1993). A new method for introducing double-strand breaks into cellular DNA. Radiat Res *13*, 160–169.

Lindahl, T., and Andersson, A. (1972). Rate of chain breakage at apurinic sites in double-stranded deoxyribonucleic acid. Biochemistry *11*, 3618-3623.

Ling, X., Harkness, T.A., Schultz, M.C., Fisher-Adams, G., and Grunstein, M. (1996). Yeast histone H3 and H4 amino termini are important for nucleosome assembly in vivo and in vitro: redundant and position-independent functions in assembly but not in gene regulation. Genes & Development *10*, 686-699.

Lipford, J.R., and Bell, S.P. (2001). Nucleosomes Positioned by ORC Facilitate the Initiation of DNA Replication. Cell *7*, 21-30.

Liu, J., Xu, L., Sandler, S.J., and Marians, K.J. (1999). Replication fork assembly at recombination intermediates is required for bacterial growth. Proceedings of the National Academy of Sciences of the United States of America *96*, 3552-3555.

Liu, Q., Guntuku, S., Cui, X.S., Matsuoka, S., Cortez, D., Tamai, K., Luo, G., Carattini-Rivera, S., DeMayo, F., Bradley, A.*, et al.* (2000). Chk1 is an essential kinase that is

regulated by Atr and required for the G(2)/M DNA damage checkpoint. Genes Dev *14*, 1448-1459.

Liu, Y., Kao, H.I., and Bambara, R.A. (2004). Flap endonuclease 1: a central component of DNA metabolism. Annu Rev Biochem *73*, 589-615.

Longhese, M.P., Paciotti, V., Fraschini, R., Zaccarini, R., Plevani, P., and Lucchini, G. (1997). The novel DNA damage checkpoint protein Ddc1p is phosphorylated periodically during the cell cycle and in response to DNA damage in budding yeast. EMBO J *16*, 5216-5226.

Lopes, M., Cotta-Ramusino, C., Pellicioli, A., Liberi, G., Plevani, P., Muzi-Falconi, M., Newlon, C.S., and Foiani, M. (2001). The DNA replication checkpoint response stabilizes stalled replication forks. Nature *412*, 557-561.

Lopez-Mosqueda, J., Maas, N.L., Jonsson, Z.O., DeFazio-Eli, L.G., Wohlschlegel, J., and Toczyski, D.P. (2010). Damage-induced phosphorylation of Sld3 is important to block late origin firing. Nature *467*, 479-483.

Lovejoy, C.A., and Cortez, D. (2009). Common mechanisms of PIKK regulation. DNA Repair (Amst) *8*, 1004-1008.

Lovett, S.T. (2003). Connecting replication and recombination. Mol Cell *11*, 554-556.

Loyola, A., Bonaldi, T., Roche, D., Imhof, A., and Almouzni, G. (2006). PTMs on H3 Variants before Chromatin Assembly Potentiate Their Final Epigenetic State. Molecular Cell *24*, 309-316.

Luder, A., and Mosig, G. (1982). Two alternative mechanisms for initiation of DNA replication forks in bacteriophage T4: priming by RNA polymerase and by recombination. Proceedings of the National Academy of Sciences of the United States of America *79*, 1101-1105.

Luger, K., Mader, A.W., Richmond, R.K., Sargent, D.F., and Richmond, T.J. (1997). Crystal structure of the nucleosome core particle at 2.8° resolution. Nature *389*, 251–260.

Lukas, C., Falck, J., Bartkova, J., Bartek, J., and Lukas, J. (2003). Distinct spatiotemporal dynamics of mammalian checkpoint regulators induced by DNA damage. Nature Cell Biology *5*, 255-260.

Lukas, J., Lukas, C., and Bartek, J. (2004). Mammalian cell cycle checkpoints: signalling pathways and their organization in space and time. DNA Repair (Amst) *3*, 997-1007.

Luke, B., Versini, G., Jaquenoud, M., Zaidi, I.W., Kurz, T., Pintard, L., Pasero, P., and Peter, M. (2006). The Cullin Rtt101p Promotes Replication Fork Progression through Damaged DNA and Natural Pause Sites. Current Biology *16*, 786-792.

Lundblad, V., and Blackburn, E.H. (1993). An alternative pathway for yeast telomere maintenance rescues est1 senescence. Cell *73*, 347-360.

Lundin, C., Erixon, K., Arnaudeau, C., Schultz, N., Jenssen, D., Meuth, M., and Helleday, T. (2002). Different Roles for Nonhomologous End Joining and Homologous Recombination following Replication Arrest in Mammalian Cells 10.1128/MCB.22.16.5869-5878.2002. Mol Cell Biol *22*, 5869-5878.

Lusetti, S.L., and Cox, M.M. (2002). THE BACTERIAL RECA PROTEIN AND THE RECOMBINATIONAL DNA REPAIR OF STALLED REPLICATION FORKS. Annual Review of Biochemistry *71*, 71-100.

Lustig, A.J., and Petes, T.D. (1986). Identification of yeast mutants with altered telomere structure Proceedings of the National Academy of Sciences of the United States of America *83* 1398-1402

Lutzmann, M., and Méchali, M. (2008). MCM9 Binds Cdt1 and Is Required for the Assembly of Prereplication Complexes. Molecular Cell *31*, 190-200.

Lydall, D., Nikolsky, Y., Bishop, D.K., and Weinert, T. (1996). A meiotic recombination checkpoint controlled by mitotic checkpoint genes. Nature *383*, 840-843.

Lydeard, J.R., Jain, S., Yamaguchi, M., and Haber, J.E. (2007). Break-induced replication and telomerase-independent telomere maintenance require Pol32. Nature *448*, 820-823.

Lydeard, J.R., Lipkin-Moore, Z., Sheu, Y.-J., Stillman, B., Burgers, P.M., and Haber, J.E. (2010). Break-induced replication requires all essential DNA replication factors except those specific for pre-RC assembly 10.1101/gad.1922610. Genes & Development *24*, 1133-1144.

Ma, Y., Pannicke, U., Schwarz, K., and Lieber, M.R. (2002). Hairpin Opening and Overhang Processing by an Artemis/DNA-Dependent Protein Kinase Complex in Nonhomologous End Joining and V(D)J Recombination. *108*, 781-794.

Mailand, N., Bekker-Jensen, S., Faustrup, H., Melander, F., Bartek, J., Lukas, C., and Lukas, J. (2007). RNF8 Ubiquitylates Histones at DNA Double-Strand Breaks and Promotes Assembly of Repair Proteins. Cell *131*, 887-900.

Mailand, N., Falck, J., Lukas, C., Sylju, aring, sen, R.G., Welcker, M., Bartek, J., and Lukas, J. (2000). Rapid Destruction of Human Cdc25A in Response to DNA Damage. Science *288*, 1425-1429.

Maiorano, D., Lutzmann, M., and Mechali, M. (2006). MCM proteins and DNA replication. Curr Opin Cell Biol *18*, 130-136.

Majka, J., and Burgers, P.M. (2004). The PCNA-RFC families of DNA clamps and clamp loaders. Prog Nucleic Acid Res Mol Biol *78*, 227-260.

Majka, J., Niedziela-Majka, A., and Burgers, P.M.J. (2006). The Checkpoint Clamp Activates Mec1 Kinase during Initiation of the DNA Damage Checkpoint. Molecular Cell *24*, 891-901.

Malkova, A., Ivanov, E.L., and Haber, J.E. (1996). Double-strand break repair in the absence of RAD51 in yeast: a possible role for break-induced DNA replication . Proceedings of the National Academy of Sciences of the United States of America *93*, 7131-7136.

Malkova, A., Naylor, M.L., Yamaguchi, M., Ira, G., and Haber, J.E. (2005a). RAD51-Dependent Break-Induced Replication Differs in Kinetics and Checkpoint Responses from RAD51-Mediated Gene Conversion. Mol Cell Biol *25*, 933-944.

Malkova, A., Naylor, M.L., Yamaguchi, M., Ira, G., and Haber, J.E. (2005b). RAD51-Dependent Break-Induced Replication Differs in Kinetics and Checkpoint Responses from RAD51-Mediated Gene Conversion 10.1128/MCB.25.3.933-944.2005. Mol Cell Biol *25*, 933-944.

Manke, I.A., Nguyen, A., Lim, D., Stewart, M.Q., Elia, A.E., and Yaffe, M.B. (2005). MAPKAP kinase-2 is a cell cycle checkpoint kinase that regulates the G2/M transition and S phase progression in response to UV irradiation. Mol Cell *17*, 37-48.

Mankouri, H.W., Ngo, H.-P., and Hickson, I.D. (2007). Shu Proteins Promote the Formation of Homologous Recombination Intermediates That Are Processed by Sgs1-Rmi1-Top3. Mol Biol Cell *18*, 4062-4073.

Mao, Y.M., Cheng, H.P., Lu, J.W., and Sheng, Z.J. (1989). [Dependence of the recA gene for the replication of the bacterial chromosome initiated by the integrated F' plasmid in Escherichia coli]. Yi Chuan Xue Bao *16*, 56-66.

Marnett, L.J. (2000). Oxyradicals and DNA damage. Carcinogenesis *21*, 361-370.

Masai, H., Asai, T., Kubota, Y., Arai, K.I., and Kogoma, T. (1994). Escherichia coli PriA protein is essential for inducible and constitutive stable DNA replication. EMBO Journal *13*, 5338-5345.

Masai, H., Matsumoto, S., You, Z., Yoshizawa-Sugata, N., and Oda, M. (2010). Eukaryotic Chromosome DNA Replication: Where, When, and How? Annual Review of Biochemistry *79*, 89-130.

Masumoto, H., Hawke, D., Kobayashi, R., and Verreault, A. (2005). A role for cell-cycle-regulated histone H3 lysine 56 acetylation in the DNA damage response. Nature *436*, 294-298.

Matsumoto, Y., and Kim, K. (1995). Excision of deoxyribose phosphate residues by DNA polymerase beta during DNA repair. Science *269*, 699-702.

Matsuoka, S., Ballif, B.A., Smogorzewska, A., McDonald, E.R., 3rd, Hurov, K.E., Luo, J., Bakalarski, C.E., Zhao, Z., Solimini, N., Lerenthal, Y.*, et al.* (2007). ATM and ATR substrate analysis reveals extensive protein networks responsive to DNA damage. Science *316*, 1160-1166.

Maya, R., Balass, M., Kim, S.T., Shkedy, D., Leal, J.F., Shifman, O., Moas, M., Buschmann, T., Ronai, Z., Shiloh, Y.*, et al.* (2001). ATM-dependent phosphorylation of Mdm2 on serine 395: role in p53 activation by DNA damage. Genes Dev *15*, 1067-1077.

Maya-Mendoza, A., Petermann, E., Gillespie, D.A.F., Caldecott, K.W., and Jackson, D.A. (2007). Chk1 regulates the density of active replication origins during the vertebrate S phase. EMBO J *26*, 2719-2731.

McEachern, M.J., and Haber, J.E. (2006). Break-Induced Replication and Recombinational Telomere Elongation in Yeast. Annual Review of Biochemistry *75*, 111-135.

McFarlane, R.J., and Whitehall, S.K. (2009). tRNA genes in eukaryotic genome organization and reorganization. Cell Cycle *8*, 3102 - 3106.

McGlynn, P., Al-Deib, A.A., Liu, J., Marians, K.J., and Lloyd, R.G. (1997). The DNA replication protein PriA and the recombination protein RecG bind D-loops. Journal of Molecular Biology *270*, 212-221.

McHugh, P.J., Sones, W.R., and Hartley, J.A. (2000). Repair of Intermediate Structures Produced at DNA Interstrand Cross-Links in Saccharomyces cerevisiae. Mol Cell Biol *20*, 3425-3433.

McHugh, P.J., Spanswick, V.J., and Hartley, J.A. (2001). Repair of DNA interstrand crosslinks: molecular mechanisms and clinical relevance. Lancet Oncol *2*, 483-490.

McIlwraith, M.J., Vaisman, A., Liu, Y., Fanning, E., Woodgate, R., and West, S.C. (2005). Human DNA Polymerase [eta] Promotes DNA Synthesis from Strand Invasion Intermediates of Homologous Recombination. Molecular Cell *20*, 783-792.

McIlwraith, M.J., and West, S.C. (2008). DNA Repair Synthesis Facilitates RAD52-Mediated Second-End Capture during DSB Repair. Molecular Cell *29*, 510-516.

McInerney, P., and O'Donnell, M. (2004). Functional Uncoupling of Twin Polymerases. Journal of Biological Chemistry *279*, 21543-21551.

McIlwraith, M.J., and West, S.C. (2008). DNA repair synthesis facilitates RAD52-mediated second-end capture during DSB repair. Molecular Cell *29*, 510-516.

Meeks-Wagner, D., and Hartwell, L.H. (1986). Normal stoichiometry of histone dimer sets is necessary for high fidelity of mitotic chromosome transmission. Cell *44*, 43-52.

Meister, P., Taddei, A., Vernis, L., Poidevin, M.l., Gasser, S.M., and Baldacci, G. (2005). Temporal separation of replication and recombination requires the intra-S checkpoint. The Journal of Cell Biology *168*, 537-544.

Menees, T.M., and Roeder, G.S. (1989). ME14, a Yeast Gene Required for Meiotic Recombination. Genetics *123*, 675-682.

Merrick, C.J., Jackson, D., and Diffley, J.F.X. (2004). Visualization of Altered Replication Dynamics after DNA Damage in Human Cells. Journal of Biological Chemistry *279*, 20067-20075.

Meyn, M.S. (1993). High spontaneous intrachromosomal recombination rates in ataxia-telangiectasia. Science *260*, 1327-1330.

Michaelis, C., Ciosk, R., and Nasmyth, K. (1997a). Cohesins: Chromosomal Proteins that Prevent Premature Separation of Sister Chromatids. Cell *91*, 35-45.

Michaelis, C., Ciosk, R., and Nasmyth, K. (1997b). Cohesins: Chromosomal Proteins that Prevent Premature Separation of Sister Chromatids. Cell *91*, 35-45.

Michel, B. (2000). Replication fork arrest and DNA recombination. Trends in Biochemical Sciences *25*, 173-178.

Michel, B., Ehrlich, S.D., and Uzest, M. (1997). DNA double-strand breaks caused by replication arrest. Embo J *16*, 430-438.

Michel, B., Grompone, G., Flores, M.-J., and Bidnenko, V. (2004). Multiple pathways process stalled replication forks. Proceedings of the National Academy of Sciences *101*, 12783-12788.

Mimitou, E.P., and Symington, L.S. (2008). Sae2, Exo1 and Sgs1 collaborate in DNA double-strand break processing. Nature *455*, 770-774.

Mimitou, E.P., and Symington, L.S. (2009a). DNA end resection: many nucleases make light work. DNA Repair (Amst) *8*, 983-995.

Mimitou, E.P., and Symington, L.S. (2009b). Nucleases and helicases take center stage in homologous recombination. Trends in Biochemical Sciences *34*, 264-272.

Minca, E.C., and Kowalski, D. (2010). Multiple Rad5 Activities Mediate Sister Chromatid Recombination to Bypass DNA Damage at Stalled Replication Forks. Molecular Cell *38*, 649-661.

Minko, I.G., Kozekov, I.D., Kozekova, A., Harris, T.M., Rizzo, C.J., and Lloyd, R.S. (2008). Mutagenic potential of DNA-peptide crosslinks mediated by acrolein-derived DNA adducts. Mutat Res *637*, 161-172.

Miotto, B., and Struhl, K. HBO1 Histone Acetylase Activity Is Essential for DNA Replication Licensing and Inhibited by Geminin. Molecular Cell *37*, 57-66.

Miotto, B., and Struhl, K. (2008). HBO1 histone acetylase is a coactivator of the replication licensing factor Cdt1. Genes & Development *22*, 2633-2638.

Mirkin, E.V., and Mirkin, S.M. (2007). Replication Fork Stalling at Natural Impediments. Microbiol Mol Biol Rev *71*, 13-35.

Miyazaki, T., Bressan, D.A., Shinohara, M., Haber, J.E., and Shinohara, A. (2004). In vivo assembly and disassembly of Rad51 and Rad52 complexes during double-strand break repair. EMBO J *23*, 939-949.

Modesti, M., and Kanaar, R. (2001). Homologous recombination: from model organisms to human disease. Genome Biology *2*, reviews1014.1011 - reviews1014.1015.

Mohindra, A., Bolderson, E., Stone, J., Wells, M., Helleday, T., and Meuth, M. (2004). A tumour-derived mutant allele of XRCC2 preferentially suppresses homologous recombination at DNA replication forks. Hum Mol Genet *13*, 203-212.

Moldovan, G.-L., Pfander, B., and Jentsch, S. (2007). PCNA, the Maestro of the Replication Fork. Cell *129*, 665-679.

Moldovan, G.L., and D'andrea, A.D. (2009). How the Fanconi Anemia Pathway Guards the Genome. Annual Review of Genetics *43*, 223-249.

Mordes, D.A., and Cortez, D. (2008). Activation of ATR and related PIKKs. Cell Cycle *7*, 2809-2812.

Morrison, A.J., Highland, J., Krogan, N.J., Arbel-Eden, A., Greenblatt, J.F., Haber, J.E., and Shen, X. (2004). INO80 and [gamma]-H2AX Interaction Links ATP-Dependent Chromatin Remodeling to DNA Damage Repair. Cell *119*, 767-775.

Morrow, D.M., Connelly, C., and Hieter, P. (1997). ``Break Copy'' Duplication: A Model for Chromosome Fragment Formation in Saccharomyces cerevisiae. Genetics *147*, 371-382.

Morrow, D.M., Tagle, D.A., Shiloh, Y., Collins, F.S., and Hieter, P. (1995). TEL1, an S. cerevisiae homolog of the human gene mutated in ataxia telangiectasia, is functionally related to the yeast checkpoint gene MEC1. Cell *82*, 831-840.

Mortensen, U.H., Bendixen, C., Sunjevaric, I., and Rothstein, R. (1996). DNA strand annealing is promoted by the yeast Rad52 protein

. Proceedings of the National Academy of Sciences of the United States of America *93*, 10729-10734.

Moshous, D., Callebaut, I., de Chasseval, R., Corneo, B., Cavazzana-Calvo, M., Le Deist, F., Tezcan, I., Sanal, O., Bertrand, Y., Philippe, N.*, et al.* (2001). Artemis, a Novel DNA Double-Strand Break Repair/V(D)J Recombination Protein, Is Mutated in Human Severe Combined Immune Deficiency. *105*, 177-186.

Moshous, D., Li, L., Chasseval, R.d., Philippe, N., Jabado, N., Cowan, M.J., Fischer, A., and Villartay, J.-P.d. (2000). A new gene involved in DNA double-strand break repair and V(D)J recombination is located on human chromosome 10p 10.1093/hmg/9.4.583. Hum Mol Genet *9*, 583-588.

Mosig, G. (1987). The Essential Role of Recombination in Phage T4 Growth. Annual Review of Genetics *21*, 347-371.

Moyer, S.E., Lewis, P.W., and Botchan, M.R. (2006). Isolation of the Cdc45/Mcm2-7/GINS (CMG) complex, a candidate for the eukaryotic DNA replication fork helicase. Proc Natl Acad Sci U S A *103*, 10236-10241.

Moynahan, M.E., and Jasin, M. (2010a). Mitotic homologous recombination maintains genomic stability and suppresses tumorigenesis. Nat Rev Mol Cell Biol *11*, 196-207.

Moynahan, M.E., and Jasin, M. (2010b). Mitotic homologous recombination maintains genomic stability and suppresses tumorigenesis. *11*, 196-207.

Munoz, I.M., Hain, K., Declais, A.C., Gardiner, M., Toh, G.W., Sanchez-Pulido, L., Heuckmann, J.M., Toth, R., Macartney, T., Eppink, B.*, et al.* (2009). Coordination of structure-specific nucleases by human SLX4/BTBD12 is required for DNA repair. Mol Cell *35*, 116-127.

Murakami, Y., Eki, T., and Hurwitz, J. (1992). Studies on the initiation of simian virus 40 replication in vitro: RNA primer synthesis and its elongation. Proceedings of the National Academy of Sciences of the United States of America *89*, 952-956.

Murakami, Y., Wobbe, C.R., Weissbach, L., Dean, F.B., and Hurwitz, J. (1986). Role of DNA polymerase alpha and DNA primase in simian virus 40 DNA replication in vitro. Proceedings of the National Academy of Sciences of the United States of America *83*, 2869-2873.

Murr, R., Loizou, J.I., Yang, Y.G., Cuenin, C., Li, H., Wang, Z.Q., and Herceg, Z. (2006). Histone acetylation by Trrap-Tip60 modulates loading of repair proteins and repair of DNA double-strand breaks. Nat Cell Biol *8*, 91-99.

Murray, J.M., Tavassoli, M., Al-Harithy, R., Sheldrick, K.S., Lehmann, A.R., Carr, A.M., and Watts, F.Z. (1994). Structural and functional conservation of the human homolog of the Schizosaccharomyces pombe rad2 gene, which is required for chromosome segregation and recovery from DNA damage. Molecular and Cellular Biology *14*, 4878-4888.

Myers, J.S., and Cortez, D. (2006). Rapid activation of ATR by ionizing radiation requires ATM and Mre11. J Biol Chem *281*, 9346-9350.

Nabatiyan, A., and Krude, T. (2004). Silencing of Chromatin Assembly Factor 1 in Human Cells Leads to Cell Death and Loss of Chromatin Assembly during DNA Synthesis. Mol Cell Biol *24*, 2853-2862.

Nakada, D., Matsumoto, K., and Sugimoto, K. (2003). ATM-related Tel1 associates with double-strand breaks through an Xrs2-dependent mechanism. Genes Dev *17*, 1957-1962.

Neecke, H., Lucchini, G., and Longhese, M.P. (1999). Cell cycle progression in the presence of irreparable DNA damage is controlled by a Mec1- and Rad53-dependent checkpoint in budding yeast. Embo J *18*, 4485-4497.

New, J.H., Sugiyama, T., Zaitseva, E., and Kowalczykowski, S.C. (1998). Rad52 protein stimulates DNA strand exchange by Rad51 and replication protein A. Nature *391*, 407-410.

Nguyen, V.Q., Co, C., and Li, J.J. (2001). Cyclin-dependent kinases prevent DNA re-replication through multiple mechanisms. Nature *411*, 1068-1073.

Nick McElhinny, S.A., Gordenin, D.A., Stith, C.M., Burgers, P.M.J., and Kunkel, T.A. (2008). Division of Labor at the Eukaryotic Replication Fork. Molecular Cell *30*, 137-144.

Nick McElhinny, S.A., Havener, J.M., Garcia-Diaz, M., Juarez, R., Bebenek, K., Kee, B.L., Blanco, L., Kunkel, T.A., and Ramsden, D.A. (2005). A gradient of template dependence defines distinct biological roles for family X polymerases in nonhomologous end joining. Mol Cell *19*, 357-366.

Niedernhofer, L.J., Daniels, J.S., Rouzer, C.A., Greene, R.E., and Marnett, L.J. (2003). Malondialdehyde, a product of lipid peroxidation, is mutagenic in human cells. J Biol Chem *278*, 31426-31433.

Niedzwiedz, W., Mosedale, G., Johnson, M., Ong, C.Y., Pace, P., and Patel, K.J. (2004). The Fanconi anaemia gene FANCC promotes homologous recombination and error-prone DNA repair. Mol Cell *15*, 607-620.

Niida, H., and Nakanishi, M. (2006). DNA damage checkpoints in mammals. Mutagenesis *21*, 3-9.

Nimonkar, A.V., Ã–zsoy, A.Z., Genschel, J., Modrich, P., and Kowalczykowski, S.C. (2008). Human exonuclease 1 and BLM helicase interact to resect DNA and initiate DNA repair
10.1073/pnas.0809380105. Proceedings of the National Academy of Sciences *105*, 16906-16911.

Nimonkar, A.V., Sica, R.A., and Kowalczykowski, S.C. (2009). Rad52 promotes second-end DNA capture in double-stranded break repair to form complement-stabilized joint molecules
10.1073/pnas.0813247106. Proceedings of the National Academy of Sciences *106*, 3077-3082.

Nitiss, K.C., Malik, M., He, X., White, S.W., and Nitiss, J.L. (2006). Tyrosyl-DNA phosphodiesterase (Tdp1) participates in the repair of Top2-mediated DNA damage. Proceedings of the National Academy of Sciences *103*, 8953-8958.

Noll, D.M., Mason, T.M., and Miller, P.S. (2006). Formation and repair of interstrand cross-links in DNA. Chem Rev *106*, 277-301.

Norman, D., and Barton, P. (2000). Isolation, sequence, and chromosomal localisation of the human IkappaBR gene (NFKBIL2). Ann Hum Genet *64*, 15-23.

Nyberg, K.A., Michelson, R.J., Putnam, C.W., and Weinert, T.A. (2002). Toward maintaining the genome: DNA damage and replication checkpoints. Annu Rev Genet *36*, 617-656.

O'Driscoll, M., Ruiz-Perez, V.L., Woods, C.G., Jeggo, P.A., and Goodship, J.A. (2003). A splicing mutation affecting expression of ataxia-telangiectasia and Rad3-related protein (ATR) results in Seckel syndrome. Nat Genet *33*, 497-501.

Ogawa, T., Yu, X., Shinohara, A., and Egelman, E. (1993). Similarity of the yeast RAD51 filament to the bacterial RecA filament 10.1126/science.8456314. Science *259*, 1896-1899.

Ogiwara, H., Ui, A., Lai, M.S., Enomoto, T., and Seki, M. (2007). Chl1 and Ctf4 are required for damage-induced recombinations. Biochemical and Biophysical Research Communications *354*, 222-226.

Olavarrieta, L., Hern·ndez, P., Krimer, D.B., and Schvartzman, J.B. (2002). DNA Knotting Caused by Head-on Collision of Transcription and Replication. Journal of Molecular Biology *322*, 1-6.

Olivera, B., and Bonhoeffer, F. (1972). Discontinuous DNA replication in vitro. I. Two distinct size classes of intermediates. Nat New Biol *240*, 233-235.

Olivier, H., Kathrin, M., and Arach, G. (2003). Paradoxes of eukaryotic DNA replication: MCM proteins and the random completion problem. BioEssays *25*, 116-125.

Osborn, A.J., and Elledge, S.J. (2003). Mrc1 is a replication fork component whose phosphorylation in response to DNA replication stress activates Rad53. Genes Dev *17*, 1755-1767.

Paciotti, V., Clerici, M., Lucchini, G., and Longhese, M.P. (2000a). The checkpoint protein Ddc2, functionally related to S. pombe Rad26, interacts with Mec1 and is regulated by Mec1-dependent phosphorylation in budding yeast. Genes Dev *14*, 2046-2059.

Paciotti, V., Clerici, M., Lucchini, G., and Longhese, M.P. (2000b). The checkpoint protein Ddc2, functionally related to S. pombe Rad26, interacts with Mec1 and is regulated by Mec1-dependent phosphorylation in budding yeast. Genes and Development *14*, 2046-2059.

Pages, V., and Fuchs, R.P. (2002). How DNA lesions are turned into mutations within cells? Oncogene *21*, 8957-8966.

Pages, V., and Fuchs, R.P. (2003). Uncoupling of Leading- and Lagging-Strand DNA Replication During Lesion Bypass in Vivo. Science *300*, 1300-1303.

Pan, X., Ye, P., Yuan, D.S., Wang, X., Bader, J.S., and Boeke, J.D. (2006). A DNA Integrity Network in the Yeast Saccharomyces cerevisiae. Cell *124*, 1069-1081.

Pandita, T.K., Pathak, S., and Geard, C.R. (1995). Chromosome end associations, telomeres and telomerase activity in ataxia telangiectasia cells. Cytogenet Cell Genet *71*, 86-93.

Paques, F., and Haber, J.E. (1999). Multiple pathways of recombination induced by double-strand breaks in Saccharomyces cerevisiae. Microbiol Mol Biol Rev *63*, 349-404.

Paull, T.T., and Gellert, M. (1998). The 3' to 5' exonuclease activity of Mre 11 facilitates repair of DNA double-strand breaks. Mol Cell *1*, 969-979.

Paull, T.T., and Gellert, M. (1999). Nbs1 potentiates ATP-driven DNA unwinding and endonuclease cleavage by the Mre11/Rad50 complex

. Genes & Development *13*, 1276-1288.

Pellegrini, L., Yu, D.S., Lo, T., Anand, S., Lee, M., Blundell, T.L., and Venkitaraman, A.R. (2002). Insights into DNA recombination from the structure of a RAD51-BRCA2 complex. Nature *420*, 287-293.

Pellicioli, A., Lucca, C., Liberi, G., Marini, F., Lopes, M., Plevani, P., Romano, A., Di Fiore, P.P., and Foiani, M. (1999). Activation of Rad53 kinase in response to DNA damage and its effect in modulating phosphorylation of the lagging strand DNA polymerase. Embo J *18*, 6561-6572.

Petermann, E., Orta, M.L., Issaeva, N., Schultz, N., and Helleday, T. (2010). Hydroxyurea-Stalled Replication Forks Become Progressively Inactivated and Require Two Different RAD51-Mediated Pathways for Restart and Repair. Molecular Cell *37*, 492-502.

Pierce, A.J., and Jasin, M. (2005). Measuring recombination proficiency in mouse embryonic stem cells. Methods Mol Biol *291*, 373-384.

Pierce, A.J., Johnson, R.D., Thompson, L.H., and Jasin, M. (1999a). XRCC3 promotes homology-directed repair of DNA damage in mammalian cells. Genes & Development *13*, 2633-2638.

Pierce, A.J., Johnson, R.D., Thompson, L.H., and Jasin, M. (1999b). XRCC3 promotes homology-directed repair of DNA damage in mammalian cells. Genes Dev *13*, 2633-2638.

Poirier, G.G., de Murcia, G., Jongstra-Bilen, J., Niedergang, C., and Mandel, P. (1982). Poly(ADP-ribosyl)ation of polynucleosomes causes relaxation of chromatin structure. Proc Natl Acad Sci U S A *79*, 3423-3427.

Pommier, Y. (2006). Topoisomerase I inhibitors: camptothecins and beyond. Nat Rev Cancer *6*, 789-802.

Pommier, Y., Barcelo, J.M., Rao, V.A., Sordet, O., Jobson, A.G., Thibaut, L., Miao, Z., Seiler, J.A., Zhang, H., Marchand, C.*, et al.* (2006). Repair of Topoisomerase I-Mediated DNA Damage. In Progress in Nucleic Acid Research and Molecular Biology (Academic Press), pp. 179-229.

Poot, R.A., Bozhenok, L., van den Berg, D.L.C., Steffensen, S., Ferreira, F., Grimaldi, M., Gilbert, N., Ferreira, J., and Varga-Weisz, P.D. (2004). The Williams syndrome transcription factor interacts with PCNA to target chromatin remodelling by ISWI to replication foci. Nat Cell Biol *6*, 1236-1244.

Possoz, C., Filipe, S.R., Grainge, I., and Sherratt, D.J. (2006). Tracking of controlled Escherichia coli replication fork stalling and restart at repressor-bound DNA in vivo. Embo J *25*, 2596-2604.

Postow, L., Crisona, N.J., Peter, B.J., Hardy, C.D., and Cozzarelli, N.R. (2001). Topological challenges to DNA replication: Conformations at the fork. Proceedings of the National Academy of Sciences of the United States of America *98*, 8219-8226.

Pouliot, J.J., Yao, K.C., Robertson, C.A., and Nash, H.A. (1999a). Yeast gene for a Tyr-DNA phosphodiesterase that repairs topoisomerase I complexes. Science *286*, 552-555.

Pouliot, J.J., Yao, K.C., Robertson, C.A., and Nash, H.A. (1999b). Yeast Gene for a Tyr-DNA Phosphodiesterase that Repairs Topoisomerase I Complexes. Science *286*, 552-555.

Prakash, L. (1981). Characterization of postreplication repair in Saccharomyces cerevisiae and effects of rad6, rad18, rev3 and rad52 mutations. Mol Gen Genet *184*, 471-478.

Prakash, L., and Prakash, S. (1977). Isolation and characterization of MMS-sensitive mutants of Saccharomyces cerevisiae. Genetics *86*, 33-55.

Prakash, R., Satory, D., Dray, E., Papusha, A., Scheller, J., Kramer, W., Krejci, L., Klein, H., Haber, J.E., Sung, P.*, et al.* (2009). Yeast Mph1 helicase dissociates Rad51-made D-

loops: implications for crossover control in mitotic recombination. Genes & Development *23*, 67-79.

Prakash, S., Johnson, R.E., and Prakash, L. (2005). Eukaryotic translesion synthesis DNA polymerases: specificity of structure and function. Annu Rev Biochem *74*, 317-353.

Prakash, S., and Prakash, L. (2000). Nucleotide excision repair in yeast. Mutat Res *451*, 13-24.

Prelich, G., Kostura, M., Marshak, D.R., Mathews, M.B., and Stillman, B. (1987). The cell-cycle regulated proliferating cell nuclear antigen is required for SV40 DNA replication in vitro. Nature *326*, 471-475.

Probst, A.V., Dunleavy, E., and Almouzni, G. (2009). Epigenetic inheritance during the cell cycle. Nat Rev Mol Cell Biol *10*, 192-206.

Pursell, Z.F., Isoz, I., Lundstrom, E.-B., Johansson, E., and Kunkel, T.A. (2007). Yeast DNA Polymerase {epsilon} Participates in Leading-Strand DNA Replication 10.1126/science.1144067. Science *317*, 127-130.

Rainey, M.D., Black, E.J., Zachos, G., and Gillespie, D.A. (2008). Chk2 is required for optimal mitotic delay in response to irradiation-induced DNA damage incurred in G2 phase. Oncogene *27*, 896-906.

Raisner, R.M., and Madhani, H.D. (2008). Genomewide Screen for Negative Regulators of Sirtuin Activity in Saccharomyces cerevisiae Reveals 40 Loci and Links to Metabolism. Genetics *179*, 1933-1944.

Ramey, C.J., Howar, S., Adkins, M., Linger, J., Spicer, J., and Tyler, J.K. (2004). Activation of the DNA Damage Checkpoint in Yeast Lacking the Histone Chaperone Anti-Silencing Function 1. Mol Cell Biol *24*, 10313-10327.

Randell, J.C.W., Bowers, J.L., Rodríguez, H.K., and Bell, S.P. (2006). Sequential ATP Hydrolysis by Cdc6 and ORC Directs Loading of the Mcm2-7 Helicase. Molecular Cell *21*, 29-39.

Ransom, M., Dennehey, B.K., and Tyler, J.K. (2010). Chaperoning Histones during DNA Replication and Repair. Cell *140*, 183-195.

Rass, U., Compton, S.A., Matos, J., Singleton, M.R., Ip, S.C.Y., Blanco, M.G., Griffith, J.D., and West, S.C. (2010). Mechanism of Holliday junction resolution by the human GEN1 protein. Genes & Development *24*, 1559-1569.

Raveendranathan, M., Chattopadhyay, S., Bolon, Y.-T., Haworth, J., Clarke, D.J., and Bielinsky, A.-K. (2006). Genome-wide replication profiles of S-phase checkpoint mutants reveal fragile sites in yeast. The EMBO Journal *25*, 3627–3639.

Ray, P., Zhang, D.-H., Elias, J.A., and Ray, A. (1995). Cloning of a Differentially Expressed IB-related Protein. Journal of Biological Chemistry *270*, 10680-10685.

Raymond, W.E., and Kleckner, N. (1993). RAD50 protein of S. cerevisiae exhibits ATP-dependent DNA binding. Nucl Acids Res *21*, 3851–3856.

Reed, S.H. (2005). Nucleotide excision repair in chromatin: the shape of things to come. DNA Repair (Amst) *4*, 909-918.

Revy, P., Malivert, L., and de Villartay, J.P. (2006). Cernunnos-XLF, a recently identified non-homologous end-joining factor required for the development of the immune system. Curr Opin Allergy Clin Immunol *6*, 416-420.

Rich, T., Allen, R.L., and Wyllie, A.H. (2000). Defying death after DNA damage. Nature *407*, 777-783.

Rijkers, T., Van den Ouweland, J., Morolli, B., Rolink, A.G., Baarends, W.M., Van Sloun, P.P.H., Lohman, P.H.M., and Pastink, A. (1998). Targeted inactivation of mouse RAD52 reduces homologous recombination but not resistance to ionizing radiation. Molecular and Cellular Biology *18*, 6423-6429.

Roberts, J.W., Phizicky, E.M., Burbee, D.G., Roberts, C.W., and Moreau, P.L. (1982). A brief consideration of the SOS inducing signal. Biochimie *64*, 805-807.

Roberts, T.M., Kobor, M.S., Bastin-Shanower, S.A., Ii, M., Horte, S.A., Gin, J.W., Emili, A., Rine, J., Brill, S.J., and Brown, G.W. (2006). Slx4 Regulates DNA Damage Checkpoint-dependent Phosphorylation of the BRCT Domain Protein Rtt107/Esc4. Mol Biol Cell *17*, 539-548.

Rogakou, E.P., Boon, C., Redon, C., and Bonner, W.M. (1999). Megabase Chromatin Domains Involved in DNA Double-Strand Breaks in Vivo. The Journal of Cell Biology *146*, 905-916.

Rogakou, E.P., Pilch, D.R., Orr, A.H., Ivanova, V.S., and Bonner, W.M. (1998). DNA Double-stranded Breaks Induce Histone H2AX Phosphorylation on Serine 139 10.1074/jbc.273.10.5858 Journal of Biological Chemistry *273* 5858-5868

Roland, B., Dorothea, S., Bing, H., Christine, M., Frank, G., and Rolf, K. (1995). Interactions of Human Nuclear Proteins P1Mcm3 and P1Cdc46. European Journal of Biochemistry *228*, 431-438.

Romanienko, P.J., and Camerini-Otero, R.D. (1999). Cloning, Characterization, and Localization of Mouse and Human SPO11. Genomics *61*, 156-169.

Romanienko, P.J., and Camerini-Otero, R.D. (2000). The Mouse Spo11 Gene Is Required for Meiotic Chromosome Synapsis. Molecular Cell *6*, 975-987.

Rooney, S., Sekiguchi, J., Zhu, C., Cheng, H.-L., Manis, J., Whitlow, S., DeVido, J., Foy, D., Chaudhuri, J., Lombard, D*., et al.* (2002). Leaky Scid Phenotype Associated with Defective V(D)J Coding End Processing in Artemis-Deficient Mice. *10*, 1379-1390.

Rosenkranz, H., and Levy, J. (1965). HYDROXYUREA: A SPECIFIC INHIBITOR OF DEOXYRIBONUCLEIC ACID SYNTHESIS. Biochim Biophys Acta *95*, 181-183.

Rothfuss, A., and Grompe, M. (2004). Repair kinetics of genomic interstrand DNA cross-links: Evidence for DNA double-strand break-dependent activation of the Fanconi anemia/BRCA pathway. Molecular and Cellular Biology *24*, 123-134.

Rothstein, R., Michel, B., and Gangloff, S. (2000). Replication fork pausing and recombination or "gimme a break". Genes Dev *14*, 1-10.

Rouse, J. (2004). Esc4p, a new target of Mec1p (ATR), promotes resumption of DNA synthesis after DNA damage. The EMBO Journal *23*, 1188–1197.

Rouse, J., and Jackson, S.P. (2000). LCD1: an essential gene involved in checkpoint control and regulation of the MEC1 signalling pathway in Saccharomyces cerevisiae. Embo J *19*, 5801-5812.

Rouse, J., and Jackson, S.P. (2002a). Interfaces Between the Detection, Signaling, and Repair of DNA Damage. Science *297*, 547-551.

Rouse, J., and Jackson, S.P. (2002b). Interfaces between the detection, signaling, and repair of DNA damage. Science *297*, 547-551.

Rouse, J., and Jackson, S.P. (2002c). Lcd1p recruits Mec1p to DNA lesions in vitro and in vivo. Mol Cell *9*, 857-869.

Rowles, A., Chong, J.P.J., Brown, L., Howell, M., Evan, G.I., and Blow, J.J. (1996). Interaction between the Origin Recognition Complex and the Replication Licensing Systemin Xenopus. Cell *87*, 287-296.

Rudin, N., and Haber, J.E. (1988). Efficient repair of HO-induced chromosomal breaks in Saccharomyces cerevisiae by recombination between flanking homologous sequences. Mol Cell Biol *8*, 3918-3928.

Rupp, W.D., and Howard-flanders, P. (1968). Discontinuities in the DNA synthesized in an Excision-defective strain of Escherichia coli following ultraviolet irradiation. Journal of Molecular Biology *31*, 291-304.

Rupp, W.D., Wilde, C.E., Reno, D.L., and Howard-Flanders, P. (1971). Exchanges between DNA strands in ultraviolet-irradiated Escherichia coli. Journal of Molecular Biology *61*, 25-44.

Saito, T.T., Youds, J.L., Boulton, S.J., and Colaiacovo, M.P. (2009). Caenorhabditis elegans HIM-18/SLX-4 interacts with SLX-1 and XPF-1 and maintains genomic integrity in the germline by processing recombination intermediates. PLoS Genet *5*, e1000735.

Sakaguchi, K., Ishibashi, T., Uchiyama, Y., and Iwabata, K. (2009). The multi-replication protein A (RPA) system - a new perspective. Febs Journal *276*, 943-963.

Saleh-Gohari, N., Bryant, H.E., Schultz, N., Parker, K.M., Cassel, T.N., and Helleday, T. (2005a). Spontaneous homologous recombination is induced by collapsed replication forks that are caused by endogenous DNA single-strand breaks. Mol Cell Biol *25*, 7158-7169.

Saleh-Gohari, N., Bryant, H.E., Schultz, N., Parker, K.M., Cassel, T.N., and Helleday, T. (2005b). Spontaneous Homologous Recombination Is Induced by Collapsed Replication Forks That Are Caused by Endogenous DNA Single-Strand Breaks 10.1128/MCB.25.16.7158-7169.2005. Mol Cell Biol *25*, 7158-7169.

San Filippo, J., Sung, P., and Klein, H. (2008a). Mechanism of Eukaryotic Homologous Recombination. Annual Review of Biochemistry *77*, 229-257.

San Filippo, J., Sung, P., and Klein, H. (2008b). Mechanism of Eukaryotic Homologous Recombination doi:10.1146/annurev.biochem.77.061306.125255. Annual Review of Biochemistry *77*, 229-257.

Sancar, A., Lindsey-Boltz, L.A., Unsal-Kacmaz, K., and Linn, S. (2004). Molecular mechanisms of mammalian DNA repair and the DNA damage checkpoints. Annu Rev Biochem *73*, 39-85.

Sancar, A., and Reardon, J.T. (2004). Nucleotide excision repair in E. coli and man. Adv Protein Chem *69*, 43-71.

Sancar, G.B., Siede, W., and van Zeeland, A.A. (1996). Repair and processing of DNA damage: a summary of recent progress. Mutat Res *362*, 127-146.

Sanchez, Y., Bachant, J., Wang, H., Hu, F., Liu, D., Tetzlaff, M., and Elledge, S.J. (1999). Control of the DNA damage checkpoint by chk1 and rad53 protein kinases through distinct mechanisms. Science *286*, 1166-1171.

Sanchez, Y., Desany, B.A., Jones, W.J., Liu, Q., Wang, B., and Elledge, S.J. (1996). Regulation of RAD53 by the ATM-like kinases MEC1 and TEL1 in yeast cell cycle checkpoint pathways. Science *271*, 357-360.

Sanderson, B.J., and Shield, A.J. (1996). Mutagenic damage to mammalian cells by therapeutic alkylating agents. Mutat Res *355*, 41-57.

Sandler, S.J. (2000). Multiple genetic pathways for restarting DNA replication forks in Escherichia coli K-12. Genetics *155*, 487–497.

Sanematsu, F., Takami, Y., Barman, H.K., Fukagawa, T., Ono, T., Shibahara, K.-i., and Nakayama, T. (2006). Asf1 Is Required for Viability and Chromatin Assembly during DNA Replication in Vertebrate Cells. Journal of Biological Chemistry *281*, 13817-13827.

Santocanale, C., and Diffley, J.F. (1998a). A Mec1- and Rad53-dependent checkpoint controls late-firing origins of DNA replication. Nature *395*, 615-618.

Santocanale, C., and Diffley, J.F.X. (1998b). A Mec1- and Rad53-dependent checkpoint controls late-firing origins of DNA replication. Nature *395*, 615-618.

Santocanale, C., and Diffley, J.F.X. (1998c). A Mec1-and Rad53-dependent checkpoint controls late-firing origins of DNA replication. Nature *395*, 615-618.

Santocanale, C., Sharma, K., and Diffley, J.F.X. (1999). Activation of dormant origins of DNA replication in budding yeast. Genes & Development *13*, 2360-2364.

Sarkar, S., Davies, A.A., Ulrich, H.D., and McHugh, P.J. (2006). DNA interstrand crosslink repair during G1 involves nucleotide excision repair and DNA polymerase zeta. Embo Journal *25*, 1285-1294.

Sarraf, S.A., and Stancheva, I. (2004). Methyl-CpG Binding Protein MBD1 Couples Histone H3 Methylation at Lysine 9 by SETDB1 to DNA Replication and Chromatin Assembly. *15*, 595-605.

Sartori, A.A., Lukas, C., Coates, J., Mistrik, M., Fu, S., Bartek, J., Baer, R., Lukas, J., and Jackson, S.P. (2007). Human CtIP promotes DNA end resection. Nature *450*, 509-514.

Sassanfar, M., and Roberts, J.W. (1990). Nature of the SOS-inducing signal in Escherichia coli : The involvement of DNA replication. Journal of Molecular Biology *212*, 79-96.

Savitsky, K., Bar-Shira, A., Gilad, S., Rotman, G., Ziv, Y., Vanagaite, L., Tagle, D.A., Smith, S., Uziel, T., Sfez, S.*, et al.* (1995a). A single ataxia telangiectasia gene with a product similar to PI-3 kinase. Science *268*, 1749-1753.

Savitsky, K., Sfez, S., Tagle, D.A., Ziv, Y., Sartiel, A., Collins, F.S., Shiloh, Y., and Rotman, G. (1995b). The complete sequence of the coding region of the ATM gene reveals similarity to cell cycle regulators in different species. Hum Mol Genet *4*, 2025-2032.

Schaer, P., Herrmann, G., Daly, G., and Lindahl, T. (1997). A newly identified DNA ligase of Saccharomyces cerevisiaeinvolved in RAD52-independent repair of DNA double-strand‚Äâbreaks. Genes & Development *11*, 1912-1924.

Schmid, C.W. (1996). Alu: Structure, Origin, Evolution, Significance, and Function of One-Tenth of Human DNA
Progress in Nucleic Acid Research and Molecular Biology. In, W.E.C.a.K. Moldave, ed. (Academic Press), pp. 283-319.

Schon, O., Friedler, A., Bycroft, M., Freund, S.M., and Fersht, A.R. (2002). Molecular mechanism of the interaction between MDM2 and p53. J Mol Biol *323*, 491-501.

Schultz, L.B., Chehab, N.H., Malikzay, A., and Halazonetis, T.D. (2000). p53 binding protein 1 (53BP1) is an early participant in the cellular response to DNA double-strand breaks. J Cell Biol *151*, 1381-1390.

Schulz, L.L., and Tyler, J.K. (2006). The histone chaperone ASF1 localizes to active DNA replication forks to mediate efficient DNA replication. FASEB J, 05-5020fje.

Schwacha, A., and Kleckner, N. (1995). Identification of double holliday junctions as intermediates in meiotic recombination. Cell *83*, 783-791.

Schwacha, A., and Kleckner, N. (1997). Interhomolog Bias during Meiotic Recombination: Meiotic Functions Promote a Highly Differentiated Interhomolog-Only Pathway. Cell *90*, 1123-1135.

Schwarz, K., Ma, Y., Pannicke, U., and Lieber, M.R. (2003). Human severe combined immune deficiency and DNA repair. Bioessays *25*, 1061-1070.

Scicchitano, D., Jones, R.A., Kuzmich, S., Gaffney, B., Lasko, D.D., Essigmann, J.M., and Pegg, A.E. (1986). Repair of oligodeoxynucleotides containing O6-methylguanine by O6-alkylguanine-DNA-alkyltransferase. Carcinogenesis *7*, 1383-1386.

Sclafani, R.A., and Holzen, T.M. (2007). Cell Cycle Regulation of DNA Replication. Annual Review of Genetics *41*, 237-280.

Scully, R., Chen, J., Ochs, R.L., Keegan, K., Hoekstra, M., Feunteun, J., and Livingston, D.M. (1997). Dynamic changes of BRCA1 subnuclear location and phosphorylation state are initiated by DNA damage. Cell *90*, 425-435.

Segurado, M., and Diffley, J.F.X. (2008). Separate roles for the DNA damage checkpoint protein kinases in stabilizing DNA replication forks. Genes Dev *22*, 1816-1827.

Segurado, M., GÛmez, M., and Antequera, F. (2002). Increased Recombination Intermediates and Homologous Integration Hot Spots at DNA Replication Origins. Molecular Cell *10*, 907-916.

Seigneur, M., Ehrlich, S.D., and Michel, B. (1997). Blocking rolling circle replication with a UV lesion creates a deletion hotspot. Mol Microbiol *26*, 569-580.

Senga, T., Sivaprasad, U., Zhu, W., Park, J.H., Arias, E.E., Walter, J.C., and Dutta, A. (2006). PCNA is a cofactor for Cdt1 degradation by CUL4/DDB1-mediated N-terminal ubiquitination. J Biol Chem *281*, 6246-6252.

Senshu, T., and Ohashi, M. (1979). Fate of newly synthesized histones shortly after interruption of DNA replication. Journal of Biochemistry *86*, 1259-1267.

Sheu, Y.J., and Stillman, B. (2006). Cdc7-Dbf4 phosphorylates MCM proteins via a docking site-mediated mechanism to promote S phase progression. Mol Cell *24*, 101-113.

Shibahara, K.-i., and Stillman, B. (1999). Replication-Dependent Marking of DNA by PCNA Facilitates CAF-1-Coupled Inheritance of Chromatin. Cell *96*, 575-585.

Shiloh, Y. (2003). ATM and related protein kinases: safeguarding genome integrity. Nat Rev Cancer *3*, 155-168.

Shinohara, A., Ogawa, H., Matsuda, Y., Ushio, N., Ikeo, K., and Ogawa, T. (1993). Cloning of human, mouse and fission yeast recombination genes homologous to RAD51 and recA. Nature Genetics *4*, 239 - 243.

Shinohara, A., Ogawa, H., and Ogawa, T. (1992). Rad51 protein involved in repair and recombination in S. cerevisiae is a RecA-like protein. Cell *69*, 457-470.

Shinohara, A., and Ogawa, T. (1998). Stimulation by Rad52 of yeast Rad51-mediated recombination. Nature *391*, 404-407.

Shirahige, K., Hori, Y., Shiraishi, K., Yamashita, M., Takahashi, K., Obuse, C., Tsurimoto, T., and Yoshikawa, H. (1998). Regulation of DNA-replication origins during cell-cycle progression. Nature *395*, 618-621.

Shivji, M.K., Podust, V.N., Hubscher, U., and Wood, R.D. (1995). Nucleotide excision repair DNA synthesis by DNA polymerase epsilon in the presence of PCNA, RFC, and RPA. Biochemistry *34*, 5011-5017.

Shor, E., Weinstein, J., and Rothstein, R. (2005). A Genetic Screen for top3 Suppressors in Saccharomyces cerevisiae Identifies SHU1, SHU2, PSY3 and CSM2: Four Genes Involved in Error-Free DNA Repair. Genetics *169*, 1275-1289.

Shroff, R., Arbel-Eden, A., Pilch, D., Ira, G., Bonner, W.M., Petrini, J.H., Haber, J.E., and Lichten, M. (2004). Distribution and Dynamics of Chromatin Modification Induced by a Defined DNA Double-Strand Break. Current Biology *14*, 1703-1711.

Sidorova, J.M., and Breeden, L.L. (1997). Rad53-dependent phosphorylation of Swi6 and down-regulation of CLN1 and CLN2 transcription occur in response to DNA damage in Saccharomyces cerevisiae. Genes Dev *11*, 3032-3045.

Sidorova, J.M., and Breeden, L.L. (2003). Rad53 checkpoint kinase phosphorylation site preference identified in the Swi6 protein of Saccharomyces cerevisiae. Mol Cell Biol *23*, 3405-3416.

Siede, W., Allen, J.B., Elledge, S.J., and Friedberg, E.C. (1996). The Saccharomyces cerevisiae MEC1 gene, which encodes a homolog of the human ATM gene product, is required for G1 arrest following radiation treatment. J Bacteriol *178*, 5841-5843.

Silljé, H.H.W., and Nigg, E.A. (2001). Identification of human Asf1 chromatin assembly factors as substrates of Tousled-like kinases. Current Biology *11*, 1068-1073.

Sjögren, C., and Nasmyth, K. (2001). Sister chromatid cohesion is required for postreplicative double-strand break repair in Saccharomyces cerevisiae. Current Biology *11*, 991-995.

Sjögren, C., and Ström, L. (2010). S-phase and DNA damage activated establishment of Sister chromatid cohesion--importance for DNA repair. Experimental Cell Research *316*, 1445-1453.

Skoog, L., and Nordenskjöld, B. (1971). Effects of hydroxyurea and 1-beta-D-arabinofuranosyl-cytosine on deoxyribonucleotide pools in mouse embryo cells. Eur J Biochem *19*, 81-89.

Slater, M.L. (1973). Effect of Reversible Inhibition of Deoxyribonucleic Acid Synthesis on the Yeast Cell Cycle. J Bacteriol *113*, 263-270.

Sleeth, K.M., Sørensen, C.S., Issaeva, N., Dziegielewski, J., Bartek, J., and Helleday, T. (2007). RPA Mediates Recombination Repair During Replication Stress and Is Displaced from DNA by Checkpoint Signalling in Human Cells. Journal of Molecular Biology *373*, 38-47.

Smerdon, M.J., Lan, S.Y., Calza, R.E., and Reeves, R. (1982). Sodium butyrate stimulates DNA repair in UV-irradiated normal and xeroderma pigmentosum human fibroblasts. Journal of Biological Chemistry *257*, 13441-13447.

Smerdon, M.J., and Lieberman, M.W. (1978). Nucleosome rearrangement in human chromatin during UV-induced DNA- reapir synthesis. Proceedings of the National Academy of Sciences of the United States of America *75*, 4238-4241.

Smirnova, M., and Klein, H.L. (2003). Role of the error-free damage bypass postreplication repair pathway in the maintenance of genomic stability. Mutat Res *532*, 117-135.

Smit, A.F. (1996). The origin of interspersed repeats in the human genome. Current Opinion in Genetics & Development *6*, 743-748.

Smith, C.E., Llorente, B., and Symington, L.S. (2007). Template switching during break-induced replication. Nature *447*, 102-105.

Smith, S., and Stillman, B. (1989). Purification and characterization of CAF-I, a human cell factor required for chromatin assembly during DNA replication in vitro. Cell *58*, 15-25.

Sobel, R.E., Cook, R.G., Perry, C.A., Annunziato, A.T., and Allis, C.D. (1995). Conservation of deposition-related acetylation sites in newly synthesized histones H3 and H4. Proceedings of the National Academy of Sciences of the United States of America *92*, 1237-1241.

Sogo, J.M., Lopes, M., and Foiani, M. (2002). Fork reversal and ssDNA accumulation at stalled replication forks owing to checkpoint defects. Science *297*, 599-602.

Sogo, J.M., Stahl, H., Koller, T., and Knippers, R. (1986). Structure of replicating simian virus 40 minichromosomes : The replication fork, core histone segregation and terminal structures. Journal of Molecular Biology *189*, 189-204.

Solinger, J.A., Kiianitsa, K., and Heyer, W.-D. (2002). Rad54, a Swi2/Snf2-like Recombinational Repair Protein, Disassembles Rad51:dsDNA Filaments. Molecular Cell *10*, 1175-1188.

Speck, C., Chen, Z., Li, H., and Stillman, B. (2005). ATPase-dependent cooperative binding of ORC and Cdc6 to origin DNA. *12*, 965-971.

Srivastava, N., Gochhait, S., de Boer, P., and Bamezai, R.N.K. (2009). Role of H2AX in DNA damage response and human cancers. Mutation Research/Reviews in Mutation Research *681*, 180-188.

Stelter, P., and Ulrich, H.D. (2003). Control of spontaneous and damage-induced mutagenesis by SUMO and ubiquitin conjugation. Nature *425*, 188-191.

Stewart, G.S., Panier, S., Townsend, K., Al-Hakim, A.K., Kolas, N.K., Miller, E.S., Nakada, S., Ylanko, J., Olivarius, S., Mendez, M.*, et al.* (2009). The RIDDLE Syndrome Protein Mediates a Ubiquitin-Dependent Signaling Cascade at Sites of DNA Damage. Cell *136*, 420-434.

Stewart, G.S., Wang, B., Bignell, C.R., Taylor, A.M., and Elledge, S.J. (2003a). MDC1 is a mediator of the mammalian DNA damage checkpoint. Nature *421*, 961-966.

Stewart, G.S., Wang, B., Bignell, C.R., Taylor, A.M.R., and Elledge, S.J. (2003b). MDC1 is a mediator of the mammalian DNA damage checkpoint. Nature *421*, 961-966.

Strahl, B.D., and Allis, C.D. (2000). The language of covalent histone modifications. Nature *403*, 41-45.

Ström, L., Lindroos, H.B., Shirahige, K., and Sjögren, C. (2004). Postreplicative Recruitment of Cohesin to Double-Strand Breaks Is Required for DNA Repair. Molecular Cell *16*, 1003-1015.

Stucki, M., Clapperton, J.A., Mohammad, D., Yaffe, M.B., Smerdon, S.J., and Jackson, S.P. (2005). MDC1 directly binds phosphorylated histone H2AX to regulate cellular responses to DNA double-strand breaks. Cell *123*, 1213-1226.

Studitsky, V.M., Clark, D.J., and Felsenfeld, G. (1995). Overcoming a nucleosomal barrier to transcription. Cell *83*, 19-27.

Su, X., Bernal, J.A., and Venkitaraman, A.R. (2008). Cell-cycle coordination between DNA replication and recombination revealed by a vertebrate N-end rule degron-Rad51. Nat Struct Mol Biol *advanced online publication*.

Sugawara, N., Ira, G., and Haber, J.E. (2000). DNA Length Dependence of the Single-Strand Annealing Pathway and the Role of Saccharomyces cerevisiae RAD59 in Double-Strand Break Repair
10.1128/MCB.20.14.5300-5309.2000. Mol Cell Biol *20*, 5300-5309.

Sugiyama, T., Kantake, N., Wu, Y., and Kowalczykowski, S.C. (2006). Rad52-mediated DNA annealing after Rad51-mediated DNA strand exchange promotes second ssDNA capture. Embo J *25*, 5539-5548.

Sun, H., Treco, D., and Szostak, J.W. (1991). Extensive 3'-overhanging, single-stranded DNA associated with the meiosis-specific double-strand breaks at the ARG4 recombination initiation site. Cell *64*, 1155-1161.

Sun, Z., Fay, D.S., Marini, F., Foiani, M., and Stern, D.F. (1996). Spk1/Rad53 is regulated by Mec1-dependent protein phosphorylation in DNA replication and damage checkpoint pathways. Genes Dev *10*, 395-406.

Sun, Z., Hsiao, J., Fay, D.S., and Stern, D.F. (1998). Rad53 FHA domain associated with phosphorylated Rad9 in the DNA damage checkpoint. Science *281*, 272-274.

Sung, P. (1994). Catalysis of ATP-dependent homologous DNA pairing and strand exchange by yeast RAD51 protein
10.1126/science.8066464. Science *265*, 1241-1243.

Sung, P., and Robberson, D.L. (1995). DNA strand exchange mediated by a RAD51-ssDNA nucleoprotein filament with polarity opposite to that of RecA. Cell *82*, 453-461.

Suzuki, T., Inagaki, S., Nakajima, S., Akashi, T., Ohto, M., Kobayashi, M., Seki, M., Shinozaki, K., Kato, T., Tabata, S.*, et al.* (2004). A novel Arabidopsis gene TONSOKU is required for proper cell arrangement in root and shoot apical meristems. Plant Journal *38*, 673-684.

Suzuki, T., Nakajima, S., Inagaki, S., Hirano-Nakakita, M., Matsuoka, K., Demura, T., Fukuda, H., Morikami, A., and Nakamura, K. (2005a). TONSOKU is Expressed in S Phase of the Cell Cycle and its Defect Delays Cell Cycle Progression in Arabidopsis. Plant Cell Physiol *46*, 736-742.

Suzuki, T., Nakajima, S., Inagaki, S., Hirano-Nakakita, M., Matsuoka, K., Demura, T., Fukuda, H., Morikami, A., and Nakamura, K. (2005b). TONSOKU is expressed in S phase of the cell cycle and its defect delays cell cycle progression in Arabidopsis. Plant and Cell Physiology *46*, 736-742.

Svendsen, J.M., Smogorzewska, A., Sowa, M.E., O'Connell, B.C., Gygi, S.P., Elledge, S.J., and Harper, J.W. (2009). Mammalian BTBD12/SLX4 assembles a Holliday junction resolvase and is required for DNA repair. Cell *138*, 63-77.

Symington, L.S. (2002). Role of RAD52 Epistasis Group Genes in Homologous Recombination and Double-Strand Break Repair. Microbiol Mol Biol Rev *66*, 630-670.

Szyjka, S.J., Aparicio, J.G., Viggiani, C.J., Knott, S., Xu, W., Tavare, S., and Aparicio, O.M. (2008). Rad53 regulates replication fork restart after DNA damage in Saccharomyces cerevisiae. Genes Dev *22*, 1906-1920.

Tagami, H., Ray-Gallet, D., Almouzni, G., and Nakatani, Y. (2004). Histone H3.1 and H3.3 Complexes Mediate Nucleosome Assembly Pathways Dependent or Independent of DNA Synthesis. Cell *116*, 51-61.

Takayama, Y., Kamimura, Y., Okawa, M., Muramatsu, S., Sugino, A., and Araki, H. (2003). GINS, a novel multiprotein complex required for chromosomal DNA replication in budding yeast. Genes & Development *17*, 1153-1165.

Takeda, S., Tadele, Z., Hofmann, I., Probst, A.V., Angelis, K.J., Kaya, H., Araki, T., Mengiste, T., Scheid, O.M., Shibahara, K.-i.*, et al.* (2004). BRU1, a novel link between responses to DNA damage and epigenetic gene silencing in Arabidopsis. Genes & Development *18*, 782-793.

Takeuchi, Y., Horiuchi, T., and Kobayashi, T. (2003). Transcription-dependent recombination and the role of fork collision in yeast rDNA. Genes & Development *17*, 1497-1506.

Tamburini, B.A., and Tyler, J.K. (2005). Localized Histone Acetylation and Deacetylation Triggered by the Homologous Recombination Pathway of Double-Strand DNA Repair. Mol Cell Biol *25*, 4903-4913.

Tan, B.C.-M., Chien, C.-T., Hirose, S., and Lee, S.-C. (2006). Functional cooperation between FACT and MCM helicase facilitates initiation of chromatin DNA replication. EMBO J *25*, 3975-3985.

Tang, Y., Zhao, W., Chen, Y., Zhao, Y., and Gu, W. (2008). Acetylation is indispensable for p53 activation. Cell *133*, 612-626.

Taniguchi, T., Garcia-Higuera, I., Andreassen, P.R., Gregory, R.C., Grompe, M., and D'Andrea, A.D. (2002). S-phase-specific interaction of the Fanconi anemia protein, FANCD2, with BRCA1 and RAD51. Blood *100*, 2414-2420.

Teng, S.-C., Chang, J., McCowan, B., and Zakian, V.A. (2000). Telomerase-Independent Lengthening of Yeast Telomeres Occurs by an Abrupt Rad50p-Dependent, Rif-Inhibited Recombinational Process. *6*, 947-952.

Teo, S.-H., and Jackson, S.P. (1997). Identification of Saccharomyces cerevisiae DNA ligase IV: involvement in DNA double-strand break repair. EMBO J *16*, 4788-4795.

Tercero, J.A., and Diffley, J.F. (2001a). Regulation of DNA replication fork progression through damaged DNA by the Mec1/Rad53 checkpoint. *412*, 553-557.

Tercero, J.A., and Diffley, J.F.X. (2001b). Regulation of DNA replication fork progression through damaged DNA by the Mec1/Rad53 checkpoint. Nature *412*, 553-557.

Tercero, J.A., Longhese, M.P., and Diffley, J.F. (2003). A central role for DNA replication forks in checkpoint activation and response. Mol Cell *11*, 1323-1336.

Tewey, K.M., Rowe, T.C., and Yang, L. (1984). Adriamycin-induced DNA damage mediated by mammalian DNA topoisomerase II. Science *226*, 466-468.

Tibbetts, R.S., Cortez, D., Brumbaugh, K.M., Scully, R., Livingston, D., Elledge, S.J., and Abraham, R.T. (2000). Functional interactions between BRCA1 and the checkpoint kinase ATR during genotoxic stress. Genes Dev *14*, 2989-3002.

Timson, D.J., Singleton, M.R., and Wigley, D.B. (2000). DNA ligases in the repair and replication of DNA. Mutation Research/DNA Repair *460*, 301-318.

Toh, G., Sugawara, N., Dong, J., Toth, R., Lee, S.E., Haber, J.E., and Rouse, J. (2010). Mec1/Tel1-dependent phosphorylation of Slx4 stimulates Rad1-Rad10-dependent cleavage of non-homologous DNA tails. DNA Repair *9*, 718-726.

Traven, A., and Heierhorst, J. (2005). SQ/TQ cluster domains: concentrated ATM/ATR kinase phosphorylation site regions in DNA-damage-response proteins. Bioessays *27*, 397-407.

Trujillo, K.M., and Sung, P. (2001). DNA Structure-specific Nuclease Activities in theSaccharomyces cerevisiae Rad50Â·Mre11 Complex 10.1074/jbc.M105482200. Journal of Biological Chemistry *276*, 35458-35464.

Tsang, E., and Carr, A.M. (2008). Replication fork arrest, recombination and the maintenance of ribosomal DNA stability. DNA Repair (Amst) *7*, 1613-1623.

Tse, A.N., Carvajal, R., and Schwartz, G.K. (2007). Targeting checkpoint kinase 1 in cancer therapeutics. Clin Cancer Res *13*, 1955-1960.

Tsubota, T., Berndsen, C.E., Erkmann, J.A., Smith, C.L., Yang, L., Freitas, M.A., Denu, J.M., and Kaufman, P.D. (2007). Histone H3-K56 Acetylation Is Catalyzed by Histone Chaperone-Dependent Complexes. Molecular Cell *25*, 703-712.

Tsukuda, T., Lo, Y.-C., Krishna, S., Sterk, R., Osley, M.A., and Nickoloff, J.A. (2009). INO80-dependent chromatin remodeling regulates early and late stages of mitotic homologous recombination. DNA Repair *8*, 360-369.

Tsurimoto, T., and Stillman, B. (1989). Purification of a cellular replication factor, RF-C, that is required for coordinated synthesis of leading and lagging strands during simian virus 40 DNA replication in vitro. Mol Cell Biol *9*, 609-619.

Tsurimoto, T., and Stillman, B. (1990). Functions of replication factor C and proliferating-cell nuclear antigen: functional similarity of DNA polymerase accessory proteins from human cells and bacteriophage T4. Proceedings of the National Academy of Sciences of the United States of America *87*, 1023-1027.

Tsurimoto, T., and Stillman, B. (1991). Replication factors required for SV40 DNA replication in vitro. I. DNA structure-specific recognition of a primer-template junction by eukaryotic DNA polymerases and their accessory proteins. Journal of Biological Chemistry *266*, 1950-1960.

Tuduri, S., Crabbe, L., Conti, C., Tourriere, H., Holtgreve-Grez, H., Jauch, A., Pantesco, V., De Vos, J., Thomas, A., Theillet, C.*, et al.* (2009). Topoisomerase I suppresses genomic instability by preventing interference between replication and transcription. Nat Cell Biol *11*, 1315-1324.

Turchi, J.J., and Henkels, K. (1996). Human Ku Autoantigen Binds Cisplatin-damaged DNA but Fails to Stimulate Human DNA-activated Protein Kinase. Journal of Biological Chemistry *271*, 13861-13867.

Tyler, J.K., Adams, C.R., Chen, S.-R., Kobayashi, R., Kamakaka, R.T., and Kadonaga, J.T. (1999). The RCAF complex mediates chromatin assembly during DNA replication and repair. Nature *402*, 555-560.

Uhlmann, F., Lottspeich, F., and Nasmyth, K. (1999). Sister-chromatid separation at anaphase onset is promoted by cleavage of the cohesin subunit Scc1. Nature *400*, 37-42.

Ui, A., Seki, M., Ogiwara, H., Lai, M.S., Yamamoto, K., Tada, S., and Enomoto, T. (2007). Activation of a novel pathway involving Mms1 and Rad59 in sgs1 cells. Biochemical and Biophysical Research Communications *356*, 1031-1037.

Ulrich, H.D. (2005). The RAD6 pathway: control of DNA damage bypass and mutagenesis by ubiquitin and SUMO. Chembiochem *6*, 1735-1743.

Ulrich, H.D., and Jentsch, S. (2000). Two RING finger proteins mediate cooperation between ubiquitin-conjugating enzymes in DNA repair. EMBO J *19*, 3388-3397.

Unal, E., Arbel-Eden, A., Sattler, U., Shroff, R., Lichten, M., Haber, J.E., and Koshland, D. (2004). DNA Damage Response Pathway Uses Histone Modification to Assemble a Double-Strand Break-Specific Cohesin Domain. Molecular Cell *16*, 991-1002.

Valencia, M., Bentele, M., Vaze, M.B., Herrmann, G., Kraus, E., Lee, S.E., Schar, P., and Haber, J.E. (2001). NEJ1 controls non-homologous end joining in Saccharomyces cerevisiae. Nature *414*, 666-669.

van Attikum, H., Fritsch, O., and Gasser, S.M. (2007). Distinct roles for SWR1 and INO80 chromatin remodeling complexes at chromosomal double-strand breaks. EMBO J *26*, 4113-4125.

van Attikum, H., Fritsch, O., Hohn, B., and Gasser, S.M. (2004). Recruitment of the INO80 Complex by H2A Phosphorylation Links ATP-Dependent Chromatin Remodeling with DNA Double-Strand Break Repair. Cell *119*, 777-788.

van Gent, D.C., Hoeijmakers, J.H., and Kanaar, R. (2001). Chromosomal stability and the DNA double-stranded break connection. Nat Rev Genet *2*, 196-206.

Vas, A., Mok, W., and Leatherwood, J. (2001). Control of DNA Rereplication via Cdc2 Phosphorylation Sites in the Origin Recognition Complex. Mol Cell Biol *21*, 5767-5777.

Vazquez, M.V., Rojas, V., and Tercero, J.A. (2008). Multiple pathways cooperate to facilitate DNA replication fork progression through alkylated DNA. DNA Repair *7*, 1693-1704.

Venclovas, C., and Thelen, M.P. (2000). Structure-based predictions of Rad1, Rad9, Hus1 and Rad17 participation in sliding clamp and clamp-loading complexes. Nucleic Acids Res *28*, 2481-2493.

Vermeulen, W., Stefanini, M., Giliani, S., Hoeijmakers, J.H., and Bootsma, D. (1991). Xeroderma pigmentosum complementation group H falls into complementation group D. Mutat Res *255*, 201-208.

Verreault, A., Kaufman, P.D., Kobayashi, R., and Stillman, B. (1996). Nucleosome Assembly by a Complex of CAF-1 and Acetylated Histones H3/H4. Cell *87*, 95-104.

Vilenchik, M.M., and Knudson, A.G. (2003). Endogenous DNA double-strand breaks: production, fidelity of repair, and induction of cancer. Proc Natl Acad Sci U S A *100*, 12871-12876.

Vincent, J.A., Kwong, T.J., and Tsukiyama, T. (2008). ATP-dependent chromatin remodeling shapes the DNA replication landscape. Nat Struct Mol Biol *15*, 477-484.

Voelkel-Meiman, K., and Roeder, G.S. (1990). Gene Conversion Tracts Stimulated by HOT1-Promoted Transcription Are Long and Continuous. Genetics *126*, 851-867.

Vogelauer, M., Rubbi, L., Lucas, I., Brewer, B.J., and Grunstein, M. (2002). Histone Acetylation Regulates the Time of Replication Origin Firing. Molecular Cell *10*, 1223-1233.

Wakayama, T., Kondo, T., Ando, S., Matsumoto, K., and Sugimoto, K. (2001). Pie1, a protein interacting with Mec1, controls cell growth and checkpoint responses in Saccharomyces cerevisiae. Mol Cell Biol *21*, 755-764.

Walker, J.R., Corpina, R.A., and Goldberg, J. (2001). Structure of the Ku heterodimer bound to DNA and its implications for double-strand break repair. Nature *412*, 607-614.

Wang, J.C. (2002). Cellular roles of DNA topoisomerases: a molecular perspective. Nat Rev Mol Cell Biol *3*, 430-440.

Wang, W. (2007). Emergence of a DNA-damage response network consisting of Fanconi anaemia and BRCA proteins. Nat Rev Genet *8*, 735-748.

Ward, I.M., Minn, K., and Chen, J. (2004). UV-induced ataxia-telangiectasia-mutated and Rad3-related (ATR) activation requires replication stress. J Biol Chem *279*, 9677-9680.

Ward, I.M., Minn, K., van Deursen, J., and Chen, J. (2003). p53 Binding protein 53BP1 is required for DNA damage responses and tumor suppression in mice. Mol Cell Biol *23*, 2556-2563.

Ward, J.F. (1985). Biochemistry of DNA lesions. Radiat Res Suppl *8*, S103-111.

Ward, J.F. (1995). Radiation mutagenesis: the initial DNA lesions responsible. Radiat Res *142*, 362-368.

Ward, J.F. (2002). The radiation-induced lesions which trigger the bystander effect. Mutat Res *499*, 151-154.

Warren, S.T., and Nelson, D.L. (1993). Trinucleotide repeat expansions in neurological disease. Curr Opin Neurobiol *3*, 752-759.

Watanabe, K., Tateishi, S., Kawasuji, M., Tsurimoto, T., Inoue, H., and Yamaizumi, M. (2004). Rad18 guides poleta to replication stalling sites through physical interaction and PCNA monoubiquitination. Embo J *23*, 3886-3896.

Weinert, T., and Lydall, D. (1993a). Cell cycle checkpoints, genetic instability and cancer. Semin Cancer Biol *4*, 129-140.

Weinert, T., and Lydall, D. (1993b). Cell cycle checkpoints, genetic instability and cancer. Semin Cancer Biol *4*, 129-140.

Weinert, T.A., Kiser, G.L., and Hartwell, L.H. (1994). Mitotic checkpoint genes in budding yeast and the dependence of mitosis on DNA replication and repair. Genes Dev *8*, 652-665.

Weinstock, D.M., Nakanishi, K., Helgadottir, H.R., and Jasin, M. (2006). Assaying double-strand break repair pathway choice in mammalian cells using a targeted endonuclease or the RAG recombinase. Methods Enzymol *409*, 524-540.

Weitzmann, M.N., Woodford, K.J., and Usdin, K. (1997). DNA secondary structures and the evolution of hypervariable tandem arrays. J Biol Chem *272*, 9517-9523.

Whitby, M.C., Osman, F., and Dixon, J. (2003). Cleavage of model replication forks by fission yeast Mus81-Eme1 and budding yeast Mus81-Mms4. J Biol Chem *278*, 6928-6935. Epub 2002 Dec 6908.

White, C.I., and Haber, J.E. (1990). Intermediates of recombination during mating type switching in Saccharomyces cerevisiae. EMBO J *9*, 663–673.

Wilmes, G.M., Archambault, V., Austin, R.J., Jacobson, M.D., Bell, S.P., and Cross, F.R. (2004). Interaction of the S-phase cyclin Clb5 with an 'RXL' docking sequence in the initiator protein Orc6 provides an origin-localized replication control switch. Genes & Development *18*, 981-991.

Wilson, T.E., Grawunder, U., and Lieber, M.R. (1997). Yeast DNA ligase IV mediates non-homologous DNA end joining. Nature *388*, 495-498.

Witkin, E.M., Roegner-Maniscalco, V., Sweasy, J.B., and McCall, J.O. (1987). Recovery from ultraviolet light-induced inhibition of DNA synthesis requires umuDC gene products in recA718 mutant strains but not in recA+ strains of Escherichia coli. Proceedings of the National Academy of Sciences of the United States of America *84*, 6805-6809.

Woodgate, R. (1999). A plethora of lesion-replicating DNA polymerases. Genes Dev *13*, 2191-2195.

Wuarin, J., Buck, V., Nurse, P., and Millar, J.B.A. (2002). Stable Association of Mitotic Cyclin B/Cdc2 to Replication Origins Prevents Endoreduplication. Cell *111*, 419-431.

Wyatt, M.D., and Pittman, D.L. (2006). Methylating Agents and DNA Repair Responses: Methylated Bases and Sources of Strand Breaks. Chemical Research in Toxicology *19*, 1580-1594.

Xu, F., Zhang, Q., Zhang, K., Xie, W., and Grunstein, M. (2007). Sir2 Deacetylates Histone H3 Lysine 56 to Regulate Telomeric Heterochromatin Structure in Yeast. Molecular Cell *27*, 890-900.

Yamane, K., Wu, X., and Chen, J. (2002). A DNA damage-regulated BRCT-containing protein, TopBP1, is required for cell survival. Mol Cell Biol *22*, 555-566.

Yang, S.S., Yeh, E., Salmon, E.D., and Bloom, K. (1997). Identification of a Mid-anaphase Checkpoint in Budding Yeast. J Cell Biol *136*, 345-354.

Yang, S.W., Burgin, A.B., Huizenga, B.N., Robertson, C.A., Yao, K.C., and Nash, H.A. (1996). A eukaryotic enzyme that can disjoin dead-end covalent complexes between DNA and type I topoisomerases. Proceedings of the National Academy of Sciences of the United States of America *93*, 11534-11539.

Yang, Y.-G., Cortes, U., Patnaik, S., Jasin, M., and Wang, Z.-Q. (2004). Ablation of PARP-1 does not interfere with the repair of DNA double-strand breaks, but compromises the reactivation of stalled replication forks. Oncogene *23*, 3872-3882.

Yao, R., Zhang, Z., An, X., Bucci, B., Perlstein, D.L., Stubbe, J., and Huang, M. (2003). Subcellular localization of yeast ribonucleotide reductase regulated by the DNA replication and damage checkpoint pathways. Proceedings of the National Academy of Sciences of the United States of America *100*, 6628-6633.

Ye, X., Franco, A.A., Santos, H., Nelson, D.M., Kaufman, P.D., and Adams, P.D. (2003). Defective S Phase Chromatin Assembly Causes DNA Damage, Activation of the S Phase Checkpoint, and S Phase Arrest. Molecular Cell *11*, 341-351.

Yeo, T.C., Xia, D., Hassouneh, S., Yang, X.O., Sabath, D.E., Sperling, K., Gatti, R.A., Concannon, P., and Willerford, D.M. (2000). V(D)J rearrangement in Nijmegen breakage syndrome. Molecular Immunology *37*, 1131-1139.

Yu, X., Chini, C.C., He, M., Mer, G., and Chen, J. (2003). The BRCT domain is a phospho-protein binding domain. Science *302*, 639-642.

Yu, X., Fu, S., Lai, M., Baer, R., and Chen, J. (2006). BRCA1 ubiquitinates its phosphorylation-dependent binding partner CtIP. Genes & Development *20*, 1721-1726.

Yudelevich, A., Ginsberg, B., and Hurwitz, J. (1968). Discontinuous synthesis of DNA during replication. Proc Natl Acad Sci U S A *61*, 1129-1136.

Yun, M.H., and Hiom, K. (2009). CtIP-BRCA1 modulates the choice of DNA double-strand-break repair pathway throughout the cell cycle. Nature *459*, 460-463.

Zaidi, I.W., Rabut, G., Poveda, A., Scheel, H., Malmström, J., Ulrich, H., Hofmann, K., Pasero, P., Peter, M., and Luke, B. (2008). Rtt101 and Mms1 in budding yeast form a CUL4DDB1-like ubiquitin ligase that promotes replication through damaged DNA. EMBO reports *9*, 1034–1040.

Zegerman, P., and Diffley, J.F.X. (2010). Checkpoint-dependent inhibition of DNA replication initiation by Sld3 and Dbf4 phosphorylation. Nature *467*, 474-478.

Zhang, H., and Freudenreich, C.H. (2007). An AT-Rich Sequence in Human Common Fragile Site FRA16D Causes Fork Stalling and Chromosome Breakage in S. cerevisiae. Molecular Cell *27*, 367-379.

Zhang, H., and Lawrence, C.W. (2005). The error-free component of the RAD6/RAD18 DNA damage tolerance pathway of budding yeast employs sister-strand recombination. Proceedings of the National Academy of Sciences *102*, 15954-15959.

Zhang, N., Liu, X., Li, L., and Legerski, R. (2007). Double-strand breaks induce homologous recombinational repair of interstrand cross-links via cooperation of MSH2, ERCC1-XPF, REV3, and the Fanconi anemia pathway. DNA Repair (Amst) *6*, 1670-1678.

Zhao, H., Watkins, J.L., and Piwnica-Worms, H. (2002). Disruption of the checkpoint kinase 1/cell division cycle 25A pathway abrogates ionizing radiation-induced S and G2 checkpoints. Proc Natl Acad Sci U S A *99*, 14795-14800.

Zhao, X., Chabes, A., Domkin, V., Thelander, L., and Rothstein, R. (2001). The ribonucleotide reductase inhibitor Sml1 is a new target of the Mec1/Rad53 kinase cascade during growth and in response to DNA damage. EMBO J *20*, 3544-3553.

Zhao, X., Muller, E.G., and Rothstein, R. (1998). A suppressor of two essential checkpoint genes identifies a novel protein that negatively affects dNTP pools. Mol Cell *2*, 329-340.

Zhao, X., and Rothstein, R. (2002). The Dun1 checkpoint kinase phosphorylates and regulates the ribonucleotide reductase inhibitor Sml1. Proceedings of the National Academy of Sciences of the United States of America *99*, 3746-3751.

Zhou, Z., and Elledge, S.J. (1993). DUN1 encodes a protein kinase that controls the DNA damage response in yeast. Cell *75*, 1119-1127.

Zhu, Z., Chung, W.-H., Shim, E.Y., Lee, S.E., and Ira, G. (2008). Sgs1 Helicase and Two Nucleases Dna2 and Exo1 Resect DNA Double-Strand Break Ends. Cell *134*, 981-994.

Zou, H., and Rothstein, R. (1997). Holliday Junctions Accumulate in Replication Mutants via a RecA Homolog-Independent Mechanism. Cell *90*, 87-96.

Zou, L., and Elledge, S.J. (2003a). Sensing DNA damage through ATRIP recognition of RPA-ssDNA complexes. Science *300*, 1542-1548.

Zou, L., and Elledge, S.J. (2003b). Sensing DNA Damage Through ATRIP Recognition of RPA-ssDNA Complexes 10.1126/science.1083430. Science *300*, 1542-1548.

Zou, L., Liu, D., and Elledge, S.J. (2003). Replication protein A-mediated recruitment and activation of Rad17 complexes. Proc Natl Acad Sci U S A *100*, 13827-13832.

Zou, L., and Stillman, B. (1998). Formation of a Preinitiation Complex by S-phase Cyclin CDK-Dependent Loading of Cdc45p onto Chromatin. Science *280*, 593-596.

Zou, L., and Stillman, B. (2000). Assembly of a Complex Containing Cdc45p, Replication Protein A, and Mcm2p at Replication Origins Controlled by S-Phase Cyclin-Dependent Kinases and Cdc7p-Dbf4p Kinase. Mol Cell Biol *20*, 3086-3096.